Oxidative Medicine and Cellular Longevity

Oxidative Stress Signalling in Neurodegenerative Diseases

Lead Guest Editor: Marco Feligioni
Guest Editors: Kambiz Hassanzadeh, Massimo Corbo, and Esmael Izadpanah

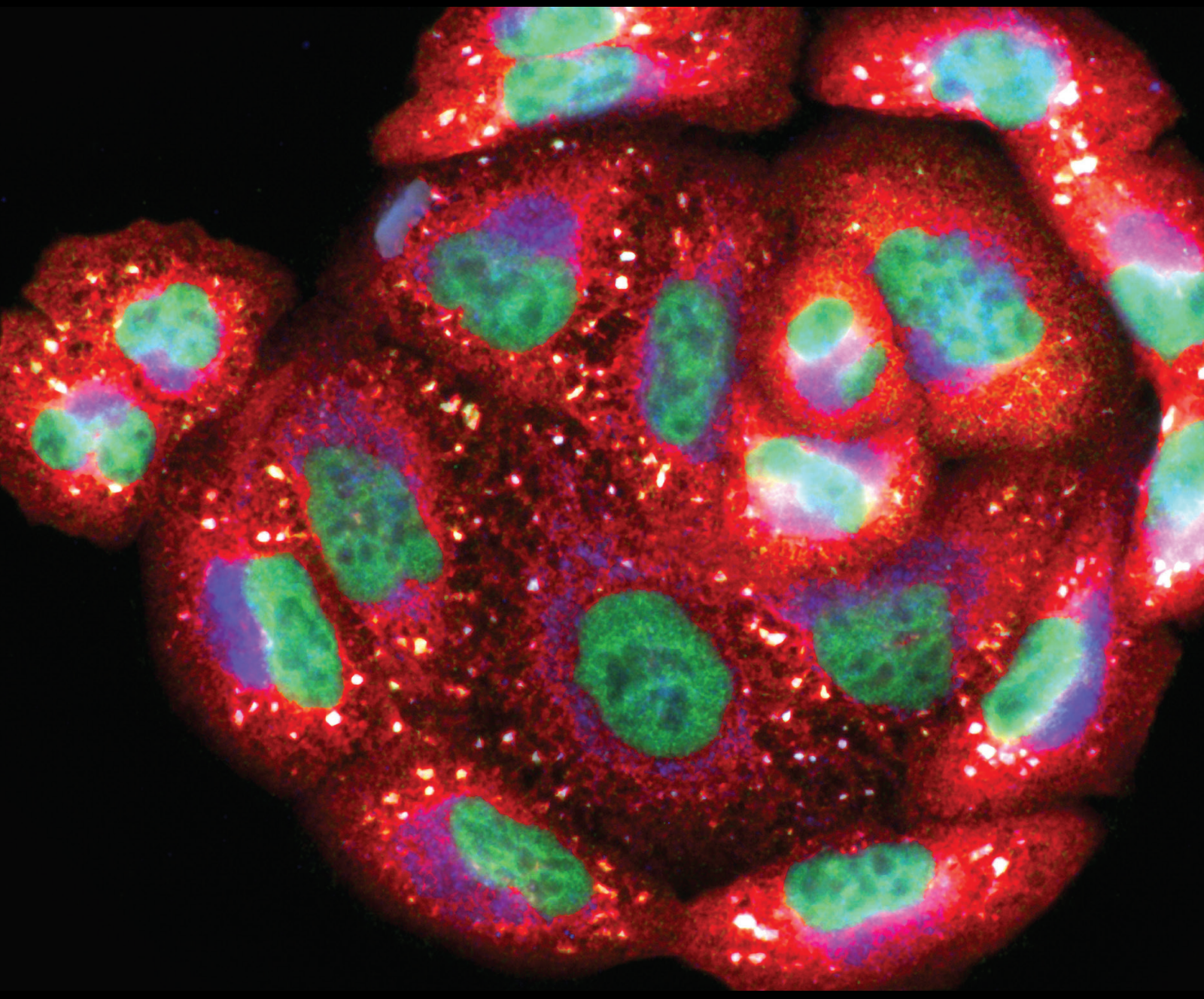

Oxidative Stress Signalling in Neurodegenerative Diseases

Oxidative Medicine and Cellular Longevity

Oxidative Stress Signalling in Neurodegenerative Diseases

Lead Guest Editor: Marco Feligioni
Guest Editors: Kambiz Hassanzadeh, Massimo Corbo, and Esmael Izadpanah

Contents

Hindawi
Oxidative Medicine and Cellular Longevity
Volume 2021, Article ID 6655122, 14 pages
https://doi.org/10.1155/2021/6655122

Research Article

Increase in Blood-Brain Barrier (BBB) Permeability Is Regulated by MMP3 via the ERK Signaling Pathway

Qin Zhang,[1,2] Mei Zheng,[1] Cristian E. Betancourt,[1] Lifeng Liu,[1] Albert Sitikov,[1] Nikola Sladojevic,[1] Qiong Zhao,[3] John H. Zhang,[4] James K. Liao,[1] and Rongxue Wu[1]

[1]*Department of Biological Sciences Division-Cardiology, University of Chicago, USA*
[2]*Department of Anesthesiology, Tongji Hospital, Tongji Medical College, Huazhong University of Science and Technology, China*
[3]*Division of Cardiology, Department of Medicine, Inova Heart and Vascular Institute, USA*
[4]*Center for Neuroscience Research, Loma Linda University, School of Medicine, USA*

Correspondence should be addressed to Rongxue Wu; rwu3@medicine.bsd.uchicago.edu

Received 9 October 2020; Revised 24 November 2020; Accepted 9 March 2021; Published 31 March 2021

Academic Editor: Kambiz Hassanzadeh

Background. The blood-brain barrier (BBB) regulates the exchange of molecules between the brain and peripheral blood and is composed primarily of microvascular endothelial cells (BMVECs), which form the lining of cerebral blood vessels and are linked via tight junctions (TJs). The BBB is regulated by components of the extracellular matrix (ECM), and matrix metalloproteinase 3 (MMP3) remodels the ECM's basal lamina, which forms part of the BBB. Oxidative stress is implicated in activation of MMPs and impaired BBB. Thus, we investigated whether MMP3 modulates BBB permeability. *Methods*. Experiments included *in vivo* assessments of isoflurane anesthesia and dye extravasation from brain in wild-type (WT) and MMP3-deficient (MMP3-KO) mice, as well as *in vitro* assessments of the integrity of monolayers of WT and MMP3-KO BMVECs and the expression of junction proteins. *Results*. Compared to WT mice, measurements of isoflurane usage and anesthesia induction time were higher in MMP3-KO mice and lower in WT that had been treated with MMP3 (WT+MMP3), while anesthesia emergence times were shorter in MMP3-KO mice and longer in WT+MMP3 mice than in WT. Extravasation of systemically administered dyes was also lower in MMP3-KO mouse brains and higher in WT+MMP3 mouse brains, than in the brains of WT mice. The results from both TEER and Transwell assays indicated that MMP3 deficiency (or inhibition) increased, while MMP3 upregulation reduced barrier integrity in either BMVEC or the coculture. MMP3 deficiency also increased the abundance of TJs and VE-cadherin proteins in BMVECs, and the protein abundance declined when MMP3 activity was upregulated in BMVECs, but not when the cells were treated with an inhibitor of extracellular signal related-kinase (ERK). *Conclusion*. MMP3 increases BBB permeability following the administration of isoflurane by upregulating the ERK signaling pathway, which subsequently reduces TJ and VE-cadherin proteins in BMVECs.

1. Introduction

The blood-brain barrier (BBB) regulates the exchange of molecules between the brain and peripheral blood and is composed primarily of endothelial cells (ECs), as well as pericytes and the endfeet of astrocytes [1]. Brain microvascular endothelial cells (BMVECs) form the lining of cerebral blood vessels and are linked to each other via tight junctions (TJs), and the structural stability of TJs is maintained, in part, by adherens junctions (AJs) [2, 3]. Numerous studies have shown that increases in BBB permeability are associated with the degradation of TJs and AJs in ECs [4–7], which can disrupt brain function [8, 9] by augmenting the passage of macrophages, leukocytes, endotoxins, bacteria, and drugs from the peripheral circulation into the brain [10–12]. Thus, the regulation of BBB permeability is crucial both for protecting the brain from harmful components of the peripheral circulation and for the treatment of central nervous system (CNS) disorders. The BBB is regulated primarily via interactions between its cellular components and the extracellular matrix (ECM); thus, matrix metalloproteinases (MMPs), which are the principal drivers of ECM degradation and

remodeling, appear to have a key role in breaking down the BBB. [13]. Furthermore, activation of the extracellular signal-related kinase (ERK) pathway has been shown to induce BBB hyperpermeability by changing the composition of TJs [14–16], but TJ proteins in sheep pleura remained intact after exposure to MMP2 or MMP9 [17, 18], which suggests that these two MMPs regulate BBB permeability via an alternative mechanism. MMP3, another member of the MMP family, is a zinc-dependent protease that is activated through autocleavage, and activated MMP3 remodels the basal lamina of the ECM, which forms part of the BBB [19]. However, whether MMP3 regulates BBB integrity, and if so, whether its role is mediated by ERK signaling and/or changes in TJ stability, remains unclear.

For most molecules, passive permeability of the BBB is low, but inhaled anesthetics such as isoflurane are highly fat soluble and, consequently, can traverse the BBB and enter brain tissue [20]. Nevertheless, factors that increase BBB permeability augment the passage of isoflurane into the CNS and enhance anesthesia [9]. Thus, the experiments presented in this report evaluated the potential role of MMP3 in BBB permeability by combining *in vivo* assessments of isoflurane anesthesia and dye extravasation in wild-type (WT) and MMP3-deficient mice with *in vitro* assessments of the integrity of BMVEC cell layers and the expression of junction proteins. Our results indicate that MMP3 could be therapeutically targeted to manipulate BBB permeability and treat neurological disease.

2. Materials and Methods

2.1. Animals. All animal procedures were carried out in accordance with the guidelines provided by the Institutional Animal Care and Use Committee of the University of Chicago (Chicago, Illinois). The C57BL/6-MMP3 deficient (MMP3−/−) mice were a GEM Collection Model TTM-610 and were generated as described before [21]. The line was backcrossed for 12 generations with C57BL/6 mice, which were provided by the Taconic Biosciences company. A PCR-based analysis was employed to genotype mice. Mice were housed in a room at 22-24°C on a 12-hour light/dark cycle and received drinking water *ad libitum*. We used 8-week-old male mice in this study.

Genotyping: We isolated genomic DNA from mouse tail clips using the Puregene DNA isolation kit from Gentra Systems according to the manufacturer's instruction. About 10 ng of the genomic DNA was used for PCR.

2.2. Experimental Design. The experimental design of the current study is described below and illustrated in Figure 1. All experiments were conducted in a blinded fashion to investigate the influence of MMP3 on the BBB integrity, we assigned all the mice to three different groups under isoflurane, including WT (MMP3+/+), KO (MMP3-/-), and WT +MMP3 (the mice were administered a recombinant human MMP3 via tail intravenous injection (iv), which was purchased from Abcam). Each experimental group contained 8 mice. *In vivo*, the BBB permeability was evaluated by measuring Evans blue and sodium-FITC-dextrans extravasation [22]. In vitro study, the BBB permeability was detected in an *in vitro* model of BBB. To evaluate the role of MMP3 on BBB junction proteins, we used the MMP3 recombinant human protein to stimulate brain microvascular endothelial cells (BMVECs). Afterward, we detected the protein level of MMP3, ZO-1, occludin, VE-cadherin, and claudin-5 by Western blot and fluorescence staining. To increase the MMP3 levels, lipopolysaccharide (LPS) in a dose of 100 μg/mL as a stimulus to increase the MMP3 levels [23, 24], and then, the ERK inhibitor FR1080204 [25] (purchased from Sigma-Aldrich) was administered to investigate the mechanism behind the effects of MMP3 on the BBB.

2.3. In Vitro Model of the Blood-Brain Barrier. To mimic the anatomic structure of the *in vivo* BBB, we developed an *in vitro* BBB model based on the coculture of brain ECs with astrocytes, as described in other publications [26]. In this model, BMVECs were seeded in the Transwell insert, and then, primary isolated astrocytes were grown on the undersurface of the Transwell insert. Isolation of the BMVECs and astrocytes are described in detail in the supplemental file (available here).

2.4. MMP3 Administration In Vivo and In Vitro Study. The MMP3 recombinant human protein purchased from Sigma was diluted to 20 μg/mL in the assay buffer: 50 mM Tris, 10 mM CaCl2, 150 mM NaCl, 0.05% (w/v), and Brij-35, pH 7.5. For the next step, MMP3 was then activated by adding chymotrypsin (Sigma, 1 mg/mL stock in 1 mM HCl) to a final concentration of 5 μg/mL. Afterward, the preparation was incubated at 37°C for 30 minutes [27], and a dose of 50 μg/kg of the MMP3 preparation was injected into the tail vein 30 minutes before an Evans blue injection *in vivo*. The activated MMP3 was added to the *in vitro* cells at a dose of 150 ng/mL for 24 hours.

2.5. Isoflurane Exposure. We anesthetized the mice with isoflurane in the chamber until they lost consciousness and respiration showed to an appropriate rate. A typical exposure includes 3% isoflurane and 100% O2, which corresponds to a respiration rate of 1 breath every 2 sec. A response to a toe pinch or tail pinch was used to confirm the appropriate state of anesthesia. The mice were orally intubated with a 22G IV catheter and artificially ventilated with a rodent respirator (Harvard 1. Apparatus or similar device, tidal volume 0.3 mL, rate 105 strokes/min) [28]. The air from the thorax was evacuated through a tub, which was connected from the mice noses and extended to a Fluosorber canister. Anesthesia was maintained with 1–2% isoflurane in 100% oxygen for 1 hour. The concentration of isoflurane was adjusted according to the loss and regain of reflexes. During anesthesia, mice were placed on a heating pad to maintain body temperature at 37°C and monitored until fully ambulatory. Anesthesia was terminated by discontinuing isoflurane administration. The anesthetic effect of isoflurane (induction time, emergence time, and isoflurane usage volume) was recorded carefully.

2.6. In Vivo BBB Permeability Assay in Mice. Either Evans blue [29, 30] or a sodium-Fluorescein Isothiocyanate (FITC)

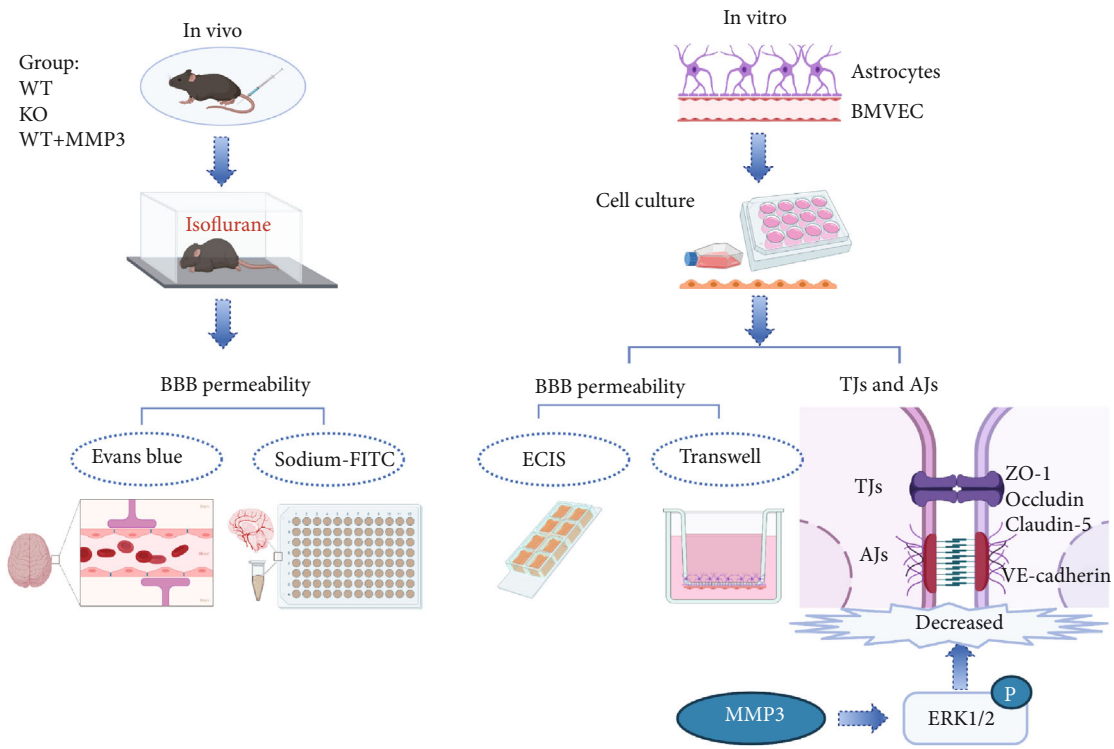

Figure 1: Experimental design. Experiments were conducted both *in vivo* and *in vitro*, as indicated. *In vivo* experiments were conducted in wild-type mice (WT), MMP3-KO mice (KO) mice, and WT mice administered MMP3 (WT + MMP3) and included assessments of susceptibility to isoflurane anesthesia and BBB permeability to intravenously administered dyes (Evans blue, sodium-FITC). *In vitro* assessments included measurements of barrier integrity via TEER using ECIS system in monolayers of BMVECs and in cocultures of BMVECs and astrocytes via Transwell assay. The abundance of junctional proteins was also evaluated via Western blot.

assay [31] was used for the assessment of the BBB integrity. The mice were injected with 2% of Evans blue or sodium-FITC (1 mg/mL in saline) 200 μL through the tail vein 2 hours before sacrificing them. Moreover, they were anesthetized with 1-2% isoflurane for 1 hour and then transcardially perfused with 10 mL normal saline to remove the Evans blue dye and the sodium-FITC from the blood vessels. Brain tissue from the bilateral temporal lobes was carefully removed from the animals following sacrifice. Regarding the mice injected with Evans blue dye, a total of 0.5 mL of formamide was added to the brain tissue homogenate to dissolve the Evans blue dye. After incubation in a 55°C water bath for 48 hours, the samples were centrifuged at 12000 × g for 30 minutes. The supernatant was then collected before absorbance measurements at 632 nm were performed using a UV spectrophotometer (Hitachi, Ltd.). The Evans blue content was calculated according to the standard curve. For mice that were injected with sodium-FITC, a total of 1 mL 50 mM of Tris buffer solution was added to the brain tissue homogenate and then centrifuged at 3000 rpm for 30 minutes. We proceeded to collect the supernatant, which was then mixed with methanol (1 : 1) and centrifuged at 3000 rpm for 30 min. The supernatant was collected, and its fluorescent intensity measured on a plate reader. Finally, the concentration per mg of tissue was calculated using a standard curve.

2.7. RNA Isolation, Reverse Transcription, and Quantitative PCR. Total RNA was isolated from cells and tissue using a RNeasy mini kit (Qiagen, Valencia, CA) according to the manufacturer's protocol. The extracted RNA was treated with recombinant DNAse (Invitrogen, Grand Island, NY) according to the manufacturer's protocol to remove any DNA contamination. cDNA was synthesized from 500 ng of RNA using the Superscript III reverse transcription kit (Invitrogen). Quantitative real-time PCR was performed using a 7300 Real-Time PCR System (Applied Biosystems, Foster City, CA) to determine the gene expression for MMP3 using validated TaqMan® gene expression assay primer/probe combinations (Applied Biosystems). All qPCR results were normalized to the expression of the endogenous control 18S. Folding changes in the transcripts were determined using the delta cycle threshold (i.e., $\Delta\Delta$Ct) method.

2.8. Transendothelial Electrical Resistance (TEER) Measurement. Measurements of transendothelial electrical resistance (TEER) across the mice brain EC monolayers were performed using the electrical cell-substrate impedance sensing system (ECIS) (Applied BioPhysics, Troy, NY, USA), as described in a previous study [32, 33]. For impedance measurements, cells were grown on 8W10E+ arrays. The arrays were treated with 10 mM L-cysteine (cat#C7352-25G, Sigma-Aldrich) followed by coating with collagen type I (cat#A1048301, Thermo Fisher Scientific) at 1 μg/cm^2. The arrays of the electrical stabilization command in the ECIS software were used to sterilize and clean the gold electrodes. BMVECs were seeded onto the arrays at a density of

60,000 cells/cm^2 in 400 μL of L-DMEM growth media. ECIS was conducted using the multiple frequency/time (MFT) option to record the impedance measurements over a broad spectrum of frequencies.

2.9. Detection of BBB Permeability In Vitro Study. To construct an *in vitro* BBB model [34], we isolated and identified mice BMVECs and astrocytes (Supplementary Figure 1). We placed a Transwell chamber insert with a 0.4-μm aperture (Corning, New York, USA) into volumetric flasks. Astrocytes (1×10^6/mL) were added to the underside of the Transwell and incubated at 37°C and 5% CO_2 for 24 hours. The chambers were then placed carefully into a 6-well plate (Corning) (Figure 1(b)). When the astrocytes reached 60% confluence under an inverted microscope, ECs (1×10^7/mL) were seeded on top of the Transwell (Figure 1(c)) at 37°C and 5% CO_2. Furthermore, we observed the cells under an inverted microscope until the astrocytes and BMVECs reached a high-density coculture and, at that point, a FITC-dextran (Dextran-blue-3KD and Dextran-red-40KD) [35] Transwell assay was used to assess the *in vitro* BBB permeability.

2.10. Western Blot. Cells were placed on ice, and the media was aspirated prior to washing twice with ice-cold PBS. A cell lysis buffer was prepared by adding a complete mini protease inhibitor tablet (Roche Diagnostics, Indianapolis, IN) and phosphatase inhibitors (Sigma-Aldrich) to a protein isolation buffer (40 mM HEPES, 120 mM NaCl, 1 mM EDTA, 3% CHAPS *w/v*). Ice-cold buffer was added to each well, and the cells were mechanically disrupted using a rubber scraper. We performed Western blots, as described before in my paper [36]. Briefly, protein extracts from the cells were subjected to a freeze/thaw cycle before being centrifuged (6,000 rpm ×20 min). Supernatants were collected, protein concentrations were determined using a BCA assay (Thermo Fisher SDS-PAGE was performed using 4–12% Bis/Tris gels (Biorad), and proteins were transferred to nitrocellulose membranes. After blocking with 5% non-fat milk in TBST, we incubated the membrane with anti-MMP3 (1 : 1000; Abcam), anti-ZO-1 (1 : 1000, Invitrogen), anti-occludin (1 : 1000, Invitrogen), anti-VE-cadherin (1 : 500, Invitrogen), anti-claudin-5 (1 : 1000, Invitrogen), and anti-p-ERK (1 : 2000 Invitrogen) antibodies for 16 hours at 4°C. After incubating with a Horseradish peroxidase- (HRP-) conjugated secondary antibody, the membranes were developed with enhanced chemiluminescence (ECL) reagent and imaged with a ChemiDoc imaging system (Biorad). A quantitative assessment was performed using Image Lab software (Biorad).

2.11. Assessment of Protein Expression by Quantitative Immunofluorescence. Fixed samples were thawed and rehydrated with PBS containing glycine at 50 mM (Sigma-Aldrich) for 10 minutes. Cells were then permeabilized with 0.1% Triton X-100, and nonspecific binding sites were blocked with a blocking buffer (PBS containing 1% bovine serum albumin BSA and 10% serum from the species the secondary antibodies were raised in). Cells were incubated overnight at 4°C with primary antibodies against one of the following targets: vWF (1 : 500 dilution; Dako, Carpentaria, CA), GFAP (1 : 50 dilution; Invitrogen, Carlsbad, CA), MMP3 (1 : 50 dilution; Invitrogen, Carlsbad, CA), or ZO-1 (1 : 50 dilution; Invitrogen, Carlsbad, CA). After incubation with the primary antibodies, the slides were washed and incubated with fluorescent-labeled secondary antibodies (1 : 200 dilution; Invitrogen, Carlsbad, CA) and mounted under glass coverslips with Vectashield-containing DAPI for nuclear identification (Vector Laboratories, Burlingame, CA). Slides were imaged on a fluorescent microscope and analyzed using Image J software. The average maximum intensity was calculated, and this value was used as the measurement threshold. Next, ten fields were selected at random, and the average of the maximum and mean intensities were calculated correcting for the background threshold. Three images per animal were assessed.

2.12. Detection of MMP3 Levels. Both MMP3 serum levels and MMP3 protein expression levels in cultured BMVECs were also determined using a specific ELISA kit by following the manufacturer's instructions (ELISA kit Abcam; ab203363). 50 μL of serum (diluted 100 times) and cell culture supernatants or standards were added together with an antibody cocktail to appropriate wells. After incubating for 1 hour at room temperature on a plate shaker set to 400 rpm, the microplate was washed 3 times. Further, 100 μL of TMB Substrate was added to each well. Finally, the OD was recorded at 450 nm after stopping the reaction by adding 100 μL of Stop Solution.

2.13. Statistical Analysis. All data are shown as the mean ± SD. Data were determined to be normal by the Shapiro-Wilks test, and unpaired *t*-tests were used for comparisons between two groups. For comparisons between multiple groups, a one-way ANOVA with Tukey's multiple comparisons test or a two-way ANOVA with Bonferroni post hoc test were performed depending on the number of experimental variables. A two-tailed *p* value of less than 0.05 was considered statistically significant. Data were visualized and analyzed using SPSS version 17.0 (Armonk, NY) and GraphPad Prism version 8.0.0 (San Diego, CA).

3. Results

3.1. MMP3 Is Highly Expressed in BMVECs. Measurements of MMP3 mRNA (1 vs. 0.117 ± 0.014, $p < 0.0001$; Figure 2(a)) and protein abundance (581.2 ± 25.11 pg/mL vs. 350.7 ± 29.33 pg/mL, $p < 0.0001$; Figure 2(b)) confirmed that the MMP3-KO mutation dramatically reduced MMP3 levels in BMVECs and astrocytes. However, measurements in WT mice indicated that MMP3 expression was significantly higher in BMVECs than in primary astrocytes or in microvascular endothelial cells (MVECs) isolated from the heart, lung, kidney, or spleen (1 vs. 0.111 ± 0.016 vs. 0.037 ± 0.007 vs. 0.404 ± 0.056 vs. 0.058 ± 0.011, $p < 0.0001$) Figure 2(c)), which suggests that MMP3 may have a unique and important role in BMVECs that differs from its roles in ECs from other organs. Thus, we began to investigate

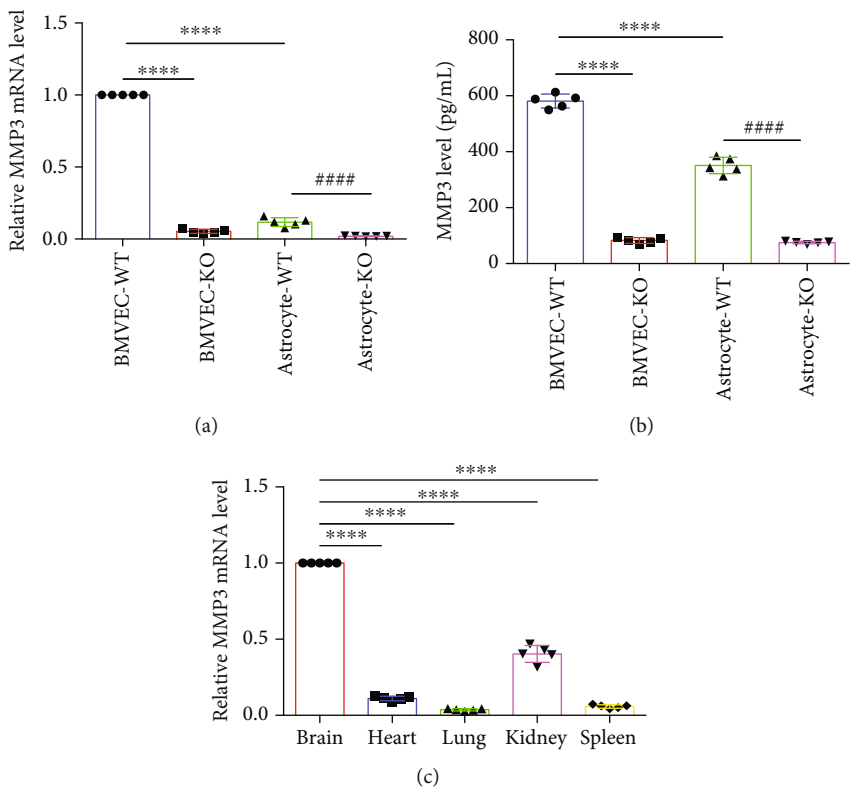

Figure 2: MMP3 is predominantly expressed in BMVECs. (a) MMP3 mRNA abundance was evaluated via q-PCR in BMVECs and astrocytes isolated from the brains of WT (BMVEC-WT and Astrocyte-WT) and MMP3-KO (BMVEC-KO and Astrocyte-KO) mice; results were normalized to measurements in BMVEC-WT. $^{****}p < 0.0001$, $^{\#\#\#\#}p < 0.0001$. (b) MMP3 protein abundance was evaluated via ELISA in culture medium from the indicated cell populations. $^{****}p < 0.0001$, $^{\#\#\#\#}p < 0.0001$. (c) MMP3 mRNA abundance was evaluated in microvascular endothelial cells (MVECs) isolated from the brains, hearts, lungs, kidneys, and spleens of WT mice results were normalized to measurements in brain MVECs. $^{****}p < 0.0001$.

whether MMP3 modulates BBB integrity by monitoring the effect of isoflurane anesthesia in MMP3-KO mice ($n = 8$), in WT mice ($n = 8$) (Figures 3(a) and 3(b)), and in WT mice that had been treated with intravenous injections of recombinant human MMP3 (WT+MMP3; $n = 8$) (bodyweight: 28.73 ± 1.111 g, 28.13 ± 0.75 g, and 28.05 ± 1.09 g, respectively, $n = 8$, $p = 0.352$). Compared to assessments in WT mice, measurements of anesthesia induction time were higher in MMP3-KO mice (3.058 ± 0.088 min vs. 1.598 ± 0.080 min; $p < 0.0001$; Figure 3(c)) and lower in WT +MMP3 mice (1.148 ± 0.104 min vs. 1.598 ± 0.080 min; $p < 0.0001$; Figure 3(c)), anesthesia emergence times were shorter in MMP3-KO mice (0.882 ± 0.073 min vs. 5.233 ± 0.173 min; $p < 0.0001$; Figure 3(d)), and longer in WT + MMP3 mice (11.780 ± 1.883 vs. 5.233 ± 0.173; $p < 0.0001$; Figure 3(d)), and isoflurane usage volumes were larger in MMP3-KO mice (83.750 ± 0.959 mL vs. 63.250 ± 0.700 mL; $p < 0.0001$; Figure 3(e)) and smaller in WT+MMP3 mice (54.630 ± 0.822 mL vs. 63.250 ± 0.700 mL; $p < 0.0001$; Figure 3(e)). Thus, MMP3 appears to increase susceptibility to isoflurane anesthesia.

3.2. MMP3 Promotes BBB Permeability in Mice. To determine whether the relationship between MMP3 expression and isoflurane anesthesia was mediated by changes in BBB permeability, mice were systemically injected with Evans blue dye or sodium-FITC and anesthetized; then, the dyes were cleared from the vessels via saline infusion, and extravasation of the dyes into the brain parenchyma was evaluated [22, 37]. Little evidence of Evans blue extravasation was observed in the brains of MMP3-KO mice, and MMP3 treatment visibly increased the amount of Evans blue in WT mouse brains (Figure 4(a)). Furthermore, both Evans blue (90.796 ± 13.112 μg per gram of tissue vs. 32.009 ± 8.620 μg per gram of tissue; $p < 0.0001$; Figure 4(b)) and sodium-FITC (33.660 ± 8.457 μg per gram of tissue vs. 63.107 ± 6.710 μg per gram of tissue; $p < 0.001$; Figure 4(c)) levels were significantly lower in MMP3-KO mouse brains, and significantly greater in WT+MMP3 mouse brains (180.971 ± 26.829 μg per gram of tissue vs. 90.796 ± 13.112 μg per gram of tissue; $p < 0.001$; 94.111 ± 7.464 μg per gram of tissue vs. 63.107 ± 6.710 μg per gram of tissue; $p < 0.001$; Figures 4(b) and 4(c)), than in the brains of WT mice. Collectively, these observations suggest that MMP3 may regulate BBB permeability.

3.3. MMP3 Regulates the Integrity of BMVEC Monolayers In Vitro. The potential role of MMP3 in BBB permeability was also evaluated *in vitro* by using an electrical cell-substrate impedance sensing system (ECIS 8W10E+ array) to measure

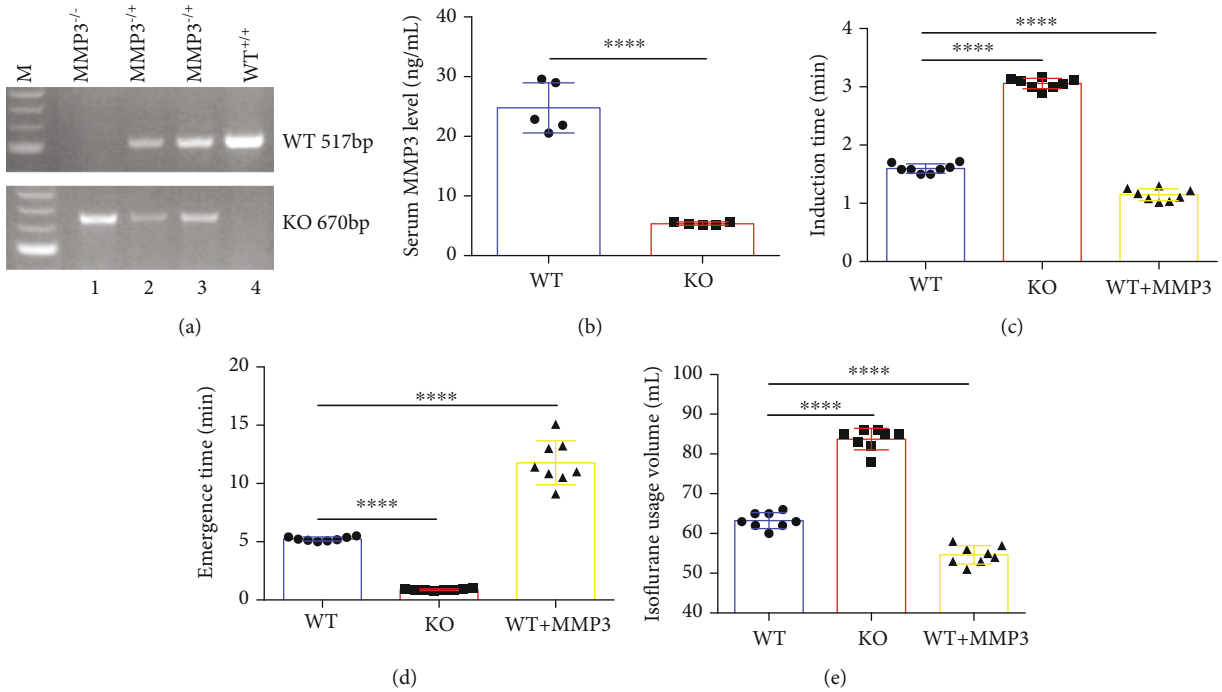

Figure 3: MMP3 enhances the anesthetic effect of isoflurane. (a) The genotypes of WT (WT+/+), heterozygous MMP3-KO (MMP3−/+), and homozygous MMP3-KO (MMP3−/−) mice were confirmed via PCR; the WT and KO alleles were identified with 517-bp and 670-bp fragments, respectively. (b) MMP3 protein abundance was evaluated via ELISA in the serum of WT and homozygous MMP3-KO (KO) mice. $^{****}p < 0.0001$. (c–e) WT mice, MMP3-KO mice, and WT mice treated with MMP3 were anesthetized with inhaled isoflurane, and the (c) time to the onset of anesthesia, (d) time to emergence from anesthesia, and (e) total volume of isoflurane was recorded. $^{****}p < 0.0001$.

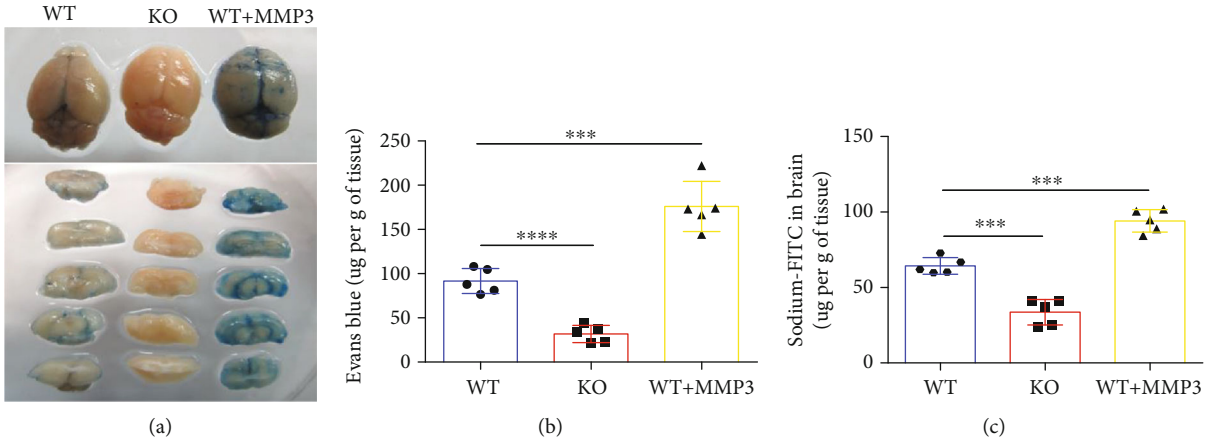

Figure 4: MMP3 increases BBB permeability. (a, b) Evans blue dye was administered via tail-vein intracardial injection to WT mice, MMP3-KO mice (KO), and WT mice that had been treated with MMP3. Two hours later, saline was injected to clear the dye from the vasculature, and the brains were harvested. Extravasation of the dye was evaluated (a) qualitatively in brain images and (b) quantitatively via spectrophotometric measurements of absorbance (632-nm wavelength). Dye quantities were calculated by comparing absorbance measurements to a standard curve. $^{****}p < 0.0001$, $^{***}p < 0.001$. (c) Sodium-FITC was administered via tail-vein injection to mice, and dye extravasation was quantified 2 hours later via fluorescence intensity. Dye quantities were calculated by comparing fluorescence measurements to a standard curve. $^{***}p < 0.001$.

transendothelial electrical resistance (TEER) in monolayers of MMP3-KO or WT BMVECs. Because resistance measurements are inversely correlated with membrane permeability, the significantly lower measurements observed in isoflurane-treated (30 μL/mL) WT cells than in WT cells that had been treated with saline indicated that isoflurane mildly increased BMVEC permeability. Resistance measurements in MMP3-KO BMVECs also declined in response to isoflurane treatment, but not significantly, and measurements were significantly greater in MMP3-KO BMVECs than in WT BMVECs regardless of treatment (Figures 5(a) and 5(b)). Furthermore, resistance measurements in both saline- and

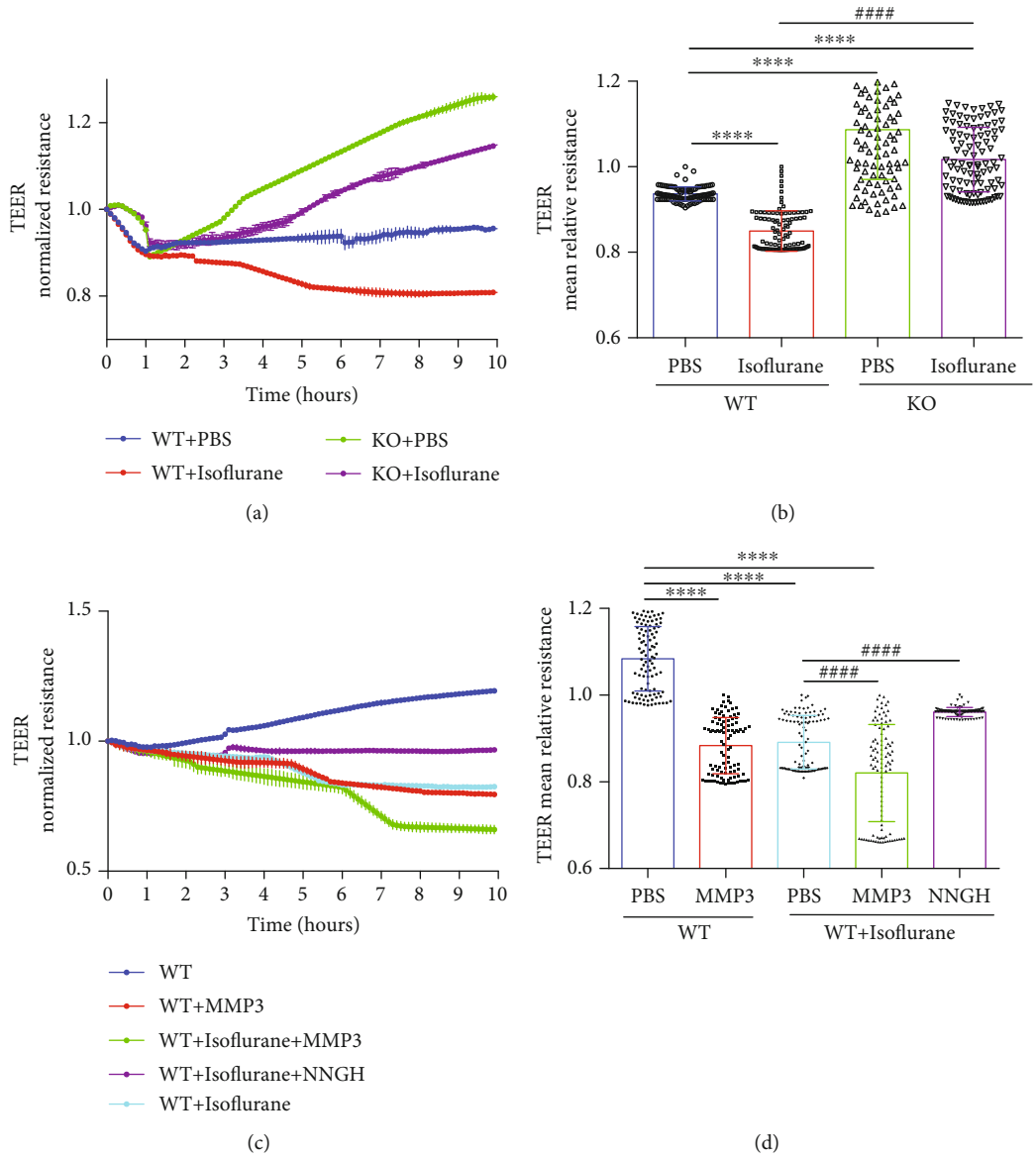

Figure 5: Continued.

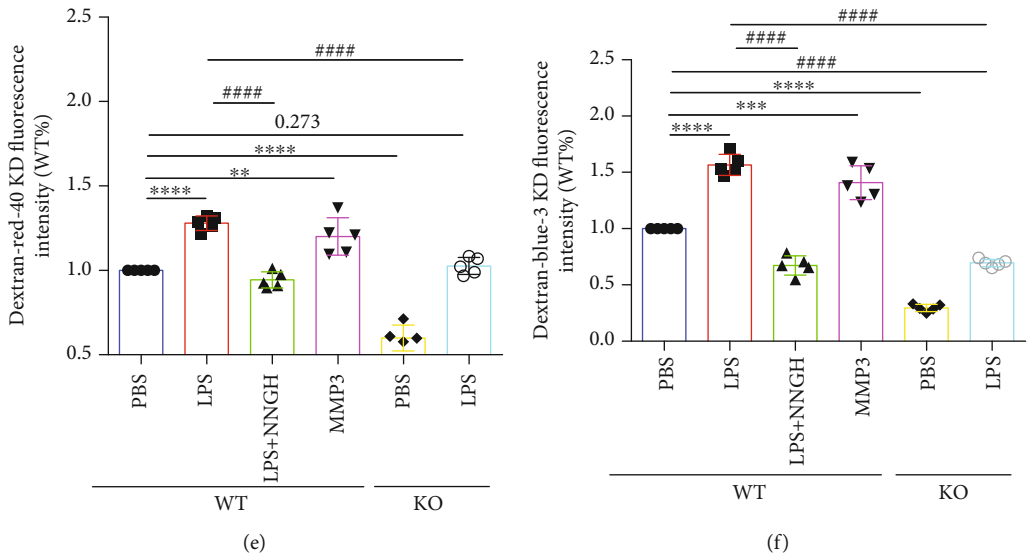

Figure 5: MMP3 reduces the integrity of BMVEC monolayers. (a, c) TEER measurements were recorded in monolayers of WT and MMP3-KO (KO) BMVECs during treatment with the indicated combinations of phosphate-buffered saline (PBS), isoflurane, MMP3, and/or NNGH; treatment was administered one hour after TEER was initiated. (b, d) Endothelial barrier integrity was evaluated by calculating the mean TEER. $^{****}p < 0.0001$, $^{\#\#\#\#}p < 0.0001$. (e, f) WT or MMP3-KO (KO) BMVECs were grown with primary mouse astrocytes in Transwell chambers and treated with PBS, LPS, LPS, and NNGH, or MMP3, as indicated; then, the chambers were suspended in the wells of a 6-well plate, (e) red (40KD) or (f) blue (3KD) FITC-dextran was added to the chamber, and permeability was evaluated 24 hours later by measuring the intensity of dextran fluorescence in the plate wells. $^{****}p < 0.0001$, $^{***}p < 0.001$, $^{**}p < 0.010$, $^{\#\#\#\#}p < 0.0001$. Quantified data are summarized for 5 independent experiments.

isoflurane-treated WT BMVECs declined significantly when the cells were cotreated with activated MMP3 (150 ng/mL) and increased significantly when isoflurane-treated WT BMVECs were cotreated with the MMP3 inhibitor N-isobutyl-N-(4- methoxyphenylsulfonyl)-glycyl hydroxamic acid (NNGH; 25 μM) (Figures 5(c) and 5(d)).

To more accurately mimic *in vivo* conditions, permeability assessments were also conducted with cocultures of freshly isolated mouse BMVECs and primary mouse astrocytes. The cells were grown in Transwell chambers, and the chambers were suspended in the wells of a 6-well plate; then, FITC-dextran (Dextran-blue-3KD and Dextran-red-40KD) was added to the Transwell chamber, and permeability was evaluated by measuring the intensity of dextran fluorescence in the plate wells. Measurements were significantly lower in cocultures with MMP3-KO BMVECs than in cocultures with WT BMVECs and increased significantly in WT BMVEC cocultures after treatment with MMP3. Furthermore, measurements in both WT and MMP3-KO BMVEC cocultures increased significantly after treatment with lipopolysaccharide (LPS; 100 μg/mL), which stimulates MMP3 activity and disrupts the BBB, but remained significantly lower in LPS-treated MMP3-KO cocultures than in LPS-treated WT cocultures, and the LPS-induced increase in permeability observed in WT cocultures was abolished by cotreatment with NNGH (Figures 5(e) and 5(f)). Collectively, the results from both our TEER and Transwell assays suggest that MMP3 increases BMVEC permeability and are consistent with our observations in MMP3-KO, WT, and WT+MMP3 mice.

3.4. MMP3 Regulates the Abundance of TJ Proteins and Adhesion Molecules by Modulating ERK Pathway Activity.

The selective permeability of the BBB is crucially dependent on the formation of tight junctions (TJs) and adherens junctions (AJs) [38]; thus, we investigated whether MMP3 may increase BBB permeability by disrupting expression of the TJ proteins ZO-1, occludin, and claudin-5, as well as the AJ protein vascular endothelial (VE)-cadherin; experiments were conducted with primary BMVECs isolated from the brains of MMP3-KO mice or their WT littermates. Notably, treatment with activated MMP3 did not change MMP3 expression in WT BMVECs; nevertheless, the expression of all four junction proteins was significantly lower in MMP3-treated WT BMVECs and significantly greater in MMP3-KO BMVECs, than in WT BMVECs without MMP3 treatment (Figures 6(a)–6(f)). ZO-1 expression was also evaluated via immunofluorescence in BMVECs that had been incubated with primary ZO-1 antibodies and fluorescent secondary antibodies (Figure 6(g)): measurements of fluorescence intensity declined significantly in WT cells after treatment with MMP3 and was significantly greater in MMP3-KO cells than in WT cells without MMP3 treatment (Figure 6(h)).

The ERK1/2 pathway induces BBB hyperpermeability by changing the composition of TJs [15, 16]; thus, we investigated whether ERK has a role in MMP3-regulated TJ protein expression by comparing measurements in BMVECs treated with saline or an ERK inhibitor. Experiments were conducted with both WT and MMP3-KO BMVECs, and since the expression of MMP3 in WT BMVECs did not change when the cells were treated with recombinant MMP3, MMP3 expression was upregulated via treatment with LPS (100 μg/mL). LPS induced ERK phosphorylation in BMVECs, and induction was prevented by either MMP3 KO or the use of an ERK inhibitor. p-ERK abundance was also lower in all MMP3

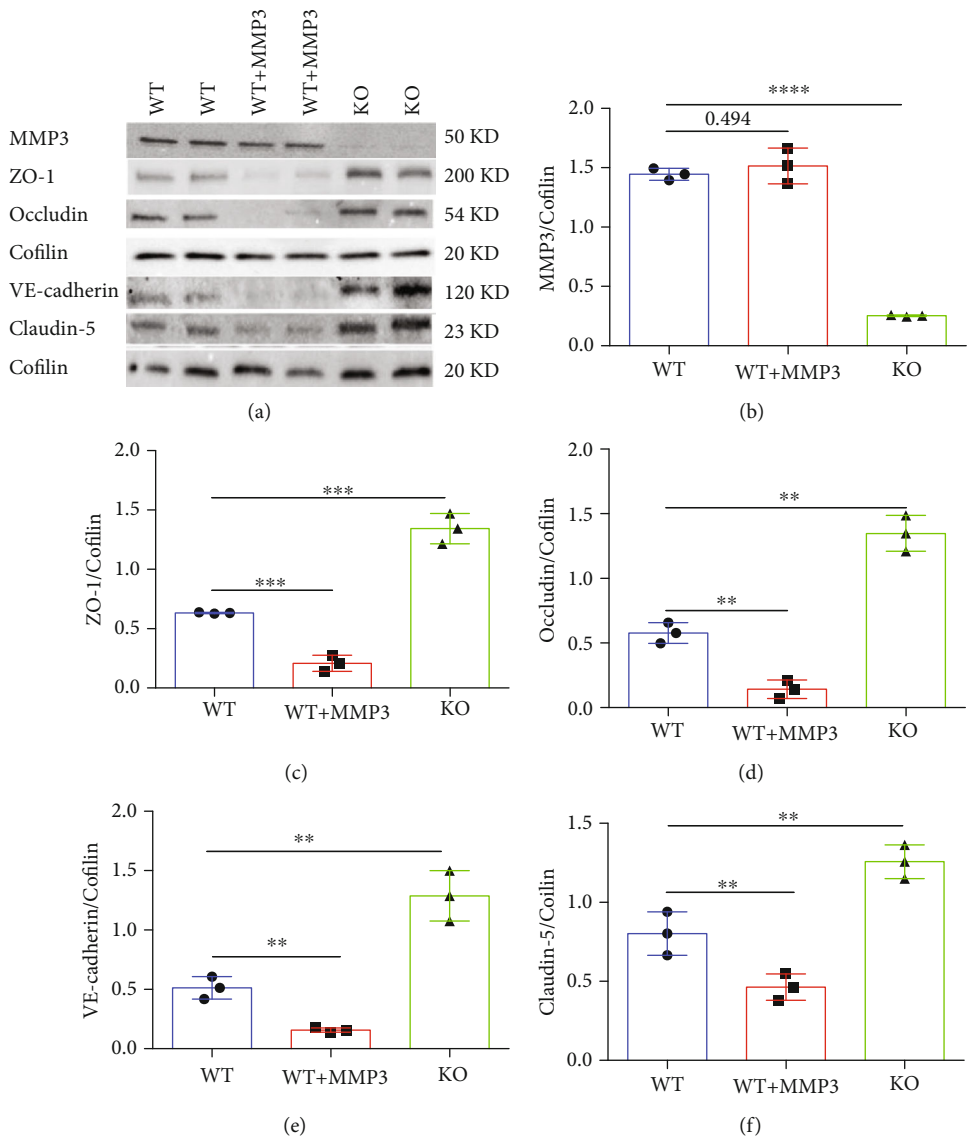

Figure 6: MMP3 regulates the abundance of junction proteins in BMVECs. (a–f) The abundance of MMP3, ZO-1, Occludin, VE-cadherin, and Claudin 5 were (a) evaluated via Western blot in WT BMVECs, WT BMVECs that had been treated with MMP3 (WT+MMP3), and MMP3-KO BMVECs (KO). Cofilin abundance was also evaluated to confirm equal loading, and then (b) MMP3, (c) ZO-1, (d) Occludin, (e) VE-cadherin, and (f) Claudin 5 measurements were quantified via normalization to Cofilin. $^{****}p < 0.0001$, $***p < 0.001$, $^{**}p < 0.010$. (g) WT, WT+MMP3, and MMP3-KO BMVECs were incubated with ZO-1 primary antibodies and fluorescent secondary antibodies (bar = 20 μm), nuclei were counterstained with DAPI, and then (h) ZO-1 abundance was quantified via measurements of fluorescence intensity. $^{****}p < 0.0001$. Quantified data are summarized for 3 experiments.

KO groups than in the WT group, and in WT BMVECs, ERK inhibition did not alter MMP3 expression either with or without concomitant LPS treatment, but measures of TJ protein expression were significantly higher in cells treated with the ERK inhibitor alone or cotreated with the ERK inhibitor and LPS than in the saline-alone or saline-LPS treatment groups, respectively. Neither ERK inhibition nor LPS treatment altered MMP3 expression, ERK activation, or TJ protein expression in MMP3-KO BMVECs, but TJ protein levels were significantly higher than in WT BMVECs (Figures 7(a)–7(f)). Thus, MMP3 appears to reduce the integrity of BMVEC monolayers, at least in part, by upregulating ERK signaling, which subsequently reduces the abundance of junction proteins.

4. Discussion

To the best of our knowledge, the study presented here is the first to demonstrate that MMP3 deficiencies suppress, while treatment with activated MMP3 enhances, isoflurane anesthesia in mice. BBB permeability was also quantified in mouse brains via the extravasation of intravenously administered dyes (Evans blue and sodium FITC) and in monolayers of BMVECs via TEER and Transwell assays: barrier integrity

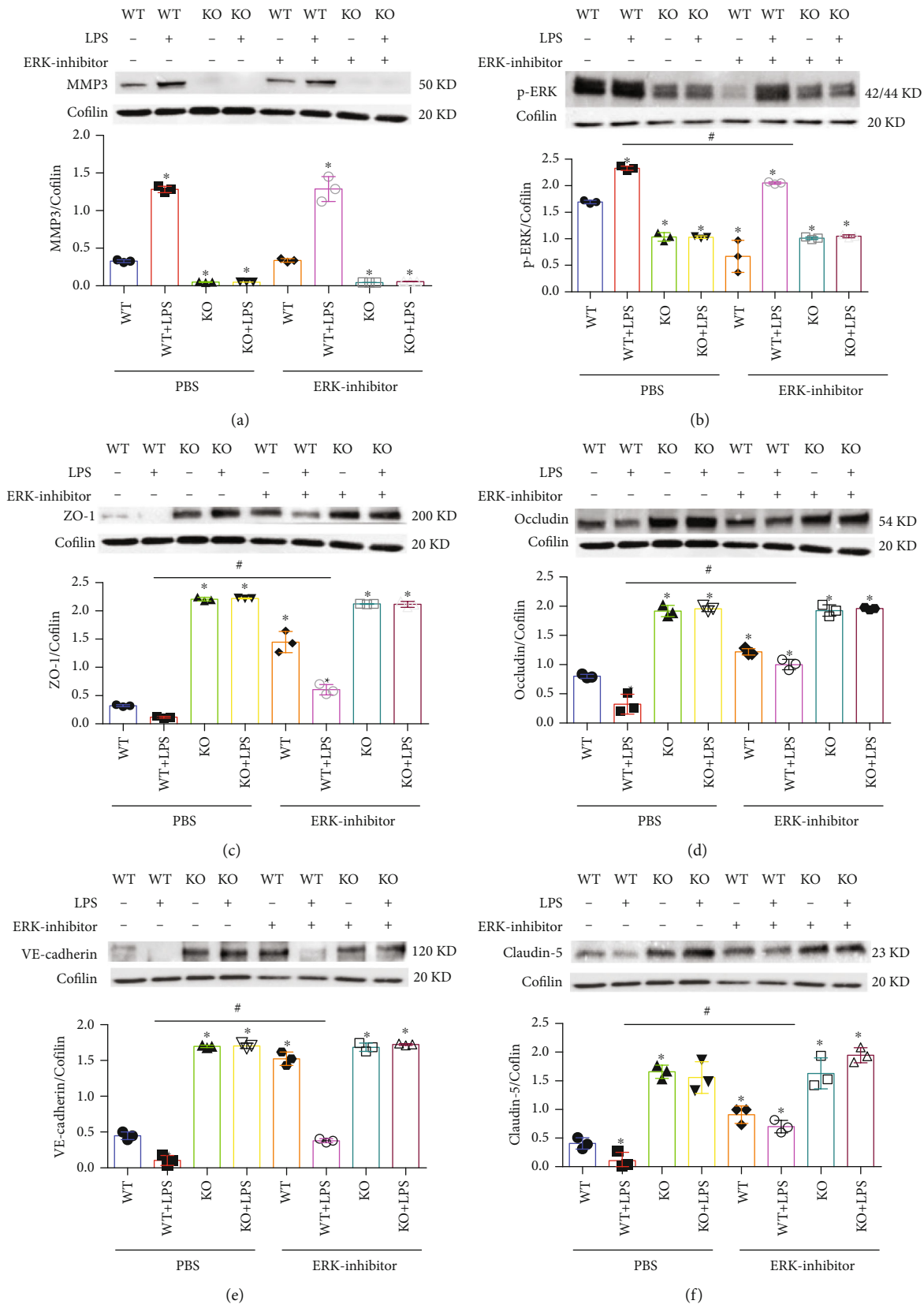

Figure 7: MMP3 regulation of BMVEC junction proteins is mediated by ERK. WT and MMP3-KO (KO) BMVECs were treated with LPS, saline, and/or an ERK inhibitor as indicated; then (a) MMP3, (b) phosphorylated ERK (p-ERK), (c) ZO-1, (d) Occludin, (e) VE-cadherin, and (f) Claudin 5 abundance were evaluated via Western blot and normalized to Cofilin abundance ($^{*}p < 0.001$ vs. WT+PBS in a; $^{*}p < 0.010$ vs. WT+PBS, $^{\#}p < 0.010$ for all other panels (Please verify)). Quantified data are summarized for 3 experiments.

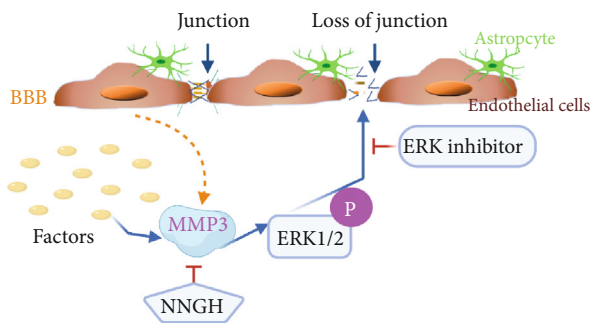

Figure 8: Schematic model for MMP3 regulation of BBB permeability. MMP3 is produced by BMVECs in response to external factors and phosphorylates ERK, which subsequently disrupts tight junctions between adjacent ECs, thereby increasing BBB permeability. BBB integrity can be preserved via ERK inhibition or by blocking MMP3 activity with NNGH.

was significantly greater in the brains of MMP3-KO mice and in monolayers of MMP3-KO BMVECs than in WT mice and WT BMVEC monolayers, respectively, whereas MMP3 upregulation reduced BBB integrity *in vivo* and the integrity of BMVEC monolayers *in vitro*. Notably, isoflurane significantly reduced TEER assessments of integrity in monolayers of WT BMVECs, but not MMP-KO BMVECs, and treatment with MMP3 exaggerated isoflurane-induced BMVEC barrier dysfunction, but not in the presence of NNGH, an MMP3 inhibitor, which suggests that the BBB permeability of isoflurane may also increase in an MMP3-dependent manner. Furthermore, MMP3 activated ERK signaling, and MMP levels were negatively correlated with the abundance of TJ and AJ proteins in BMVECs, but not when the cells were cotreated with an ERK inhibitor. Taken together, the results from our experiments with WT and MMP3-KO mice and BMVECs suggest that MMP3 increases BBB permeability and that this effect may be at least partially mediated by increases in ERK pathway activity and the ERK-induced disruption of inter-EC junctions (Figure 8).

In vivo assessments of MMP activity are technically challenging, which may partially explain why the results from previous investigations of MMPs in endothelial barrier function have been limited and somewhat inconsistent. For example, both MMP2 and MMP9 downregulated ZO-1 expression and enhanced BBB permeability in response to focal cerebral ischemia-reperfusion injury [39], but MMP9 deficiency did not reduce disruption of the BBB during viral encephalomyelitis [40]. The role of MMP3 in BBB maintenance is even less well-studied, but our observation that MMP3 increases BBB permeability by reducing the expression of several junction proteins, including ZO-1, claudin-5, and occludin, is consistent with a previous report that MMP3 disrupts the blood-spinal cord barrier [41]. Furthermore, ERK signaling appears to regulate TJ protein expression in the proximal epididymis of mice [42], and the results reported here indicate that MMP3-induced declines in TJ protein levels are strongly dependent on ERK activation: levels of ERK phosphorylation correlated positively with MMP3 activity and negatively with TJ protein levels, and ERK inhibition increased TJ protein levels in WT BMVEC monolayers, but not in monolayers of MMP3-KO BMVECs. The mechanism that links ERK phosphorylation to the disruption of BBB junctional proteins is unknown but could involve the ubiquitin ligase complex, which targets phosphorylated proteins for degradation [43]; these topics will be addressed in future studies.

MMPs are essential for normal brain function, but elevated levels of MMP expression are believed to contribute to pathological CNS conditions by damaging the neurovascular unit and disrupting the BBB, perhaps via the degradation of TJ and basement-membrane proteins [13, 44]. Oxidative stress is also implicated in activation of MMPs and impaired BBB [45]. Several studies have suggested that MMP2 and MMP9 may contribute to BBB breakdown [13, 17]—for example, MMP9 appears to mediate the loss of TJ stability observed in mice with 1,2-dichloroethane-induced brain edema [46]—and our observation that MMP3 mRNA levels were much higher in BMVECs than in MVECs from other organs (e.g., the heart, lungs, spleen, and kidney) suggests that it may have a unique and essential role in BMVECs, particularly since many of the ECM proteins that form the basal lamina of cerebral blood vessels can be proteolysed by MMP3 [19]. Isoflurane has also been linked to BBB disruption [47, 48], but may protect against acute lung injury by maintaining endothelial barrier integrity [11], so the effect of isoflurane on BBB permeability remains somewhat unclear.

One of the significant findings of this study is that MMP3 was associated with elevated anesthetic sensitivity and BBB opening. Because the BBB is the primary regulator of exchange between the peripheral circulation and the brain, and is the key surface through which systemically administered drugs access the CNS [8], the complexity of the BBB provides many unique opportunities for drug delivery. Thus, our results suggest that MMP3 may be a useful adjunctive treatment for enhancing the efficacy of other neurotherapeutics [49], which could reduce the occurrence and/or severity of side effects (as well as cost) by enabling patients to be treated with lower doses of the primary treatment [35, 50]. However, increases in BBB permeability could also enable blood-borne immune cells to enter the brain and provoke a neuroinflammatory response [51], as illustrated by growing evidence that BBB disruption is associated with brain inflammatory conditions such as Alzheimer's disease and multiple sclerosis [52]. Oxidative stress is also implicated in MMP activation and blood-brain barrier injury [53]. However, despite enormous efforts, CNS drug discovery still relies on improving the BBB, and the success of CNS therapeutic development depends on techniques for modulating BBB permeability and the kinetics of drug distribution to ensure optimal CNS penetration [35].

Unlike other MMPs, MMP3 is predominantly expressed in ECs, and our results indicate that it is more highly expressed in the brain than in other organs; nevertheless, our *in vivo* experiments were conducted with global MMP3-KO mice, so our observations in these animals could have been influenced by the loss of MMP3 expression in non-ECs, as well as BMVECs. Furthermore, since direct MMP3 administration did not increase MMP3 levels in BMVECs,

LPS was used to upregulate MMP3 expression in our in vitro studies and, consequently, we cannot exclude a potentially MMP3-independent role for LPS in TJ stability. Future studies will address these limitations by conducting experiments in EC-specific MMP3-KO mice, by investigating the use of other MMP3 inhibitors, and by determining how LPS regulates MMP3 expression and BBB integrity.

5. Conclusions

In summary, the results presented here are the first to reveal the function of MMP3 in the BBB and suggest that it has an essential role in the brain microvasculature that differs from its function in other vessels. We have shown that MMP3 increases BBB permeability by upregulating the ERK signaling pathway, which subsequently reduces TJ and AJ protein abundance in BMVECs. Oxidative stress often leads to impairment of BBB. Since the BBB is the primary regulator of exchange between the peripheral blood and the brain, our observations likely have important implications for treating neuroinflammatory conditions and other CNS disorders involving the endothelial MMP3 pathway.

Data Availability

Data are available on request.

Conflicts of Interest

The authors declare that there is no conflict of interest regarding the publication of this article.

Authors' Contributions

Qin and Rongxue conceived the study design and wrote the manuscript. Qin performed experiments with assistance from Mei, Cristian, Lifeng, Albert, and Nikola. Qin analyzed the data. Qiong, John, and JK reviewed and contributed to the writing of the manuscript. Rongxue supervised the research. All the authors read and approved the final version of the manuscript.

Funding

Rongxue Wu is supported by 1R01HL140114-01A1. James K. Liao is supported by HL136962.

Acknowledgments

We want to thank Stephanie Besser for careful review of the manuscript and statistical advice and W. Kevin Meisner, PhD, ELS, for editorial assistance. Imaging work was performed at the University of Chicago Integrated Light Microscopy Core Facility, which is supported by Rongxue Wu's CTSA-ITM Core subsidies funding, University of Chicago (through NIH UL1 TR000430). M Manuscript was submitted to Research Square. Rongxue Wu is supported by Chicago DRTC (NIH/P30 DK020595) and CTSA-ITM Core subsidies funding (through NIH UL1 TR000430).

Supplementary Materials

Primary culture and identification of astrocytes. Primary culture and identification of BMVECs. Supplementary results: identification and morphology of primary cultured astrocytes and BMVECs. Supplementary Figure 1. *(Supplementary Materials)*

References

[1] S. Tietz and B. Engelhardt, "Brain barriers: crosstalk between complex tight junctions and adherens junctions," *The Journal of Cell Biology*, vol. 209, no. 4, pp. 493–506, 2015.

[2] E. Dejana, E. Tournier-Lasserve, and B. M. Weinstein, "The control of vascular integrity by endothelial cell junctions: molecular basis and pathological implications," *Developmental Cell*, vol. 16, no. 2, pp. 209–221, 2009.

[3] F. Shimizu, Y. Sano, T. Maeda et al., "Peripheral nerve pericytes originating from the blood-nerve barrier expresses tight junctional molecules and transporters as barrier-forming cells," *Journal of Cellular Physiology*, vol. 217, no. 2, pp. 388–399, 2008.

[4] J. T. Chen, Y. L. Lin, T. L. Chen, Y. T. Tai, C. Y. Chen, and R. M. Chen, "Ketamine alleviates bradykinin-induced disruption of the mouse cerebrovascular endothelial cell-constructed tight junction barrier via a calcium-mediated redistribution of occludin polymerization," *Toxicology*, vol. 368-369, pp. 142–151, 2016.

[5] J. Tian, R. Shi, T. Liu et al., "Brain infection by hepatitis E virus probably via damage of the blood-brain barrier due to alterations of tight junction proteins," *Frontiers in Cellular and Infection Microbiology*, vol. 9, p. 52, 2019.

[6] Z. Maherally, H. L. Fillmore, S. L. Tan et al., "Real-time acquisition of transendothelial electrical resistance in an all-human, in vitro, 3-dimensional, blood-brain barrier model exemplifies tight-junction integrity," *The FASEB Journal*, vol. 32, no. 1, pp. 168–182, 2018.

[7] N. Nathoo, H. Jalal, S. S. Natah, Q. Zhang, Y. Wu, and J. F. Dunn, "Hypoxia and inflammation-induced disruptions of the blood-brain and blood-cerebrospinal fluid barriers assessed using a novel T1-based MRI method," *Acta Neurochirurgica. Supplement*, vol. 121, pp. 23–28, 2016.

[8] B. V. Zlokovic, "The blood-brain barrier in health and chronic neurodegenerative disorders," *Neuron*, vol. 57, no. 2, pp. 178–201, 2008.

[9] A. M. S. Hartz and B. Bauer, "Regulation of ABC transporters at the blood-brain barrier: new targets for CNS therapy," *Molecular Interventions*, vol. 10, no. 5, pp. 293–304, 2010.

[10] B. Dong, Y. Yang, Z. Zhang, K. Xie, L. Su, and Y. Yu, "Hemopexin alleviates cognitive dysfunction after focal cerebral ischemia-reperfusion injury in rats," *BMC Anesthesiology*, vol. 19, no. 1, p. 13, 2019.

[11] J. A. Englert, A. A. Macias, D. Amador-Munoz et al., "Isoflurane ameliorates acute lung injury by preserving epithelial tight junction integrity," *Anesthesiology*, vol. 123, no. 2, pp. 377–388, 2015.

[12] L. Librizzi, F. Noe, A. Vezzani, M. de Curtis, and T. Ravizza, "Seizure-induced brain-borne inflammation sustains seizure recurrence and blood-brain barrier damage," *Annals of Neurology*, vol. 72, no. 1, pp. 82–90, 2012.

[13] P. M. Abdul-Muneer, N. Chandra, and J. Haorah, "Interactions of oxidative stress and neurovascular inflammation in

the pathogenesis of traumatic brain injury," *Molecular Neurobiology*, vol. 51, no. 3, pp. 966–979, 2015.

[14] M. Hisada, M. Hiranuma, M. Nakashima, N. Goda, T. Tenno, and H. Hiroaki, "High dose of baicalin or baicalein can reduce tight junction integrity by partly targeting the first PDZ domain of zonula occludens-1 (ZO-1)," *European Journal of Pharmacology*, vol. 887, p. 173436, 2020.

[15] L. Gonzalez-Mariscal, R. Tapia, and D. Chamorro, "Crosstalk of tight junction components with signaling pathways," *Biochimica et Biophysica Acta (BBA) - Biomembranes*, vol. 1778, no. 3, pp. 729–756, 2008.

[16] L. F. Wang, X. Li, Y. B. Gao et al., "Activation of VEGF/Flk-1-ERK pathway induced blood-brain barrier injury after microwave exposure," *Molecular Neurobiology*, vol. 52, no. 1, pp. 478–491, 2015.

[17] E. Apostolidou, E. Paraskeva, K. Gourgoulianis, P. A. Molyvdas, and C. Hatzoglou, "Matrix metalloproteinases 2 and 9 increase permeability of sheep pleura in vitro," *BMC Physiology*, vol. 12, no. 1, p. 2, 2012.

[18] H. Zhu, R. Dai, Y. Zhou, H. Fu, and Q. Meng, "TLR2 ligand Pam3CSK4 regulates MMP-2/9 expression by MAPK/NF-κB signaling pathways in primary brain microvascular endothelial cells," *Neurochemical Research*, vol. 43, no. 10, pp. 1897–1904, 2018.

[19] E. M. Kim and O. Hwang, "Role of matrix metalloproteinase-3 in neurodegeneration," *Journal of Neurochemistry*, vol. 116, no. 1, pp. 22–32, 2011.

[20] E. I. Eger 2nd, "Current and future perspectives on inhaled anesthetics," *Pharmacotherapy*, vol. 18, no. 5, pp. 895–910, 1998.

[21] J. S. Mudgett, N. I. Hutchinson, N. A. Chartrain et al., "Susceptibility of stromelysin 1-deficient mice to collagen-induced arthritis and cartilage destruction," *Arthritis and Rheumatism*, vol. 41, no. 1, pp. 110–121, 1998.

[22] M. Kaya and B. Ahishali, "Assessment of permeability in barrier type of endothelium in brain using tracers: Evans blue, sodium fluorescein, and horseradish peroxidase," *Methods in Molecular Biology*, vol. 763, pp. 369–382, 2011.

[23] M. Zhang, Y. Xue, H. Chen et al., "Resveratrol inhibits MMP3 and MMP9 expression and secretion by suppressing TLR4/NF-κB/STAT3 activation in Ox-LDL-treated HUVECs," *Oxidative Medicine and Cellular Longevity*, vol. 2019, Article ID 9013169, 15 pages, 2019.

[24] K. Klein, M. Kato, M. Frank-Bertoncelj et al., "Evaluating the bromodomain protein BRD1 as a therapeutic target in rheumatoid arthritis," *Scientific Reports*, vol. 8, no. 1, article 11125, 2018.

[25] M. Ohori, T. Kinoshita, M. Okubo et al., "Identification of a selective ERK inhibitor and structural determination of the inhibitor-ERK2 complex," *Biochemical and Biophysical Research Communications*, vol. 336, no. 1, pp. 357–363, 2005.

[26] H. Vernon, K. Clark, and J. P. Bressler, "In vitro models to study the blood brain barrier," *Methods in Molecular Biology*, vol. 758, pp. 153–168, 2011.

[27] J. O'Callaghan, D. E. Crosbie, P. S. Cassidy et al., "Therapeutic potential of AAV-mediated MMP-3 secretion from corneal endothelium in treating glaucoma," *Human Molecular Genetics*, vol. 26, no. 7, pp. 1230–1246, 2017.

[28] E. N. Spoelstra, C. Ince, A. Koeman et al., "A novel and simple method for endotracheal intubation of mice," *Laboratory Animals*, vol. 41, no. 1, pp. 128–135, 2016.

[29] M. Kumar, N. Tyagi, K. S. Moshal et al., "$GABA_A$ receptor agonist mitigates homocysteine-induced cerebrovascular remodeling in knockout mice," *Brain Research*, vol. 1221, pp. 147–153, 2008.

[30] A. Mujagic, A. Marushima, Y. Nagasaki et al., "Antioxidant nanomedicine with cytoplasmic distribution in neuronal cells shows superior neurovascular protection properties," *Brain Research*, vol. 1743, article 146922, 2020.

[31] C. Gurses, O. Ekizoglu, N. Orhan et al., "Levetiracetam decreases the seizure activity and blood-brain barrier permeability in pentylenetetrazole-kindled rats with cortical dysplasia," *Brain Research*, vol. 1281, pp. 71–83, 2009.

[32] R. Szulcek, H. J. Bogaard, and G. P. van Nieuw Amerongen, "Electric cell-substrate impedance sensing for the quantification of endothelial proliferation, barrier function, and motility," *Journal of Visualized Experiments*, no. 85, 2014.

[33] Y. Ke, O. V. Oskolkova, N. Sarich et al., "Effects of prostaglandin lipid mediators on agonist-induced lung endothelial permeability and inflammation," *American Journal of Physiology-Lung Cellular and Molecular Physiology*, vol. 313, no. 4, pp. L710–L721, 2017.

[34] Y. Wang, N. Wang, B. Cai, G. Y. Wang, J. Li, and X. X. Piao, "In vitro model of the blood-brain barrier established by co-culture of primary cerebral microvascular endothelial and astrocyte cells," *Neural Regeneration Research*, vol. 10, no. 12, pp. 2011–2017, 2015.

[35] A. Ben-Zvi, B. Lacoste, E. Kur et al., "Mfsd2a is critical for the formation and function of the blood-brain barrier," *Nature*, vol. 509, no. 7501, pp. 507–511, 2014.

[36] R. Wu, H. C. Chang, A. Khechaduri et al., "Cardiac-specific ablation of ARNT leads to lipotoxicity and cardiomyopathy," *The Journal of Clinical Investigation*, vol. 124, no. 11, pp. 4795–4806, 2014.

[37] M. Spatz and I. Klatzo, "Pathological aspects of brain transport phenomena," *Advances in Experimental Medicine and Biology*, vol. 69, pp. 479–495, 1976.

[38] L. Cucullo, M. Hossain, V. Puvenna, N. Marchi, and D. Janigro, "The role of shear stress in blood-brain barrier endothelial physiology," *BMC Neuroscience*, vol. 12, no. 1, p. 40, 2011.

[39] Y. Gu, G. Zheng, M. Xu et al., "Caveolin-1 regulates nitric oxide-mediated matrix metalloproteinases activity and blood-brain barrier permeability in focal cerebral ischemia and reperfusion injury," *Journal of Neurochemistry*, vol. 120, no. 1, pp. 147–156, 2012.

[40] C. Savarin, S. A. Stohlman, A. M. Rietsch, N. Butchi, R. M. Ransohoff, and C. C. Bergmann, "MMP9 deficiency does not decrease blood-brain barrier disruption, but increases astrocyte MMP3 expression during viral encephalomyelitis," *Glia*, vol. 59, no. 11, pp. 1770–1781, 2011.

[41] J. Y. Lee, H. Y. Choi, H. J. Ahn, B. G. Ju, and T. Y. Yune, "Matrix metalloproteinase-3 promotes early blood-spinal cord barrier disruption and hemorrhage and impairs long-term neurological recovery after spinal cord injury," *The American Journal of Pathology*, vol. 184, no. 11, pp. 2985–3000, 2014.

[42] B. Kim and S. Breton, "The MAPK/ERK-signaling pathway regulates the expression and distribution of tight junction proteins in the mouse proximal epididymis," *Biology of Reproduction*, vol. 94, no. 1, p. 22, 2016.

[43] J. Zhao, J. Wei, R. Mialki, C. Zou, R. K. Mallampalli, and Y. Zhao, "Extracellular signal-regulated kinase (ERK) regulates

cortactin ubiquitination and degradation in lung epithelial cells," *The Journal of Biological Chemistry*, vol. 287, no. 23, pp. 19105–19114, 2012.

[44] Y. Yang and G. A. Rosenberg, "Matrix metalloproteinases as therapeutic targets for stroke," *Brain Research*, vol. 1623, pp. 30–38, 2015.

[45] P. J. Kelly, J. D. Morrow, M. Ning et al., "Oxidative stress and matrix metalloproteinase-9 in acute ischemic stroke: the Biomarker Evaluation for Antioxidant Therapies in Stroke (BEAT-Stroke) study," *Stroke*, vol. 39, no. 1, pp. 100–104, 2008.

[46] X. Jin, T. Wang, Y. Liao et al., "Neuroinflammatory reactions in the brain of 1,2-DCE-intoxicated mice during brain edema," *Cell*, vol. 8, no. 9, p. 987, 2019.

[47] N. K. Acharya, E. L. Goldwaser, M. M. Forsberg et al., "Sevoflurane and isoflurane induce structural changes in brain vascular endothelial cells and increase blood–brain barrier permeability: possible link to postoperative delirium and cognitive decline," *Brain Research*, vol. 1620, pp. 29–41, 2015.

[48] Y. Cao, C. Ni, Z. Li et al., "Isoflurane anesthesia results in reversible ultrastructure and occludin tight junction protein expression changes in hippocampal blood-brain barrier in aged rats," *Neuroscience Letters*, vol. 587, pp. 51–56, 2015.

[49] C. Betsholtz, "Double function at the blood-brain barrier," *Nature*, vol. 509, no. 7501, pp. 432-433, 2014.

[50] L. N. Nguyen, D. Ma, G. Shui et al., "Mfsd2a is a transporter for the essential omega-3 fatty acid docosahexaenoic acid," *Nature*, vol. 509, no. 7501, pp. 503–506, 2014.

[51] H. Chen and E. E. Konofagou, "The size of blood-brain barrier opening induced by focused ultrasound is dictated by the acoustic pressure," *Journal of Cerebral Blood Flow and Metabolism*, vol. 34, no. 7, pp. 1197–1204, 2014.

[52] J. P. Patel and B. N. Frey, "Disruption in the blood-brain barrier: the missing link between brain and body inflammation in bipolar disorder?," *Neural Plasticity*, vol. 2015, Article ID 708306, 12 pages, 2015.

[53] C. Lehner, R. Gehwolf, H. Tempfer et al., "Oxidative stress and blood-brain barrier dysfunction under particular consideration of matrix metalloproteinases," *Antioxidants & Redox Signaling*, vol. 15, no. 5, pp. 1305–1323, 2011.

Hindawi
Oxidative Medicine and Cellular Longevity
Volume 2021, Article ID 9875639, 9 pages
https://doi.org/10.1155/2021/9875639

Research Article

Redox Imbalance Associates with Clinical Worsening in Spinocerebellar Ataxia Type 2

Almaguer-Gotay Dennis,[1,2] Luis E. Almaguer-Mederos,[1,2] Rodríguez-Aguilera Raúl,[1,2] Rodríguez-Labrada Roberto,[1] Velázquez-Pérez Luis,[1,3] Cuello-Almarales Dany,[1,2] González-Zaldívar Yanetza,[1,2] Vázquez-Mojena Yaimeé,[1] Estupiñán-Domínguez Annelié,[1] Peña-Acosta Arnoy,[1] and Torres-Vega Reydenis[1]

[1]*Center for the Investigation and Rehabilitation of Hereditary Ataxias (CIRAH), Holguín, Cuba*
[2]*University of Medical Sciences of Holguín, Cuba*
[3]*Cuban Academy of Sciences, Cuba*

Correspondence should be addressed to Almaguer-Gotay Dennis; dennisalmaguer@gmail.com

Received 28 July 2020; Revised 24 December 2020; Accepted 5 February 2021; Published 22 February 2021

Academic Editor: Kambiz Hassanzadeh

Background. Spinocerebellar ataxia type 2 (SCA2) is a neurodegenerative disease presenting with redox imbalance. However, the nature and implications of redox imbalance in SCA2 physiopathology have not been fully understood. *Objective*. The objective of this study is to assess the redox imbalance and its association with disease severity in SCA2 mutation carriers. *Methods*. A case-control study was conducted involving molecularly confirmed SCA2 patients, presymptomatic individuals, and healthy controls. Several antioxidant parameters were assessed, including serum thiol concentration and the superoxide dismutase, catalase, and glutathione S-transferase enzymatic activities. Also, several prooxidant parameters were evaluated, including thiobarbituric acid-reactive species and protein carbonyl concentrations. Damage, protective, and OXY scores were computed. Clinical correlates were established. *Results*. Significant differences were found between comparison groups for redox markers, including protein carbonyl concentration ($F = 3.30$; $p = 0.041$), glutathione S-transferase activity ($F = 4.88$; $p = 0.009$), and damage ($F = 3.20$; $p = 0.045$), protection ($F = 12.75$; $p < 0.001$), and OXY ($F = 7.29$; $p = 0.001$) scores. Protein carbonyl concentration was positively correlated with CAG repeat length ($r = 0.27$; $p = 0.022$), while both protein carbonyl concentration ($r = -0.27$; $p = 0.018$) and OXY score ($r = -0.25$; $p = 0.013$) were inversely correlated to the disease duration. Increasing levels of antioxidants and decreasing levels of prooxidant parameters were associated with clinical worsening. *Conclusions*. There is a disruption of redox balance in SCA2 mutation carriers which depends on the disease stage. Besides, redox changes associate with markers of disease severity, suggesting a link between disruption of redox balance and SCA2 physiopathology.

1. Introduction

Spinocerebellar ataxias (SCAs) are a heterogeneous group of neurodegenerative diseases characterized by progressive neuronal loss and shared clinical manifestations, including gait ataxia, dysmetria, dysarthria, and adiadochokinesia [1]. To date, 48 molecular variants of SCAs have been reported [2]. In particular, spinocerebellar ataxia type 2 (SCA2) is due to a CAG repeat expansion mutation in the *ATXN2* gene and it reaches the highest worldwide prevalence in Holguín province, Cuba [3].

SCA2 is a polyglutamine disorder causing neurodegeneration at different levels, including cerebellar Purkinje cells, thalamic and cholinergic basal forebrain neurons, brainstem pontine, and olivary neurons, spinal and cortical motor neurons, as a result of mutant Ataxin-2 expression [4]. However, the primary mechanisms by which the polyQ expansion in Ataxin-2 causes SCA2 remain unknown. Nonetheless,

evidence shows the occurrence of cytoplasmic aggregation of mutant Ataxin-2 [5], disturbed RNA metabolism [6, 7], dysregulation of calcium homeostasis [8, 9], altered methylation patterns in the *ATXN2* promoter [10], and oxidative stress as part of SCA2 physiopathology.

Oxidative stress was initially defined as "a disturbance in the prooxidant-antioxidant balance in favor of the former" and more recently as "a disruption of redox signaling and control" [11–14]. Enzymes like superoxide dismutase (SOD), catalase (CAT), and glutathione S-transferases (GSTs), or thiols as reduced glutathione (GSH), are part of the main antioxidant systems minimizing the damage caused by free radicals on lipids and proteins and regulate the cellular redox state [11, 12]. Oxidative stress has been linked to neurodegenerative disorders, including Alzheimer's disease (AD), Parkinson's disease (PD), amyotrophic lateral sclerosis (ALS), Huntington's disease (HD), and spinocerebellar ataxias [15–18].

Opposite to oxidative stress, the concept of "reductive stress" refers to a redox condition characterized by an abnormal increase in the levels of reducing agents in the forms of NADH, NADPH, and GSH and associated with increased mitochondrial oxidation and cytotoxicity [19]. Reductive stress has been poorly studied in the context of neurodegenerative disorders; however, evidence supporting its occurrence was gathered in young healthy individuals at risk of Alzheimer's disease [20] and in cellular and *Drosophila* models for Huntington's disease [21].

Few studies have shown the occurrence of redox imbalance in SCA2 patients. Indeed, increased levels of malondialdehyde (a product of lipids' oxidative damage), increased GST activity [22, 23], and decreased extracellular superoxide dismutase activity [24], were reported in SCA2 patients' blood serum. Besides, increased mitochondrial superoxide dismutase and decreased catalase expression were found in SCA2 patients' fibroblasts [25].

Even though evidence supporting the occurrence of redox imbalance in SCA2 was collected, its nature and implications in disease physiopathology have not been fully understood. Hence, the present study is aimed at assessing the redox imbalance and its association with disease severity in SCA2 mutation carriers by examining antioxidant and prooxidant parameters in a large sample of SCA2 patients and presymptomatic individuals.

2. Materials and Methods

2.1. Reagents. Pyrogallol (Alfa Aesar Co., Ward Hill, MA 01835, USA), hydrogen peroxide (H_2O_2) (Sigma-Aldrich, St. Louis, MO 63103, USA), 1-chloro-2,4-dinitrobenzene (Alfa Aesar, Ward Hill, MA 01835, USA), reduced glutathione (GSH) (Sigma-Aldrich, St. Louis, MO 63103, USA), 1,1,3,3-tetraethoxypropane (Sigma-Aldrich, St. Louis, MO 63103, USA), and bovine albumin (Calbiochem, San Diego, CA 92121, USA).

2.2. The Study Design. A case-control study was conducted to assess the redox status in SCA2 patients and presymptomatic individuals. Thirty-six molecularly confirmed SCA2 patients with mild to moderate clinical presentation (M/F: 4/32; aged 25 to 65 years) were recruited at the Center for the Investigation and Rehabilitation of Hereditary Ataxias, Holguín, Cuba. SCA2 patients were matched by age and gender with 36 presymptomatic individuals (mutation carriers with no clinical presentation at the time of the study) (M/F: 4/32; aged 23 to 66 years) and an equal number of healthy control individuals (M/F: 3/33; aged 23 to 65 years). To further verify differences between patients and controls regarding redox parameters, a data set consisting of 60 molecularly confirmed SCA2 patients (M/F: 27/33; aged 22 to 68 years) and 60 control individuals (M/F: 27/33; aged 23 to 70 years) matched by age and gender were assessed. A maximal age difference of two years between patients and presymptomatic and control individuals was allowed.

To assess the relationships between redox parameters, CAG repeat length, and clinical and neurophysiological variables, the sample of SCA2 patients was enlarged to one hundred (M/F: 48/52; aged 19 to 68 years). The study was approved by the institutional ethics committee, and it was conducted according to the Declaration of Helsinki. Written informed consent was obtained from all participants after a complete description of the study.

2.3. Clinical, Neurophysiological, and Genetic Assessment. The clinical diagnosis was based on the identification of gait ataxia, dysarthria, dysmetria, and dysdiadochokinesia and the slowing of saccade eye movements. Age at onset (AO) was defined as the onset of motor impairment. Disease duration (DD) was defined as the time elapsed between the clinical debut and the time when the neurological evaluation was made. Clinical severity was estimated by using the scale for the assessment and rating of ataxia (SARA) score [26]. The progression rate was calculated as the rate between the SARA score and age. Maximal saccade velocity (MSV) (in 60°/second) and saccade latency (SL) (in milliseconds) were determined as previously reported [27]. The mean estimated age at onset of the presymptomatic group was calculated with the individuals' current age and CAG repeat length at the *ATXN2* locus, as previously reported [28]. Predicted time to onset (in years) was calculated with the formula [predicted age of onset − current age]. The CAG repeat length at the *ATXN2* locus was determined by polymerase chain reaction (PCR) followed by polyacrylamide gel electrophoresis as previously reported [29].

2.4. Blood Sample Collection. Fasting blood samples were collected from subjects by venipuncture at the time when neurological and neurophysiological evaluations were made. Serum was obtained *via* blood centrifugation at 3,000 rpm at 4°C for 10 minutes, frozen immediately, and stored at −20°C until biochemical analysis.

2.5. Assessment of Antioxidant Biomarkers in Blood Serum. SOD3 and CAT enzymatic activities were measured at 37°C, following standard methods based on the use of pyrogallol and H_2O_2 as substrates [30, 31]. GST activity was measured at 37°C, following the Habig and Jacoby method, using 1-chloro-2,4-dinitrobenzene and GSH as substrates

[32]. Reducing thiol (R-SH) total concentration was assessed at 25°C, following the Ellman protocol [33].

2.6. Assessment of Oxidative Modification on Lipids and Proteins. Thiobarbituric acid-reactive species (TBARS) and protein carbonyl (PC) concentration were assessed in blood serum following Yagi [34] and Levine [35] standard methods.

All samples were assayed in triplicate using a BioMate 3 Spectrophotometer (Thermo Spectronic Company, USA).

2.7. Redox Global Index Computation. The damage score (DS), protection score (PS), and OXY score were computed following a modified procedure to that reported by Veglia et al. [36]. The DS was computed with a base on log-transformed TBARS and PC concentrations; meanwhile, the PS was computed with a base on log-transformed SOD3, CAT, and GST enzymatic activities and R-SH concentrations. Individual redox parameters were standardized following Veglia et al. [36]. The OXY score was computed as the difference between DS and PS, reflecting the balance between oxidants and antioxidants.

2.8. Statistical Analysis. Descriptive statistics were used to assess central tendencies and dispersion of data. The Kolmogorov-Smirnov test was used to assess the normality of data distribution. The chi-square test (χ^2) was used to establish comparisons between patients, presymptomatic individuals, and controls for gender. One-way ANOVA was utilized to assess differences between comparison groups for age and redox parameters. Tukey's post-hoc test was applied to identify differences between comparison groups. Student's *t*-test was used to compare redox parameters between patients and controls.

Pearson's correlation test was utilized to assess the relationship between redox parameters, clinical and neurophysiological variables, and CAG repeat length. Correction for repeat length or disease duration was applied to redox and clinical variables by simple or multiple linear regression analyses. Statistical significance was defined as $p \leq 0.05$.

Type-I error in multiple comparisons was adjusted by the Benjamini-Hochberg (BH) method for controlling the false discovery rate [37]. Analyses were performed using the commercially available Statistica software package (StatSoft Inc., 2003 Statistica data analysis software system, version 6. http://www.statsoft.com).

3. Results

3.1. Redox Balance in SCA2 Mutation Carriers. To know if redox disturbances are present in SCA2 mutation carriers and to determine if these disturbances take place since the presymptomatic stage of the disease, comparisons for redox parameters were established between affected SCA2 patients and presymptomatic and control individuals. No significant differences were found between comparison groups for gender ($\chi^2 = 0.20$; $p = 0.904$) or age distributions ($F = 0.656$, $p = 0.521$). Also, no significant associations were found between age or gender and redox parameters in the comparison groups ($p > 0.05$).

There was no significant difference between SCA2 patients and presymptomatic and control individuals regarding SOD3 or CAT activities, SOD3/CAT index, R-SH, or TBARS concentrations. However, there were significant differences in GST activity, protein carbonyl concentration, damage score, and protective and OXY scores (Table 1). Nonetheless, only GST activity and protective and OXY scores remained significant after adjustment for multiple comparisons.

Post-hoc analyses showed significant decreases in GST activity and protection score and significant increases in protein carbonyl concentration and OXY score in presymptomatic individuals relative to affected patients. A significant decrease in the protection score was found in presymptomatic individuals relative to control individuals, and a significant decrease in the damage score was found in patients relative to control individuals (Figure 1). After correction for multiple comparisons, only the difference between presymptomatic individuals and affected patients relative to protein carbonyl concentration and the decrease in the damage score between patients and control individuals lost their statistical significance.

In the enlarged data consisting of 60 patients and 60 control subjects, significant decreases in the protein carbonyl concentration ($t = -3.44$; $p < 0.001$), damage score ($t = -3.15$; $p = 0.002$), and the OXY score ($t = -2.55$; $p = 0.012$) were found in patients relative to control individuals. These differences remained significant after adjustment for multiple comparisons.

3.2. Associations between Redox Parameters, CAG Repeat Length, and Clinical Biomarkers in SCA2 Mutation Carriers. Taking into account that the CAG repeat length in the *ATXN2* gene is the major determinant of clinical severity in SCA2, correlations were established between CAG repeat length and redox parameters in presymptomatic individuals and the enlarged sample of one hundred SCA2 patients. Besides, the relevance of redox parameters to clinical severity was assessed.

In presymptomatic individuals, a highly significant negative correlation between time to onset and repeat length ($r = -0.48$; $p = 0.005$) was found. However, no significant correlation was obtained between repeat length and redox parameters ($p > 0.05$). As expected, in the enlarged sample of one hundred SCA2 patients, the age at onset showed a highly significant negative correlation with the repeat length ($r = -0.73$; $p < 0.001$), and the SARA score was significantly correlated to the disease duration ($r = 0.57$; $p < 0.001$) and repeat length ($r = 0.21$; $p = 0.038$). Also, the progression rate showed significant correlations with repeat length ($r = 0.71$; $p < 0.001$) and disease duration ($r = 0.23$; $p = 0.022$). Besides, saccade velocity was significantly correlated to repeat length ($r = -0.46$; $p < 0.001$). Nonetheless, saccade latency showed no significant correlations with repeat length or disease duration.

On correlation analysis, the repeat length showed a significant association only with protein carbonyl concentration. Similarly, the disease duration showed significant negative correlations with protein carbonyl concentrations and OXY score (Figure 2).

Table 1: Comparison of redox parameters between SCA2 mutation carriers and control individuals.

Redox parameters	Controls ($n = 36$)		Presymptomatics ($n = 36$)		Patients ($n = 36$)		F	p
	Mean	SD	Mean	SD	Mean	SD		
SOD3 (KU/L)	2.02	0.52	1.85	0.46	1.99	0.38	1.46	0.238
CAT (KUI/L)	19.14	8.74	15.48	7.68	20.00	13.81	1.91	0.153
CAT/SOD3	9.97	5.46	9.30	6.39	10.35	6.86	0.26	0.773
GST (UI/L)	14.00	4.73	11.54	5.08	15.09	4.98	4.88	*0.009*
R-SH (μmol/L)	136.92	71.29	105.09	43.30	124.32	63.17	2.54	0.084
TBARS (μmol/L)	2.17	0.72	1.90	0.72	1.97	1.07	0.88	0.420
PC (nmol/mg)	1.65	0.43	1.74	0.41	1.48	0.43	3.30	*0.041*
DS	0.03	0.74	−0.11	0.83	−0.44	0.86	3.20	*0.045*
PS	−0.01	0.51	−0.49	0.50	0.01	0.41	12.75	*<0.001*
OXY score	0.04	0.97	0.38	0.87	−0.46	0.97	7.29	*0.001*

SOD3: superoxide dismutase activity; CAT: catalase activity; GST: glutathione S-transferase activity; R-SH: reducing thiol total concentration; TBARS: thiobarbituric acid-reactive species; PC: protein carbonyl concentration; DS: damage score; PS: protection score; SD: standard deviation.

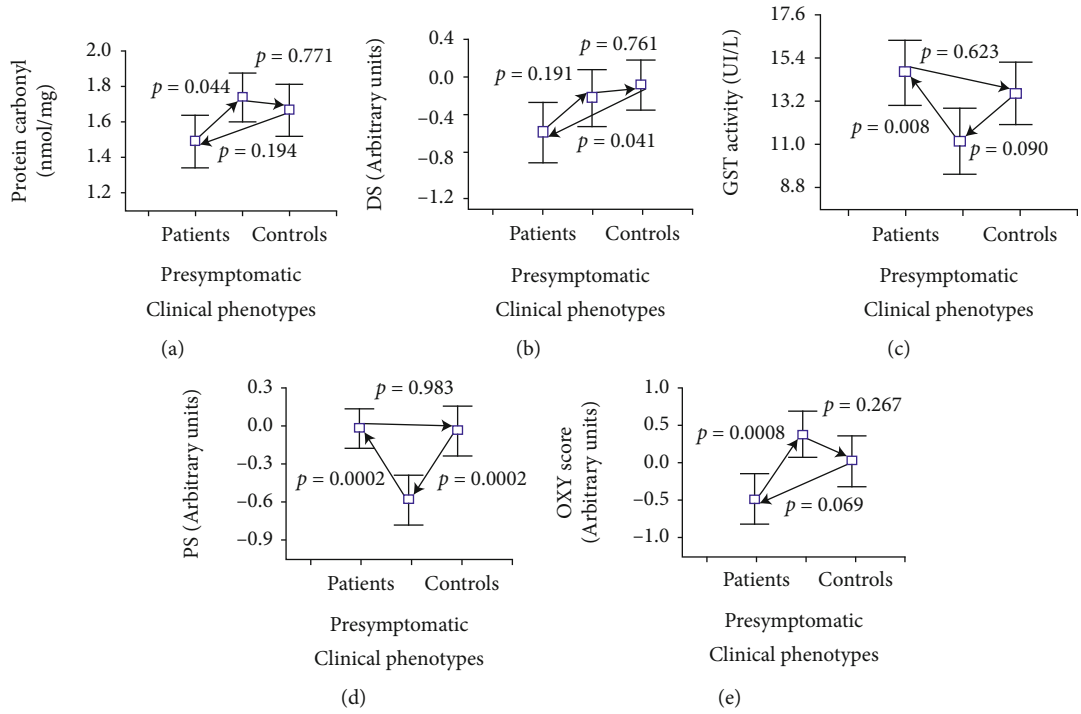

Figure 1: Post-hoc analyses for comparison of redox parameters between SCA2 mutation carriers and control individuals. DS: damage score; PS: protection score.

Significant effects were obtained for the repeat length ($\beta = 0.283$, SE = 0.11; $p = 0.012$) and disease duration ($\beta = -0.280$, SE = 0.11; $p = 0.014$) on protein carbonyl concentration by multiple linear regression analysis ($R = 0.387$; $p = 0.003$). Besides, significant effects were obtained for the repeat length ($\beta = 0.268$, SE = 0.10; $p = 0.009$) and disease duration ($\beta = -0.240$, SE = 0.10; $p = 0.019$) on the OXY score ($R = 0.357$; $p = 0.003$).

Regarding the associations between redox parameters and clinical biomarkers, the time to onset in presymptomatic individuals showed significant correlations with R-SH ($r = 0.41$; $p = 0.025$) and protein carbonyl concentration ($r = 0.35$; $p = 0.049$). However, after correction for repeat length, only the association with protein carbonyl concentration remained significant. Also, a correlation of marginal significance was obtained for the damage score (Table 2).

In affected patients, there was no significant correlation between the age at onset and redox parameters. Nonetheless, after correction for repeat length, the age at onset showed significant negative correlations with R-SH concentration and the protection score. Corrected age at onset also showed significant positive correlations with protein carbonyl concentration and the OXY score (Table 2).

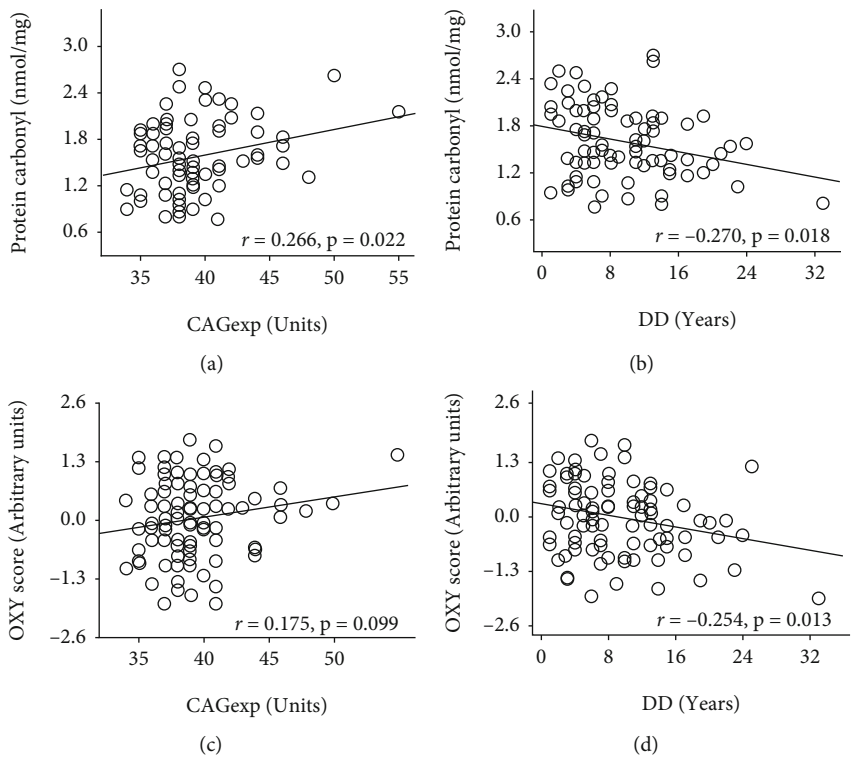

Figure 2: Correlation analyses for redox parameters, repeat length, and disease duration. CAGexp: CAG repeat length in ATXN2 expanded alleles; DD: disease duration.

Table 2: Correlation analyses for redox and clinical parameters.

Redox/clinical parameters	Correlation coefficient (p level)					
	TTO✦	AO✦	SARA score◊	PR◊	Sac. veloc.✦	Sac. lat.
SOD3	−0.04 (0.811)	−0.04 (0.714)	0.09 (0.428)	0.10 (0.358)	−0.031 (0.824)	0.15 (0.294)
CAT	−0.06 (0.751)	−0.07 (0.504)	0.44 (*<0.001*)	0.50 (*<0.001*)	-0.31 (*0.025*)	0.31 (*0.022*)
CAT/SOD3	0.08 (0.650)	−0.06 (0.574)	0.34 (*0.002*)	0.38 (*<0.001*)	−0.21 (0.127)	0.14 (0.303)
GST	−0.03 (0.885)	−0.09 (0.407)	0.25 (*0.017*)	0.21 (0.051)	0.17 (0.221)	−0.16 (0.249)
R-SH	0.28 (0.131)	−0.23 (*0.027*)	0.07 (0.493)	0.17 (0.112)	−0.26 (0.060)	0.21 (0.122)
TBARS	−0.18 (0.347)	0.07 (0.510)	−0.19 (0.083)	−0.16 (0.16)	−0.05 (0.742)	0.06 (0.653)
PC	−0.43 (*0.014*)	0.29 (*0.013*)	−0.20 (0.094)	−0.25 (*0.033*)	−0.04 (0.799)	0.006 (0.971)
DS	−0.34 (0.058)	0.18 (0.084)	−0.24 (*0.025*)	−0.22 (*0.036*)	−0.04 (0.782)	−0.02 (0.880)
PS	−0.05 (0.774)	−0.30 (*0.004*)	0.35 (*0.001*)	0.44 (*<0.001*)	−0.21 (0.134)	0.25 (0.072)
OXY score	−0.29 (0.111)	0.30 (*0.005*)	−0.38 (*<0.001*)	−0.41 (*<0.001*)	0.09 (0.528)	−0.15 (0.261)

SOD3: superoxide dismutase activity; CAT: catalase activity; GST: glutathione S-transferase activity; R-SH: reducing thiol total concentration; TBARS: thiobarbituric acid-reactive species; PC: protein carbonyl concentration; DS: damage score; PS: protection score; SD: standard deviation; TTO: time to onset (in presymptomatic individuals); AO: age at onset; PR: progression rate. ✦Corrected for repeat length; ◊corrected for disease duration and CAG repeat length.

The SARA score showed significant correlations with GST activity ($r = 0.22$; $p = 0.036$), CAT activity ($r = 0.29$; $p = 0.004$), CAT/SOD3 index score ($r = 0.29$; $p = 0.006$), protein carbonyl concentration ($r = -0.30$; $p = 0.01$), damage score ($r = -0.27$; $p = 0.008$), protection score ($r = 0.31$; $p = 0.002$), and OXY score ($r = -0.39$; $p < 0.001$). After correction for disease duration and repeat length, the SARA score showed significant positive correlations with GST and CAT activities, the CAT/SOD3 index score, and the protection score.

Likewise, corrected the SARA score showed significant negative correlations with the damage and OXY scores (Table 2). Similarly, the progression rate showed significant correlations with CAT ($r = 0.25$; $p = 0.015$) activity and the CAT/SOD3 index score ($r = 0.32$; $p = 0.002$). After correction for repeat length and disease duration, the progression rate was positively correlated to CAT activity, the CAT/SOD3 index score, and the protection score. Besides, the corrected progression rate was negatively correlated to protein carbonyl concentration and the damage and OXY scores

(Table 2). On the other hand, saccade velocity showed significant correlations with CAT activity ($r = -0.35$; $p = 0.008$) and the CAT/SOD3 index score ($r = -0.33$; $p = 0.013$). After correction for repeat length, saccade velocity showed a highly significant negative correlation with CAT activity. On the contrary, saccade latency showed a significant positive correlation with CAT activity (Table 2).

4. Discussion

In this study, taking advantage of the largest and genetically homogeneous SCA2 population worldwide, the evidence is provided for the role of oxidative stress in the presymptomatic stage of the disease, which seems to evolve into reductive stress in symptomatic stages, then contributing to clinical worsening. To our knowledge, this is the first study on redox balance in SCA2 which includes presymptomatic individuals, showing a redox shift in the transition from presymptomatic to symptomatic stages of the disease.

Presymptomatic individuals presented a significantly higher protein carbonyl concentration and OXY score, in parallel to lower GST activity than affected patients. Besides, presymptomatic individuals presented significantly lower protection scores than affected patients and healthy controls. Overall, this evidence indicates the occurrence of oxidative stress in the presymptomatic stage of the disease, which seems to be harmful as the corrected protein carbonyl concentration is negatively associated with the time to disease onset. This finding suggests that protein carbonyl concentration might be a good predictor of disease onset in mutation carriers.

As far as we know, only two studies have assessed the relevance of redox parameters in presymptomatic individuals for polyglutamine disorders. In presymptomatic individuals for Huntington's disease, higher levels of lipid peroxidation and protein carbonyl concentration and lower GSH concentration were found, suggesting the occurrence of oxidative stress before the onset of HD symptoms [38]. Also similar to our findings in SCA2, no significant associations were found for repeat length and redox parameters in HD presymptomatic individuals [38].

Contrary to our results in SCA2 presymptomatic individuals, higher SOD3 and glutathione peroxidase activities and decreased levels of reactive oxygen species were found in presymptomatic individuals with spinocerebellar ataxia type 3 (SCA3), suggesting a potential antioxidant adaptive response to an oxidative challenge taking place before disease onset. Nonetheless, these results seem to be of limited pathological significance as no correlations of redox markers with the predicted age of onset or repeat length were found [18].

Though oxidative stress has been suggested to be playing key roles in neurodegenerative disorders, this oxidative stress-centered view was challenged by evidence of little or no protection by free radical-scavenging antioxidants [39–41] and by evidences showing no association between clinical progressions and the oxidation induced by free radicals in the brain [42, 43]. In addition, findings relative to increased glucose 6-phosphate dehydrogenase (G6PDH) in AD and PD [44, 45] and increased thioredoxin reductase (TrxR) [46], neuronal thiols, and GSH/GSSG ratio in AD [44, 47] suggest that reductive reprogramming has an important role in these disorders. Also, the occurrence of lower GSSG and P-p38 levels and higher expression of glutamylcysteinyl ligase and glutathione peroxidase in young healthy individuals at risk of Alzheimer's disease [20] and the enhancing of the neurodegenerative phenotype in cellular and *Drosophila* models for Huntington's disease by treatment with N-acetyl-L-cysteine and overexpression of SOD1 support a relevant role for reductive stress in these neurodegenerative disorders [21].

In this study, it was found that affected SCA2 patients show a significant decrease in the protein carbonyl concentration and damage and OXY scores relative to controls, probably as a result of increased antioxidant activity. In addition, longer CAG repeats were associated to increased protein carbonyl concentration, as a reflection of the damaging effects of mutant Ataxin-2. Unexpectedly, there was a decrease in protein carbonyl concentration and OXY score with the advance of the disease, suggesting the sustained activation of the antioxidant machinery. Indeed, increased GST activity was observed in our patients and increased concentration of GSH was found in the white matter of SCA2 patients in a previous report [48].

Similar increases in the antioxidant defenses have been traditionally interpreted as an adaptive response to counteract the damaging effects of prooxidants on the cellular major macromolecular components, with a global protective effect [15, 16, 49]. However, we found that SCA2 patients with early disease onset show higher reducing thiol total concentration and protection score, suggesting harmful effects for increased antioxidant defenses. Moreover, positive associations were found for antioxidant parameters and SARA score, progression rate, and saccade latency, as well as a negative association with saccade velocity, reinforcing the suggestion that increased antioxidant defenses have worsening effects on the clinical presentation. In particular, catalase activity seems to be of great relevance as it was associated with the SARA score, disease progression, saccade velocity, and latency. In addition, SCA2 patients with early disease onset show lower protein carbonyl concentration and there were inverse significant associations between prooxidant parameters and disease severity.

Overall, this evidence suggests the potential occurrence of reductive stress in the symptomatic stage of SCA2, which reinforces the neurodegenerative process probably by contributing to the loss of ROS physiological effects on normal neuronal development and function.

It has been shown that ROS are important in the establishment of neuronal polarity and growth cone pathfinding [50, 51] and in the regulation of synaptic transmission and plasticity [52, 53]. Indeed, superoxide is essential to induce long-term depression in the cerebellar Purkinje neurons [54] and physiological concentrations of hydrogen peroxide are necessary for structural plasticity dependent on neuronal activity and for the maintenance of evoked synaptic transmission in *Drosophila* [55]. On the contrary, activation of catalase inhibited the adaptive morphological changes of the neuromuscular junction in *Drosophila* [55]. Besides,

overexpression of mitochondrial catalase, producing an astrocyte-specific decrease of endogenous mitochondrial ROS in mice, causes profound changes in brain energy and redox metabolism, eventually leading to neuronal dysfunction and cognitive impairment [56]. This evidence suggests that overactivation of the antioxidant machinery might have negative effects on the physiology of the nervous system.

It has been proved that neuronal polarization depends heavily on the activity of protein kinases including PI3K, whose signaling can be regulated by ROS-mediated inhibition of PTEN [57]. PTEN and PI3K were also involved in synaptic terminal growth by DJ-1β oxidation in *Drosophila* [58, 59]. In addition, the release of calcium from intracellular stores was involved in the mechanisms by which ROS contribute to neuronal polarity and to synaptic plasticity [54, 60, 61]. Importantly, Ataxin-2 protein was implicated in calcium signaling and PI3K/Akt/mTOR pathways [8, 9, 62]. These findings provide potential links between Ataxin-2 and redox-mediated neuronal development and function.

In conclusion, there is a disruption of redox balance in SCA2 mutation carriers which depends on the disease stage. Besides, redox changes associate with markers of disease severity, suggesting a link between disruption of redox balance and SCA2 physiopathology. Further studies are needed to confirm these findings, to clarify the molecular mechanisms involved and to assess the usefulness of redox parameters as biomarkers of disease progression and to monitor the effects of therapeutic interventions.

Data Availability

The molecular and clinical data used to support the findings of this study are restricted by the Ethics Committee at the Center for the Investigation and Rehabilitation of Hereditary Ataxias in order to protect patient privacy. Data are available from D Almaguer-Gotay for researchers who meet the criteria for access to confidential data.

Conflicts of Interest

The authors declare that they have no conflicts of interest.

Acknowledgments

The authors are grateful to patients and control individuals for their cooperation with this research. We are also indebted to M.D. Patrick MacLeod and to the Cuban Ministry of Public Health for technical and financial support.

References

[1] Y. M. Sun, C. Lu, and Z. Y. Wu, "Spinocerebellar ataxia: relationship between phenotype and genotype - a review," *Clinical Genetics*, vol. 90, no. 4, pp. 305–314, 2016.

[2] D. Genis, S. Ortega-Cubero, H. S. Nicolás et al., "HeterozygousSTUB1mutation causes familial ataxia with cognitive affective syndrome (SCA48)," *Neurology*, vol. 91, no. 21, pp. e1988–e1998, 2018.

[3] L. C. Velázquez-Pérez, R. Rodríguez-Labrada, and J. Fernandez-Ruiz, "Spinocerebellar ataxia type 2: clinicogenetic aspects, mechanistic insights, and management approaches," *Frontiers in Neurology*, vol. 8, p. 472, 2017.

[4] A. Antenora, C. Rinaldi, A. Roca, C. Pane, M. Lieto, and F. Saccà, "The multiple faces of spinocerebellar ataxia type 2," *Annals of Clinical Translational Neurology*, vol. 4, no. 9, pp. 687–695, 2017.

[5] D. P. Huynh, H. T. Yang, H. Vakharia, D. Nguyen, and S. M. Pulst, "Expansion of the polyQ repeat in ataxin-2 alters its Golgi localization, disrupts the Golgi complex and causes cell death," *Human Molecular Genetics*, vol. 12, no. 13, pp. 1485–1496, 2003.

[6] E. Damrath, M. V. Heck, S. Gispert, M. Azizov, J. Nowock, and C. Seifried, "ATXN2-CAG42 sequesters PABPC1 into insolubility and induces FBXW8 in cerebellum of old ataxic knock-in mice," *PLoS Genetics*, vol. 8, no. 8, p. e1002920, 2012.

[7] S. Paul, W. Dansithong, K. P. Figueroa, D. R. Scoles, and S. M. Pulst, "Staufen1 links RNA stress granules and autophagy in a model of neurodegeneration," *Nature Communications*, vol. 9, no. 1, p. 3648, 2018.

[8] J. Liu, T. S. Tang, H. Tu, O. Nelson, E. Herndon, and D. P. Huynh, "Deranged calcium signaling and neurodegeneration in spinocerebellar ataxia type 2," *The Journal of Neuroscience*, vol. 29, no. 29, pp. 9148–9162, 2009.

[9] M. V. Halbach, S. Gispert, T. Stehning, E. Damrath, M. Walter, and G. Auburger, "Atxn2 knockout and CAG42-knock-in cerebellum shows similarly dysregulated expression in calcium homeostasis pathway," *Cerebellum*, vol. 16, no. 1, pp. 68–81, 2017.

[10] J. M. Laffita-Mesa, P. O. Bauer, V. Kourí, L. P. Serrano, J. Roskams, and D. Almaguer-Gotay, "Epigenetics DNA methylation in the core ataxin-2 gene promoter: novel physiological and pathological implications," *Human Genetics*, vol. 131, no. 4, pp. 625–638, 2012.

[11] I. Mironczuk-Chodakowska, A. M. Witkowska, and M. E. Zujko, "Endogenous non-enzymatic antioxidants in the human body," *Advances in Medical Sciences*, vol. 63, no. 1, pp. 68–78, 2018.

[12] A. E. Azab, A. A. Adwas, A. S. I. Elsayed, A. A. Adwas, A. S. I. Elsayed, and F. A. Quwaydir, "Oxidative stress and antioxidant mechanisms in human body," *Journal of Applied Biotechnology & Bioengineering*, vol. 6, no. 1, pp. 43–47, 2019.

[13] H. Sies, "Oxidative stress: introductory remarks," in *Oxidative Stress*, H. Sies, Ed., pp. 1–8, London, London, Academic Press, 1985.

[14] D. P. Jones, "Redefining oxidative stress," *Antioxidants & Redox Signaling*, vol. 8, no. 9-10, pp. 1865–1879, 2006.

[15] H. Sies, C. Berndt, and D. P. Jones, "Oxidative stress," *Annual Review of Biochemistry*, vol. 86, no. 1, pp. 715–748, 2017.

[16] J. I. Sbodio, S. H. Snyder, and B. D. Paul, "Redox mechanisms in neurodegeneration: from disease outcomes to therapeutic opportunities," *Antioxidants & Redox Signaling*, vol. 30, no. 11, pp. 1450–1499, 2019.

[17] B. D. Paul and S. H. Snyder, "Impaired redox signaling in Huntington's disease: therapeutic implications," *Frontiers in Molecular Neuroscience*, vol. 12, p. 68, 2019.

[18] M. A. de Assis, S. J. A. Morales, A. Longoni, H. C. Branco, T. V. Rocco, and B. A. Wigner, "Peripheral oxidative stress biomarkers in spinocerebellar ataxia type 3/Machado–Joseph disease," *Frontiers in Neurology*, vol. 8, p. 485, 2017.

[19] P. Korge, G. Calmettes, and J. N. Weiss, "Increased reactive oxygen species production during reductive stress: the roles

of mitochondrial glutathione and thioredoxin reductases," *Biochimica et Biophysica Acta*, vol. 1847, no. 6-7, pp. 514–525, 2015.

[20] M. C. Badía, E. Giraldo, F. Dasí et al., "Reductive stress in young healthy individuals at risk of Alzheimer disease," *Free Radical Biology & Medicine*, vol. 63, pp. 274–279, 2013.

[21] R. B. Underwood, S. Imarisio, A. Fleming, C. Rose, G. Krishna, and P. Heard, "Antioxidants can inhibit basal autophagy and enhance neurodegeneration in models of polyglutamine disease," *Human Molecular Genetics*, vol. 19, no. 17, pp. 3413–3429, 2010.

[22] F. G. Riverón, B. O. Martínez, G. R. Gutiérrez et al., "Oxidative damage and antioxidant enzymes in blood of patients with spinocerebellar ataxia type 2," *Rev. Cubana Genet. Comunit.*, vol. 4, no. 1, pp. 42–47, 2010.

[23] D. Almaguer-Gotay, L. E. Almaguer-Mederos, R. Aguilera-Rodríguez et al., "Role of glutathione S-transferases in the spinocerebellar ataxia type 2 clinical phenotype," *Journal of the Neurological Sciences*, vol. 341, no. 1-2, pp. 41–45, 2014.

[24] D. Almaguer-Gotay, L. E. Almaguer-Mederos, R. Aguilera-Rodríguez, R. Rodríguez-Labrada, D. Cuello-Almarales, and A. Estupiñán-Domínguez, "Spinocerebellar ataxia type 2 is associated with the Extracellular loss of superoxide dismutase but not catalase activity," *Frontiers in Neurology*, vol. 8, 2017.

[25] N. Cornelius, H. J. Wardman, P. I. Hargreaves, V. Neergheen, B. A. Sigaard, and Z. Tümer, "Evidence of oxidative stress and mitochondrial dysfunction in spinocerebellar ataxia type 2 (SCA2) patient fibroblasts: effect of coenzyme Q10 supplementation on these parameters," *Mitochondrion*, vol. 34, pp. 103–114, 2017.

[26] T. Schmitz-Hübsch, S. T. du Montcel, L. Baliko, J. Berciano, S. Boesch, and C. Depondt, "Scale for the assessment and rating of ataxia: development of a new clinical scale," *Neurology*, vol. 66, no. 11, pp. 1717–1720, 2006.

[27] R. Rodríguez-Labrada, L. Velázquez-Pérez, C. Seigfried, N. Canales-Ochoa, G. Auburger, and J. Medrano-Montero, "Saccadic latency is prolonged in spinocerebellar ataxia type 2 and correlates with the frontal-executive dysfunctions," *Journal of the Neurological Sciences*, vol. 306, no. 1-2, pp. 103–107, 2011.

[28] L. E. Almaguer-Mederos, N. S. Falcon, Y. R. Almira, Y. G. Zaldivar, D. C. Almarales, and E. M. Góngora, "Estimation of the age at onset in spinocerebellar ataxia type 2 Cuban patients by survival analysis," *Clinical Genetics*, vol. 78, no. 2, pp. 169–174, 2010.

[29] G. Imbert, F. Saudou, G. Yvert, D. Devys, Y. Trottier, and J. M. Garnier, "Cloning of the gene for spinocerebellar ataxia 2 reveals a locus with high sensitivity to expanded CAG/glutamine repeats," *Nature Genetics*, vol. 14, no. 3, pp. 285–291, 1996.

[30] S. Marklund and G. Marklund, "Involvement of the superoxide anion radical in the autoxidation of pyrogallol and a convenient assay for superoxide dismutase," *European Journal of Biochemistry*, vol. 47, no. 3, pp. 469–474, 1974.

[31] B. Chance, "Catalases and peroxidases, part II. Special methods," *Methods of Biochemical Analysis*, vol. 1, pp. 408–424, 1954.

[32] W. H. Habig and W. B. Jacoby, "[51] Assays for differentiation of glutathione S-transferases," *Methods in Enzymology*, vol. 77, pp. 398–405, 1981.

[33] L. G. Ellman, "Tissue sulfhydryl groups," *Archives of Biochemistry and Biophysics.*, vol. 82, no. 1, pp. 70–77, 1959.

[34] K. A. Yagi, "A simple fluorometric assay for lipoperoxide in blood plasma," *Biochemical Medicine*, vol. 15, no. 2, pp. 212–216, 1976.

[35] R. L. Levine, J. A. Williams, E. R. Stadtman, and E. Shacter, "[37] Carbonyl assays for determination of oxidatively modified proteins," *Methods in Enzymology*, vol. 233, pp. 346–357, 1994.

[36] F. Veglia, V. Cavalca, and E. Tremoli, "OXY-SCORE: a global index to improve evaluation of oxidative stress by combining pro- and antioxidant markers," *Methods in Molecular Biology*, vol. 594, pp. 197–213, 2010.

[37] Y. Benjamini and Y. Hochberg, "Controlling the false discovery rate: a practical and powerful approach to multiple testing," *Journal of the Royal Statistical Society: Series B (Methodological)*, vol. 57, pp. 289–300, 1995.

[38] N. Klepac, M. Relja, R. Klepac, S. Hećimović, T. Babić, and V. Trkulja, "Oxidative stress parameters in plasma of Huntington's disease patients, asymptomatic Huntington's disease gene carriers and healthy subjects: a cross-sectional study," *Journal of Neurology*, vol. 254, no. 12, pp. 1676–1683, 2007.

[39] A. Lloret, D. Esteve, P. Monllor, A. Cervera-Ferri, and A. Lloret, "The Effectiveness of vitamin E treatment in Alzheimer's disease," *International Journal of Molecular Sciences*, vol. 20, no. 4, 2019.

[40] R. Filograna, M. Beltramini, L. Bubacco, and M. Bisaglia, "Anti-oxidants in Parkinson's disease therapy: a critical point of view," *Current Neuropharmacology*, vol. 14, no. 3, pp. 260–271, 2016.

[41] M. M. Essa, M. Moghadas, T. Ba-Omar, M. Walid Qoronfleh, G. J. Guillemin, and T. Manivasagam, "Protective effects of antioxidants in Huntington's disease: an extensive review," *Neurotoxicity Research*, vol. 35, no. 3, pp. 739–774, 2019.

[42] A. Nunomura, G. Perry, G. Aliev, K. Hirai, A. Takeda, and E. K. Balraj, "Oxidative damage is the earliest event in Alzheimer disease," *Journal of Neuropathology and Experimental Neurology*, vol. 60, no. 8, pp. 759–767, 2001.

[43] D. R. Galasko, E. Peskind, C. M. Clark, J. F. Quinn, J. M. Ringman, and G. A. Jicha, "Antioxidants for Alzheimer disease: a randomized clinical trial with cerebrospinal fluid biomarker measures," *Archives of Neurology*, vol. 69, no. 7, pp. 836–841, 2012.

[44] R. L. Russell, S. L. Siedlak, A. K. Raina, J. M. Bautista, M. A. Smith, and G. Perry, "Increased neuronal glucose-6-phosphate dehydrogenase and sulfhydryl levels indicate reductive compensation to oxidative stress in Alzheimer disease," *Archives of Biochemistry and Biophysics*, vol. 370, no. 2, pp. 236–239, 1999.

[45] L. Dunn, G. F. Allen, A. Mamais, H. Ling, A. Li, and K. E. Duberley, "Dysregulation of glucose metabolism is an early event in sporadic Parkinson's disease," *Neurobiology of Aging*, vol. 35, no. 5, pp. 1111–1115, 2014.

[46] M. A. Lovell, C. Xie, S. P. Gabbita, and W. R. Markesbery, "Decreased thioredoxin and increased thioredoxin reductase levels in Alzheimer's disease brain," *Free Radical Biology and Medicine*, vol. 28, no. 3, pp. 418–427, 2000.

[47] J. D. Adams, L. K. Klaidman, I. N. Odunze, H. C. Shen, and C. A. Miller, "Alzheimer's and Parkinson's disease," *Molecular and Chemical Neuropathology*, vol. 14, pp. 213–226, 1991.

[48] J. M. Joers, D. K. Deelchand, T. Lyu et al., "Neurochemical abnormalities in premanifest and early spinocerebellar ataxias," *Annals of Neurology*, vol. 83, no. 4, pp. 816–829, 2018.

[49] Y. Torres-Ramos, A. Montoya-Estrada, B. Cisneros, K. Tercero-Pérez, G. León-Reyes, and N. Leyva-García, "Oxidative stress in spinocerebellar ataxia type 7 is associated with disease severity," *Cerebellum*, vol. 17, no. 5, pp. 601–609, 2018.

[50] M. Nitti, A. L. Furfaro, C. Cevasco, N. Traverso, U. M. Marinari, and M. A. Pronzato, "PKC delta and NADPH oxidase in retinoic acid-induced neuroblastoma cell differentiation," *Cellular Signalling*, vol. 22, no. 5, pp. 828–835, 2010.

[51] R. J. Hung, U. Yazdani, J. Yoon, H. Wu, T. Yang, and N. Gupta, "Mical links semaphorins to F-actin disassembly," *Nature*, vol. 463, no. 7282, pp. 823–827, 2010.

[52] S. Sanyal, D. J. Sandstrom, C. A. Hoeffer, and M. Ramaswami, "AP-1 functions upstream of CREB to control synaptic plasticity in Drosophila," *Nature*, vol. 416, no. 6883, pp. 870–874, 2002.

[53] K. Y. Lee, K. Chung, and J. M. Chung, "Involvement of reactive oxygen species in long-term potentiation in the spinal cord dorsal hor n," *Journal of Neurophysiology*, vol. 103, no. 1, pp. 382–391, 2010.

[54] H. Fujii and T. Hirano, "Calcineurin regulates induction of late phase of cerebellar long-term depression in rat cultured Purkinje neurons," *The European Journal of Neuroscience*, vol. 16, no. 9, pp. 1777–1788, 2002.

[55] C. W. M. Oswald, S. P. Brooks, F. M. Zwart, A. Mukherjee, J. H. R. West, and N. G. C. Giachello, "Reactive oxygen species regulate activity-dependent neuronal plasticity in Drosophila," *eLife*, vol. 7, article e39393, 2018.

[56] C. Vicente-Gutierrez, N. Bonora, V. Bobo-Jimenez, D. Jimenez-Blasco, I. Lopez-Fabuel, and E. Fernandez, "Astrocytic mitochondrial ROS modulate brain metabolism and mouse behavior," *Nature Metabolism*, vol. 1, no. 2, pp. 201–211, 2019.

[57] Y. C. Kim, H. Kitaura, T. Taira, S. M. M. Iguchi-Ariga, and H. Ariga, "Oxidation of DJ-1-dependent cell transformation through direct binding of DJ-1 to PTEN," *International Journal of Oncology*, vol. 35, no. 6, pp. 1331–1341, 2009.

[58] V. Kumar, M. X. Zhang, M. W. Swank, J. Kunz, and G. Y. Wu, "Regulation of dendritic morphogenesis by Ras-PI3K-Akt-mTOR and Ras-MAPK signaling pathways," *The Journal of Neuroscience*, vol. 25, no. 49, pp. 11288–11299, 2005.

[59] S. Jordán-Alvarez, W. Fouquet, S. J. Sigrist, and A. Acebes, "Presynaptic PI3K activity triggers the formation of glutamate receptors at neuromuscular terminals of Drosophila," *Journal of Cell Science*, vol. 125, no. 15, pp. 3621–3629, 2012.

[60] R. J. Gasperini, M. Pavez, A. C. Thompson, C. B. Mitchell, H. Hardy, and K. M. Young, "How does calcium interact with the cytoskeleton to regulate growth cone motility during axon pathfinding?," *Molecular and Cellular Neurosciences*, vol. 84, pp. 29–35, 2017.

[61] B. E. Herring and R. A. Nicoll, "Long-term potentiation: from CaMKII to AMPA receptor trafficking," *Annual Review of Physiology*, vol. 78, no. 1, pp. 351–365, 2016.

[62] I. Lastres-Becker, D. Nonis, F. Eich, M. Klinkenberg, M. Gorospe, and P. Kötter, "Mammalian ataxin-2 modulates translation control at the pre-initiation complex via PI3K/mTOR and is induced by starvation," *Biochimica et Biophysica Acta*, vol. 1862, no. 9, pp. 1558–1569, 2016.

Hindawi
Oxidative Medicine and Cellular Longevity
Volume 2021, Article ID 8845064, 15 pages
https://doi.org/10.1155/2021/8845064

Research Article

Protective Effect of Biobran/MGN-3 against Sporadic Alzheimer's Disease Mouse Model: Possible Role of Oxidative Stress and Apoptotic Pathways

Mamdooh H. Ghoneum [1] **and Nesrine S. El Sayed** [2]

[1] *Department of Surgery, Charles Drew University of Medicine and Science, Los Angeles, California, USA*
[2] *Department of Pharmacology and Toxicology, Faculty of Pharmacy, Cairo University, Cairo, Egypt*

Correspondence should be addressed to Nesrine S. El Sayed; nesrine_salah2002@yahoo.com

Received 28 September 2020; Revised 14 December 2020; Accepted 3 January 2021; Published 27 January 2021

Academic Editor: Kambiz Hassanzadeh

Alzheimer's disease (AD) is a debilitating and irreversible brain disease that affects an increasing number of aged individuals, mandating the development of protective nutraceuticals. Biobran/MGN-3, an arabinoxylan from rice bran, has potent antioxidant, antiaging, and immunomodulatory effects. The aim of the present study was to investigate the protective effect of Biobran against sporadic Alzheimer's disease (SAD). SAD was induced in mice via intracerebroventricular injection of streptozotocin (STZ) (3 mg/kg). STZ-treated mice were administered with Biobran for 21 days. The effects of Biobran on memory and learning were measured via the Morris water maze, novel object recognition, and Y-maze tests. Biomarkers for apoptosis, oxidative stress, and amyloidogenesis were measured using ELISA and western blot analysis. Histopathological examination was performed to confirm neuronal damage and amyloid-beta deposition. Biobran reversed the spatial memory deficit in SAD-induced mice, and it increased the expression of glutathione, reduced malondialdehyde, decreased IL-6, decreased intercellular adhesion molecule-1 (ICAM-1), and significantly increased nuclear factor erythroid 2-related factor 2 (Nrf2) and antioxidant response element (ARE). Moreover, Biobran exerted a protective effect against amyloid-beta-induced apoptosis via the suppression of both cleaved caspase-3 and the proapoptotic protein Bax and via the upregulation of the antiapoptotic protein Bcl-2. Furthermore, it reduced the expression of forkhead box class O proteins. It could be concluded from this study that Biobran may be a useful nutritional antioxidant agent for protection against SAD through its activation of the gene expression of Nrf2/ARE, which in turn modulates the apoptotic and amyloidogenic pathways.

1. Introduction

Alzheimer's disease (AD) is the most common neurodegenerative disorder characterized by progressive loss of memory and cognition. The appearance of oxidative stress markers is one of the hallmarks of AD; it leads to the build-up of amyloid deposits and neurofibrillary tangles and to the progression of the disease [1]. Oxidative stress is involved in many disorders, including Parkinson's disease, chronic inflammation, and AD [2]. Neurons produce energy at a high rate and show high oxygen consumption; they are at extremely high risk to oxidative damage from reactive oxygen species (ROS) [3]. Currently, the process by which amyloid-beta (Aβ) accumulation occurs in the central nervous system is uncertain, but the generation of ROS during Aβ self-aggregation is a potential mechanism by which Aβ may cause neuronal damage and death. This effect ultimately leads to synaptic membrane depolarization, excessive calcium influx, and mitochondrial impairment [4, 5]. One of the common regulators of the oxidative stress pathway in AD is the expression of the nuclear factor erythroid 2-related factor 2 (Nrf2). It is present mainly in the cytoplasm of the

hippocampal neurons [6], and in AD animal models, the pathology of Aβ is linked with altered expression of Nrf2 target genes [7]. Nrf2 can act as a molecular switch in neurons that mediates the antioxidant system [8]. Active Nrf2 protects cells against oxidative injury by binding to the antioxidant response element (ARE) under oxidative stimuli and promoting antioxidative genes [9]. Therefore, the restoration of Nrf2 expression could alleviate cognitive impairment by protecting neurons against oxidative injury and decreasing Aβ accumulation [10].

Neuroinflammation plays an important role in AD pathogenesis through the production of inflammatory cytokines like IL-6, which is highly prevalent in AD [11, 12], and the intercellular adhesion molecule-1 (ICAM-1), which is highly expressed in the neuritic plaques in AD brains. ICAM-1 has been implicated in neurodegeneration through its role as an important mediator of immune cell activation and inflammatory response in AD [13]. ICAM-1 plays a key role in cell survival in the brain and induced the upregulation of proapoptotic proteins, Bax and cleaved caspase-3, and downregulation of the antiapoptotic proteins, Bcl-2 [14, 15]. This pathway has many downstream targets like the transcriptional factor forkhead box proteins of class O3a (FOXO3a), a factor that, when translocated to the nucleus, can trigger cell apoptosis. Evidence is growing that apoptotic markers can directly target FOXO3a and lead to cell apoptosis [16]. The family of FOXO proteins is extensively involved in the cell signal transduction of apoptosis and in oxidative stress. This effect is important in the survival of cerebral endothelial vascular cells [17], oxidative stress injury in mouse cerebellar granule neurons [18], and hippocampal neuronal injury [19]; and it can also lead to caspase 3-induced apoptotic death [20, 21].

STZ injection in the brain is linked to brain insulin resistance, neuroinflammation, oxidative stress, and deposition of Aβ, as well as tau protein aggregation leading to impairment in memory and learning functions that mimic sporadic Alzheimer's disease (SAD) in humans [22]. ICV-STZ injection induces the activation of microglial cells, which produce massive amounts of inflammatory mediators and free radicals that provoke neuronal damage [23].

Currently, there are no dietary supplements or prescribed medications for decreasing the risk of AD [24], and current FDA-approved treatments for AD are only symptomatic [25]. Biobran/MGN-3 is a denatured hemicellulose from rice bran that has shown promising effect as a natural adjuvant to existing immunotherapies for cancer [26, 27] through its antioxidant properties [28]. Biobran was shown previously to enhance natural killer cell activity in aged mice [29] as well as healthy elderly human subjects [30], with improvement in their health-related quality of life [31]. Few studies have been done on the beneficial effects of Biobran on aging and neurodegenerative diseases. So, the present study is aimed at investigating the possible protective effect of Biobran in a SAD model through the modulation of oxidative stress, amyloidogenesis, inflammation, and apoptotic pathways. Behavioral and biochemical experiments were performed to illuminate the mechanisms underlying its potential neuroprotective effect in the STZ model of SAD.

2. Material and Methods

2.1. Animals. Adult male Swiss albino mice, weighing 25-30 g, were used in the present study. Mice were obtained from the animal facility of the National Research Center, Cairo, Egypt, and they were housed 6 mice per cage. Mice were allowed to acclimate to their environment for a period of one week prior to the study. Animals were maintained in a controlled environment with constant temperatures ($25 \pm 2^{\circ}$C), light/dark cycles (12/12 h), and relative humidity ($60 \pm 10\%$). Animals were provided with a standard chow diet and allowed water ad libitum. This study complied with the Guide for the Care and Use of Laboratory Animals published by the US National Institutes of Health [32] and was approved by the Institutional Animal Care and Use Committee, Cairo University (CU-IACUC), approval number: CU-III-F-26-20. Animal discomfort and suffering was minimized as much as possible.

2.2. Drug Treatments. STZ was purchased from Sigma-Aldrich Co. (St Louis, MO, USA) and dissolved in saline solution (0.9% NaCl). Biobran is a denatured hemicellulose that is extracted from rice bran by reacting rice bran hemicellulose with carbohydrate-hydrolyzing enzymes obtained from Shiitake mushrooms. Biobran's main chemical structure is arabinoxylan with an arabinose polymer in its side chain and a xylose in its main chain [26]. Daiwa Pharmaceutical Co. Ltd. (Tokyo, Japan) kindly provided Biobran. Biobran was prepared in saline (0.9% w/v) and was freshly prepared each day (Figure 1).

2.3. Acute Toxicity Study. Earlier studies have shown Biobran to be a nontoxic and safe agent. The Ames mutagenicity test is negative, Biobran's 50% lethal dose (LD50) is greater than 36 g/kg, and several toxicity studies have all confirmed the safety of Biobran in both humans and animals [27, 33]. 8-month-long periods of treatment of animals with Biobran as well as 5-year-long treatment for humans [34] have not resulted in any adverse side effects. In the present study, Biobran's acute toxicity in mice was assessed via the up and down procedure according to Guideline No. 423 from the Organization for Economic Cooperation and Development [35]. A starting dose of 2 g/kg Biobran was given to mice. For 24 hours, the mice were observed continuously for toxic symptoms, following which they were observed daily over an additional 20 days of maintenance.

2.4. Induction of SAD. SAD was induced in mice by ICV injection of STZ (3 mg/kg) into their lateral ventricle using the freehand procedure [36] updated by Warnock [37] for the avoidance of cerebral vein penetration. Thiopental (50 mg/kg, i.p.) was used to anesthetize the mice. The mouse head was secured using downward pressure above the ears, followed by insertion of the needle directly through the skin and skull into the lateral ventricle. Visualization of an equilateral triangle between the eyes and center of the skull was used to locate the bregma and target the lateral ventricle allowing the needle to be inserted at the following coordinates from bregma: 1 mm mediolateral, 0.1 mm anteroposterior,

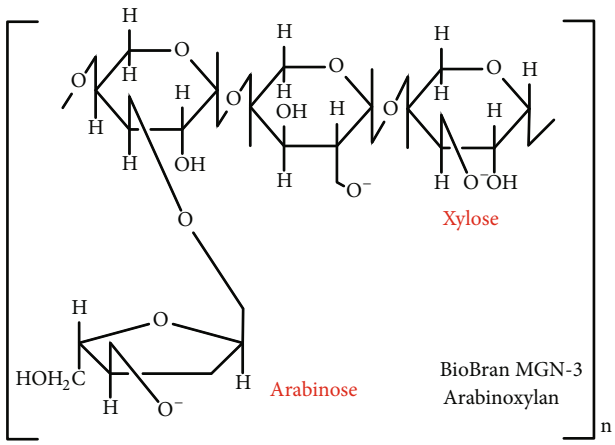

Figure 1: Chemical structure of Biobran/MGN-3.

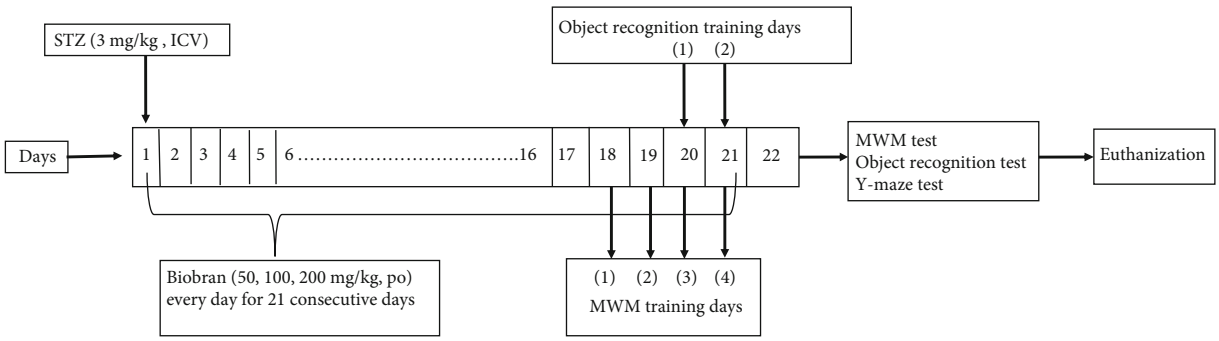

Figure 2: Experimental design.

and 3 mm dorsoventral. The mice exhibited normal behavior approximately 1 minute after injection.

2.5. Experimental Design. Mice were randomly allocated into five groups, each containing 12 mice. Group 1, the sham control group, received one ICV saline injection followed by intraperitoneal (i.p.) saline injections for 21 consecutive days. Group 2 received STZ (3 mg/kg, ICV) once and served as the SAD model [38]. Group 3 received STZ (3 mg/kg, ICV), five hours later, it is followed by Biobran (50 mg/kg, i.p.) daily for 21 consecutive days. Group 4 received STZ (3 mg/kg, ICV), five hours later, it is followed by Biobran (100 mg/kg, i.p.) daily for 21 consecutive days. Group 5 received STZ (3 mg/kg, ICV), five hours later, it is followed by Biobran (200 mg/kg, i.p.) daily for 21 consecutive days. Once the treatment period ended, mice were given behavioral tests assessing cognitive functions (Figure 2).

2.6. Behavioral Assessments

2.6.1. Object Recognition Test. To assess long-term memory and estimate cognition, we used the object recognition test. It is based on the concept of preference for novelty, which is the innate tendency of animals to exhibit an affinity for exploring a novel object rather than a familiar one [39]. This test was administered over three consecutive days. On day 1, each mouse was placed in a wooden box ($30 \times 30 \times 30$) dimension and was left for thirty minutes to adapt to the surroundings.

On day 2, two wooden cubes identical in shape, color, and size were placed at opposite corners in the box, 2 cm from the walls. Each mouse was placed in the box's middle and given ten minutes to explore the new objects. On day 3, one of the cubes was replaced by a novel object of different shape, size and color, and mice were each given five minutes to explore the box's objects. Objects and the arena were thoroughly cleaned with 70% ethanol between experiments with individual mice to ensure that their behavior was not guided by odor cues. Each mouse was faced toward the same wall at the beginning of each trial and was prevented from displacing the objects. Animals were video-recorded and measured for the following:

(1) *Discrimination Index.* Time difference between the exploration of novel and familiar objects divided by the total exploration time

(2) *Recognition Index.* Time spent exploring the novel object as a percentage of the total exploration time

2.6.2. Morris Water Maze (MWM) Test. The MWM test was used to investigate spatial memory and learning [40]. The maze consisted of stainless-steel circular tanks (210 cm in diameter, 51 cm high) filled with water ($25 \pm 2^{\circ}$C) to a depth of 35 cm and divided into four quadrants. A black platform

(10 cm wide, 28 cm high) was placed inside the target quadrant and submerged by 2 cm. The platform remained in the same location during training and testing procedures, and it was made invisible by coloring the water with a purple-colored nontoxic dye. Memory-acquisition trials (120 s/trail) were performed over four consecutive days, twice/day, with at least 15 min between trials. Animals were left free during each acquisition trial to locate the hidden platform. If the mouse located the platform, it was given 20 additional seconds for rest, while if the mouse did not reach the platform within 120 s, it was guided to the platform and allowed to rest there for 20 s. Mean escape latency (MEL) was calculated as the time taken by each mouse to find the hidden platform. After four acquisition trial days, mice were allowed 60 seconds to probe a pool in which the platform had been removed. Mice were put into the water in the Northeast position (Q4), and this is a fixed release point during the test. Measurements were made of the time each mouse spent in the target quadrant as an indicator of retrieval or memory.

2.6.3. Y-Maze Test. The Y-maze is used to measure spatial working memory in rodents via the spontaneous alternation behavior (SAB) calculation [41]. Spontaneous alternation measures the ability of the animal to alternate its choice of arm entry on subsequent trials based on its memory of previous arm entries performed, which depends on the natural exploratory behavior of animals for new environments. The maze is a Y-shaped apparatus consisting of three arms, each one with the same dimensions, 35 cm long, 25 cm high, and 10 cm wide at 120° extending from a central platform. The apparatus was placed on the floor of the experimental room. The test was performed for 2 days. The first day was for the purpose of training; each mouse was positioned in the central platform and allowed to explore the maze freely for 8 minutes. The same procedure was followed on the second testing day, with the addition of manual recording of each arm entry, scored only when all four limbs of the mouse were inside the arm. After each session, the maze was cleaned with 70% ethanol to exclude any olfactory cues that might interfere with subsequent testing. An alternation was considered to have occurred if three successive different arms were entered during an overlapping triplet set. The percentage of spontaneous alternation activity (SAB%) was calculated as the "number of alternations consecutively" divided by "the total number of arm entries minus 2" and multiplied by 100.

2.7. Biochemical Assessments. Following the behavioral tests, animals ($n = 12$) were anesthetized using thiopental sodium (50 mg/kg, i.p.) and then euthanized by cervical dislocation. The brains were rapidly dissected on ice/salt mixture and washed with ice-cold saline. The hippocampi were homogenized in ice-cold saline to prepare 10% homogenates; these were split into several aliquots and stored at -80°C for estimation of the biochemical parameters ($n = 6$), western blot analysis ($n = 3$), and histopathological examination ($n = 3$).

2.8. Biochemical Measurements

2.8.1. Determination of GSH and MDA. The hippocampal glutathione (GSH) content was measured spectrophotometrically using Ellman's reagent [42]. The peroxidation of hippocampal lipids was estimated by measuring malondialdehyde (MDA) levels via thiobarbituric acid reactive substances [43]. The results are expressed as mmol/mg protein.

2.8.2. Determination of IL-6, ICAM-1, Cleaved Caspase-3, and Amyloid-$\beta_{1\text{-}42}$. Hippocampal IL-6 and ICAM-1 levels were estimated using mouse ELISA kits purchased from RayBiotech Inc. (Norcross, Georgia, USA) and MyBioSource Inc. (San Diego, CA, USA), respectively. Cleaved caspase-3 and amyloid-$\beta_{1\text{-}42}$ mouse ELISA kits were provided from Cusabio, Wuhan, China. The hippocampal levels of these markers were measured according to the manufacturer's instructions for each respective ELISA kit and expressed as their corresponding units to the tissue protein content determined by Salama et al. [44]. The ELISA assay measures the amount of sample by sandwiching it between two antibodies, one of which is precoated to the microtiter plate, and the other of which acts as a detector antibody. The microtiter plate provided in each kit was precoated with an antibody specific to each marker. Standards or samples are then added to the appropriate microtiter plate wells with a biotin-conjugated antibody preparation specific for the marker, and avidin conjugated to HRP is added to each microplate well and incubated. Then, a TMB substrate solution is added to each well. Only those wells that contain the protein, biotin-conjugated antibody, and enzyme-conjugated avidin will exhibit a change in color. The enzyme–substrate reaction is terminated by the addition of a sulfuric acid solution, and the color change is measured spectrophotometrically at a wavelength of 450 nm.

2.8.3. Western Blot Analysis. Western blot is a method to quantify the expression level of specific proteins. Protein solutions were extracted from hippocampal tissues, $n = 3$. SDS-PAGE (10% acrylamide gel) was used to separate equal amounts of protein (averaging 20–30 μg of total protein). Proteins were subsequently transferred to polyvinylidene difluoride membranes (Pierce, Rockford, IL, USA) with a Bio-Rad Trans-Blot system. Western blot immunodetection was performed by incubating the membranes at room temperature for 1 hour with blocking solution comprised of 20 mM Tris-Cl, pH 7.5, 150 mM NaCl, 0.1% Tween 20, and 3% bovine serum albumin. Membranes were incubated overnight at 4°C with one of the following primary antibodies: Nrf2 (catalog no: 31163), FOXO3a (catalog no: 1950), and β-actin (catalog no: 8227) obtained from Thermo Fisher Scientific Inc. (Rockford, IL, USA). Peroxidase-labelled secondary antibodies (1 : 1000; Novus Biologicals, Colorado, USA) were added after washing, followed by 1 h of membrane incubation at room temperature. Incubation with the substrate permits the detection of the amount of protein through optical documentation systems. The quantification of the band intensity can be used to determine specific protein levels in the tested tissues. Detection of a second "housekeeping" protein is necessary to control for variability in protein loading between samples. The band intensity was analyzed using the ChemiDoc™ imaging system with Image LabTM software version 5.1 (Bio-Rad Laboratories Inc., Hercules, CA,

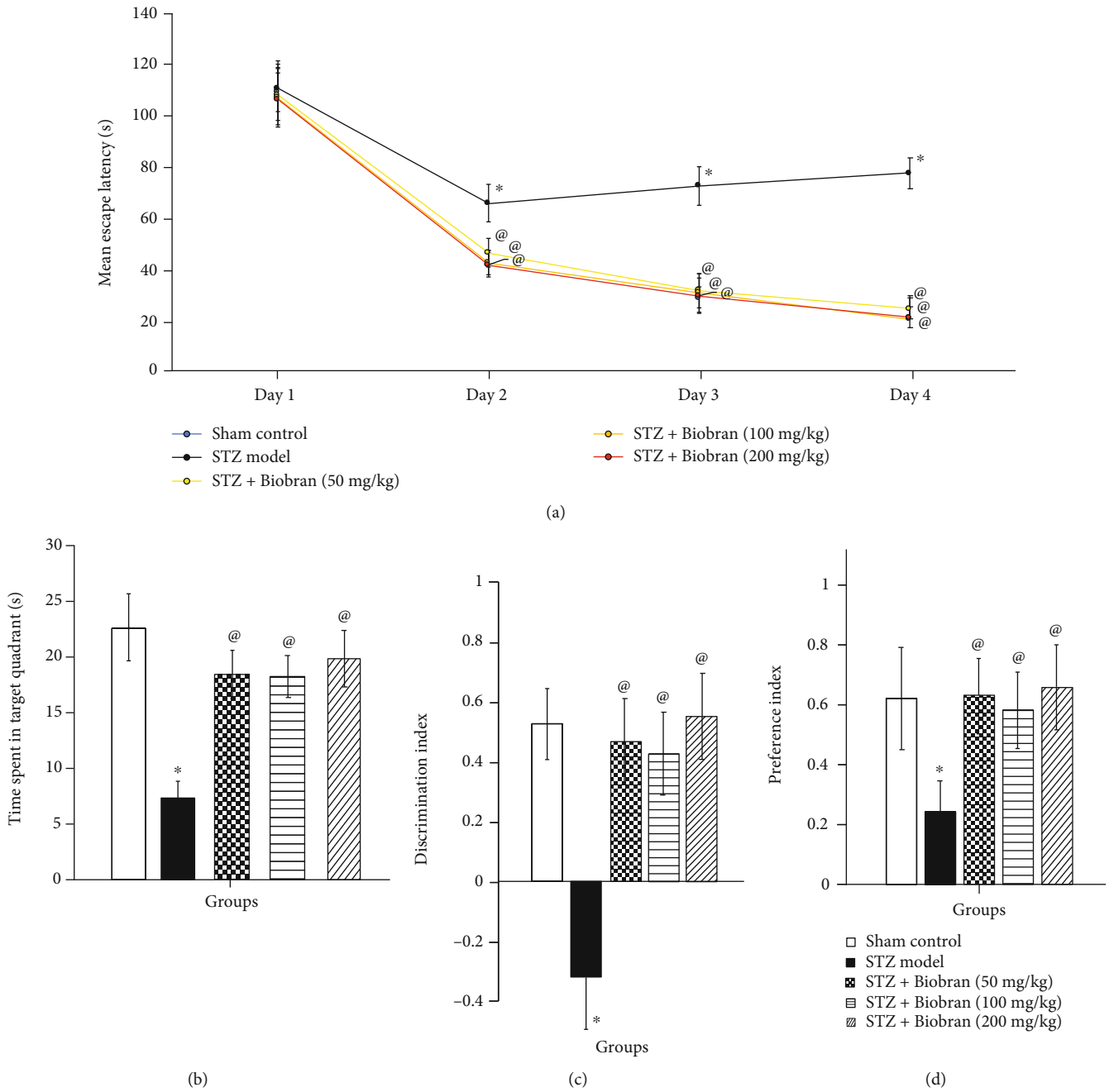

Figure 3: Effect of Biobran on the cognitive functions in MWM and NOR tasks in ICV-STZ injected mice. (a) Effect of Biobran on MEL in MWM. (b) Effect of Biobran on time spent in target quadrant in MWM. (c) Effect of Biobran on the discrimination index in NOR. (d) Effect of Biobran on the preference index in NOR. Values are expressed as mean ± SD; $n = 12$. Statistical analyses were performed using one-way analysis of variance (ANOVA) followed by the Tukey-Kramer post hoc test. *Significantly different from normal group at $p < 0.05$. @Significantly different from ICV-STZ group at $p < 0.05$.

USA). The results are presented in arbitrary units after normalization to levels of the β-actin protein.

2.8.4. Histopathological Analysis of Brain

(1) H & E Staining. The brain of 3 mice in each group was excised and fixed in 10% formol saline for 24 h. Washing was done in tap water then serial dilutions of alcohol (methyl, ethyl, and absolute ethyl) were used for dehydration. Specimens were cleared in xylene and embedded in paraffin at 56°C in a hot air oven for 24 h. Paraffin bees wax tissue blocks were prepared for sectioning at 4 μm thickness by sledge microtome. The obtained tissue sections were collected on glass slides, deparaffinized, and stained by hematoxylin & eosin (H&E) stain for examination using a light electric microscope [45].

Table 1: Effect of Biobran (50, 100, and 200 mg/kg) on spontaneous alternation behavior in Y-maze task in ICV-STZ-injected mice. Values are expressed as mean ± SD; $n = 12$. Statistical analyses were performed using one-way analysis of variance (ANOVA) followed by the Tukey-Kramer post hoc test. * Significantly different from the normal group at $P < 0.05$, @Significantly different from the ICV-STZ group at $P < 0.05$.

Groups	Sham control	STZ model	STZ + Biobran (50 mg/kg)	STZ + Biobran (100 mg/kg)	STZ + Biobran (200 mg/kg)
% Spontaneous alternation	68.29 ± 2.07	*35.72 ± 1.72	@55.79 ± 1.55	@59.32 ± 1.68	@65.87 ± 2.05

(2) Congo Red Staining. For Congo red staining, sections were stained with Congo red solution (0.2%) for 1 h and then counter-stained with hematoxylin solution. Plaques were observed and captured at 400 X magnification under a fluorescent microscope.

2.9. Statistical Analysis. Data are presented as mean ± S.D. Mean escape latency in Morris water maze trials was analyzed by repeated-measures analysis of variance (ANOVA). The remaining results were analyzed using one-way ANOVA followed by Tukey's multiple comparison test. Statistical analysis was performed using GraphPad Prism© software (version 6.01; Graph Pad Software, California, USA). For all the statistical tests, the level of significance was fixed at $P < 0.05$.

3. Results

3.1. Biobran's acute toxicity was investigated. We found no mortality, toxicity, or general behavior changes over a 24 h period at a dose of 2 g/kg

3.2. Neurobehavioral Analysis. The effects of STZ and Biobran (50, 100, and 200 mg/kg) on neurobehavioral tests were conducted within 24 h of the last day of Biobran injection.

3.2.1. Mean Escape Latency (MEL). Figure 3(a) shows that the MEL in the MWM for STZ-treated mice was significantly higher (159%) than the MEL of the sham control mice at day 2, an effect that further increased at day 3 and 4. Mice treated with Biobran, on the other hand, had MEL values that were similar to the sham control starting on day 2.

3.2.2. Time Spent in the Target Quadrant. Studies of Biobran's effect on time spent in the target quadrant of the MWM revealed that STZ-treated mice spent 32.6% of the time in the quadrant in comparison with the sham control, while animals treated with 50, 100, and 200 mg/kg of Biobran spent 81.7%, 81.0%, and 88.1% of the time, respectively, as compared to STZ-treated mice [$F(4, 55) = 92.80$, $P < 0.0001$] (Figure 3(b)).

3.2.3. Discrimination and Preference Indices in the Novel Object Recognition (NOR) Test. The NOR test is used to examine the effect of STZ and Biobran on discrimination and preference indices. Administration of STZ in mice resulted in a decrease of the discrimination index compared to sham-control mice; on the other hand, it was increased significantly after Biobran administration in a dose-dependent manner. Additionally, the time ICV-STZ injected mice spent exploring the novel object was 39% of the time of the sham control group, which reflects a lower preference index. On the other hand, mice supplemented with Biobran were observed to prefer the novel object over the familiar object, normalizing the preference index in a dose-dependent manner (Figures 3(c) and 3(d)).

3.2.4. Spontaneous Alternation Behavior in Y-Maze Task. The ICV-STZ group exhibited a significantly lower percentage of spontaneous alteration behavior, as compared to sham control mice. Treatment with different doses of Biobran resulted in a significant increase in the percentage of spontaneous alteration behavior, as compared to the ICV-STZ group [$F(4, 55) = 37.90$, $P < 0.0001$]. Thus, Biobran attenuated the STZ-induced impairment in short term memory as its administration caused a significant elevation in the percentage of spontaneous alteration behavior (Table 1).

3.3. Oxidative Stress Biomarkers. The levels of MDA and GSH in the hippocampus were measured to investigate Biobran's protective effect on oxidative stress biomarkers. Administration of STZ resulted in a significant decrease of the GSH level by 15.5% compared to the sham control mice However, the administration of Biobran resulted in a significant increase in GSH content in a dose-dependent manner that was maximized at 82.8% at 200 mg/kg compared to ICV-STZ-injected mice [$F(4, 40) = 771.4$, $P < 0.0001$]. On the other hand, intracerebroventricular injection of STZ produced a significant increase in the MDA levels compared to sham control mice. Biobran supplementation for SAD mice reduced the MDA level in a dose-dependent manner compared to STZ-injected mice [$F(4, 40) = 2180$, $P < 0.0001$]. Moreover, Biobran (200 mg/kg) decreased significantly the MDA level as compared to Biobran (50 mg/kg) (Figure 4).

Oxidative stress was further studied via the expression of Nrf2 and ARE. Mice treated with STZ exhibited a significant decrease in hippocampal Nrf2 and ARE levels as compared to sham control mice, while exposure to Biobran resulted in a dose-dependent reversal of the expression of Nrf2 and ARE as compared to STZ-injected mice [$F(4, 40) = 285.5$, $P < 0.0001$], [$F(4, 40) = 455.5$, $P < 0.0001$], respectively, where a high dose of Biobran (200 mg) approximately returned Nrf2 and ARE levels to that of control (Figure 5).

3.4. Amyloid $\beta_{1\text{-}42}$. STZ-treated mice exhibited approximately a 4-fold increase in Aβ expression in comparison with the sham control. The Aβ levels were significantly decreased in STZ-treated mice after administration of Biobran to STZ injected mice [$F(4, 40) = 2348$, $P < 0.0001$]. The effect was

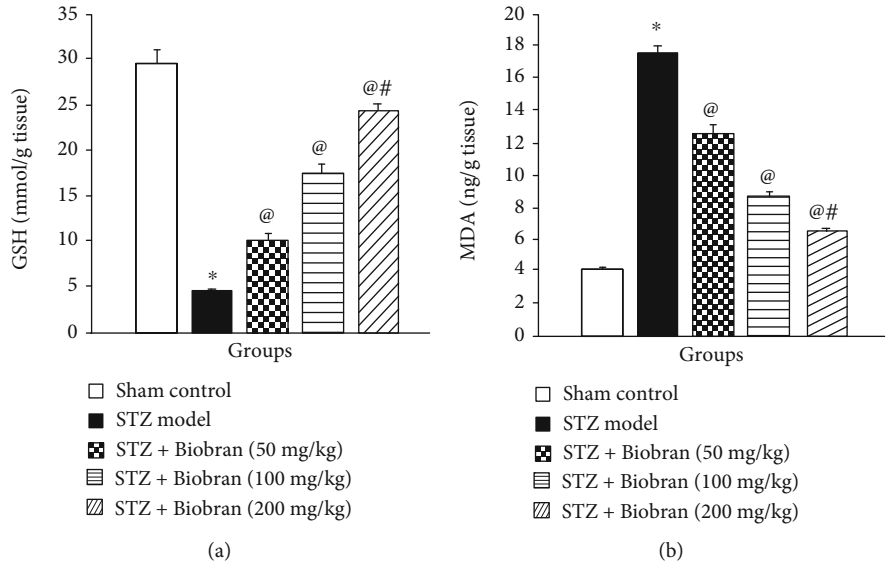

Figure 4: Effect of Biobran on MDA and GSH in ICV-STZ-injected mice. Values are expressed as mean ± SD; $n = 6$. Statistical analyses were performed using one-way analysis of variance (ANOVA) followed by the Tukey-Kramer post hoc test. *Significantly different from normal group at $p < 0.05$. @Significantly different from ICV-STZ group at $p < 0.05$. #Significantly different from Biobran (50 mg/kg) at $p < 0.05$.

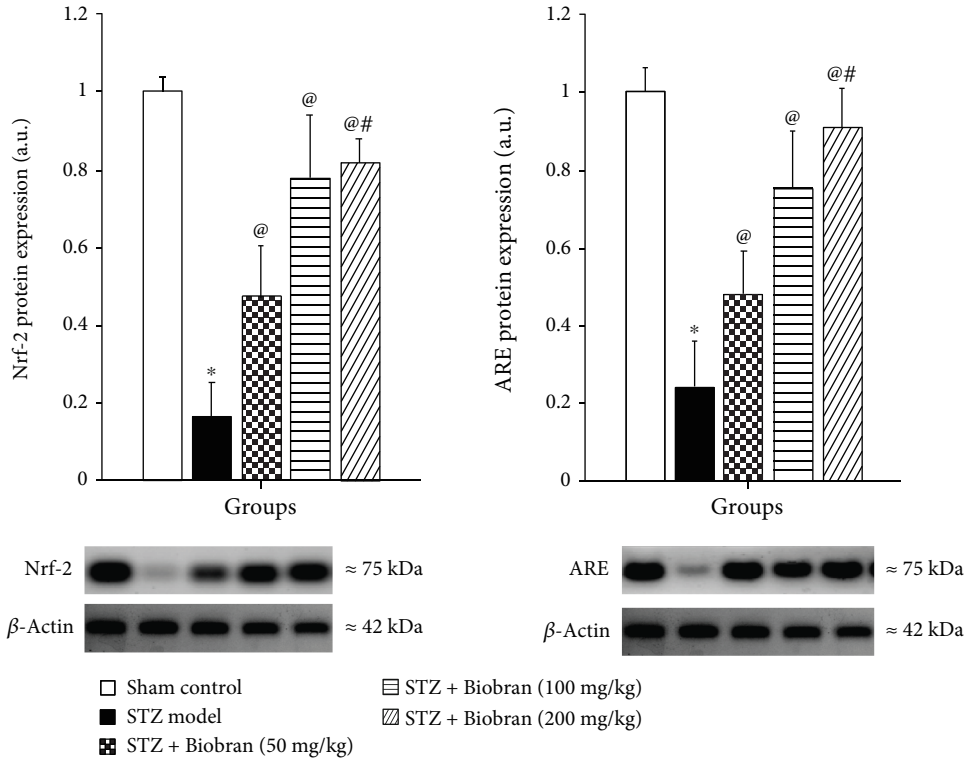

Figure 5: The effect of Biobran on Nrf2 and ARE in ICV-STZ-injected mice. Values are expressed as mean ± SD; $n = 3$. Statistical analyses were performed using one-way analysis of variance (ANOVA) followed by the Tukey-Kramer post hoc test. *Significantly different from normal group at $p < 0.05$. @Significantly different from ICV-STZ group at $p < 0.05$. #Significantly different from Biobran (50 mg/kg) at $p < 0.05$.

dose-dependent, reaching the lowest level for 200 mg/kg (Figure 6).

3.5. Inflammatory Biomarkers. In AD and many other diseases, autoimmune and inflammatory processes can be stimulated by IL-6. STZ-treated mice had a significant increase in IL-6 and ICAM-1 expression as compared to control mice. However, Biobran supplementation suppressed the levels of these markers in a dose-dependent manner that reached the control level at 200 mg/kg as compared to ICV-STZ mice

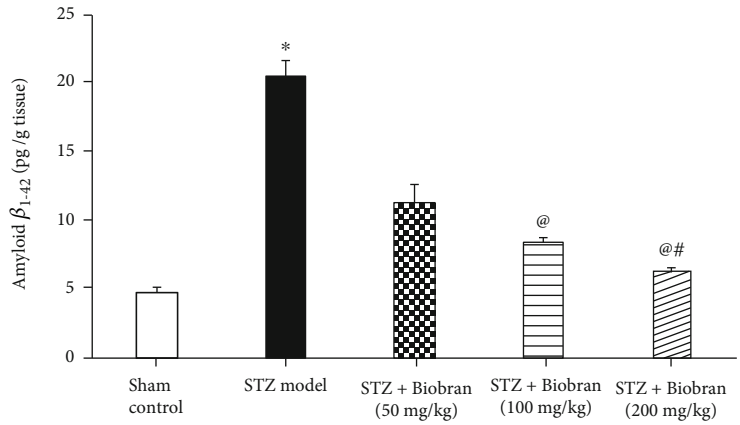

Figure 6: The effect of Biobran on $A\beta_{1-42}$ in ICV-STZ-injected mice. Values are expressed as mean ± SD; $n = 6$. Statistical analyses were performed using one-way analysis of variance (ANOVA) followed by the Tukey-Kramer post hoc test, *Significantly different from normal group at $p < 0.05$. @Significantly different from ICV-STZ group at $p < 0.05$. #Significantly different from Biobran (50 mg/kg) at $p < 0.05$.

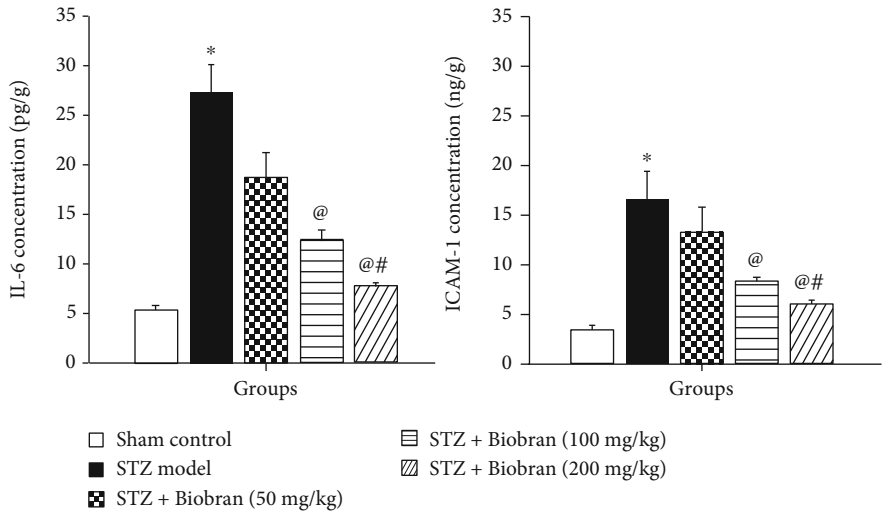

Figure 7: Effect of Biobran on IL-6 and ICAM-1 in ICV-STZ-injected mice. Values are expressed as mean ± SD; $n = 6$. Statistical analyses were performed using one-way analysis of variance (ANOVA) followed by the Tukey-Kramer post hoc test. *Significantly different from normal group at $p < 0.05$. @Significantly different from ICV-STZ group at $p < 0.05$. #Significantly different from Biobran (50 mg/kg) at $p < 0.05$.

$[F(4, 40) = 646.2,\ P < 0.0001]$ and $[F(4, 40) = 857.1,\ P < 0.0001]$, respectively (Figure 7).

3.6. Apoptotic Biomarkers. STZ-treated mice exerted a significantly increased expression of Bax while simultaneously showing a decrease in Bcl-2 expression in comparison to sham control. The Bax/Bcl-2 ratio in STZ-treated mice is 38 times greater compared to the ratio for sham control mice. In contrast, mice supplemented with Biobran demonstrated a dose-dependent reversal of Bax and Bcl-2 expression relative to STZ-treated mice. At the highest Biobran concentration, both Bax and Bcl-2 expression were comparable to the sham control level, with the Bax/Bcl-2 ratio being only 1.5 times as high as the sham control (Figure 8(a)). A similar effect was seen for cleaved caspase-3 expression. In STZ mice, cleaved caspase-3 levels increased approximately 5-fold relative to control. Following supplementation with Biobran, STZ-treated mice exhibited a gradual decrease in cleaved caspase-3 expression in a dose-dependent manner $[F(4, 40) = 1728,\ P < 0.0001]$ (Figure 8(b)).

We furthermore analyzed the expression of FOXO3a protein. A significant increase by 5-fold in the expression of FOXO3a was revealed in STZ-treated mice relative to control. Following supplementation with Biobran, FOXO3a expression in STZ-treated mice decreased in a dose-dependent manner, with the highest dose (200 mg) nearly bringing FOXO3a expression back to the level of control compared to STZ-injected mice $[F(4, 25) = 670.3,\ P < 0.0001]$, respectively] (Figure 9).

3.7. Histopathology Analysis. Brains of sham control mice showed normal structure of the brain tissue including the cerebral cortex and the hippocampus. Microscopic

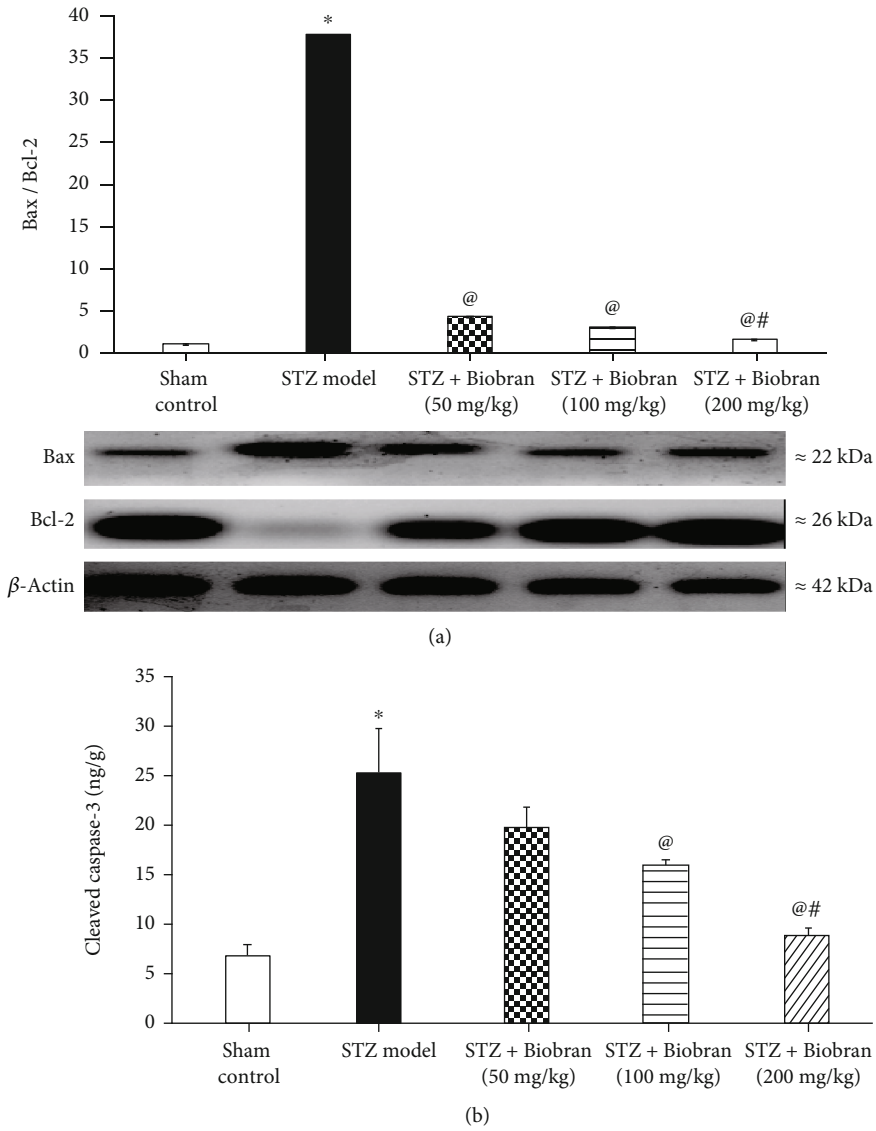

Figure 8: Effect of Biobran on the ratio of Bax to Bcl-2 (a) and cleaved Caspase-3 (b) in ICV-STZ-injected mice. Values are expressed as mean ± SD; $n = 3$. Statistical analyses were performed using one-way analysis of variance (ANOVA) followed by the Tukey-Kramer post hoc test. *Significantly different from normal group at $p < 0.05$. @Significantly different from ICV-STZ group at $p < 0.05$. #Significantly different from Biobran (50 mg/kg) at $p < 0.05$.

examination of the STZ group showed several histopathological changes in the brain tissue. The cerebral cortex showed numerous scattered dark degenerated neurons that were associated with neuronophagia and diffuse gliosis. The hippocampus showed multifocal haemorrhagic areas with dark degenerated neurons in the CA3, CA4, and DG regions.

Mice treated with Biobran (50 mg/kg) ameliorated the effects of STZ. Sections of the cerebral cortex showed decreased numbers of dark neurons with healthy neurons in most examined sections. The hippocampus showed normal neurons in the various neurological regions.

Mice treated with Biobran (100 mg/kg and 200 mg/kg) showed normal histological structure of the cerebral cortex except for few degenerated neurons and neuronophagia. The hippocampus appeared apparently normal.

The administration of Biobran showed no histopathological alterations in the brain tissue with normal structure of the cerebral cortex and the hippocampus (Figures 10 and 11).

The number of amyloid plaques was investigated in different experimental groups through visualization with Congo red stain. Normal mice showed no amyloid deposition in the brain sections. Meanwhile, ICV injection of STZ showed multifocal deposition of the amyloid deposition in the brain tissue especially in the inflammatory lesion that showed focal gliosis. The administration of Biobran (50 mg/kg) resulted in a marked reduction of the number of amyloid plaques in the brain tissue. Moreover, mice that received Biobran (100 mg/kg) showed few amyloid plaques, and mice that received Biobran (200 mg/kg) showed an absence of amyloid plaques in most examined brain tissue (Figure 12).

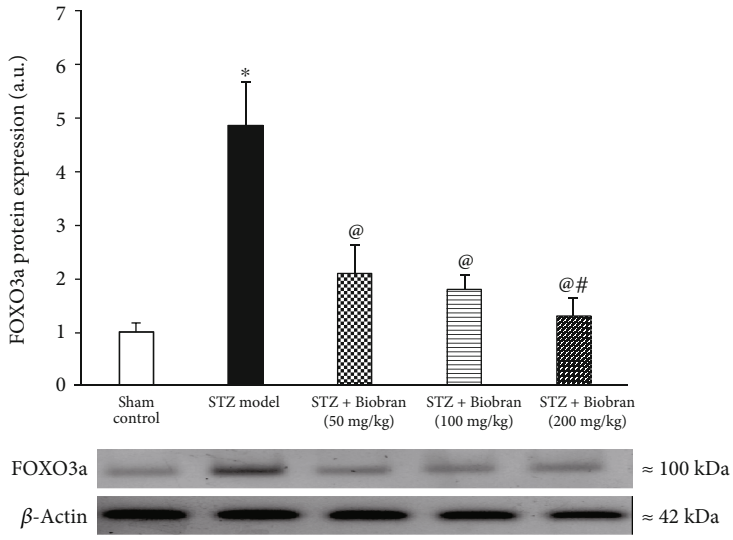

Figure 9: Effect of Biobran on FOXO3a in ICV-STZ injected mice. Values are expressed as mean ± SD; $n = 3$. Statistical analyses were performed using one-way analysis of variance (ANOVA) followed by the Tukey-Kramer post hoc test. *Significantly different from normal group at $p < 0.05$. @Significantly different from ICV-STZ group at $p < 0.05$. #Significantly different from Biobran (50 mg/kg) at $p < 0.05$.

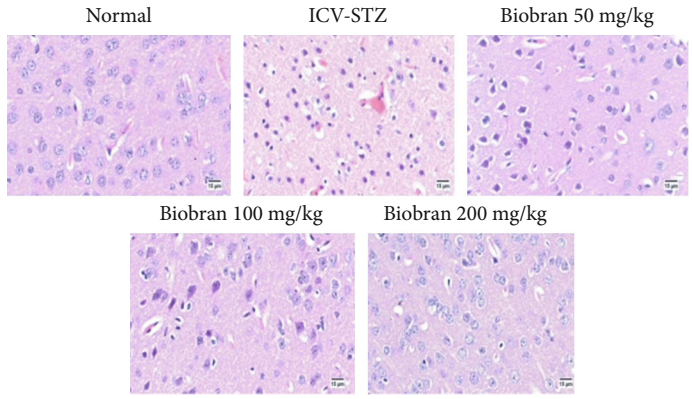

Figure 10: Effect of Biobran (50, 100, and 200 mg/kg) on histopathological changes in the cerebral cortex of ICV-STZ injected mice, $n = 3$. Control: showing normal histological structure of the cerebral cortex of normal mice; ICV-STZ: showing diffuse gliosis in the cerebral cortex admixed with numerous degenerated neurons in the injected mice; Biobran 50 mg/kg: showing moderate number of degenerated neurons; Biobran 100 mg/kg: showing few injured neurons; Biobran 200 mg/kg: showing apparently normal cerebral cortex structure.

4. Discussion

The current study evaluated the protective effect of Biobran/MGN-3 against STZ-induced SAD in mice. Biobran, a natural biological response modifier, has been shown to possess antiaging [29–31] and antioxidant [37] properties. Biobran is proved previously to exhibit potent immunomodulatory functions [26, 27, 46–48] and exert beneficial effects against cancer, viruses, and microbes [49–52].

In the present study, STZ-treated mice were unable to discriminate between novel and familiar objects, as demonstrated by the NOR task. The ICV-STZ group revealed marked deterioration in memory and learning functions as observed in the Morris water maze and manifested by a significant decrease in the time spent in the target quadrant as well as in the Y-maze tests demonstrated by a significant decline in the spontaneous alternation behavior. These findings are in agreement with previous studies reporting that ICV-STZ injection was implicated in decreased spontaneous alternation behavior in the Y-maze test and a decline in spatial learning and reference memory in Morris water maze trials as well as the test day [53, 54]. This indicates obvious memory and learning deficits in these mice. The ICV injection of STZ is a well-known model of sporadic Alzheimer's disease in rodents with similar progressive pathology of AD as in the human brain [55–57]. However, it was of great interest to note that Biobran supplementation prevented the STZ-induced impairments of short-term and spatial memory. In a dose-dependent manner, Biobran reduced the MEL time, extended the time spent in the target quadrant, and reversed the discrimination and preference indices as well as decreasing the spontaneous alternation behavior in the Y-maze task.

Coherent to the aforementioned findings, it was found that the cognitive dysfunction exerted a positive impact on

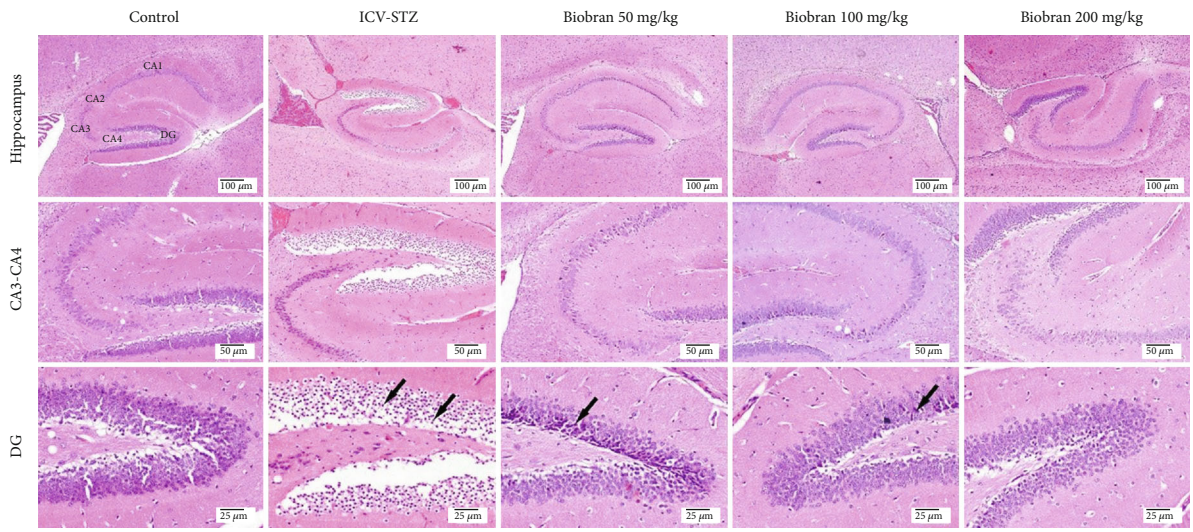

Figure 11: Effect of Biobran (50, 100, and 200 mg/kg) on histopathological changes in the hippocampus of ICV-STZ-injected mice, $n = 3$. Control: showing normal histological structure of different CA regions and DG of the hippocampus of normal mice; ICV-STZ: showing edema of CA1, CA2, and DG with dark-degenerated neurons in CA3, CA4, and DG (arrows) in the hippocampus and congestion in the surrounding brain parenchyma; Biobran 50 mg/Kg: showing dark degenerated neurons in the CA1, CA4, and DG regions (arrow) of the hippocampus; Biobran 100 mg/Kg: showing apparently normal neurons in the hippocampus with few scattered neurons in CA4 and DG (arrow); Biobran 200 mg/Kg: showing apparently normal neurons in the hippocampus.

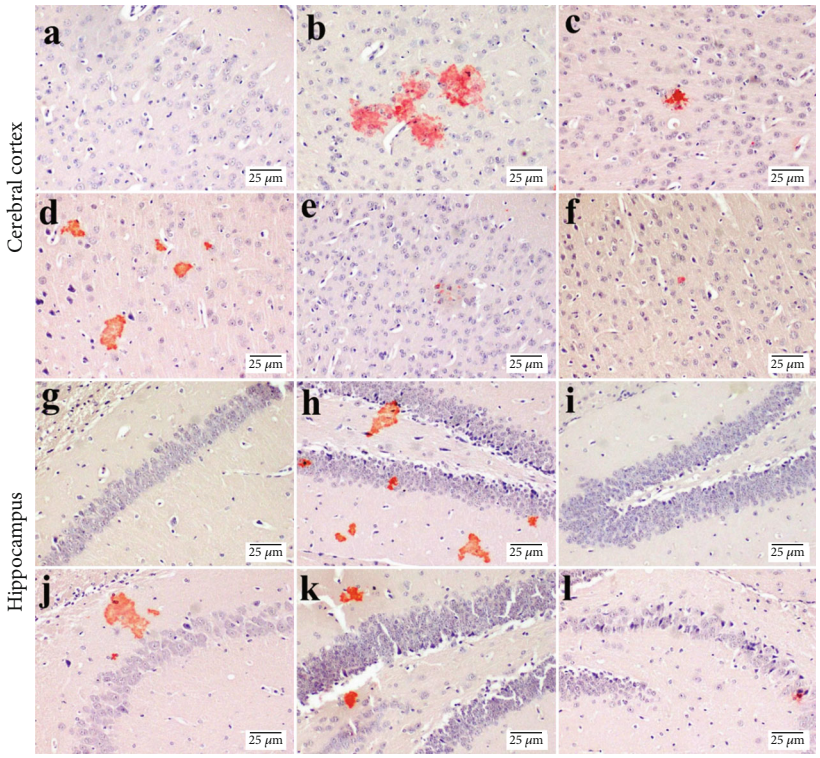

Figure 12: Congo red—brain-stained sections of mice for amyloid plaques visualization in the cerebral cortex and hippocampus ($n = 3$). (a, g, i) represent the normal group showing no deposition of amyloid plaques. (b, h) represent the STZ group showing multifocal deposition in the cerebral cortex in the cerebral cortex and the hippocampus, respectively. (c, d, j) represent Biobran (50 mg/kg) in STZ-injected mice, showing multifocal scattered plaques. (e, k) represent Biobran (100 mg/kg) in STZ-injected mice, showing few deposition in the cerebral cortex and multifocal deposition in the hippocampus. (f, l) represent Biobran (200 mg/kg) in STZ-injected mice showing minute deposition of amyloid plaques.

the amyloidogenic and oxidative stress pathways. Aβ peptide is one of the hallmarks of AD causing neuronal loss in the brain and resulting into deficits in memory and learning. Previous studies revealed that antioxidant compounds could be promising therapeutic or preventive interventions for AD patients because they inhibit Aβ fibril formation and protect the brain from Aβ neurotoxicity [58]. In the current study, Biobran exerted a significant antioxidant effect in the model of SAD, which is in agreement with previous studies that revealed Biobran's antioxidant activity against murine solid Ehrlich carcinoma [28], as well as its ability to significantly alleviate the increase in MDA content and prevent the irradiation-induced depletion of GSH in mice spleens [59].

ROS generation caused by mitochondrial oxidative phosphorylation can have profound effects on cellular functions and result in the initiation of many diseases, including aging [60] and AD [2, 61]. During oxidative stress, ROS can lead to neuronal synaptic dysfunction [62, 63] and may cause neuronal damage and death during Aβ self-aggregation [64]. Biobran has been shown previously to upregulate the oxidative stress in the liver and to inhibit the levels of these biomarkers including MDA, total free radicals, and nitric oxide in murine Ehrlich carcinoma [28]. This suggests that Biobran induces oncostatic activity by providing protection against oxidative stress, modulating lipid peroxidation, and enhancing the antioxidant defense system. Moreover, it was reported previously that Nrf2 is suppressed in AD patients' neurons [65], which is in harmony with the results of the present study. For AD animals, there is a decrease in Nrf2 expression, as well as in the expression of the Nrf2/ARE pathway's target genes [66]. Altered expression in Nrf2 is associated with cognitive deficits and impaired spatial memory in mouse models of AD [6] and a deficiency in Nrf2 results in vulnerability to oxidative stress [67], phosphorylated-Tau [68], and enhanced autophagic dysfunction [7]. On the other hand, it was revealed previously that neurons can be protected against Aβ pathology and oxidative proteotoxic stress by the upregulation of the Nrf2/ARE pathway [69, 70]. Several studies have shown that neuropathological changes such as AD and Parkinson's are also associated with faulty inflammatory processes such as increased expression of the proinflammatory cytokine IL-6 in the brain [11, 12]. In the current study, IL-6 and ICAM-1 were significantly increased after STZ administration, but Biobran supplementation caused a significant decrease in the levels of these biomarkers. Interestingly, a recent clinical study revealed the increased concentrations of IL-6 and ICAM-1 in AD patients' cerebrospinal fluid (CSF) [71, 72]. These effects were more evident in patients with abnormal CSF Aβ levels, indicating that, in the presence of Aβ pathology, associations between cerebrovascular, neurodegenerative, and neuroinflammatory processes may be aggravated and contribute to tau aggregation, leading to cognitive impairment and disease progression [71]. Therefore, focusing on these biomarkers offers potential targets for novel therapeutic interventions. In the present work, the administration of Biobran significantly inhibited the levels of ICAM-1 and IL-6 in the hippocampi of SAD-induced mice with significant accumulation of amyloid plaques.

In the present study, Biobran exerted an antiapoptotic effect against STZ in a dose-dependent manner. This effect could be due to suppression of cleaved caspase-3 as well as the proapoptotic protein Bax and through the downregulation of the antiapoptotic protein Bcl-2. It has been suggested previously that Aβ activates the neuronal apoptotic pathway via its accumulation in the mitochondrial membrane and impairment of mitochondrial function [73]. The membrane of mitochondria becomes permeable during mitochondrial apoptosis, and ROS gets released [74]. Apoptogenic proteins such as cytochrome c can thereby be produced, and proapoptotic factors can be introduced into the cytosol from the mitochondria, ultimately activating procaspases and inducing apoptosis [75]. Neuronal loss can be caused by mitochondrial dysfunction via the regulation of proapoptotic proteins like caspase-3 and Bax and antiapoptotic proteins like Bcl-2 [14, 15, 20]. The ability of Biobran to exert a protective effect against STZ-induced apoptosis is in accordance with our earlier studies showing that Biobran treatment upregulated Bax expression, activated caspase-3, and downregulated Bcl-2 expression; these well-established molecular events in apoptosis have shown that Biobran can protect against glandular stomach carcinogenesis in rats [49], inhibit hepatocarcinogenesis in rats [50], and enhance fractionated X-ray irradiation's anticancer effects for Ehrlich solid tumor-bearing mice [59].

The effect of Biobran on FOXO protein expression in STZ-injected mice hippocampi was also examined. FOXO proteins have a range of biological functions. They are present throughout the body and are selectively expressed in the nervous system. The complex interaction between signal transduction pathways and FOXO proteins in the presence of oxidative stress can significantly impact apoptosis and autophagy [18, 20, 76]. Under oxidative stress conditions, autophagy can be induced by FOXO proteins along with the promotion of cell survival [64]. STZ-injected mice showed significantly higher levels of the FOXO protein expression. Biobran decreased significantly these values in a dose-dependent manner. This demonstrates Biobran's protective effect against FOXO-mediated apoptosis in STZ-treated mice. Recently, it was reported that Biobran/MGN-3 is a promising psychoneuroimmune modulatory agent that could improve the quality of life in healthy old adults [31].

Histopathological analysis using H&E and Congo red stainings further revealed the protective effect of Biobran against STZ-induced neuronal damage in the cerebral cortex and hippocampal sections of mice. Treatment with Biobran reduced the neuronal toxicity observed in STZ-injected mice, with fewer eosinophilic-stained neurons and more healthy neurons with prominent nuclei. This indicates that Biobran could act as a potential candidate to attenuate neurodegeneration and preserve cognitive functions. Hippocampal sections of Biobran-treated groups also exhibited a dose-dependent protective effect against Aβ plaque formation. These positive histological effects of Biobran are in agreement with our behavioral and biochemical assessments. The highest dose of Biobran exerted better protection compared to the low and moderate doses.

5. Conclusions

Biobran exerts a dose-dependent protective effect against sporadic AD. This effect is achieved through the targeting of the Nrf2/ARE antioxidant signaling that modulates amyloidogenesis as well as the Bcl2/Bax/caspase-3 pathway. To our knowledge, the present study is the first to investigate the protective effect of Biobran against SAD. Our findings suggest that Biobran's activity is able to reduce Aβ generation and promotes cognitive function recovery. They may suggest the possible applicability of Biobran in clinical trials of human subjects in the management of SAD.

Data Availability

The data of the present study including the figures and western blot analysis used to support the findings of this study are included within the article.

Conflicts of Interest

The authors declare there are no conflicts of interest.

Authors' Contributions

M Ghoneum and N El Sayed planned the study and wrote the manuscript. N El Sayed designed and performed the experiments. Both authors approved the manuscript.

Acknowledgments

Biobran/MGN-3 was provided by Daiwa Pharm. Co., Ltd, Japan. This work was funded by Diawa Pharmaceutical Co., Ltd., Tokyo, Japan; Grant #T0099108.

References

[1] A. Nunomura, G. Perry, M. A. Pappolla et al., "Neuronal oxidative stress precedes amyloid-beta deposition in Down syndrome," *Journal of Neuropathology and Experimental Neurology*, vol. 59, no. 11, pp. 1011–1017, 2000.

[2] M. C. Polidori, "Oxidative stress and risk factors for Alzheimer's disease: clues to prevention and therapy," *Journal of Alzheimer's Disease*, vol. 6, no. 2, pp. 185–191, 2004.

[3] M. Bélanger, I. Allaman, and P. J. Magistretti, "Brain energy metabolism: focus on astrocyte-neuron metabolic cooperation," *Cell Metabolism*, vol. 14, no. 6, pp. 724–738, 2011.

[4] M. P. Mattson, "Pathways towards and away from Alzheimer's disease," *Nature*, vol. 430, no. 7000, pp. 631–639, 2004.

[5] P. Flagmeier, S. De, D. C. Wirthensohn et al., "Ultrasensitive Measurement of CA^{2+} Influx into Lipid Vesicles Induced by Protein Aggregates," *Angewandte Chemie (International Ed. in English)*, vol. 56, no. 27, pp. 7750–7754, 2017.

[6] K. Kanninen, R. Heikkinen, T. Malm et al., "Intrahippocampal injection of a lentiviral vector expressing Nrf2 improves spatial learning in a mouse model of Alzheimer's disease," *Proceedings of the National Academy of Sciences of the United States of America*, vol. 106, no. 38, pp. 16505–16510, 2009.

[7] G. Joshi, K. A. Gan, D. A. Johnson, and J. A. Johnson, "Increased Alzheimer's disease-like pathology in the APP/PS1ΔE9 mouse model lacking Nrf2 through modulation of autophagy," *Neurobiology of Aging*, vol. 36, no. 2, pp. 664–679, 2015.

[8] P. Milani, G. Ambrosi, O. Gammoh, F. Blandini, and C. Cereda, "SOD1 and DJ-1 Converge at Nrf2 Pathway: A Clue for Antioxidant Therapeutic Potential in Neurodegeneration," *Oxidative Medicine and Cellular Longevity*, vol. 2013, Article ID 836760, 12 pages, 2013.

[9] A. Gugliandolo, P. Bramanti, and E. Mazzon, "Role of Vitamin E in the Treatment of Alzheimer's Disease: Evidence from Animal Models," *International Journal of Molecular Sciences*, vol. 18, no. 12, p. 2504, 2017.

[10] Y. Tian, W. Wang, L. Xu et al., "Activation of Nrf2/ARE pathway alleviates the cognitive deficits in PS1V97L Tg mouse model of Alzheimer's disease through modulation of oxidative stress," *Journal of Neuroscience Research*, vol. 97, no. 4, pp. 492–505, 2018.

[11] I. M. Cojocaru, M. Cojocaru, G. Miu, and V. Sapira, "Study of interleukin-6 production in Alzheimer's disease," *Romanian Journal of Internal Medicine*, vol. 49, no. 1, pp. 55–58, 2011.

[12] Q. Alam, M. Zubair Alam, G. Mushtaq et al., "Inflammatory Process in Alzheimer's and Parkinson's Diseases: Central Role of Cytokines," *Current Pharmaceutical Design*, vol. 22, no. 5, pp. 541–548, 2016.

[13] R. Pola, A. Flex, E. Gaetani et al., "Intercellular adhesion molecule-1 K469E gene polymorphism and Alzheimer's disease," *Neurobiology of Aging*, vol. 24, no. 2, pp. 385–387, 2003.

[14] L. H. Broise, A. R. Gottschalk, J. Quintáns, and C. B. Thompson, "Bcl-2 and Bcl-2-related proteins in apoptosis regulation," *Current Topics in Microbiology and Immunology*, vol. 200, pp. 107–121, 1995.

[15] E. Castre´n, Y. Ohga, M. P. Berzaghi, G. Tzimagiorgis, H. Thoenen, and D. Lindholm, "*bcl*-2 Messenger RNA is localized in neurons of the developing and adult rat brain," *Neuroscience*, vol. 61, no. 1, pp. 165–177, 1994.

[16] V. M. Renault, P. U. Thekkat, K. L. Hoang et al., "The prolongevity gene *FoxO3* is a direct target of the p53 tumor suppressor," *Oncogene*, vol. 30, no. 29, pp. 3207–3221, 2011.

[17] J. Hou, S. Wang, Y. Chen Shang, Z. Zhong Chong, and K. Maiese, "Erythropoietin employs cell longevity pathways of SIRT1 to foster endothelial vascular integrity during oxidant stress," *Current Neurovascular Research*, vol. 8, no. 3, pp. 220–235, 2011.

[18] S. Peng, S. Zhao, F. Yan et al., "HDAC2 selectively regulates foxo3a-mediated gene transcription during oxidative stress induced neuronal cell death," *The Journal of Neuroscience*, vol. 35, no. 3, pp. 1250–1259, 2015.

[19] S. Wang, Z. Zhong Chong, Y. Chen Shang, and K. Maiese, "WISP1 neuroprotection requires FoxO3a post-translational modulation with autoregulatory control of SIRT1," *Current Neurovascular Research*, vol. 10, no. 1, pp. 54–69, 2013.

[20] C. Charvet, I. Alberti, F. Luciano et al., "Proteolytic regulation of Forkhead transcription factor FOXO3a by caspase-3-like proteases," *Oncogene*, vol. 22, no. 29, pp. 4557–4568, 2003.

[21] Y. C. Shang, Z. Z. Chong, J. Hou, and K. Maiese, "Wnt1, FoxO3a, and NF-κB oversee microglial integrity and activation during oxidant stress," *Cellular Signalling*, vol. 22, no. 9, pp. 1317–1329, 2010.

[22] M. Salkovic-Petrisic, A. Knezovic, S. Hoyer, and P. Riederer, "What have we learned from the streptozotocin-induced animal model of sporadic Alzheimer's disease, about the

therapeutic strategies in Alzheimer's research," *Journal of Neural Transmission (Vienna)*, vol. 120, no. 1, pp. 233–252, 2013.

[23] P. K. Kamat, A. Kalani, S. Rai, S. K. Tota, A. Kumar, and A. S. Ahmad, "Streptozotocin Intracerebroventricular-Induced Neurotoxicity and Brain Insulin Resistance: a Therapeutic Intervention for Treatment of Sporadic Alzheimer's Disease (sAD)-Like Pathology," *Molecular Neurobiology*, vol. 53, no. 7, pp. 4548–4562, 2016.

[24] D. Hsu and G. A. Marshall, "Primary and Secondary Prevention Trials in Alzheimer Disease: Looking Back, Moving Forward," *Current Alzheimer Research*, vol. 14, no. 4, pp. 426–440, 2017.

[25] C. Patterson, *World Alzheimer Report 2018: The state of the art of dementia research: new frontiers*, Alzheimer's Disease International, London, 2018.

[26] M. Ghoneum, "Anti-HIV Activity *in Vitro* of MGN-3, an Activated Arabinoxylane from Rice Bran," *Biochemical and Biophysical Research Communications*, vol. 243, no. 1, pp. 25–29, 1998.

[27] M. Ghoneum, "From bench to bedside: The growing use of arabinoxylan rice bran (MGN-3/Biobran) in cancer immunotherapy," *Austin Immunology*, vol. 1, p. 1006, 2016.

[28] E. Noaman, N. K. Badr el-Din, M. A. Bibars, A. A. Abou Mossallam, and M. Ghoneum, "Antioxidant potential by arabinoxylan rice bran, MGN-3/biobran, represents a mechanism for its oncostatic effect against murine solid Ehrlich carcinoma," *Cancer Letters*, vol. 268, no. 2, pp. 348–359, 2008.

[29] M. Ghoneum and S. Abedi, "Enhancement of natural killer cell activity of aged mice by modified arabinoxylan rice bran (MGN-3/Biobran)," *The Journal of Pharmacy and Pharmacology*, vol. 56, no. 12, pp. 1581–1588, 2004.

[30] A. F. Elsaid, M. Shaheen, and M. Ghoneum, "Biobran/MGN-3, an arabinoxylan rice bran, enhances NK cell activity in geriatric subjects: A randomized, double-blind, placebo-controlled clinical trial," *Experimental and Therapeutic Medicine*, vol. 15, no. 3, pp. 2313–2320, 2018.

[31] A. F. Elsaid, R. M. Fahmi, M. Shaheen, and M. Ghoneum, "The enhancing effects of Biobran/MGN-3, an arabinoxylan rice bran, on healthy old adults' health-related quality of life: a randomized, double-blind, placebo-controlled clinical trial," *Quality of Life Research*, vol. 29, no. 2, pp. 357–367, 2020.

[32] National Institutes of Health, *National Institutes of Health Guide for Care and Use of Laboratory Animals*, 2011.

[33] K. Tazawa, *BioBran/MGN-3 (Rice Bran Arabinoxylan Deritive): Basic and clinical application to integrative medicine*, Iyakushuppan Co. Publishers, 2006.

[34] M. Ghoneum and J. Brown, "NK immunorestoration of cancer patients by MGN-3, a modified arabinoxylan rice bran (study of 32 patients followed for up to 4 years)," *Wheat and rice in disease prevention and health. Anti-aging medical therapeutics. Vol. III. Klatz R, Goldman R*, R. R. Watson, V. Preedy, and S. Zibadi, Eds., pp. 217–226, 1999.

[35] OECD, "Organization for Economic Cooperation and Development (OECD) Guidelines for Testing of Chemicals. Acute Oral Toxic," *Acute Toxic Class Method*, vol. 423, 2001.

[36] M. A. Pelleymounter, M. Joppa, N. Ling, and A. C. Foster, "Pharmacological evidence supporting a role for central corticotropin-releasing Factor2Receptors in behavioral, but not endocrine, response to environmental stress," *The Journal of Pharmacology and Experimental Therapeutics*, vol. 302, no. 1, pp. 145–152, 2002.

[37] G. I. Warnock, *Study Of The Central Corticotrophin-Releasing Factor System Using The 2- Deoxyglucose Method For Measurement Of Local Cerebral Glucose Utilisation*, Dissertation. University of Bath, 2010.

[38] J. Mehla, M. Pahuja, and Y. K. Gupta, "Streptozotocin-Induced Sporadic Alzheimer's Disease: Selection of Appropriate Dose," *Journal of Alzheimer's Disease*, vol. 33, no. 1, pp. 17–21, 2012.

[39] A. Ennaceur, "One-trial object recognition in rats and mice: Methodological and theoretical issues," *Behavioural Brain Research*, vol. 215, no. 2, pp. 244–254, 2010.

[40] G. M. Morris, "Spatial Localization Does Not Require the Presence of Local Cues," *Learning and Motivation*, vol. 260, pp. 239–260, 1981.

[41] K. Yamada, T. Tanaka, T. Mamiya, T. Shiotani, T. Kameyama, and T. Nabeshima, "Improvement by nefiracetam of β-amyloid-(1-42)-induced learning and memory impairments in rats," *British Journal of Pharmacology*, vol. 126, no. 1, pp. 235–244, 1999.

[42] E. Beutler, O. Duron, and B. Kelly, "Improved method for the determination of blood glutathione," *The Journal of Laboratory and Clinical Medicine*, vol. 61, pp. 882–888, 1963.

[43] M. Mihara and M. Uchiyama, "Determination of malonaldehyde precursor in tissues by thiobarbituric acid test," *Analytical Biochemistry*, vol. 86, no. 1, pp. 271–278, 1978.

[44] O. H. Lowry, N. J. Rosebrough, A. L. Farr, and R. J. Randall, "Protein measurement with the Folin phenol reagent," *The Journal of Biological Chemistry*, vol. 193, no. 1, pp. 265–275, 1951.

[45] J. D. Banchroft, A. Stevens, and D. R. Turner, *Theory and Practice of Histological Techniques*, Churchil Livingstone, New York, London, San Francisco, Tokyo, Fourth edition, 1996.

[46] M. Ghoneum, "Enhancement of human natural killer cell activity by modified arabinoxylan from rice bran (MGN-3)," *International Journal of Immunotherapy*, vol. 14, pp. 89–99, 1998.

[47] A. Pérez-Martínez, J. Valentín, L. Fernández et al., "Arabinoxylan rice bran (MGN-3/Biobran) enhances natural killer cell-mediated cytotoxicity against neuroblastoma *in vitro* and *in vivo*," *Cytotherapy*, vol. 17, no. 5, pp. 601–612, 2015.

[48] M. Ghoneum and S. Agrawal, "Activation of Human Monocyte-Derived Dendritic Cells *in Vitro* by the Biological Response Modifier Arabinoxylan Rice Bran (MGN-3/BIOBRAN)," *International Journal of Immunopathology and Pharmacology*, vol. 24, no. 4, pp. 941–948, 2011.

[49] N. K. Badr El-Din, S. M. Abdel Fattah, D. Pan, L. Tolentino, and M. Ghoneum, "Chemopreventive Activity of MGN-3/Biobran Against Chemical Induction of Glandular Stomach Carcinogenesis in Rats and Its Apoptotic Effect in Gastric Cancer Cells," *Integrative Cancer Therapies*, vol. 15, no. 4, pp. -NP26–NP34, 2016.

[50] N. K. Badr El-Din, D. A. Ali, R. Othman, S. W. French, and M. Ghoneum, "Chemopreventive role of arabinoxylan rice bran, MGN-3/Biobran, on liver carcinogenesis in rats," *Biomedicine & Pharmacotherapy*, vol. 126, p. 110064, 2020.

[51] H. Salama, E. Medhat, M. Shaheen, A. R. N. Zekri, T. Darwish, and M. Ghoneum, "Arabinoxylan rice bran (Biobran) suppresses the viremia level in patients with chronic HCV infection: A randomized trial," *International Journal of Immunopathology and Pharmacology*, vol. 29, no. 4, pp. 647–653, 2016.

[52] M. Ghoneum, M. Matsuura, and S. Gollapudp, "Modified arabinoxylan rice bran (Mgn-3/Biobran) enhances intracellular

killing of microbes by human phagocytic Cellsin vitro," *International Journal of Immunopathology and Pharmacology*, vol. 21, no. 1, pp. 87–95, 2008.

[53] A. M. El Halawany, N. S. E. L. Sayed, H. M. Abdallah, and R. S. E. Dine, "Protective effects of gingerol on streptozotocin-induced sporadic Alzheimer's disease: emphasis on inhibition of β-amyloid, COX-2, alpha-, beta - secretases and APH1a," *Scientific Reports*, vol. 7, no. 1, p. 2902, 2017.

[54] N. O. Abdel Rasheed, N. S. El Sayed, and A. S. El-Khatib, "Targeting central β2 receptors ameliorates streptozotocin-induced neuroinflammation via inhibition of glycogen synthase kinase3 pathway in mice," *Progress in Neuro-Psychopharmacology & Biological Psychiatry*, vol. 86, pp. 65–75, 2018.

[55] A. Sgarbossa, D. Giacomazza, and M. di Carlo, "Ferulic Acid: A Hope for Alzheimer's Disease Therapy from Plants," *Nutrients*, vol. 7, no. 7, pp. 5764–5782, 2015.

[56] M. Khalili and F. Hamzeh, "Effects of active constituents of Crocus sativus L., crocin on streptozocin-induced model of sporadic Alzheimer's disease in male rats," *Iranian Biomedical Journal*, vol. 14, no. 1–2, pp. 59–65, 2010.

[57] P. Liu, L. B. Zou, L. H. Wang et al., "Xanthoceraside attenuates tau hyperphosphorylation and cognitive deficits in intracerebroventricular- streptozotocin injected rats," *Psychopharmacologia*, vol. 231, pp. 345–356, 2014.

[58] S. Bhatt, L. Puli, and C. R. Patil, "Role of reactive oxygen species in the progression of Alzheimer's disease," *Drug Discovery Today*, 2020.

[59] M. Ghoneum, N. K. Badr El-Din, S. M. Abdel Fattah, and L. Tolentino, "Arabinoxylan rice bran (MGN-3/Biobran) provides protection against whole-body γ-irradiation in mice via restoration of hematopoietic tissues," *Journal of Radiation Research*, vol. 54, no. 3, pp. 419–429, 2013.

[60] Y. V. Nikitchenko, V. K. Klochkov, N. S. Kavok et al., "Anti-aging Effects of Antioxidant Rare-Earth Orthovanadate Nanoparticles in Wistar Rats," *Biological Trace Element Research*, 2021.

[61] J. Poddar, S. Singh, P. Kumar, S. Bali, S. Gupta, and S. Chakrabarti, "Inhibition of complex I-III activity of brain mitochondria after intracerebroventricular administration of streptozotocin in rats is possibly related to loss of body weight," *Heliyon*, vol. 6, no. 7, article e04490, 2020.

[62] J. Alam and L. Sharma, "Potential Enzymatic Targets in Alzheimer's: A Comprehensive Review," *Current Drug Targets*, vol. 20, no. 3, pp. 316–339, 2019.

[63] A. Armada-Moreira, J. I. Gomes, C. C. Pina et al., "Going the Extra (Synaptic) Mile: Excitotoxicity as the Road Toward Neurodegenerative Diseases," *Frontiers in Cellular Neuroscience*, vol. 14, 2020.

[64] C. A. Massaad, "Neuronal and vascular oxidative stress in Alzheimer's disease," *Current Neuropharmacology*, 2011.

[65] C. P. Ramsey, C. A. Glass, M. B. Montgomery et al., "Expression of Nrf2 in neurodegenerative diseases," *Journal of Neuropathology and Experimental Neurology*, vol. 66, no. 1, pp. 75–85, 2007.

[66] K. Kanninen, T. M. Malm, H. K. Jyrkkänen et al., "Nuclear factor erythroid 2-related factor 2 protects against beta amyloid," *Molecular and Cellular Neurosciences*, vol. 39, no. 3, pp. 302–313, 2008.

[67] T. W. Kensler, N. Wakabayashi, and S. Biswal, "Cell survival responses to environmental stresses via the Keap1-Nrf2-ARE pathway," *Annual Review of Pharmacology and Toxicology*, vol. 47, no. 1, pp. 89–116, 2007.

[68] A. I. Rojo, M. Pajares, P. Rada et al., "NRF2 deficiency replicates transcriptomic changes in Alzheimer's patients and worsens APP and TAU pathology," *Redox Biology*, vol. 13, pp. 444–451, 2017.

[69] M. J. Calkins, D. A. Johnson, J. A. Townsend et al., "The Nrf2/ARE pathway as a potential therapeutic target in neurodegenerative disease," *Antioxidants & Redox Signaling*, vol. 11, no. 3, pp. 497–508, 2009.

[70] X. Wang, M. R. Campbell, S. E. Lacher et al., "A Polymorphic Antioxidant Response Element Links NRF2/sMAF Binding to Enhanced *MAPT* Expression and Reduced Risk of Parkinsonian Disorders," *Cell Reports*, vol. 15, no. 4, pp. 830–842, 2016.

[71] S. Janelidze, N. Mattsson, E. Stomrud et al., "CSF biomarkers of neuroinflammation and cerebrovascular dysfunction in early Alzheimer disease," *Neurology*, vol. 91, no. 9, pp. e867–e877, 2018.

[72] I. Morales, G. Farías, and R. B. Maccioni, "Neuroimmunomodulation in the pathogenesis of Alzheimer's disease," *Neuroimmunomodulation*, vol. 17, no. 3, pp. 202–204, 2010.

[73] M. Y. Cha, S. H. Han, S. M. Son et al., "Mitochondria-Specific Accumulation of Amyloid β Induces Mitochondrial Dysfunction Leading to Apoptotic Cell Death," *PLoS One*, vol. 7, no. 4, article e34929, 2012.

[74] Z. C. Zhao, F. Li, and K. Maiese, "Stress in the brain: novel cellular mechanisms of injury linked to Alzheimer's disease," *Brain Research. Brain Research Reviews*, vol. 49, pp. 1–21, 2005.

[75] W. Ahmad, B. Ijaz, K. Shabbiri, F. Ahmed, and S. Rehman, "Oxidative toxicity in diabetes and Alzheimer's disease: mechanisms behind ROS/ RNS generation," *Journal of Biomedical Science*, vol. 24, no. 1, p. 76, 2017.

[76] K. Maiese, "FoxO proteins in the nervous system," *Analytical Cellular Pathology (Amsterdam)*, vol. 2015, article 569392, 15 pages, 2015.

Hindawi
Oxidative Medicine and Cellular Longevity
Volume 2020, Article ID 2638130, 16 pages
https://doi.org/10.1155/2020/2638130

Review Article

RNA and Oxidative Stress in Alzheimer's Disease: Focus on microRNAs

Akihiko Nunomura[1] **and George Perry**[2]

[1]*Department of Psychiatry, Jikei University School of Medicine, Tokyo, Japan*
[2]*Department of Biology and Neurosciences Institute, University of Texas at San Antonio, San Antonio, USA*

Correspondence should be addressed to Akihiko Nunomura; anunomura@jikei.ac.jp

Received 23 July 2020; Revised 21 October 2020; Accepted 29 October 2020; Published 30 November 2020

Academic Editor: Esmael Izadpanah

Oxidative stress (OS) is one of the major pathomechanisms of Alzheimer's disease (AD), which is closely associated with other key events in neurodegeneration such as mitochondrial dysfunction, inflammation, metal dysregulation, and protein misfolding. Oxidized RNAs are identified in brains of AD patients at the prodromal stage. Indeed, oxidized mRNA, rRNA, and tRNA lead to retarded or aberrant protein synthesis. OS interferes with not only these translational machineries but also regulatory mechanisms of noncoding RNAs, especially microRNAs (miRNAs). MiRNAs can be oxidized, which causes misrecognizing target mRNAs. Moreover, OS affects the expression of multiple miRNAs, and conversely, miRNAs regulate many genes involved in the OS response. Intriguingly, several miRNAs embedded in upstream regulators or downstream targets of OS are involved also in neurodegenerative pathways in AD. Specifically, seven upregulated miRNAs (miR-125b, miR-146a, miR-200c, miR-26b, miR-30e, miR-34a, miR-34c) and three downregulated miRNAs (miR-107, miR-210, miR-485), all of which are associated with OS, are found in vulnerable brain regions of AD at the prodromal stage. Growing evidence suggests that altered miRNAs may serve as targets for developing diagnostic or therapeutic tools for early-stage AD. Focusing on a neuroprotective transcriptional repressor, REST, and the concept of hormesis that are relevant to the OS response may provide clues to help us understand the role of the miRNA system in cellular and organismal adaptive mechanisms to OS.

1. Introduction

The process of neurodegeneration in Alzheimer's disease (AD), the most common cause of dementia and a major concern in the aging population across the world, is a dynamic, multifaceted biochemical phenomenon and is essentially lifelong. Oxidative stress (OS) is considered as one of the major underlying mechanisms of AD and related neurodegenerative disorders. Indeed, oxidative damage is closely associated with other pathological key events in neurodegeneration such as mitochondrial dysfunction, inflammation, impaired calcium homeostasis, metal dysregulation, protein misfolding, and impaired autophagy [1, 2]. Several kinds of research materials, i.e., postmortem brain samples and biological fluid from the patients with prodromal-stage of AD, genetically modified animal models of AD, as well as disease models using induced pluripotent stem cells (iPSCs), all provide consistent evidence that OS is a significant early event in the pathological cascade of AD [3–7]. Strikingly, both transgenic animals and iPSC models of AD indicate that a prominent elevation of OS markers occurs simultaneously with or even prior to the initial AD-related amyloid-β (Aβ) and tau pathology [5–7].

In contrast to DNA, oxidative damage to RNA has not been a major focus of research until recently, which is presumably due to the assumed transient nature of RNA. However, RNAs including messenger RNA (mRNA) can persist for several hours to days in certain tissues, suggesting that damaged mRNAs are detrimental to the cell if not corrected [8–10]. Increased levels of an oxidized base and an oxidized nucleoside of RNA, 8-oxo-guanine (8-oxoGua), and 8-oxo-guanosine (8-oxoGuo) were demonstrated in the vulnerable neuronal populations in postmortem brains of patients with preclinical AD and mild cognitive impairment (MCI) stage

of AD [11–13] as well as in brains of gene-driven animal models of AD at an early stage of degeneration [14, 15]. The 8-oxoGua formation in neuronal RNA is not merely an epiphenomenon but a potentially lethal insult for cells because a recent experimental study elucidates the distinct pathway between heavily oxidized mRNA and apoptotic cell death [16].

Oxidative RNA damage affects not only mRNAs but also noncoding RNA species. Among them, microRNAs (miRNAs), which interfere with the translation of target mRNAs, are of particular interest since their dysregulation has been implicated in neurodegenerative disorders like AD [17, 18]. Indeed, a cellular experiment has demonstrated that miRNAs can be directly oxidized and subsequently misrecognize mRNAs that are not their native targets [19]. Given the notion that noncoding RNAs are expected to contribute towards the biological complexity of the mammalian brain and cognitive evolution [20, 21], oxidative damage to noncoding RNAs and consequent dysregulation of the gene expression might be involved in the central pathophysiology of diverse neuropsychiatric disorders affecting higher brain functions [22, 23]. Besides direct oxidation of miRNAs, there is growing knowledge that OS affects expression levels of multiple miRNAs; conversely, miRNAs regulate lots of genes involved in the OS response [24, 25]. Intriguingly, several miRNAs embedded in oxidative stress regulation are involved also in several known pathways of neurodegeneration in AD, Parkinson's disease (PD), amyotrophic lateral sclerosis, and Huntington's disease [26, 27]. Further investigations towards elucidating the possible involvement of the oxidatively modified miRNAs and oxidatively altered miRNAs networks in the neurodegenerative pathways may open a novel avenue to establish an early intervention strategy for AD.

2. Direct Oxidation of RNA Species

2.1. Susceptibility of RNA to Oxidative Damage. Compared to oxidative DNA damage, far fewer studies have focused on oxidative damage to RNA, and only limited kinds of oxidatively modified bases in RNA have been reported previously [28–30]. Among multiple adducts of nucleoside oxidation, 8-oxo-deoxyguanosine (8-oxodGuo) and 8-oxoGuo are two of the best characterized and studied forms of DNA and RNA oxidation, respectively [31, 32]. Cellular abundance, location, lack of coating histone, and its single-stranded structure make RNA more susceptible to OS than DNA [33–35] (Table 1). Accordingly, greater oxidation to RNA than to DNA has been shown in studies with isolated DNA and RNA as well as in several kinds of cell lines and tissues [8].

2.2. Susceptibility to Oxidative Damage in Different RNA Species

2.2.1. Messenger RNA (mRNA). The extent of oxidative RNA damage varies greatly among different types of RNA in a manner that appears to show greater oxidative RNA damage in lesser association with RNA binding proteins [10]. For example, poly $(A)^+$ mRNA is found to have fivefold higher levels of 8-oxoGuo than total RNA that consists mostly of ribosomal RNA (rRNA) [9]. In the AD brain, northwestern blotting with a monoclonal anti-8-oxoGuo antibody shows that a significant amount of brain poly $(A)^+$ mRNA species are oxidized. While the identified oxidized mRNAs reveal that some species are more susceptible to OS in AD, no common motifs or structures were found in the oxidatively susceptible mRNA species in the AD brain [36]. Some of the identified known oxidized transcripts are related to the pathophysiology of AD, which included p21ras, mitogen-activated protein kinase (MAPK) kinase 1, carbonyl reductase, copper/zinc superoxide dismutase (SOD1), apolipoprotein D, and calpains, but not amyloid-β protein precursor (APP) or tau [36].

2.2.2. Ribosomal RNA (rRNA) and Transfer RNA (tRNA). In the AD brain, rRNA, extremely abundant in neurons, contains 8-oxoGuo [37, 38]. Remarkably, rRNA shows higher binding capacity to redox-active iron than tRNA, and consequently, the oxidation of rRNA by the Fenton chemistry forms 13 times more 8-oxoGuo than tRNA [37].

2.2.3. MicroRNA (miRNA). MicroRNAs (miRNAs) are small noncoding RNAs containing approximately 22 nucleotides, and they bind to complementary sequences in the three prime untranslated regions ($3'$UTRs) of target mRNA transcripts, thereby inhibiting mRNA translation or promoting mRNA degradation [39]. In the biogenesis pathway, miRNAs are transcribed from genomic loci as long as primary strands (pri-miRNAs) that undergo cleavage to precursor hairpins (premiRNAs) in the nucleus before being exported to the cytoplasm. PremiRNAs are further cleaved into double-stranded miRNA : miRNA$*$ duplexes and loaded into the RNA-induced silencing complex (RISC) containing an Argonaute (Ago) family protein as a core component. Finally, single-stranded mature miRNAs are completed by unwinding of the duplexes [40]. As a result, the repressive functions of the RISC and mature miRNAs themselves have been primarily associated with the cytoplasm, while several mature miRNAs are expressed also in the nucleus and nucleolus [41, 42]. Given cytoplasmic predominance of the subcellular localization and the single-stranded form, the mature miRNAs might be highly vulnerable to reactive oxygen species (ROS) (Table 1). Surprisingly, up to hundreds of miRNAs, besides 22 tRNAs and two rRNAs, have been identified from mitochondria, the major source of ROS [41]. Furthermore, miRNAs are often relatively long lived, and their half-lives reported to be ranged from 28 to 220 h, which is roughly 2- to 20-fold longer than that of typical mRNAs (about 10 h) [43]. Taken together, these findings support the possibility that miRNAs have abundant opportunities to be attacked by ROS.

Wang et al. have demonstrated that oxidized miRNAs containing 8-oxoGuo are produced in vitro through hydrogen peroxide (H_2O_2) treatment in a rat heart cell line as well as in vivo in the hearts of a mouse model of ischemia/reperfusion [19]. Indeed, miR-184 is the most highly oxidized but other oxidized forms of miRNAs are detected, i.e., oxidized

Table 1: Reasons why RNA species in human brain are vulnerable to oxidative insults.

RNA species	(i) Abundance in a cell (ii) Mostly single-stranded form and less protection by proteins (iii) Localization in the vicinity of mitochondria, the major source of ROS (iv) No known repair mechanisms for oxidized RNA
Human brain	(i) High oxygen consumption rate (ii) High content of easily peroxidizable polyunsaturated fatty acids (iii) High content of transition metals that catalyze ROS-generating reactions (iv) Low content of antioxidant enzyme catalase

ROS: reactive oxygen species.

miR-135a, miR-139, miR-204, miR-21, miR-23a, miR-290, miR-29a, and miR-30c. Therefore, not all miRNAs are oxidized in response to ROS stimulation, whereas several miRNAs are more susceptible to the oxidative modification. It remains to be determined whether there exists a common motif and sequence for the selective oxidation of miRNAs [19]. Although oxidized miRNAs are not identified in the human brain diseases at the current moment, possible involvement of the oxidized miRNAs in AD and related neurodegeneration is strongly suggested [8, 44, 45]. Additionally, direct oxidative modifications to other noncoding RNAs such as small nuclear RNAs, small nucleolar RNAs, long noncoding RNAs, and circular RNAs are not reported, while the role of these RNA species in the nervous system has recently drawn growing attention [46, 47].

2.3. Sources of Reactive Oxygen Species (ROS) Responsible for RNA Oxidation

2.3.1. ROS of Mitochondrial Origin and Fenton Reaction. The brain is particularly vulnerable to oxidative damage because of its high oxygen consumption rate (accounting for 20-25% of total body oxygen consumption but less than 2% of total body weight), high content of fatty acids and transition metals, and relative paucity of antioxidant enzymes compared with other organs (e.g., the content of catalase in the brain is only 10-20% of the liver and heart) [8, 48] (Table 1). Given this environment, neurons are continuously exposed to ROS such as superoxide ($O_2\cdot^-$), H_2O_2, and hydroxyl radical (·OH) that are produced from the mitochondrial electron transport chain through the normal cellular metabolism [49–51]. Among them, highly reactive ·OH can diffuse through the tissue only in the order of several nanometers [52], while $O_2\cdot^-$ is hardly permeable through cell membranes [53]. In consideration of the widespread damage to cytoplasmic RNA in AD [54, 55], RNA species are likely attacked by ·OH, which is formed from the reaction of highly diffusible H_2O_2 [56] with redox-active metals through the Fenton chemistry [37]. In the AD brain, malfunctioning mitochondria likely play a central role in producing abundant ROS as well as supplying redox-active iron into the cytosol [57, 58]. Indeed, ribosomes purified from the AD hippocampus contain was significantly higher levels of redox-active iron compared to controls, and the iron is bound to rRNA [37]. Therefore, mitochondrial abnormalities coupled with dysregulation of metal homeostasis are key features closely associated with ROS formation responsible for the RNA oxidation in AD [59].

2.3.2. Mode of Oxidized miRNA Generation. The concept that ROS originates from the mitochondria and becomes harmful when they are coupled with redox-active metals is fully compatible with the mode of the oxidized miRNA generation in the cellular model reported by Wang et al. [19]. In fact, miRNAs remain almost intact after incubation with H_2O_2 or redox-active iron (Fe^{3+}) alone. However, when miRNAs were incubated in a mixture of H_2O_2 and Fe^{3+} along with the reducing agent ascorbate, their oxidation substantially occurred, which indicates that oxidatively modified miRNAs are generated by ·OH via the Fenton reaction [19].

2.4. Biological Consequence of Oxidized RNA

2.4.1. Oxidized mRNA. Although guanine is the most reactive of the nucleic acid bases, not only 8-oxoGuo but also 8-oxo-adenosine, 5-hydroxycytidine, and 5-hydroxyuridine have been identified in oxidized RNA [28]. These oxidized nucleosides may have altered pairing capacity and thus be at the origin of erroneous protein production. Indeed, the 8-oxoGua can pair with both adenine and cytosine, and thus oxidized RNA compromises the accuracy of translation [60, 61]. The oxidized bases in mRNAs in cell lines cause ribosomal stalling on the transcripts leading to a decreased rate of full-length peptide synthesis [9, 62, 63], as well as synthesis of truncated, nonfunctional peptides, or mutated peptides [64]. Moreover, strand scission is proposed to result from as many as 40% of reactions of ·OH with RNA [65]. Recently, a distinct pathway between heavily oxidized mRNA and apoptotic cell death has been established. Mechanistically, specific binding of poly(C)-binding protein 1 (PCB1) to oxidized mRNA in which two 8-oxoGua residues are located nearby induces caspase-3 activation and subsequent apoptosis [16].

2.4.2. Oxidized rRNA. The biological consequence of rRNA oxidation has also been investigated in vitro using translation assays with oxidized ribosomes from rabbit reticulocytes and shows a significant reduction of protein synthesis [37]. Notably, studies on brains of subjects with AD and MCI have demonstrated ribosomal dysfunction associated with oxidative RNA damage. Isolated polyribosome complexes from AD and MCI brains show a decreased rate and capability for protein synthesis without alteration in the polyribosome content [38, 66]. A variety of ways that oxidative damage to

Table 2: Oxidized RNA species potentially induce apoptosis.

RNA species	Mechanism inducing apoptosis by oxidized RNAs	Ref
Oxidized messenger RNA (mRNA)	Specific binding of poly(C)-binding protein 1 (PCB1) to heavily oxidized mRNA carrying two 8-oxo-guanine residues at the 9th and 15th positions triggers caspase-3 activation and subsequent apoptosis.	[16]
Oxidized transfer RNA (tRNA)	Because tRNA is accessible in the mitochondrial intermembrane space, oxidation of tRNA can be catalyzed by cytochrome c (cyt c) and leads to the formation of cross-linking complex between tRNA and cyt c. then, oxidized tRNA facilitates cyt c release from mitochondria and subsequently induces apoptosis.	[68]
Oxidized microRNA (miRNA)	Oxidized miRNA-184 containing 8-oxo-guanosine associates with the 3′ UTRs of Bcl-xL and Bcl-w that are not its native targets. Subsequent reduction in Bcl-xL and Bcl-w is responsible for the cells undergoing apoptosis.	[19]

3′ UTRs: three prime untranslated regions.

the functional domain of rRNA which affects translation are suggested: (i) inhibiting ribosomal assembly, resulting in the nonfunctional subunit; (ii) interfering with codon-anticodon interaction or with binding of *aminoacyl-tRNA,* causing miscoding or ribosomal stalling, and (iii) blocking elongation of nascent peptide and stalling the ribosome [10].

2.4.3. Oxidized tRNA. Oxidative damage to tRNA may cause defects in codon-anticodon pairing or in aminoacylation, potentially leading to production of miscoded proteins [10]. Moreover, cleavage and fragmentation of tRNA induced by oxidative stress are observed in cell lines [67], which promotes formation of stress granules [10]. Like oxidized mRNA, a mechanism inducing apoptosis has been suggested by oxidized tRNA. Because tRNA is accessible in the mitochondrial intermembrane space, oxidized tRNA forms cross-linked complex with cytochrome *c* (cyt *c*), which facilitates cyt *c* release from the mitochondria and subsequently induces apoptosis [68].

2.4.4. Oxidized miRNA. A recent discovery of oxidized miRNAs opens new avenue in the research field of RNA oxidation. The oxidized miRNA causes misrecognizing target mRNAs, resulting in downregulation in synthesis of particular proteins and potentially inducing cellular crucial events [19]. Among several oxidized miRNAs, oxidized miR-184 containing 8-oxo-Guo shows such a prominent influence to the cell functions. Indeed, oxidized miR-184 associates with the 3′UTRs of B cell lymphoma-extra-large (Bcl-xL) and Bcl-2-like protein 2 (Bcl-w) that are not its native targets. Subsequent reduction of antiapoptotic proteins Bcl-xL and Bcl-w is involved in the initiation of apoptosis in the study with a rat heart cell line. Moreover, the reduction of these proteins by oxidized miR-184 is associated with an increase in susceptibility of the heart to infarction in a mouse model of ischemia/reperfusion injury [19]. It has been identified also that oxidized miR-204, but not native miR-204, can regulate pancreatic and duodenal homeobox 1 C-terminal inhibiting factor 1 (Pcif1), and oxidized miR-139, but not native miR-139, can regulate RNA (guanine-7-) methyltransferase (RNMT), further suggesting that oxidative modification can affect the targets of miRNAs [19]. Given the notion that miRNAs are expected to contribute towards the biological complexity of the mammalian brain and cognitive evolution [20, 21], the elucidation of other oxidized miRNAs and their targets may shed new light on understanding the complex molecular mechanism of brain aging and neurodegenerative diseases.

The mechanisms inducing apoptosis by the oxidized RNAs are summarized in Table 2. Most importantly, RNA oxidation leads to not only impaired RNA normal functions but also the gain of a signal to facilitate cellular apoptosis in response to OS.

2.5. Coping with RNA Damage

2.5.1. Degradation. Degradation of RNA plays a central role in RNA metabolism, and damaged RNA can be removed through degradation by ribonucleases (RNase), but selective degradation activity for oxidized RNA has not been established for known RNases [34, 69]. Because absence of no-go decay factors causes an accumulation of 8-oxoGuo-containing mRNA in yeast, the oxidized mRNA is likely subjected to degradation through no-go decay, a ribosome-based mRNA surveillance mechanism [9].

2.5.2. Repair Mechanisms. Alkylation damage in RNA is repaired by the same mechanism as a DNA-repair, catalyzed in the bacterium *Escherichia coli* by the enzyme AlkB, and in humans by the related protein [70]. However, specific repair mechanism for oxidized RNA, unlike DNA, has not been reported.

2.5.3. Avoidance of Oxidized Ribonucleotides Incorporation. The mechanism avoiding incorporation of the oxidized nucleotide into DNA and RNA is involved in coping with nucleic acid damage [33, 34, 71, 72]. MutT homologue 1 (MTH1) and Nudix type 5 (NUDT5) proteins participate in this error-avoiding mechanism by hydrolyzing the oxidized nucleoside diphosphates and/or triphosphates to the monophosphates [60, 61, 73]. Indeed, the expression of MTH1 is increased in vulnerable neurons in AD [74] and PD [75], indicating a compensatory upregulation of the MTH1

Table 3: Dysregulated microRNAs in association with both early-stage Alzheimer's disease (AD) pathology and oxidative stress (OS).

miRNA	Up- or downregulated in brains with AD pathology	Target gene	Specific function and association with OS regulation clarified by cellular and animal experiments	Ref
miR-107	Downregulated in the temporal cortex at BraaK stages III/IV of MCI subjects	BACE1	MiR-107 decreases BACE-1 mRNA levels by binding to the 3′ UTR of BACE1, hence decreases the production of Aβ. OS served as the key trigger to downregulate miR-107 by cell-derived soluble Aβ.	[92, 115, 116]
miR-125b	Upregulated in the frontal cortex at BraaK stages III/IV of non-demented and early AD subjects	SPHK1 NCAM	Overexpression of miR-125b promotes APP and BACE1 expression and Aβ production and apoptosis by targeting SPHK1 through inflammation (via increase in TNF-α and IL-6) and OS (via decrease in SOD). Mir-125b promotes tau phosphorylation by targeting NCAM.	[93, 99, 100]
miR-146a	Upregulated in the hippocampus at BraaK stages III/IV of preclinical or early AD subjects	CFH ROCK1 SOD2	MiRNA-146a is NF-κB-sensitive and activates inflammation by targeting 3′ UTR of CFH, an important repressor of the inflammatory response of the brain. Overexpression of miR-146a induces tau phosphorylation by targeting ROCK1 via inhibition of PTEN. Mir-146a is upregulated by ROS and downregulates SOD2 (mitochondrial manganese SOD).	[94, 101–103]
miR-200c	Upregulated in the hippocampus at BraaK stages III/IV of non-demented and early AD subjects.	PTEN S6K1	In APP/PSEN1 double-transgenic mice, Aβ deposition results in ER stress that induces miR-200c. MiR-200c supports cell survival and neurite outgrowth of cultured neuron by targeting PTEN. MiR-200c reduces Aβ secretion by targeting S6K1 via reduction of IRS-1pSer and promoting insulin signaling. MiR-200c is upregulated by ROS in primary hippocampal neuron.	[93, 111–113]
miR-210	Downregulated in the hippocampus at BraaK stages III/IV of non-demented and early AD subjects	ISCU1/2 COX10	Soluble Aβ leads to NMDAR overactivation, excessive calcium influx, mitochondrion-derived ROS production, and upregulation of miR-210. MiR-210 targets ISCU1/2 and COX10 that have important roles in mitochondrial respiration and function	[93, 116]
miR-26b	Upregulated in the temporal cortex at BraaK stage III of patients with MCI	RB1	Overexpression of miR-26b leads to aberrant cell cycle re-entry and increased tau-phosphorylation by targeting RB1 via activation of RB1/E2F cell cycle and CDK5. Sequence-specific inhibition of miR-26b in culture is neuroprotective against OS.	[95]
miR-30e	Upregulated in the hippocampus at BraaK stages III/IV of non-demented and early AD subjects	SNAI1	Overexpression of miR-30e increases the levels of SOD, GSH, and GSH-PX and decreases ROS levels by targeting SNAI1 through decreasing TGF-β and SMAD2 expression and increasing NOX4 expression.	[93, 110]
miR-34a	Upregulated in the frontal cortex and hippocampus at BraaK stages III/IV of non-demented and early AD subjects.	SIRT1 ADAM10 NMDAR 2B TREM2 BCL2	Overexpression of miR-34a increases the levels of an adaptor protein p66shc and reduces tolerance to OS by targeting SIRT1. Conditional miR-34a overexpression mouse shows cognitive impairment associated with accumulation of intracellular Aβ and tau hyperphosphorylation possibly through targeting	[93, 104–108]

Table 3: Continued.

miRNA	Up- or downregulated in brains with AD pathology	Target gene	Specific function and association with OS regulation clarified by cellular and animal experiments	Ref
miR-34c	Upregulated in the hippocampus at BraaK stages III/IV of early AD subjects	SYT1	ADAM10, NMDAR 2B, and SIRT1. MiR-34a targets also the amyloid sensing- and clearance receptor protein TREM2 as well as anti-apoptotic protein BCL2. Overexpression of miR-34c mediates synaptic and memory deficits by targeting SYT1 through ROS generation, JNK activation, and p53 accumulation.	[94, 109]
miR-485	Downregulated in the frontal cortex at BraaK stage III of early AD subjects	BACE1 RAC1	MiR-485 decreases BACE1 mRNA levels by binding to BACE1 exon 6, hence decreases the production of Aβ. MiR-485 upregulation alleviates ischemia-reperfusion injury by targeting RAC1 via NOTCH2 signaling, which are evidenced by improved cell viability, decreased OS markers, and reduced apoptotic rate.	[96, 118, 119]

3′ UTR, three prime untranslated region; Aβ, amyloid-β; *ADAM10,* A Disintegrin and metalloproteinase domain-containing protein 10; APP, amyloid precursor protein; BACE1, β-site amyloid precursor protein-cleaving enzyme 1; BCL2, B-cell lymphoma 2; CDK5, cyclin-dependent kinase 5; CFH, complement factor H; *COX10*, cytochrome c oxidase assembly protein; ER, endoplasmic reticulum; GSH, glutathione; GSH-PX, glutathione-peroxidase; IL-6, interleukin-6; IRS-1pSer, insulin receptor substrate 1 at serine residues; ISCU1/2, iron-sulfur cluster scaffold homolog 1/2; *JNK*, Jun amino terminal kinase; MCI, mild cognitive impairment; NCAM, neural cell adhesion molecule; NF-κB, nuclear transcription factor κB; NMDAR, N-methyl-d-aspartate receptor; NOTCH2, neurogenic locus notch homolog protein 2; *NOX4*, NADPH oxidase 4; p66shc, 66 kDa proto-oncogene Src homologous-collagen homologue; PSEN1, presenilin-1; *PTEN*, *phosphatase and tensin homolog; RAC1*, RAS-related C3 botulinus toxin substrate 1; RB1, *retinoblastoma* 1; ROCK1, rho-associated, coiled-coil containing protein kinase 1; ROS, reactive oxygen species; S6K1, S6 kinase B1; SIRT1, *silent mating type information regulation 2 homolog* (sirtuin) 1; SMAD2, mothers against decapentaplegic homolog 2; *SNAI1*, snail family transcriptional repressor 1; SOD, superoxide dismutase; SPHK1, sphingosine kinase 1; *SYT1*, synaptotagmin 1; TGF, transforming growth factor; TNF-α, tumor necrosis factor-α; TREM2, triggering receptor expressed in myeloid cells 2.

against OS. Moreover, several enzymes involved in the nucleotide metabolism show a discriminator activity against the oxidized nucleotides. Guanylate kinase (GK), converting GMP to GDP, is inactive on 8-oxo-GMP [76]. Similarly, ribonucleotide reductase (RNR), catalyzing reduction of four naturally occurring ribonucleoside diphosphates, is inactive on 8-oxo-GDP [76]. The final gatekeeper is RNA polymerase that incorporates 8-oxo-GTP into RNA at a much lower rate compared to the normal GTP incorporation [34, 60, 72].

2.5.4. Proteins Binding Specifically to Oxidized RNA. Proteins that bind specifically to 8-oxoGuo-containing RNA have been reported, namely, polynucleotide phosphorylase (PNPase) [77, 78], Y box-binding protein 1 (YB-1) [79], and AU-rich element RNA binding protein 1 (Auf1) [also called heterogeneous nuclear ribonucleoprotein D0 (HNRNPD)] [80, 81]. It has been proposed that these proteins are able to recognize and discriminate the oxidized RNA molecule from normal ones, thus contributing to the fidelity of translation in cells by sequestrating the damaged RNA from the translational machinery [77–80].

2.5.5. Coping with Oxidative miRNA Damage. Compared to the biogenesis and activity, the process of degradation of miRNAs has received less attention. While miRNAs are globally stable, individual miRNAs display rapid decay dynamics in some specific situations, as occurs for a few neuron-enriched miRNAs, but not constitutively expressed miRNAs, and for mature miRNAs, but not the miRNA precursors [43]. Although several miRNA-degrading enzymes have been identified, including both 3′-to-5′ and 5′-to-3′exoribonucleases [43, 82], whether they are less or more efficient for oxidized miRNAs is unknown. Among them, the human PNPase degrades certain mature miRNAs in human melanoma cells [82] and may be involved in oxidized miRNA degradation [77, 78]. A recent comprehensive review has concluded that how cells cope with oxidative damage to miRNAs is unclear, and whether they have evolved pathways to degrade or repair them should be the subject of future research [83].

2.6. Therapeutic Interventions against Oxidized RNA Species. Several experimental studies on human subjects and animal models have demonstrated successful interventions including nonpharmacological and pharmacological approaches towards reduction of oxidized RNA. Indeed, the efficacious interventions are caloric restriction and exercise in human subjects [84], as well as administrations with antioxidants and anti-inflammatory agents such as acetyl-l-carnitine [85], α-linolenic acid [86], α-lipoic acid [85], docosahexaenoic acid (DHA) [86], indomethacin [87], selenium [14], and vitamin E [88] in experimental animals. Antioxidants may reduce miRNA oxidation as well. Administration of *N*-acetylcysteine (NAC) reduces oxidized miR-184 and attenuates the reductions in Bcl-xL and Bcl-w and consequently prevents apoptosis both in the rat heart cell line and in the hearts of a mouse model of ischemia/reperfusion [19].

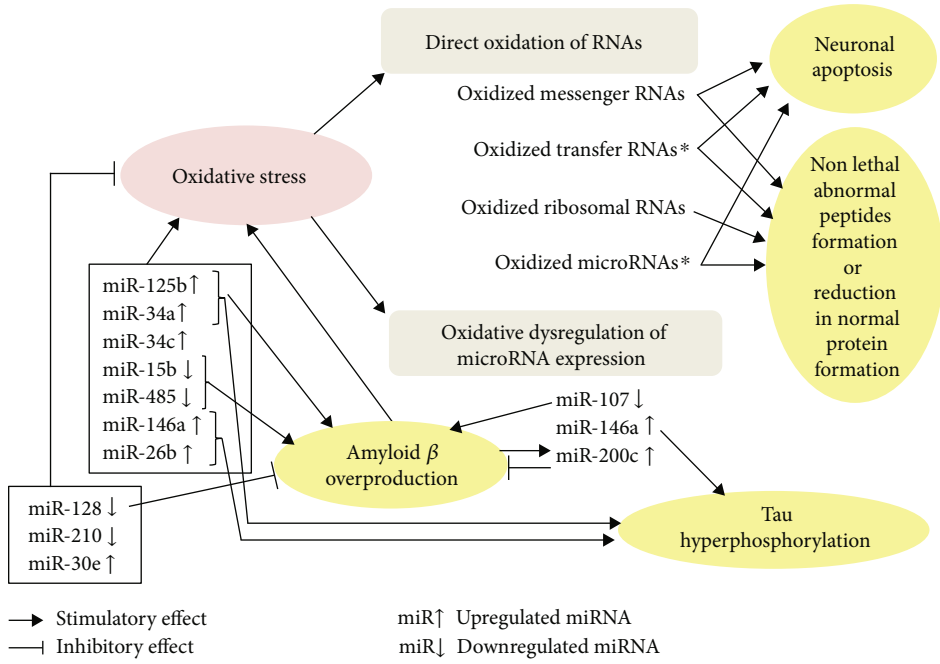

Figure 1: Overview of interrelations among oxidative stress, RNA species modification/dysregulation, and neurodegenerative changes in Alzheimer's disease. Oxidative stress can induce two modes of oxidative insults on RNA species, i.e., direct oxidation of RNAs and oxidative dysregulation of the microRNA (miRNAs) expression. These modifications and dysregulations of RNAs potentially induce neuronal apoptosis or nonlethal neuronal dysfunction as well as amyloid β overproduction and tau hyperphosphorylation. Besides these changes as consequences of oxidative stress, altered expressions of some miRNAs are associated with an acceleration of oxidative stress, while those of others are associated with a compensatory reduction of oxidative stress. Of note, dysmetabolism of amyloid β can be a cause or a consequence of oxidative stress. *Oxidized transfer RNAs and oxidized microRNAs have been reported only in cellular and animal models, but the other changes in RNAs shown in this figure have been found in the brains of Alzheimer's disease.

Overexpressing human *MTH1* in a transgenic mouse model significantly reduced 8-oxoGuo in the brain [89].

3. microRNAs and Oxidative Stress Regulation

3.1. Interplay between miRNAs and Oxidative Stress (OS) Affects Neurodegeneration. MiRNAs are embedded in complex regulatory networks, since a single miRNA can regulate up to hundreds of target mRNAs coding for different proteins [39, 90]. It has been demonstrated that miRNAs regulate lots of genes involved in the OS response, and conversely, OS affects expression levels of multiple miRNAs. Indeed, 27 different miRNAs are associated with generation but 11 different miRNAs are associated with reduction of OS. In downstream of OS, induced expression of 56 miRNAs, while reduced expression of 32 miRNAs, is observed [25]. Moreover, dysregulation of miRNAs has been implicated in neurodegenerative disorders such as AD, PD, amyotrophic lateral sclerosis, Huntington's disease, and prion disorders [27, 91]. Although the interrelations among miRNAs, OS, and neurodegeneration are often considered separately, several miRNAs embedded in OS regulation or OS targets are involved also in known pathways of neurodegeneration such as mitochondrial dysfunction, inflammation, and protein misfolding. Some classes of miRNAs *accelerate* these cellular anomalies, whereas others act in a counterregulatory, *protective* role. Also, changes in levels of certain species of miRNAs can be a *consequence* of the abovementioned anomalies [17, 27].

3.2. Specific miRNAs Associated with Both OS and Alzheimer's Disease (AD)

3.2.1. Altered miRNAs in the AD Brain at Braak Stages III/IV. The roles of individual miRNAs, i.e., seven upregulated miRNAs (miR-125b, miR-146a, miR-200c, miR-26b, miR-30e, miR-34a, miR-34c) and three downregulated miRNAs (miR-107, miR-210, miR-485) that are relevant to both OS and neurodegenerative pathways in AD are summarized in Table 3. Of note, all the alterations of these miRNAs are demonstrated in the human brain with early AD pathology at Braak stages III and IV [92–96] that are not a substrate for profound cognitive impairment [97] and largely correspond to MCI [98].

3.2.2. Upregulated miRNAs in the AD Brain at Braak Stages III/IV. A synergistic effect mechanism of accelerated AD pathology and OS in neurodegeneration is found in several upregulated miRNAs listed in Table 3, i.e., miR-125b [99, 100], miR-146a [101–103], miR-26b [95], and miR-34a [104–108]. Upregulation of these miRNAs leads to Aβ production and/or tau-phosphorylation and an increase in vulnerability to OS. Upregulation of miR-34c increases ROS production and mediates synaptic deficits through the ROS-Jun amino terminal kinase (JNK)-p53 pathway [109].

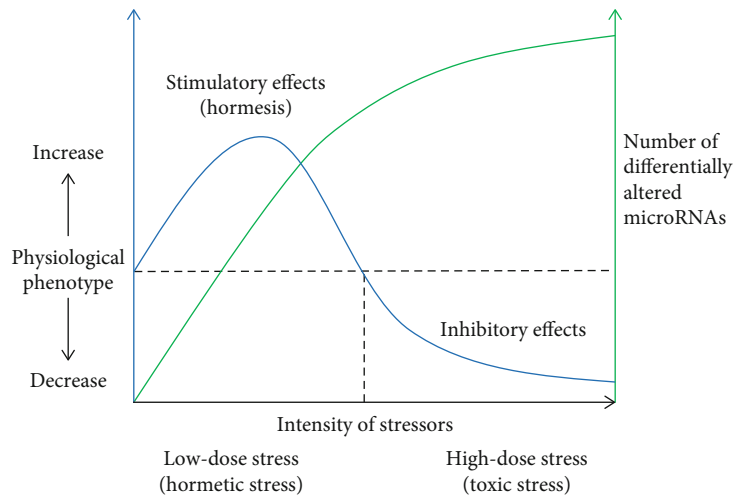

Figure 2: A microRNA system mediates hormesis. As intensity of stressors increases, the number of differentially altered miRNAs increases, which is associated with a biphasic physiological phenotype. Under low doses of hormetic stress, a moderate increase in miRNAs is associated with an increase in physiological (beneficial) phenotype. However, under high doses of toxic stress, an excessive increase in miRNAs is associated with a decrease in physiological phenotype.

In contrast, upregulation of miR-30e, being found in the hippocampus of AD [93], increases antioxidant enzymes such as SOD, glutathione (GSH), and glutathione-peroxidase (GSH-PX) and decreases ROS [110], suggesting compensatory regulation of the miRNA in the AD brain. The role of miR-200c in the pathophysiology is more complicated. MiR-200c is upregulated by Aβ-induced endoplasmic reticulum (ER) stress or OS [111, 112] and able to reduce Aβ secretion [113], suggesting a compensatory role. Indeed, upregulation of miR-200c is observed in the hippocampus of AD subjects [93] and in the cortices of APP transgenic mice at an early period of Aβ deposition [113]. In epilepsy model rats, however, downregulation of miR-200c is neuroprotective. It increases SOD and GSH-PX activities and decreases apoptosis of hippocampal neurons by upregulation of its target reversion-inducing cysteine-rich protein with kazal motifs (RECK) via inactivating protein kinase B (AKT) signaling [114].

3.2.3. Downregulated miRNAs in the AD Brain at Braak Stages III/IV. As for downregulated miRNAs listed in Table 3, each specific miRNA shows its own mode of relevance to the disease pathogenesis. OS triggers downregulation of miR-107 that normally represses Aβ production, and downregulation of miR-107 in AD is associated with an accumulation of Aβ [115, 116]. Because cell-derived soluble Aβ induces further OS [117], a vicious cycle promoting OS and Aβ production is formed. Similarly, miR-485 that normally represses Aβ production and silences OS [118, 119] is downregulated in the cortex of AD [96], where altered miR-485 exacerbates neurodegeneration through both excess of Aβ and OS. Conversely, downregulation of miR-210 in the hippocampus of AD [93] may represent compensatory regulation of the miRNA in the AD brain. Because soluble Aβ leads to upregulation of miR-210 that inhibits the mitochondrial respiration and function [116], downregulation of miR-210 should be neuroprotective through alleviating Aβ toxicity and OS silencing.

3.2.4. Other Altered miRNAs in the AD Brain. Downregulation of miR-128 is observed in the hippocampus at the Braak stage VI of advanced AD patients, but not at the Braak stage III/IV [94]. Indeed, miR-128 promotes Aβ-mediated cytotoxicity by targeting peroxisome proliferator activated receptor-γ (PPAR-γ) via activation of nuclear transcription factor κB (NF-κB) [120]. Also, miR-128 promotes OS by targeting sirtuin 1 (SIRT1) [121], indicating that downregulation of miR-128 in late-stage AD seems to be a compensatory regulation against Aβ pathology and OS. MiR-15b also downregulated in the temporal cortex and hippocampus of patients with AD. In contrast to miR-128, miR-15b reduces Aβ accumulation through directly targeting $3'$UTRs of β-site amyloid precursor protein-cleaving enzyme 1 (BACE1) and NF-κB [122] and counteracting senescence associated mitochondrial dysfunction and ROS generation by targeting stress-induced SIRT4 [123]. Therefore, downregulation of miR-15b in AD is associated with an acceleration of both Aβ pathology and OS.

The interrelations among OS, RNA species modification/dysregulation, and neurodegenerative changes in AD are summarized in Figure 1.

3.2.5. Altered miRNAs in the Mouse Model of AD. Downregulation of miR-20a is observed in the transgenic mouse model of AD carrying *Swedish* double mutation (K670 N/M671L) of the amyloid precursor protein (APP) and M146L mutation of the presenilin-1 (PSEN1) (APPswe/PSEN1M146L) [108]. While ROS upregulates miR-20a in primary hippocampal neuron [124], miR-20a reduces Aβ by targeting APP [125], indicating a decrease in the protective function of miR-20a in this model. Conversely, miR-98 is upregulated in the APPSwe/PSEN1M146L mouse model [108], which seems to represent a compensatory mechanism

against AD and OS. MiR-98 decreases the production of APP and Aβ and improves OS and mitochondrial dysfunction targeting hairy and enhancer of split- (Hes-) related with the YRPW motif protein 2 (HEY2) via inactivation of the Notch signaling pathway [126]. Similarly, a protective function of miR-330 targeting vav guanine nucleotide exchange factor 1 (VAV1) is reported in the AD mouse model through the MAPK signaling pathway. Upregulation of miR-330 reduces Aβ production and alleviates OS and mitochondrial dysfunction in AD [127]. In the transgenic mouse model of AD carrying APP Swedish mutation and PSEN1 lacking exon 9 (APPswe/PSEN1Δ9), OS-associated miR-34a, miR-34c, and miR-98 are abnormally expressed in the animal between 3 and 6 months of age [128] when initial Aβ depositions start in the hippocampus [129]. Taken together, studies on the postmortem human brain and transgenic animal model consistently suggest the altered expression of the OS-associated miRNAs as an early-stage event of AD.

3.3. Neuroprotective Function of REST and miRNAs

3.3.1. A Transcriptional Repressor, REST: AD and OS. The restrictive element-1 silencing transcription factor (REST), also known as neuron-restrictive silencing factor (NRSF), has been thought to function as a regulator of neuronal genes involved in neurogenesis and neuronal differentiation. However, recently accumulated findings strongly indicate that REST is not only a classical repressor to maintain normal neurogenesis but it is also a fine fundamental protector against neurodegeneration [130, 131]. Surprisingly, the expression of REST is increased with aging in brains of cognitively normal elderly. However, in brains of patients with MCI and AD, a significant reduction in REST has been found in cortical and hippocampal neurons, where nuclear REST levels are positively correlated with a global cognitive measure. Of particular note, elevated REST levels are associated with preservation of the cognitive function even in the presence of AD pathology [132]. Indeed, chromatin immunoprecipitation with deep sequencing shows that REST represses proapoptotic genes, e.g., FAS, FAS-associated death domain protein (FADD), TNF receptor-associated death domain protein (TRDD), Bcl-2-associated X protein (BAX), and cytochrome *c*, as well as AD pathology-associated genes, e.g., presenilin-2 (PSEN2) and presenilin enhancer 2 (PSENEN) implicated in Aβ generation and MAPK implicated in tau phosphorylation. Simultaneously, REST induces the expression of forkhead box O (FOXO) transcription factors that mediate OS resistance and the antioxidant enzymes catalase and SOD1. That REST potently protects neurons from OS and Aβ toxicity is rigorously confirmed by experiments on conditional REST knockout mice and nematode *Caenorhabditis elegans* (*C. elegans*) models with a functional orthologue of REST and SPR-4 [132].

3.3.2. Rest and miRNAs. As REST has been shown to mediate the temporal and cell-specific expression of several classes of noncoding RNAs including miRNAs [133], the loss of REST in AD might disturb the network of miRNAs. Quite recently, loss of REST causes upregulation of miR-124 and downregulation of its target protein phosphatase 1 (PTPN1) and disrupted miR-124/PTPN1 signaling that induces AD-like tau pathology in mice via activation of glycogen synthase kinase 3 (GSK-3) and inactivation of protein phosphatase 2A (PP2A) [134]. Conversely, REST is regulated by some cytokines/regulators such as miRNAs [130]. Indeed, miR-124 and miR-9 target REST and form self-enforcing loops together with the polypyrimidine tract-binding protein (PTB) to control neuronal conversion and maturation. In a double negative feedback loop consisting of PTB, miR-124, and REST (PTB-REST-miR-124 loop), REST represses miR-124, which in turn dismantles multiple components of the REST complex, and the RNA binding protein PTB serves both as a substrate for and a key inhibitor to the miR-124 targeting [135]. As is the case with the process of neurogenesis, the miRNA system likely acts both upstream and downstream of the REST expression in the aging brain, where the miRNA system participates in fine tuning of the gene to distinguish neuroprotection from neurodegeneration.

3.4. MiRNAs Mediates Hormesis under OS

3.4.1. Hormesis and OS. The relationship between the strength of a stressor and its biological effects on a physiological phenotype is not linear, but biphasic. This process is known as hormesis, whereby exposure to a low dose of a potentially harmful stressor promotes adaptive changes to the cells, organs, and living body that enables it to better tolerate subsequent stress. When we consider the hormetic response in association with neuronal adaptation to stressors, it is helpful to introduce the concepts of "neurohormesis" by Mattson [136] and "mitohormesis" by Ristow [137] in the context of maintaining cognitive health. Because these concepts indicate that moderate levels of OS are beneficial to the biological system through the adaptive preconditioning, further investigation to understand the molecular mechanisms of the regulatory hormesis may give hints on developing a new therapeutic approach for neurodegenerative diseases.

3.4.2. Hormesis and miRNAs. Recent studies indicate an involvement of changes in miRNAs in the adaptive response of hormesis or preconditioning. In an experiment using *C. elegans* exposed to nicotine in the period of postembryonic stages, the hormetic response in locomotive speed of the worm was observed by low and high dose of nicotine exposure. Of note, there was a dose-dependent increase in the degree of fold change (1 vs. 3.4-fold) and the number (1.3% vs. 16.4%) of the differentially altered miRNAs in the worm treated with low- and high-dose nicotine [138]. These observations support a speculation that miRNAs as a system mediates hormesis (Figure 2). In another study using *C. elegans*, an antibiotic enoxacin extends the lifespan of the worms by downregulating miR-34-5p. The longevity effects associated with downregulated miR-34 are abrogated by the antioxidant NAC, indicating that the mechanism of promoting longevity matches well with a prooxidant-mediated mitohormetic response [139]. Also, the involvement of miRNAs in the hormetic activation of the antioxidant system is suggested in an

experiment of preharvest ultraviolet C (UV-C) treatment that attenuates postharvest senescence of stored strawberry fruit. Indeed, miR-159 and miR-398 are downregulated by UV-C, and that their respective targets are upregulated at the early stage of storage with enhancement of the activity of antioxidant enzymes. The initial burst of ROS primes the fruit in an antioxidative activated state via ROS-mediated feedback control with posttranscriptional involvement of miRNAs [140].

3.4.3. Ischemic Preconditioning and miRNAs. Neuroprotective regulation of miRNAs is induced also in the early phase of ischemic preconditioning. MiR-200c, upregulated in the hippocampus of AD subjects [93] and in the cortices of APP transgenic mice at early period of Aβ deposition [113], is involved among miRNAs that upregulated at 3 hours after cerebral ischemic preconditioning in mice [141]. Of note, the protective function of miR-200c upregulation is mediated by targeting prolyl hydroxylase 2 (PHD2, also known as EGLN1), a sensor of oxygen and OS [142]. Similarly, downregulation of miR-15b, observed in the temporal cortex of AD patients [143], is associated with preconditioning by a volatile anesthetic sevoflurane against cerebral ischemic injury in rats by sustained expression of its target Bcl-2, an antiapoptotic protein [144].

4. MicroRNAs in Diagnosis and Therapy for Alzheimer's Disease

4.1. MiRNAs as a Diagnostic Tool for AD

4.1.1. Circulating miRNAs in Bodily Fluids. MiRNAs are not only detected in tissue but also in bodily fluids such as blood plasma and serum, cerebrospinal fluid (CSF), urine, and saliva. These miRNAs are collectively known as circulating miRNAs. miRNAs are actively and selectively excreted from cell cytoplasm to bodily fluids through exosomes, microparticles, apoptotic cell bodies, or excreted as microvesicle free miRNAs that are associated with diverse proteins such as Ago and high-density lipoprotein. Also, they can be passively excreted into bodily fluids as a result of apoptosis, metastasis, and inflammation [90]. It has been suggested that miRNAs from the brain are able to cross the blood-brain barrier (BBB) into peripheral circulation using exosomes [145, 146].

4.1.2. Circulating miRNAs in AD. According to a recent review on circulating miRNAs, collectively, 253 miRNAs have been reported with different expression levels in AD patients compared to healthy controls, of which 100 miRNAs are upregulated, 115 miRNAs are downregulated, and 38 miRNAs are both up- and downregulated in AD [90]. In another systematic review extracting dysregulated miRNAs in the peripheral blood from patients with AD, the authors have crossreferenced the dysregulated circulating miRNAs against the dysregulated miRNAs in the brain at the Braak stage III and identified 10 miRNAs [147]. Indeed, the list of 10 miRNAs are identical to those shown in Table 3, indicating that dysregulated miRNAs in association with both early-stage AD pathology and OS regulation can be detected in the peripheral blood. Four of these 10 miRNAs, namely, miR-107, miR-125b, miR-146a, and miR-34a, are found to be altered in the CSF in the same direction as observed in the brain [148, 149]. However, three miRNAs of the 10 miRNAs, namely, miR-125b, miR-146a, and miR-26b, are differently dysregulated between the brain and blood: upregulated in the brain but downregulated in the peripheral blood. This is probably due to the timing of sampling, since several miRNAs can be inversely dysregulated between early and late stage of AD. For example, miR-146a in the brain and CSF is upregulated at the Braak stage III of prodromal AD but downregulated at the Braak stage VI of advanced AD [94].

4.1.3. Diagnostic Potential of Circulating miRNAs in AD. Of particular note, among the miRNAs shown in Table 3, plasma miR-107 and serum miR-125b measured with a real-time quantitative reverse transcriptase polymerase chain reaction (qRT–PCR) method has been found to show considerably high sensitivity (0.90 for miR-107 and 0.81 for miR-125b) and specificity (0.78 for miR-107 and 0.68 for miR-125b) as a biomarker of AD [149, 150]. Furthermore, decrease in plasma miR-107 is more prominent in amnestic MCI (aMCI) than in AD. Therefore, plasma miR-107 shows even higher sensitivity of 0.98 and specificity of 0.83 to discriminate between patients with aMCI and healthy controls, suggesting a potential role of the circulating miRNA as a diagnostic biomarker at the prodromal stage of AD [149]. Also, serum miR-34c is significantly increased in patients with aMCI and might be a predictive biomarker for diagnosis of aMCI [109].

4.2. MiRNAs as a Therapeutic Target of AD

4.2.1. Recent Advances in RNA-Based Therapeutics. RNA-based therapeutics, such as small interfering RNAs (siRNAs), miRNAs, antisense oligonucleotides (ASOs), aptamers, synthetic mRNAs, and CRISPR-Cas9, have great potential to target currently undruggable genes and gene products and to generate new therapeutic paradigms in disease, ranging from cancer to pandemic influenza to AD [151]. Indeed, patisiran and givosiran are the U.S. Food and Drug Administration (*FDA*) approved, the first and second RNA interference-(RNAi-) based drugs indicated for the treatment of adults with polyneuropathy of hereditary transthyretin-mediated (hATTR) amyloidosis and acute hepatic porphyria (AHP), respectively [152, 153]. According to the recent systematic review, 28 ongoing studies are found to be related to the application of RNAs in the treatment and diagnosis of AD, i.e., ASOs (8 targets), miRNA mimics (agomirs) (7 targets), anti-miRNAs (antagomirs) (6 targets), siRNAs (5 targets), and mRNAs (2 targets) [154].

4.2.2. Agomirs and Antagomirs as Therapeutics for AD. The field of miRNAs as therapeutics for AD has attracted attention and potentially offers a variety of solutions including Aβ or tau reduction, enhancement of neuronal survival, inhibition of apoptosis, and protection of synapses [155]. The therapeutic modulation of miRNAs can be done in two ways. The levels of downregulated or upregulated miRNAs can be reversed using agomirs or antagomirs which are antisense

molecules that act to bind and thus inactivate the target miRNA sequence, respectively [156]. Specifically, an intraventricular infusion of miR-107 mimic (agomir) reverses the impairments of spatial memory and long-term potentiation and loss of pyramidal neurons caused by Aβ neurotoxicity in a mouse model of AD via the intraventricular injection of Aβ42 [157]. Conversely, the intrahippocampal delivery of a microRNA-146a specific inhibitor (antagomir) into transgenic mice with five familial AD mutations (5xFAD mice) showed enhanced hippocampal levels of rho-associated, coiled-coil containing protein kinase 1 (ROCK1) protein and repressed tau hyperphosphorylation, partly restoring the memory function in the 5xFAD mice [102]. Similarly, administration of miR-34c antagomir by the third ventricle injection or intranasal delivery markedly increased the brain levels of synaptotagmin 1 (SYT1) and ameliorated the cognitive function in SAMP8 mice [109]. Therefore, several OS-associated miRNAs summarized in Table 3 might be not only diagnostic but also therapeutic targets for AD.

5. Conclusion

Neuronal RNA oxidation in vulnerable neuronal populations in AD [54] and PD [158] was reported in 1999. Since then, involvement of RNA oxidation in the disease pathogenesis has been suggested in diverse neuropsychiatric disorders [4, 8] as well as common chronic diseases beyond the central nervous system such as diabetes and heart failure [159]. In 2015, the existence and the biological significance of oxidized miRNAs were demonstrated in cellular and animal models [19]. Cellular consequences of oxidatively altered RNAs have recently been investigated more intensively and rigorously than before, which provides still limited but an increasing amount of information about disrupted cellular functions in translational machinery and noncoding regulatory mechanisms. Indeed, three independent pathways of apoptosis induction have been identified through formations of oxidized mRNA [16], oxidized tRNA [68], and oxidized miRNA [19]. Besides direct oxidation, expression levels of several miRNAs embedded in upstream regulators or downstream targets of OS are altered in AD. It is noteworthy that both direct oxidation of RNAs and oxidative dysregulation of the miRNA expression occur at an early stage of neurodegeneration. Further understanding of the consequences and cellular handling mechanisms of the oxidatively altered RNAs may provide clues to the underlying mechanisms of neurodegenerative diseases and lead to better early intervention strategies.

Additional Points

Since the submission of this article, it has been reported that formation of 8-oxo-guanine in seed region of miR-1 is sufficient to cause cardiac hypertrophy in mice, which provides novel evidence for an epitranscriptional role of oxidized miRNA in phenotypic alteration (H. Seok, H. Lee, S. Lee et al., "Position-specific oxidation of miR-1 encodes cardiac hypertrophy," *Nature*, vol. 584, no. 7820, pp. 279-285, 2020).

Conflicts of Interest

Akihiko Nunomura has received lecture fees from Daiichi Sankyo Co., Ltd., Eisai Co., Ltd., Janssen Pharmaceutical K.K., Meiji Seika Pharma Co., Ltd., Ono Pharmaceutical Co., Ltd. and Otsuka Pharmaceutical Co., Ltd. and grant support from Eisai Co., Ltd. George Perry has served on the Board of Neurotrope and Neurotez.

Authors' Contributions

AN and GP conjointly conceptualized the idea for the review. AN performed the literature search, analyzed the cited studies, and wrote the article. GP critically revised the work and made changes and additions to its intellectual content.

Acknowledgments

This work was supported by the Japan Society for the Promotion of Science (JSPS) KAKENHI (Grants-in-Aid for Scientific Research), Grant number 18K07595 to AN.

References

[1] M. P. Mattson, "Late-onset dementia: a mosaic of prototypical pathologies modifiable by diet and lifestyle," *npj Aging and Mechanisms of Disease*, vol. 1, no. 1, 2015.

[2] D. M. A. Oliver and P. H. Reddy, "Molecular basis of Alzheimer's disease: focus on mitochondria," *Journal of Alzheimer's Disease*, vol. 72, Supplement 1, pp. S95–S116, 2019.

[3] A. Nunomura, T. Hofer, P. I. Moreira, R. J. Castellani, M. A. Smith, and G. Perry, "RNA oxidation in Alzheimer disease and related neurodegenerative disorders," *Acta Neuropathologica*, vol. 118, no. 1, pp. 151–166, 2009.

[4] A. Nunomura, P. I. Moreira, R. J. Castellani et al., "Oxidative damage to RNA in aging and neurodegenerative disorders," *Neurotoxicity Research*, vol. 22, no. 3, pp. 231–248, 2012.

[5] M. J. McManus, M. P. Murphy, and J. L. Franklin, "The mitochondria-targeted antioxidant MitoQ prevents loss of spatial memory retention and early neuropathology in a transgenic mouse model of Alzheimer's disease," *The Journal of Neuroscience*, vol. 31, no. 44, pp. 15703–15715, 2011.

[6] T. Kondo, M. Asai, K. Tsukita et al., "Modeling Alzheimer's disease with iPSCs reveals stress phenotypes associated with intracellular Aβ and differential drug responsiveness," *Cell Stem Cell*, vol. 12, no. 4, pp. 487–496, 2013.

[7] J. H. Birnbaum, D. Wanner, A. F. Gietl et al., "Oxidative stress and altered mitochondrial protein expression in the absence of amyloid-β and tau pathology in iPSC-derived neurons from sporadic Alzheimer's disease patients," *Stem Cell Research*, vol. 27, pp. 121–130, 2018.

[8] A. Nunomura, H. G. Lee, X. Zhu, and G. Perry, "Consequences of RNA oxidation on protein synthesis rate and fidelity: implications for the pathophysiology of neuropsychiatric disorders," *Biochemical Society Transactions*, vol. 45, no. 5, pp. 1053–1066, 2017.

[9] C. L. Simms, B. H. Hudson, J. W. Mosior, A. S. Rangwala, and H. S. Zaher, "An active role for the ribosome in determining the fate of oxidized mRNA," *Cell Reports*, vol. 9, no. 4, pp. 1256–1264, 2014.

[10] C. L. Simms and H. S. Zaher, "Quality control of chemically damaged RNA," *Cellular and Molecular Life Sciences*, vol. 73, no. 19, pp. 3639–3653, 2016.

[11] M. A. Lovell, S. Soman, and M. A. Bradley, "Oxidatively modified nucleic acids in preclinical Alzheimer's disease (PCAD) brain," *Mechanisms of Ageing and Development*, vol. 132, no. 8-9, pp. 443–448, 2011.

[12] M. A. Lovell and W. R. Markesbery, "Oxidatively modified RNA in mild cognitive impairment," *Neurobiology of Disease*, vol. 29, no. 2, pp. 169–175, 2008.

[13] A. Nunomura, T. Tamaoki, N. Motohashi et al., "The earliest stage of cognitive impairment in transition from normal aging to Alzheimer disease is marked by prominent RNA oxidation in vulnerable neurons," *Journal of Neuropathology and Experimental Neurology*, vol. 71, no. 3, pp. 233–241, 2012.

[14] M. A. Lovell, S. Xiong, G. Lyubartseva, and W. R. Markesbery, "Organoselenium (Sel-Plex diet) decreases amyloid burden and RNA and DNA oxidative damage in APP/PS1 mice," *Free Radical Biology & Medicine*, vol. 46, no. 11, pp. 1527–1533, 2009.

[15] S. Porcellotti, F. Fanelli, A. Fracassi et al., "Oxidative stress during the progression of β-amyloid pathology in the neocortex of the Tg2576 mouse model of Alzheimer's disease," *Oxidative Medicine and Cellular Longevity*, vol. 2015, Article ID 967203, 18 pages, 2015.

[16] T. Ishii, H. Hayakawa, T. Igawa, T. Sekiguchi, and M. Sekiguchi, "Specific binding of PCBP1 to heavily oxidized RNA to induce cell death," *Proceedings of the National Academy of Sciences of the United States of America*, vol. 115, no. 26, pp. 6715–6720, 2018.

[17] M. J. Millan, "Linking deregulation of non-coding RNA to the core pathophysiology of Alzheimer's disease: An integrative review," *Progress in Neurobiology*, vol. 156, pp. 1–68, 2017.

[18] M. L. Idda, R. Munk, K. Abdelmohsen, and M. Gorospe, "Noncoding RNAs in Alzheimer's disease," *Wiley Interdiscip Rev RNA*, vol. 9, no. 2, p. e1463, 2018.

[19] J. X. Wang, J. Gao, S. L. Ding et al., "Oxidative modification of miR-184 enables it to target Bcl-xL and Bcl-w," *Molecular Cell*, vol. 59, no. 1, pp. 50–61, 2015.

[20] X. Cao, G. Yeo, A. R. Muotri, T. Kuwabara, and F. H. Gage, "Noncoding RNAs in the mammalian central nervous system," *Annual Review of Neuroscience*, vol. 29, no. 1, pp. 77–103, 2006.

[21] M. F. Mehler and J. S. Mattick, "Noncoding RNAs and RNA editing in brain development, functional diversification, and neurological disease," *Physiological Reviews*, vol. 87, no. 3, pp. 799–823, 2007.

[22] G. Barry and J. S. Mattick, "The role of regulatory RNA in cognitive evolution," *Trends in Cognitive Sciences*, vol. 16, no. 10, pp. 497–503, 2012.

[23] G. Barry, "Integrating the roles of long and small non-coding RNA in brain function and disease," *Molecular Psychiatry*, vol. 19, no. 4, pp. 410–416, 2014.

[24] S. L. Hollins and M. J. Cairns, "MicroRNA: small RNA mediators of the brains genomic response to environmental stress," *Progress in Neurobiology*, vol. 143, pp. 61–81, 2016.

[25] M. S. Leisegang, K. Schröder, and R. P. Brandes, "Redox regulation and noncoding RNAs," *Antioxidants & Redox Signaling*, vol. 29, no. 9, pp. 793–812, 2018.

[26] N. Amakiri, A. Kubosumi, J. Tran, and P. H. Reddy, "Amyloid beta and microRNAs in Alzheimer's disease," *Frontiers in Neuroscience*, vol. 13, p. 430, 2019.

[27] J. Konovalova, D. Gerasymchuk, I. Parkkinen, P. Chmielarz, and A. Domanskyi, "Interplay between microRNAs and oxidative stress in neurodegenerative diseases," *International Journal of Molecular Sciences*, vol. 20, no. 23, p. 6055, 2019.

[28] H. Yanagawa, Y. Ogawa, and M. Ueno, "Redox ribonucleosides. Isolation and characterization of 5-hydroxyuridine, 8-hydroxyguanosine, and 8-hydroxyadenosine from Torula yeast RNA," *The Journal of Biological Chemistry*, vol. 267, pp. 13320–13326, 1992.

[29] Y. Rhee, M. R. Valentine, and J. Termini, "Oxidative base damage in RNA detected by reverse transcriptase," *Nucleic Acids Research*, vol. 23, no. 16, pp. 3275–3282, 1995.

[30] J. Barciszewski, M. Z. Barciszewska, G. Siboska, S. I. Rattan, and B. F. Clark, "Some unusual nucleic acid bases are products of hydroxyl radical oxidation of DNA and RNA," *Molecular Biology Reports*, vol. 26, no. 4, pp. 231–238, 1999.

[31] Z. Shen, W. Wu, and S. L. Hazen, "Activated leukocytes oxidatively damage DNA, RNA, and the nucleotide pool through halide-dependent formation of hydroxyl radical," *Biochemistry*, vol. 39, no. 18, pp. 5474–5482, 2000.

[32] T. Hofer, C. Badouard, E. Bajak, J. L. Ravanat, A. Mattsson, and I. A. Cotgreave, "Hydrogen peroxide causes greater oxidation in cellular RNA than in DNA," *Biological Chemistry*, vol. 386, no. 4, pp. 333–337, 2005.

[33] D. Brégeon and A. Sarasin, "Hypothetical role of RNA damage avoidance in preventing human disease," *Mutation Research*, vol. 577, no. 1-2, pp. 293–302, 2005.

[34] Z. Li, J. Wu, and C. DeLeo, "RNA damage and surveillance under oxidative stress," *IUBMB Life*, vol. 58, no. 10, pp. 581–588, 2006.

[35] P. I. Moreira, A. Nunomura, M. Nakamura et al., "Nucleic acid oxidation in Alzheimer disease," *Free Radical Biology & Medicine*, vol. 44, no. 8, pp. 1493–1505, 2008.

[36] X. Shan, H. Tashiro, and C.-l. G. Lin, "The identification and characterization of oxidized RNAs in Alzheimer's disease," *The Journal of Neuroscience*, vol. 23, no. 12, pp. 4913–4921, 2003.

[37] K. Honda, M. A. Smith, X. Zhu et al., "Ribosomal RNA in Alzheimer disease is oxidized by bound redox-active iron," *The Journal of Biological Chemistry*, vol. 280, no. 22, pp. 20978–20986, 2005.

[38] Q. Ding, W. R. Markesbery, Q. Chen, F. Li, and J. N. Keller, "Ribosome dysfunction is an early event in Alzheimer's disease," *The Journal of Neuroscience*, vol. 25, no. 40, pp. 9171–9175, 2005.

[39] D. P. Bartel, "MicroRNAs: genomics, biogenesis, mechanism, and function," *Cell*, vol. 116, no. 2, pp. 281–297, 2004.

[40] T. Kawamata, H. Seitz, and Y. Tomari, "Structural determinants of miRNAs for RISC loading and slicer-independent unwinding," *Nature Structural & Molecular Biology*, vol. 16, no. 9, pp. 953–960, 2009.

[41] A. K. L. Leung, "The whereabouts of microRNA actions: cytoplasm and beyond," *Trends in Cell Biology*, vol. 25, no. 10, pp. 601–610, 2015.

[42] B. J. Goldie, C. Fitzsimmons, J. Weidenhofer, J. R. Atkins, D. O. Wang, and M. J. Cairns, "miRNA enriched in human neuroblast nuclei bind the MAZ transcription factor and

their precursors contain the MAZ consensus motif," *Frontiers in Molecular Neuroscience*, vol. 10, p. 259, 2017.

[43] Z. Zhang, Y. W. Qin, G. Brewer, and Q. Jing, "MicroRNA degradation and turnover: regulating the regulators," *Wiley Interdisciplinary Reviews: RNA*, vol. 3, no. 4, pp. 593–600, 2012.

[44] M. Prendecki, J. Florczak-Wyspianska, M. Kowalska et al., "APOE genetic variants and apoE, miR-107 and miR-650 levels in Alzheimer's disease," *Folia Neuropathologica*, vol. 57, no. 2, pp. 106–116, 2019.

[45] M. Essack, A. Salhi, C. Van Neste et al., "DES-ROD: exploring literature to develop new links between RNA oxidation and human diseases," *Oxidative Medicine and Cellular Longevity*, vol. 2020, Article ID 5904315, 13 pages, 2020.

[46] B. Zhang, D. Han, Y. Korostelev et al., "Changes in snoRNA and snRNA abundance in the human, chimpanzee, macaque, and mouse brain," *Genome Biology and Evolution*, vol. 8, pp. 840–850, 2016.

[47] C. Yao and B. Yu, "Role of long noncoding RNAs and circular RNAs in nerve regeneration," *Frontiers in Molecular Neuroscience*, vol. 12, p. 165, 2019.

[48] J. N. Cobley, M. L. Fiorello, and D. M. Bailey, "13 reasons why the brain is susceptible to oxidative stress," *Redox Biology*, vol. 15, pp. 490–503, 2018.

[49] J. T. Coyle and P. Puttfarcken, "Oxidative stress, glutamate, and neurodegenerative disorders," *Science*, vol. 262, no. 5134, pp. 689–695, 1993.

[50] M. P. Mattson, S. L. Chan, and W. Duan, "Modification of brain aging and neurodegenerative disorders by genes, diet, and behavior," *Physiological Reviews*, vol. 82, no. 3, pp. 637–672, 2002.

[51] B. Halliwell, "Reactive oxygen species and the central nervous system," *Journal of Neurochemistry*, vol. 59, no. 5, pp. 1609–1623, 1992.

[52] H. Joenje, "Genetic toxicology of oxygen," *Mutation Research*, vol. 219, no. 4, pp. 193–208, 1989.

[53] M. A. Takahashi and K. Asada, "Superoxide anion permeability of phospholipid membranes and chloroplast thylakoids," *Archives of Biochemistry and Biophysics*, vol. 226, pp. 558–566, 1983.

[54] A. Nunomura, G. Perry, M. A. Pappolla et al., "RNA oxidation is a prominent feature of vulnerable neurons in Alzheimer's disease," *Journal of Neuroscience*, vol. 19, no. 6, pp. 1959–1964, 1999.

[55] A. Nunomura, G. Perry, G. Aliev et al., "Oxidative damage is the earliest event in Alzheimer disease," *Journal of Neuropathology and Experimental Neurology*, vol. 60, no. 8, pp. 759–767, 2001.

[56] J. Schubert and J. W. Wilmer, "Does hydrogen peroxide exist "free" in biological systems?," *Free Radical Biology and Medicine*, vol. 11, pp. 545–555, 1991.

[57] K. Hirai, G. Aliev, A. Nunomura et al., "Mitochondrial abnormalities in Alzheimer's disease," *Journal of Neuroscience*, vol. 21, no. 9, pp. 3017–3023, 2001.

[58] M. T. Lin and M. F. Beal, "Mitochondrial dysfunction and oxidative stress in neurodegenerative diseases," *Nature*, vol. 443, no. 7113, pp. 787–795, 2006.

[59] M. A. Smith, A. Nunomura, X. Zhu, A. Takeda, and G. Perry, "Metabolic, metallic, and mitotic sources of oxidative stress in Alzheimer disease," *Antioxidants & Redox Signaling*, vol. 2, no. 3, pp. 413–420, 2000.

[60] F. Taddei, H. Hayakawa, M. Bouton et al., "Counteraction by MutT protein of transcriptional errors caused by oxidative damage," *Science*, vol. 278, no. 5335, pp. 128–130, 1997.

[61] T. Ishibashi, H. Hayakawa, R. Ito, M. Miyazawa, Y. Yamagata, and M. Sekiguchi, "Mammalian enzymes for preventing transcriptional errors caused by oxidative damage," *Nucleic Acids Research*, vol. 33, no. 12, pp. 3779–3784, 2005.

[62] X. Shan, Y. Chang, and C. L. Glenn Lin, "Messenger RNA oxidation is an early event preceding cell death and causes reduced protein expression," *The FASEB Journal*, vol. 21, no. 11, pp. 2753–2764, 2007.

[63] A. Calabretta, P. A. Küpfer, and C. J. Leumann, "The effect of RNA base lesions on mRNA translation," *Nucleic Acids Research*, vol. 43, no. 9, pp. 4713–4720, 2015.

[64] M. Tanaka, P. B. Chock, and E. R. Stadtman, "Oxidized messenger RNA induces translation errors," *Proceedings of the National Academy of Sciences*, vol. 104, no. 1, pp. 66–71, 2007.

[65] A. C. Jacobs, M. J. Resendiz, and M. M. Greenberg, "Direct strand scission from a nucleobase radical in RNA," *Journal of the American Chemical Society*, vol. 132, no. 11, pp. 3668-3669, 2010.

[66] Q. Ding, W. R. Markesbery, V. Cecarini, and J. N. Keller, "Decreased RNA, and increased RNA oxidation, in ribosomes from early Alzheimer's disease," *Neurochemical Research*, vol. 31, no. 5, pp. 705–710, 2006.

[67] D. M. Thompson, C. Lu, P. J. Green, and R. Parker, "tRNA cleavage is a conserved response to oxidative stress in eukaryotes," *RNA*, vol. 14, no. 10, pp. 2095–2103, 2008.

[68] M. Tanaka, P. Jaruga, P. A. Küpfer et al., "RNA oxidation catalyzed by cytochrome c leads to its depurination and cross-linking, which may facilitate cytochrome c release from mitochondria," *Free Radical Biology & Medicine*, vol. 53, no. 4, pp. 854–862, 2012.

[69] M. P. Deutscher, "Degradation of RNA in bacteria: comparison of mRNA and stable RNA," *Nucleic Acids Research*, vol. 34, no. 2, pp. 659–666, 2006.

[70] P. A. Aas, M. Otterlei, P. O. Falnes et al., "Human and bacterial oxidative demethylases repair alkylation damage in both RNA and DNA," *Nature*, vol. 421, no. 6925, pp. 859–863, 2003.

[71] A. Bellacosa and E. G. Moss, "RNA repair: damage control," *Current Biology*, vol. 13, no. 12, pp. R482–R484, 2003.

[72] Z. Li, S. Malla, B. Shin, and J. M. Li, "Battle against RNA oxidation: molecular mechanisms for reducing oxidized RNA to protect cells," *Wiley Interdisciplinary Reviews: RNA*, vol. 5, no. 3, pp. 335–346, 2014.

[73] R. Ito, H. Hayakawa, M. Sekiguchi, and T. Ishibashi, "Multiple enzyme activities of Escherichia coli MutT protein for sanitization of DNA and RNA precursor pools," *Biochemistry*, vol. 44, no. 17, pp. 6670–6674, 2005.

[74] A. Furuta, T. Iida, Y. Nakabeppu, and T. Iwaki, "Expression of hMTH1 in the hippocampi of control and Alzheimer's disease," *Neuroreport*, vol. 12, no. 13, pp. 2895–2899, 2001.

[75] H. Shimura-Miura, N. Hattori, D. Kang, K. Miyako, Y. Nakabeppu, and Y. Mizuno, "Increased 8-oxo-dGTPase in the mitochondria of substantia nigral neurons in Parkinson's disease," *Annals of Neurology*, vol. 46, no. 6, pp. 920–924, 1999.

[76] H. Hayakawa, A. Hofer, L. Thelander et al., "Metabolic fate of oxidized guanine ribonucleotides in mammalian cells," *Biochemistry*, vol. 38, no. 12, pp. 3610–3614, 1999.

[77] H. Hayakawa, M. Kuwano, and M. Sekiguchi, "Specific binding of 8-oxoguanine-containing RNA to polynucleotide phosphorylase protein," *Biochemistry*, vol. 40, no. 33, pp. 9977–9982, 2001.

[78] H. Hayakawa and M. Sekiguchi, "Human polynucleotide phosphorylase protein in response to oxidative stress," *Biochemistry*, vol. 45, no. 21, pp. 6749–6755, 2006.

[79] H. Hayakawa, T. Uchiumi, T. Fukuda et al., "Binding capacity of human YB-1 protein for RNA containing 8-oxoguanine," *Biochemistry*, vol. 41, no. 42, pp. 12739–12744, 2002.

[80] H. Hayakawa, A. Fujikane, R. Ito, M. Matsumoto, K. I. Nakayama, and M. Sekiguchi, "Human proteins that specifically bind to 8-oxoguanine-containing RNA and their responses to oxidative stress," *Biochemical and Biophysical Research Communications*, vol. 403, no. 2, pp. 220–224, 2010.

[81] T. Ishii, H. Hayakawa, T. Sekiguchi, N. Adachi, and M. Sekiguchi, "Role of Auf1 in elimination of oxidatively damaged messenger RNA in human cells," *Free Radical Biology & Medicine*, vol. 79, pp. 109–116, 2015.

[82] S. Rüegger and H. Großhans, "MicroRNA turnover: when, how, and why," *Trends in Biochemical Sciences*, vol. 37, no. 10, pp. 436–446, 2012.

[83] L. L. Yan and H. S. Zaher, "How do cells cope with RNA damage and its consequences?," *The Journal of Biological Chemistry*, vol. 294, no. 41, pp. 15158–15171, 2019.

[84] T. Hofer, L. Fontana, S. D. Anton et al., "Long-term effects of caloric restriction or exercise on DNA and RNA oxidation levels in white blood cells and urine in humans," *Rejuvenation Research*, vol. 11, no. 4, pp. 793–799, 2008.

[85] J. Liu, E. Head, A. M. Gharib et al., "Memory loss in old rats is associated with brain mitochondrial decay and RNA/DNA oxidation: partial reversal by feeding acetyl-L-carnitine and/or R-alpha -lipoic acid," *Proceedings of the National Academy of Sciences*, vol. 99, no. 4, pp. 2356–2361, 2002.

[86] V. R. King, W. L. Huang, S. C. Dyall, O. E. Curran, J. V. Priestley, and A. T. Michael-Titus, "Omega-3 fatty acids improve recovery, whereas omega-6 fatty acids worsen outcome, after spinal cord injury in the adult rat," *The Journal of Neuroscience*, vol. 26, no. 17, pp. 4672–4680, 2006.

[87] J. Brück, B. Görg, H. J. Bidmon et al., "Locomotor impairment and cerebrocortical oxidative stress in portal vein ligated rats in vivo," *Journal of Hepatology*, vol. 54, no. 2, pp. 251–257, 2011.

[88] Y. Chang, Q. Kong, X. Shan et al., "Messenger RNA oxidation occurs early in disease pathogenesis and promotes motor neuron degeneration in ALS," *PLoS One*, vol. 3, no. 8, article e2849, 2008.

[89] G. De Luca, I. Ventura, V. Sanghez et al., "Prolonged lifespan with enhanced exploratory behavior in mice overexpressing the oxidized nucleoside triphosphatase hMTH1," *Aging Cell*, vol. 12, no. 4, pp. 695–705, 2013.

[90] M. M. J. van den Berg, J. Krauskopf, J. G. Ramaekers, J. C. S. Kleinjans, J. Prickaerts, and J. J. Briedé, "Circulating microRNAs as potential biomarkers for psychiatric and neurodegenerative disorders," *Progress in Neurobiology*, vol. 185, p. 101732, 2020.

[91] C. A. Juźwik, S. Drake, Y. Zhang et al., "microRNA dysregulation in neurodegenerative diseases: A systematic review," *Progress in Neurobiology*, vol. 182, article 101664, 2019.

[92] W. X. Wang, B. W. Rajeev, A. J. Stromberg et al., "The expression of microRNA miR-107 decreases early in Alzheimer's disease and may accelerate disease progression through regulation of -Site Amyloid Precursor Protein-Cleaving Enzyme 1," *The Journal of Neuroscience*, vol. 28, no. 5, pp. 1213–1223, 2008.

[93] J. P. Cogswell, J. Ward, I. A. Taylor et al., "Identification of miRNA changes in Alzheimer's disease brain and CSF yields putative biomarkers and insights into disease pathways," *Journal of Alzheimer's Disease*, vol. 14, no. 1, pp. 27–41, 2008.

[94] M. Müller, H. B. Kuiperij, J. A. Claassen, B. Küsters, and M. M. Verbeek, "MicroRNAs in Alzheimer's disease: differential expression in hippocampus and cell-free cerebrospinal fluid," *Neurobiology of Aging*, vol. 35, no. 1, pp. 152–158, 2014.

[95] S. Absalon, D. M. Kochanek, V. Raghavan, and A. M. Krichevsky, "MiR-26b, upregulated in Alzheimer's disease, activates cell cycle entry, tau-phosphorylation, and apoptosis in postmitotic neurons," *The Journal of Neuroscience*, vol. 33, no. 37, pp. 14645–14659, 2013.

[96] P. Lau, K. Bossers, R.'. Janky et al., "Alteration of the microRNA network during the progression of Alzheimer's disease," *EMBO Molecular Medicine*, vol. 5, no. 10, pp. 1613–1634, 2013.

[97] P. T. Nelson, H. Braak, and W. R. Markesbery, "Neuropathology and cognitive impairment in Alzheimer disease: a complex but coherent relationship," *Journal of Neuropathology and Experimental Neurology*, vol. 68, no. 1, pp. 1–14, 2009.

[98] W. R. Markesbery, "Neuropathologic alterations in mild cognitive impairment: a review," *Journal of Alzheimer's Disease*, vol. 19, no. 1, pp. 221–228, 2010.

[99] Y. Jin, Q. Tu, and M. Liu, "MicroRNA-125b regulates Alzheimer's disease through SphK1 regulation," *Molecular Medicine Reports*, vol. 18, pp. 2373–2380, 2018.

[100] L. Zhang, H. Dong, Y. Si et al., "miR-125b promotes tau phosphorylation by targeting the neural cell adhesion molecule in neuropathological progression," *Neurobiology of Aging*, vol. 73, pp. 41–49, 2019.

[101] W. J. Lukiw, Y. Zhao, and J. G. Cui, "An NF-κB-sensitive micro RNA-146a-mediated inflammatory circuit in Alzheimer disease and in stressed human brain cells," *The Journal of Biological Chemistry*, vol. 283, pp. 31315–31322, 2008.

[102] G. Wang, Y. Huang, L. L. Wang et al., "MicroRNA-146a suppresses ROCK1 allowing hyperphosphorylation of tau in Alzheimer's disease," *Scientific Reports*, vol. 6, no. 1, article 26697, 2016.

[103] G. Ji, K. Lv, H. Chen et al., "MiR-146a regulates SOD2 expression in H_2O_2 stimulated PC12 cells," *PLoS One*, vol. 8, no. 7, article e69351, 2013.

[104] S. Sarkar, S. Jun, S. Rellick, D. D. Quintana, J. Z. Cavendish, and J. W. Simpkins, "Expression of microRNA-34a in Alzheimer's disease brain targets genes linked to synaptic plasticity, energy metabolism, and resting state network activity," *Brain Research*, vol. 1646, pp. 139–151, 2016.

[105] N. Tong, R. Jin, Z. Zhou, and X. Wu, "Involvement of *microRNA-34a* in age-related susceptibility to oxidative stress in ARPE-19 cells by targeting the silent mating type information regulation 2 homolog 1/p66shc pathway: implications for

age-related macular degeneration," *Frontiers in Aging Neuroscience*, vol. 11, p. 137, 2019.

[106] S. Sarkar, E. B. Engler-Chiurazzi, J. Z. Cavendish et al., "Overexpression of miR-34a induces rapid cognitive impairment and Alzheimer's disease-like pathology," *Brain Research*, vol. 1721, p. 146327, 2019.

[107] Y. Zhao, V. Jaber, and W. J. Lukiw, "Over-expressed pathogenic miRNAs in Alzheimer's disease (AD) and prion disease (PrD) drive deficits in TREM2-mediated Aβ42 peptide clearance," *Frontiers in Aging Neuroscience*, vol. 8, p. 140, 2016.

[108] X. Wang, P. Liu, H. Zhu et al., "miR-34a, a microRNA up-regulated in a double transgenic mouse model of Alzheimer's disease, inhibits bcl2 translation," *Brain Research Bulletin*, vol. 80, no. 4-5, pp. 268–273, 2009.

[109] Z. Shi, K. Zhang, H. Zhou et al., "Increased miR-34c mediates synaptic deficits by targeting synaptotagmin 1 through ROS-JNK-p53 pathway in Alzheimer's disease," *Aging Cell*, vol. 19, no. 3, article e13125, 2020.

[110] Y. Cheng, M. Zhou, and W. Zhou, "MicroRNA-30e regulates TGF-β-mediated NADPH oxidase 4-dependent oxidative stress by Snai1 in atherosclerosis," *International Journal of Molecular Medicine*, vol. 43, pp. 1806–1816, 2019.

[111] Q. Wu, X. Ye, Y. Xiong et al., "The protective role of microRNA-200c in Alzheimer's disease pathologies is induced by beta amyloid-triggered endoplasmic reticulum stress," *Frontiers in Molecular Neuroscience*, vol. 9, p. 140, 2016.

[112] S. Xu, R. Zhang, J. Niu et al., "Oxidative stress mediated-alterations of the microRNA expression profile in mouse hippocampal neurons," *International Journal of Molecular Sciences*, vol. 13, no. 12, pp. 16945–16960, 2012.

[113] S. Higaki, M. Muramatsu, A. Matsuda et al., "Defensive effect of microRNA-200b/c against amyloid-beta peptide-induced toxicity in Alzheimer's disease models," *PLoS One*, vol. 13, no. 5, article e0196929, 2018.

[114] Y. Du, X. Chi, and W. An, "Downregulation of microRNA-200c-3p reduces damage of hippocampal neurons in epileptic rats by upregulating expression of RECK and inactivating the AKT signaling pathway," *Chemico-Biological Interactions*, vol. 307, pp. 223–233, 2019.

[115] Y. Jiao, L. Kong, Y. Yao et al., "Osthole decreases beta amyloid levels through up-regulation of miR-107 in Alzheimer's disease," *Neuropharmacology*, vol. 108, pp. 332–344, 2016.

[116] J. J. Li, G. Dolios, R. Wang, and F. F. Liao, "Soluble beta-amyloid peptides, but not insoluble fibrils, have specific effect on neuronal microRNA expression," *PLoS One*, vol. 9, no. 3, article e90770, 2014.

[117] D. A. Butterfield, A. M. Swomley, and R. Sultana, "Amyloidβ-Peptide (1-42)-induced oxidative stress in Alzheimer disease: importance in disease pathogenesis and progression," *Antioxidants & Redox Signaling*, vol. 19, no. 8, pp. 823–835, 2013.

[118] M. A. Faghihi, M. Zhang, J. Huang et al., "Evidence for natural antisense transcript-mediated inhibition of microRNA function," *Genome Biology*, vol. 11, no. 5, p. R56, 2010.

[119] X. Chen, S. Zhang, P. Shi, Y. Su, D. Zhang, and N. Li, "MiR-485-5p promotes neuron survival through mediating Rac1/-Notch2 signaling pathway after cerebral ischemia/reperfusion," *Current Neurovascular Research*, vol. 17, no. 3, pp. 259–266, 2020.

[120] L. Geng, T. Zhang, W. Liu, and Y. Chen, "Inhibition of miR-128 abates Aβ-mediated cytotoxicity by targeting PPAR-γ via NF-κB inactivation in primary mouse cortical neurons and neuro2a cells," *Yonsei Medical Journal*, vol. 59, no. 9, pp. 1096–1106, 2018.

[121] X. Zhao, Y. Jin, L. Li et al., "MicroRNA-128-3p aggravates doxorubicin-induced liver injury by promoting oxidative stress via targeting Sirtuin-1," *Pharmacological Research*, vol. 146, p. 104276, 2019.

[122] J. Li and H. Wang, "miR-15b reduces amyloid-β accumulation in SH-SY5Y cell line through targetting NF-κB signaling and BACE1," *Bioscience Reports*, vol. 38, 2018.

[123] A. Lang, S. Grether-Beck, M. Singh et al., "MicroRNA-15b regulates mitochondrial ROS production and the senescence-associated secretory phenotype through sirtuin 4/SIRT4," *Aging*, vol. 8, no. 3, pp. 484–505, 2016.

[124] R. Zhang, Q. Zhang, J. Niu et al., "Screening of microRNAs associated with Alzheimer's disease using oxidative stress cell model and different strains of senescence accelerated mice," *Journal of the Neurological Sciences*, vol. 338, no. 1-2, pp. 57–64, 2014.

[125] S. S. Hébert, K. Horré, L. Nicolaï et al., "MicroRNA regulation of Alzheimer's amyloid precursor protein expression," *Neurobiology of Disease*, vol. 33, no. 3, pp. 422–428, 2009.

[126] F. Z. Chen, Y. Zhao, and H. Z. Chen, "MicroRNA-98 reduces amyloid β-protein production and improves oxidative stress and mitochondrial dysfunction through the notch signaling pathway via HEY2 in Alzheimer's disease mice," *International Journal of Molecular Medicine*, vol. 43, pp. 91–102, 2018.

[127] Y. Zhou, Z. F. Wang, W. Li et al., "Protective effects of microRNA-330 on amyloid β-protein production, oxidative stress, and mitochondrial dysfunction in Alzheimer's disease by targeting VAV1 via the MAPK signaling pathway," *Journal of Cellular Biochemistry*, vol. 119, no. 7, pp. 5437–5448, 2018.

[128] L. L. Wang, L. Min, Q. D. Guo et al., "Profiling microRNA from brain by microarray in a transgenic mouse model of Alzheimer's disease," *BioMed Research International*, vol. 2017, 8030311 pages, 2017.

[129] J. L. Jankowsky, D. J. Fadale, J. Anderson et al., "Mutant presenilins specifically elevate the levels of the 42 residue β-amyloid peptide in vivo: evidence for augmentation of a 42-specific γ secretase," *Human Molecular Genetics*, vol. 13, no. 2, pp. 159–170, 2004.

[130] Y. Zhao, M. Zhu, Y. Yu et al., "Brain REST/NRSF is not only a silent repressor but also an active protector," *Molecular Neurobiology*, vol. 54, no. 1, pp. 541–550, 2017.

[131] J. Y. Hwang and R. S. Zukin, "REST, a master transcriptional regulator in neurodegenerative disease," *Current Opinion in Neurobiology*, vol. 48, pp. 193–200, 2018.

[132] T. Lu, L. Aron, J. Zullo et al., "REST and stress resistance in ageing and Alzheimer's disease," *Nature*, vol. 507, no. 7493, pp. 448–454, 2014.

[133] I. A. Qureshi and M. F. Mehler, "Regulation of non-coding RNA networks in the nervous system–what's the REST of the story?," *Neuroscience Letters*, vol. 466, no. 2, pp. 73–80, 2009.

[134] T. Y. Hou, Y. Zhou, L. S. Zhu et al., "Correcting abnormalities in miR-124/PTPN1 signaling rescues tau pathology in Alzheimer's disease," *Journal of Neurochemistry*, vol. 154, no. 4, pp. 441–457, 2020.

[135] Y. Xue, H. Qian, J. Hu et al., "Sequential regulatory loops as key gatekeepers for neuronal reprogramming in human cells," *Nature Neuroscience*, vol. 19, no. 6, pp. 807–815, 2016.

[136] M. P. Mattson and A. Cheng, "Neurohormetic phytochemicals: low-dose toxins that induce adaptive neuronal stress responses," *Trends in Neurosciences*, vol. 29, no. 11, pp. 632–639, 2006.

[137] M. Ristow, "Unraveling the truth about antioxidants: mitohormesis explains ROS-induced health benefits," *Nature Medicine*, vol. 20, no. 7, pp. 709–711, 2014.

[138] F. A. Taki, X. Pan, and B. Zhang, "Chronic nicotine exposure systemically alters microRNA expression profiles during post-embryonic stages in Caenorhabditis elegans," *Journal of Cellular Physiology*, vol. 229, pp. 79–89, 2013.

[139] S. Pinto, V. N. Sato, E. A. De-Souza et al., "Enoxacin extends lifespan of C. elegans by inhibiting miR-34-5p and promoting mitohormesis," *Redox Biology*, vol. 18, pp. 84–92, 2018.

[140] Y. Xu, M. T. Charles, Z. Luo et al., "Preharvest ultraviolet C treatment affected senescence of stored strawberry fruit with a potential role of microRNAs in the activation of the antioxidant system," *Journal of Agricultural and Food Chemistry*, vol. 66, no. 46, pp. 12188–12197, 2018.

[141] S. T. Lee, K. Chu, K. H. Jung et al., "MicroRNAs induced during ischemic preconditioning," *Stroke*, vol. 41, no. 8, pp. 1646–1651, 2010.

[142] T. Miyata, S. Takizawa, and C. van Ypersele de Strihou, "Hypoxia. 1. Intracellular sensors for oxygen and oxidative stress: novel therapeutic targets," *American Journal of Physiology. Cell Physiology*, vol. 300, no. 2, pp. C226–C231, 2011.

[143] S. Moncini, M. Lunghi, A. Valmadre et al., "The miR-15/107 family of microRNA genes regulates CDK5R1/p35 with implications for Alzheimer's disease pathogenesis," *Molecular Neurobiology*, vol. 54, no. 6, pp. 4329–4342, 2017.

[144] H. Shi, B. L. Sun, J. Zhang et al., "miR-15b suppression of Bcl-2 contributes to cerebral ischemic injury and is reversed by sevoflurane preconditioning," *CNS Neurol Disord Drug Targets*, vol. 12, no. 3, pp. 381–391, 2013.

[145] J. Ko, M. A. Hemphill, D. Gabrieli et al., "Smartphone-enabled optofluidic exosome diagnostic for concussion recovery," *Scientific Reports*, vol. 6, no. 1, p. 31215, 2016.

[146] B. Xu, Y. Zhang, X.-F. Du et al., "Neurons secrete miR-132-containing exosomes to regulate brain vascular integrity," *Cell Research*, vol. 27, no. 7, pp. 882–897, 2017.

[147] S. Swarbrick, N. Wragg, S. Ghosh, and A. Stolzing, "Systematic review of miRNA as biomarkers in Alzheimer's disease," *Molecular Neurobiology*, vol. 56, no. 9, pp. 6156–6167, 2019.

[148] P. N. Alexandrov, P. Dua, J. M. Hill, S. Bhattacharjee, Y. Zhao, and W. J. Lukiw, "microRNA (miRNA) speciation in Alzheimer's disease (AD) cerebrospinal fluid (CSF) and extracellular fluid (ECF). *Int*," *Journal of Biochemistry and Molecular Biology*, vol. 3, pp. 365–373, 2012.

[149] T. Wang, K. Chen, H. Li et al., "The feasibility of utilizing plasma *MiRNA107* and *BACE1* messenger RNA gene expression for clinical diagnosis of amnestic mild cognitive impairment," *The Journal of Clinical Psychiatry*, vol. 76, no. 2, pp. 135–141, 2015.

[150] L. Tan, J. T. Yu, Q. Y. Liu et al., "Circulating miR-125b as a biomarker of Alzheimer's disease," *Journal of the Neurological Sciences*, vol. 336, no. 1-2, pp. 52–56, 2014.

[151] S. Dowdy, "Overcoming cellular barriers for RNA therapeutics," *Nature Biotechnology*, vol. 35, no. 3, pp. 222–229, 2017.

[152] D. Adams, A. Gonzalez-Duarte, W. D. O'Riordan et al., "Patisiran, an RNAi therapeutic, for hereditary transthyretin amyloidosis," *The New England Journal of Medicine*, vol. 379, no. 1, pp. 11–21, 2018.

[153] E. Sardh, P. Harper, M. Balwani et al., "Phase 1 trial of an RNA interference therapy for acute intermittent porphyria," *The New England Journal of Medicine*, vol. 380, no. 6, pp. 549–558, 2019.

[154] M. Ghaffari, N. Sanadgol, and M. Abdollahi, "A systematic review of current progresses in the nucleic acid-based therapies for neurodegeneration with implications for Alzheimer's disease," *Mini Reviews in Medicinal Chemistry*, vol. 20, no. 15, pp. 1499–1517, 2020.

[155] F. Angelucci, K. Cechova, M. Valis, K. Kuca, B. Zhang, and J. Hort, "MicroRNAs in Alzheimer's disease: diagnostic markers or therapeutic agents?," *Frontiers in Pharmacology*, vol. 10, p. 665, 2019.

[156] B. Martinez and P. V. Peplow, "MicroRNAs in Parkinson's disease and emerging therapeutic targets," *Neural Regeneration Research*, vol. 12, no. 12, pp. 1945–1959, 2017.

[157] B. Shu, X. Zhang, G. Du, Q. Fu, and L. Huang, "MicroRNA-107 prevents amyloid-β-induced neurotoxicity and memory impairment in mice," *International Journal of Molecular Medicine*, vol. 41, pp. 1665–1672, 2017.

[158] J. Zhang, G. Perry, M. A. Smith et al., "Parkinson's disease is associated with oxidative damage to cytoplasmic DNA and RNA in substantia nigra neurons," *The American Journal of Pathology*, vol. 154, no. 5, pp. 1423–1429, 1999.

[159] H. E. Poulsen, E. Specht, K. Broedbaek et al., "RNA modifications by oxidation: a novel disease mechanism?," *Free Radical Biology & Medicine*, vol. 52, no. 8, pp. 1353–1361, 2012.

Hindawi
Oxidative Medicine and Cellular Longevity
Volume 2020, Article ID 3807476, 14 pages
https://doi.org/10.1155/2020/3807476

Research Article

Blood Exosomes Have Neuroprotective Effects in a Mouse Model of Parkinson's Disease

Ting Sun, Zhe-Xu Ding, Xin Luo, Qing-Shan Liu, and Yong Cheng

Key Laboratory for Ethnomedicine for Ministry of Education, Center on Translational Neuroscience, College of Life and Environmental Sciences, School of Pharmacy, Minzu University of China, Beijing, China

Correspondence should be addressed to Qing-Shan Liu; nlqsh@163.com and Yong Cheng; yongcheng@muc.edu.cn

Received 25 July 2020; Revised 7 October 2020; Accepted 28 October 2020; Published 26 November 2020

Academic Editor: Kambiz Hassanzadeh

Parkinson's disease (PD) is a common and complex neurodegenerative disease; the pathogenesis of which is still uncertain. Exosomes, nanosized extracellular vesicles, have been suggested to participate in the pathogenesis of PD, but their role is unknown. Here, a metabolomic analysis of serum and brain exosomes showed differentially expressed metabolites between 1-Methyl-4-phenyl-1, 2, 3, 6-tetrahydropyridine hydrochloride- (MPTP-) induced PD mice and control mice, such as oxidized lipids, vitamins, and cholesterol. These metabolites were enriched in coenzyme, nicotinamide, and amino acid pathways related to PD, and they could be served as preclinical biomarkers. We further found that blood-derived exosomes from healthy volunteers alleviated impaired motor coordination in MPTP-treated mice. Results from immunohistochemistry and western blotting indicated that the loss of dopaminergic neurons in substantia nigra and striatum of PD model mice was rescued by the exosome treatment. The exosome treatment also restored the homeostasis of oxidative stress, neuroinflammation, and cell apoptosis in the model mice. These results suggest that exosomes are important mediators for PD pathogenesis, and exosomes are promising targets for the diagnosis and treatment of PD.

1. Introduction

Parkinson's disease (PD) is the second most common neurodegenerative disease, affecting approximately 1% of the population aged > 60 years [1, 2]. A meta-analysis of the global data indicated the rising prevalence of PD with age along with some differences in prevalence by geographic location and sex [3, 4]. The first detailed description of PD was made approximately two centuries ago, but the pathogenesis of the disease remains unclear [5]. Its cardinal motor symptoms are bradykinesia, tremor, rigidity, flexed posture, postural instability, and freezing of gait [6, 7]. The crucial pathological feature of PD is the degeneration of dopaminergic neurons in the substantia nigra pars compacta (SNpc), a reduction in dopamine content in the striatum (Cpu), and the appearance of Lewy bodies [5, 6], which are aggregated by abnormally folded α-synuclein. Misfolded α-synuclein is the most abundant protein inclusion that can categorize PD with other neurodegenerative diseases. PD results from a complicated interplay of genetic and environmental factors, such as cigarette smoking and caffeine [8–10]. However, we cannot treat PD by modifying genetic or environmental risk factors. Neuroinflammation also contributes to PD pathology. In the early stages of diseases, astrocytes and microglia are both involved in the clearance of extracellular debris or release of nutrients and anti-inflammatory factors, which might aid the survival of neurons [11, 12]. However, activated microglia can release harmful reactive oxygen species, nitrogen species, and proinflammatory cytokines [13, 14]. Prolonged overactivation of microglia will exacerbate the death of dopaminergic neurons in the nigra [15, 16]. Accumulating evidence indicates that oxidative stress plays a key role in all forms of PD [17]. Studies of young PD patients have revealed that elevated oxidative stress is an important trait of the early disease stages and occurs before severe neuronal loss [18]. Exosomes, the smallest extracellular vesicles (diameter range 50-150 nm), are released by the fusion of multivesicular endosomal bodies with the plasma membrane [19, 20].

Exosomes can be released both *in vitro* and *in vivo* from a variety of nerve cells, such as neurons [21], microglia [22], and astrocytes [23]. Exosomes carry noncoding RNA such as miRNA, lncRNA, and circRNA, along with proteins and lipids [24, 25], and mediate intercellular and interorgan communication. In PD, exosomes secreted by neurons have been found to carry pathogenic proteins such as α-synuclein and are transmitted to other neurons or glial cells, leading to the further spread of misfolded α-synuclein and the occurrence of neuroinflammation [26–28]. There is reason to believe that the release and transmission of exosomes can dynamically reflect the pathological changes in cells in inaccessible areas such as the brain [29]. Some studies have demonstrated that the expression of proteins and RNAs in exosomes derived from the sera and cerebrospinal fluid (CSF) of PD patients significantly differ from those of healthy people [30]. The studies by Shi et al. [31] and Stuendl et al. [32] found significant differences in the exosomal α-synuclein in the plasma and CSF exosomes in PD patients and controls. The study also found a large increase in the number of exosomes in the CSF of PD patients [32]. Therefore, exosome has been suggested as a promising target for the diagnosis of PD [33]. Given the close relationship between dopamine loss and the metabolism of amino acids such as tyrosine, exosomal metabolomics analysis could receive more attention for predicting disease or discovering new potential biomarkers. However, there are no detailed studies on exosomal metabolites in relation to PD. In addition, signal molecules carried by exosomes may also affect gene expression in target cells. Many studies have indicated that exosomes derived from multiple cells may have therapeutic effects in neurological diseases such as stroke [34, 35], ischemia-reperfusion injury [36], traumatic brain injury [37, 38], and Alzheimer's disease [39]. Our latest study found that serum exosomes from major depressive disorder patients caused depressive-like behavior in healthy mice, and serum exosomes from healthy volunteers alleviated the depressive-like behaviors in unpredictable mild stress-treated mice [40]. We hypothesize that exosomes may also have potential predictive and therapeutic effects in PD. In this study, we are aimed at utilizing widely-targeted metabolomics technology to analyze the serum and brain exosomal metabolite differences between healthy and 1-Methyl-4-phenyl-1, 2, 3, 6-tetrahydropyridine hydrochloride- (MPTP-) induced PD mice, with the aim of identifying potential biomarkers of PD. In addition, we are aimed at exploring whether "normal" exosomes protect against PD.

2. Materials and Methods

2.1. Preparation of Exosomes. All volunteers were recruited from Minzu University of China (Supplementary Table 1). The blood exosome isolation and validation methods were performed as previously reported [41]. Briefly, exosomes were isolated from the diluted blood using a qEV column and concentrated with a 30 K MWCO PES protein concentrator-Vivaspin® (Sartorius, Gottingen, Germany). The concentrated exosomes were then resuspended in 200 μl phosphate-buffered saline (PBS) for further analysis.

2.2. Widely-Targeted Metabolomics. Widely-targeted metabolomics detection and quantification were conducted by the metabolomics provider METWARE on serum and brain samples from healthy control and MPTP-induced PD mice. Serum and brain exosome isolation was performed as described previously [41, 42]. Detailed methods are provided in Supplementary file 1.

2.3. Animals and Treatment. Ten-week-old male C57BL/6 mice (25 ± 2 g) were obtained from Vital River Laboratory (Beijing, China) and were housed at 24 ± 1°C and 50 ± 1% humidity under a 12 h light/dark cycle and provided with *ad libitum* access to a standard diet and drinking water. Animal procedures (including the euthanization method) were approved by the Animal Care and Use Committee of the Minzu University of China (ECMUC2019001AO). MPTP (Macklin, Shanghai, China) was used to generate the PD model. The mice were randomly divided into three groups: the control, MPTP, and exosomes+MPTP groups. The mice in the control group were intraperitoneally injected with saline. The MPTP and exosomes+MPTP groups were injected with MPTP (20 mg/kg, dissolved in saline) every 2 h for a total of four doses over an 8 h period in 1 day. The mice in the exosomes+MPTP group were caudal vein injected with exosomes (0.2 ml per mouse). The first injection was delivered 1 h before the first injection of MPTP, and thereafter once every 3 days for a total of four injections.

2.4. Behavior Test. The rotarod test was used to assess neurological impairment such as motor coordination and balance and was performed on days 1 and 11 after MPTP injection. The protocol followed was as previously reported [43]. Before MPTP injection, mice were pretrained for 3 days at 10 rpm until they were able to remain on the rod for at least 90 s. For the formal test, a rotating drum was accelerated from 4 to 40 rpm over 5 min. Each trial continued until the mice were unable to remain on the rod without falling off. The latency for the mice to fall from the rotarod was recorded ($n = 3$).

2.5. Brain Immunohistochemistry. After the rotarod test, mice were euthanized with pentobarbitone and perfused with saline. The brains were removed, postfixed in 4% paraformaldehyde overnight at 4°C, and then soaked in 20% and 30% sucrose and processed for cryoprotection. The frozen brains were cut into 40 μm coronal sections using a freezing microtome and stored in cryoprotectant (30% ethylene glycol, 30% sucrose, and 0.02 M PB) at -20°C until use. Brain sections were washed in PBS and treated with 3% H_2O_2, then blocked and perforated with 10% goat serum and 0.3% Triton X-100. The sections were then incubated overnight with primary antibodies TH (CST, Boston, MA, USA) at 4°C, followed by incubation with secondary antibodies which were goat anti-rabbit (1 : 400) for 1 h at 25°C. Sections were mounted on gelatin-coated slides, then dried, dehydrated, and coverslipped. The histological images were examined using a bright-field microscope.

2.6. Western Blot Analysis. The substantia nigra and striatum were isolated from the brain and homogenized with RIPA buffer. The protein concentration of the lysates was

determined by a BCA Protein Assay Kit and mixed with 4× loading buffer and boiled at 95°C for 5 min. Proteins were separated by sodium dodecyl sulfate–polyacrylamide gel electrophoresis and then transferred to a nitrocellulose membrane. The percentage of the SDS-PAGE gel was 10% for tyrosine hydroxylase (TH) and actin and 12% for Bax and Bcl-2. The blotted membrane was blocked with 5% skim milk for 1 h and then incubated overnight with corresponding primary antibodies at 4°C, followed by incubation with corresponding secondary antibodies for 1 h at 25°C, and subsequently visualized with an enhanced chemiluminescence reagent. The secondary antibodies were goat anti-rabbit (1 : 10,000) and goat anti-mouse (1 : 10,000) from CST.

2.7. Quantitative Real-Time Polymerase Chain Reaction. Total RNA from substantia nigra and striatum was, respectively, extracted with Trizol reagent. A PrimeScript RT reagent kit was used to synthesize first-strand cDNA. Then cDNAs were quantified by real-time polymerase chain reaction on LightCycler® 96 (Roche). GAPDH was used as a reference gene for analysis. Primers were synthesized by Sangon Biotech (Shanghai) Co., Ltd.

2.8. Oxidative Stress Marker Level/Activity Measurement. The MDA level and total SOD activity in the serum were measured by a colorimetric assay kit (Jiancheng Bioengineering Institute, China) according to the manufacturer's instructions.

2.9. Statistical Analysis. Data are presented as means ± standard deviation. Statistical significance ($p < 0.05$) was analyzed by one-way ANOVA or t-test with GraphPad Prism 7.

3. Results

3.1. Differentially Expressed Metabolites between Control and MPTP Mice. A widely-targeted metabolomics analysis was used to evaluate the differences in exosomal metabolites in the serum and the brain in healthy control and MPTP-induced PD mice. In this study, a total of 433 metabolites were detected in four groups: serum control (Sc), serum MPTP (Sm), brain control (Bc), and brain MPTP (Bm). A Score OPLS–DA Plot and an OPLS-DA S-Plot of Bc vs. Bm and Sc vs. Sm are presented in Figure 1. The metabolic data were analyzed according to the OPLS–DA model, and the Scores OPLS–DA Plot was drawn to illustrate the previous differences in each component.

The Variable Importance in Projection (VIP) of the OPLS-DA model and p value as determined by a Mann–Whitney U-test were used to screen the differential expression of metabolites. A VIP of ≥1 and p value of < 0.05 were considered to indicate differentially expressed metabolites. The results of the differential metabolism screening are provided in Supplementary Table 1. In the serum samples, 69 metabolites were found to be differentially expressed between the control group and MPTP group. In the brain tissue, 148 metabolites were found to be differentially expressed (Supplementary Tables 2 and 3). Additionally, 25 differently expressed metabolites were found in both serum and brain tissue (Table 1).

We next used the KEGG database to annotate the differentially expressed metabolites for potential biological functions. According to the KEGG pathway enrichment diagram, pathways such as the tyrosine metabolic pathway, purine metabolism, and glutamate metabolism pathways were found to be significantly enriched for differentially expressed metabolites in the serum and brain tissue (Figure 1).

3.2. Serum Exosomal Metabolites as Potential Biomarkers for PD. Receiver operating characteristic (ROC) curves were utilized to evaluate the accuracy of the metabolites in the serum for potentially differentiating MPTP mice from controls. We performed ROC curve analysis using the nine metabolites that contributed most to the differentiation of MPTP mice and controls. As indicated in Figure 2, serum exosomal phenylacetate (Figure 2(a), area under the curve [AUC] = 91.43% , 95% confidence interval [CI]: 79.16-100%), (S)-(-)-2-hydroxyisocaproic acid (Figure 2(b), AUC = 100%, 95% CI:100-100%), D-glucono-1,5-lactone (Figure 2(c), AUC = 92.14%, 95% CI: 81.74-100%), cholesterol (Figure 2(d), AUC = 97.86%, 95% CI: 93.29-100%), triethyl phosphate (Figure 2(e), AUC = 90%, 95% CI: 76.29-100%), 1,2-dichloroethane (Figure 2(f), AUC = 100%, 95% CI: 100-100%), carene (Figure 2(g), AUC = 85.71%, 95% CI: 70.16-100%), 2,4,6-trimethylphenol (Figure 2(h), AUC = 92.86%, 95% CI: 82.92-100%), and terpinolene (Figure 2(i), AUC = 95.71%, 95% CI: 88.36-100%) were found to have good to excellent performance to discriminate between MPTP mice and controls. This suggests that the above nine metabolites are likely to be potential biomarkers for PD.

3.3. Effects of Blood-Derived Exosomes from Healthy Volunteers on Motor Ability in PD Model Mice. The rotarod test was used to evaluate the motor coordination and balance of mice. The experimental design is illustrated in Figure 3(a). After pretraining and before MPTP injection, there was no significant difference in the latency of the mice in each group, indicating that the motor capacity of the mice in each group was similar (Figure 3(b)). On day 11, the rotarod test results indicated that MPTP treatment significantly decreased the latency and exosome treatment significantly improved the latency (Figure 3(c)) ($p < 0.001$).

3.4. Effects of Blood-Derived Exosomes from Healthy Volunteers on Dopamine Neurons in MPTP Mice. The improvement in motor dysfunction in exosome-treated MPTP-treated mice led us to hypothesize that exosomes may protect dopaminergic neurons from MPTP-induced injury. To test this hypothesis, we assessed whether exosomes prevent MPTP-induced neuronal damage. TH is a rate-limiting enzyme in dopamine biosynthesis and a well-known marker of dopaminergic neurons. The level of TH-positive neurons in the SNpc and CPu is recognized as an indicator of the severity of dopaminergic neuronal damage in MPTP-injured animals.

The immunohistochemical results in the SNpc indicated that the number of TH-positive neurons was significantly reduced in the MPTP group compared to that in the control

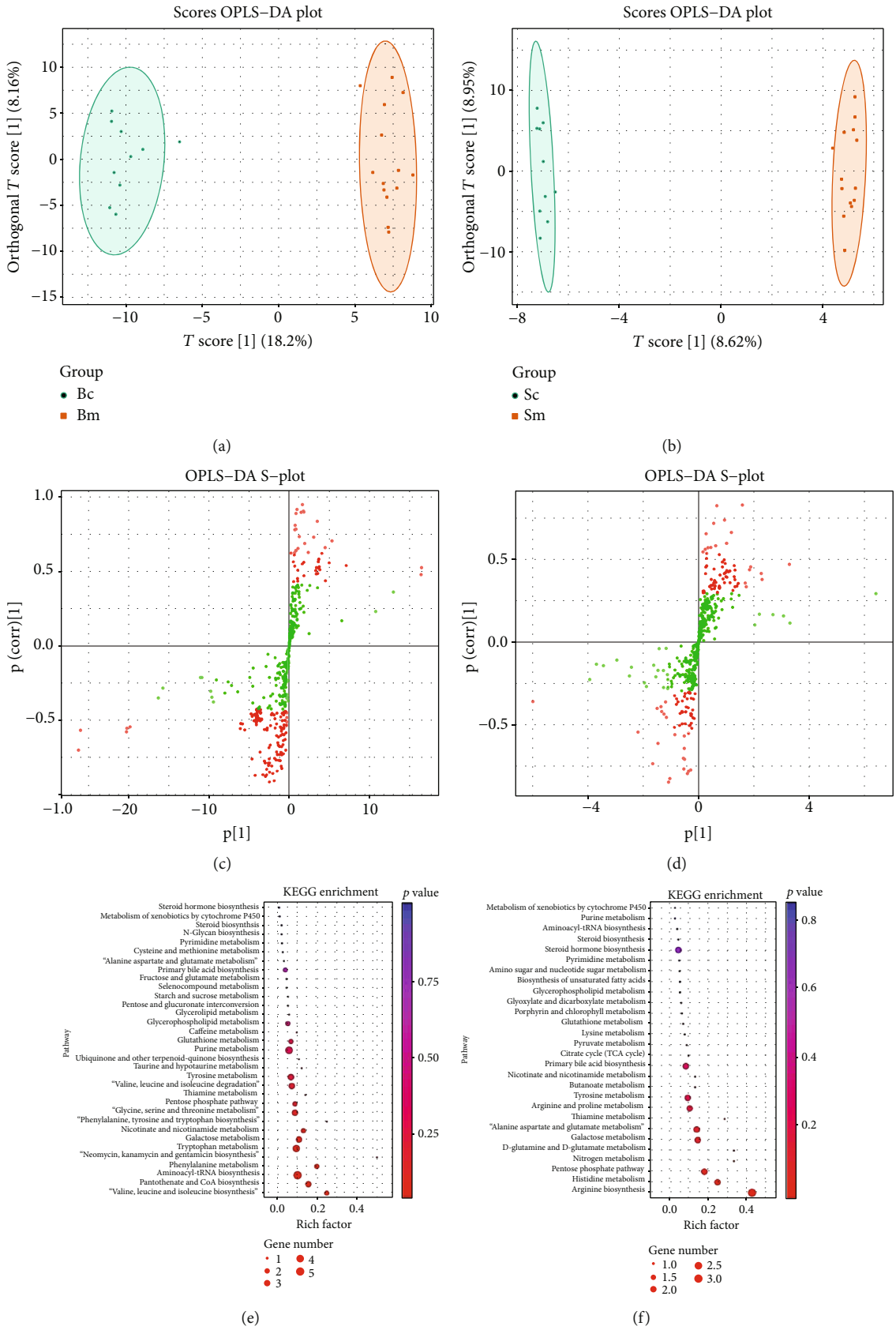

Figure 1: Widely-targeted metabolomics analysis was used to evaluate the differences of metabolites in the brain between control and PD model mice. Analysis of 14 Parkinson's disease mice and 10 control mice. A Score OPLS-DA Plot of metabolites in the brain (a) and serum (b). An OPLS-DA S-Plot of metabolites in the brain (c) and serum (d). Statistics of KEGG Enrichment in the brain (e) and serum (f).

Table 1: 25 differentially expressed metabolites in serum and brain tissue.

Compounds	Class	Serum			Brain		
		VIP	p value	Trend	VIP	p value	Trend
(5-L-Glutamyl)-L-amino acid	Amino acid metabolomics	1.50329	0.0308	Up	1.016439	0.0183	Up
Dulcitol	Carbohydrate metabolomics	1.508731	0.0283	Down	1.931532	<0.0001	Down
Phenyllactate (Pla)	Organic acid and its derivatives	2.503092	<0.0001	Down	1.087977	0.0039	Down
9,10-DiHOME [(±)9,10-dihydroxy-12Z-octadecenoic acid]	Oxidized lipid	1.826174	0.0067	Up	1.367845	0.0027	Down
Cis-11,14,17-eicosatrienoic acid (C20:3)	Lipids fatty acids	1.56911	0.0203	Up	2.024657	<0.0001	Down
(S)-(-)-2-Hydroxyisocaproic acid	Organic acid and its derivatives	2.884665	<0.0001	Down	1.71456	0.0002	Down
Neopterin	Pteridines and derivatives	1.910464	0.005	Up	2.007469	<0.0001	Down
4-Ethylbenzoic acid	Benzene and substituted derivatives	1.945169	0.0041	Up	1.970055	<0.0001	Down
2-Picolinic acid	Pyridine and pyridine derivatives	1.332943	0.0481	Down	1.325756	0.0032	Down
Adenine	Nucleotide metabolomics	1.548782	0.0288	Down	1.323111	0.0064	Down
D-Glucono-1,5-lactone	Carbohydrate metabolomics	2.446655	<0.0001	Up	1.465692	0.0013	Up
Nicotinic acid	CoOthersEnzyme factor & vitamin	1.906224	0.0066	Down	1.084725	0.0124	Down
1-Naphthylacetic acid	Organic acid and its derivatives	1.490897	0.0181	Down	1.612702	0.0008	Up
Cholesterol	Lipids	2.80908	<0.0001	Up	2.226335	<0.0001	Up
Hexadecanamide	Lipids fatty acids	1.291087	0.0274	Up	1.304757	0.0301	Up
Triethyl phosphate	Organic acid and its derivatives	2.413266	0.0001	Down	2.140886	<0.0001	Down
1,2-Dichloroethane	Hydrocarbon derivative	2.825226	<0.0001	Up	1.319369	0.0062	Up
(E)-2-Octen-1-ol	Alcohol	1.769306	0.0077	Down	1.246376	0.0071	Down
Barbituric acid	Heterocyclic compound	1.554395	0.0277	Down	1.196766	0.0072	Down
Carene	Heterocyclic compound	2.232867	0.0004	Up	2.123199	<0.0001	Down
Hexyl acetate	Fatty acyls	1.79975	0.0087	Up	1.554381	0.0003	Down
2,4,6-Trimethylphenol	Phenols and its derivatives	2.660509	<0.0001	Down	1.641595	0.0002	Down
Terpinolene	Terpenoid	2.707682	<0.0001	Down	1.474065	0.0004	Down
Octanal	Aldehyde	1.481981	0.0278	Down	1.129016	0.0196	Down
Naphthalene	Benzene and substituted derivatives	1.663639	0.0121	Down	1.255286	0.0057	Down

The name of compounds, class, VIP, p value, and trend of metabolites were shown in the table.

group ($p < 0.0001$). Exosome treatment almost completely reversed this reduction ($p < 0.0001$) (Figures 4(a) and 4(b)). Similar results were also reflected in the immunohistochemical staining of the CPu (Figure 4(c)). To further confirm these findings, we measured TH protein levels in the SNpc and CPu by western blot. Compared to the control group, TH protein expression was significantly reduced in both the SNpc and the CPu in the MPTP group ($p < 0.0001$), whereas exosome treatment significantly alleviated this reduction ($p < 0.05$) (Figures 4(d) and 4(e)).

3.5. mRNA Levels of Inflammatory and Anti-Inflammatory Factors in the SNpc and CPu. Neuroinflammation is one of the key pathogenic features of PD. In this study, we examined inflammatory and anti-inflammatory cytokine mRNA expression in the SNpc and CPu. The results revealed that the mRNA levels of interleukin (IL)-1β, IL-6, and tumor necrosis factor- (TNF-) α were significantly increased and those of IL-4, IL-10, and transforming growth factor- (TGF-) β were significantly decreased by MPTP treatment in the SNpc ($p < 0.05$). Exosome treatment significantly reduced the mRNA levels of IL1β, IL-6, and TNF-α and improved the mRNA levels of IL-4, IL-10, and TGF-β ($p < 0.05$) (Figures 5(a)–5(f)). Similar changes in IL-1β, IL-6, IL-4, IL-10, and TGF-β were observed in the CPu ($p < 0.05$) (Figures 5(g)–5(l)). These results indicate that neuroinflammation caused by MPTP could be relieved by exosome treatment.

3.6. Effects of Blood-Derived Exosomes from Healthy Volunteers on Oxidative Stress and Apoptosis. Oxidative stress has been implicated in the etiology of PD. The serum

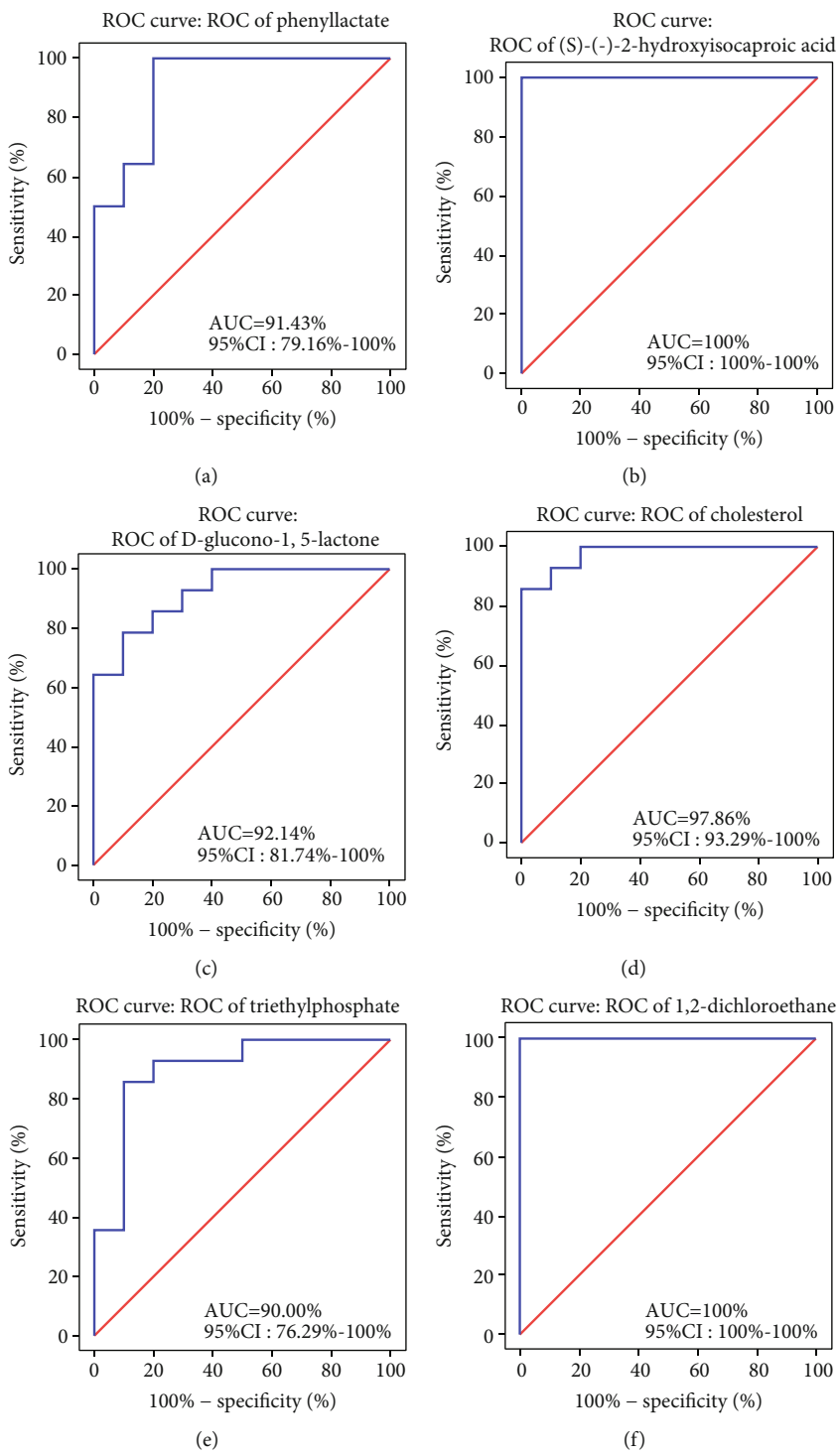

Figure 2: Continued.

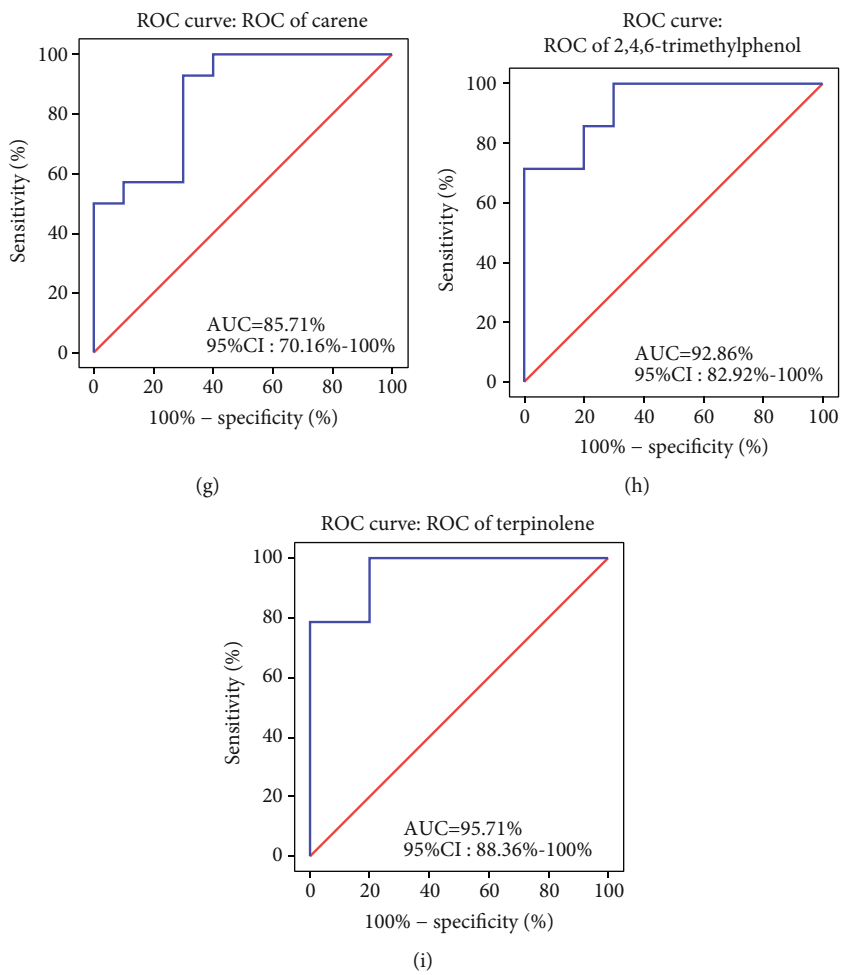

Figure 2: Serum exosomal metabolites as biomarkers for PD. ROC curves of Phenyllactate (a), (S)-(-)-2-hydroxyisocaproic acid (b), D-dlucono-1,5-lactone (c), cholesterol (d), triethyl phosphate (e), 1,2-dichloroethane (f), carene (g), 2,4,6-trimethylphenol (h), and Terpinolene (i) in serum exosomes of MPTP mice and controls. Results were analyzed with 10 controls and 14 MPTP mice.

malondialdehyde (MDA) and superoxide dismutase (SOD) levels were measured to assess the degree of oxidative stress injury and antioxidative ability. The results indicated that, compared to the control condition, MPTP treatment significantly increased the MDA level, and exosomes markedly alleviated this change ($p < 0.05$) (Figure 6(a)). Similarly, the SOD level was significantly reduced by MPTP but increased by exosomes ($p < 0.05$) (Figure 6(b)). In addition, Bcl-2 and Bax were detected, which reflected antiapoptosis and apoptosis in the brain, respectively. The results indicated a significant reduction in Bcl-2 protein expression but an increase in Bax expression with MPTP treatment ($p < 0.05$). Exosomes also upregulated Bcl-2 and downregulated Bax expression ($p < 0.05$). The above results were consistent in the SNpc (Figures 6(c) and 6(e)) and CPu (Figures 6(d) and 6(f)).

4. Discussion

The etiology of PD is complex and diverse and involves the interaction of genetic factors and the external environment. The occurrence of the disease is often associated with imbalances in neurotransmitters, lipid and energy metabolism disorders, and mitochondrial dysfunction. Neurotransmitters play a role in signal transduction via metabolic pathways such as release and reuptake. Changes in any of these metabolic pathways may affect central nervous system function. Small changes in endogenous and exogenous factors can be reflected in metabolite levels. Based on metabolomics approaches, metabolites associated with dopamine, purines, amino acids, fatty acids, and polyamines were found to be highly correlated with the progression of PD [44, 45]. Most of such studies are based on CSF and blood analysis, although some have examined other biological samples such as urine, feces, or brain tissue [46]. However, blood (serum or plasma) metabolites do not fully reflect the metabolism in the brain, and CSF samples are difficult to acquire. Therefore, exosomes, which can cross the blood-brain barrier, were used in this study to synchronously assess the metabolic changes in both the brain and the serum. Our results revealed a close relationship between exosome metabolites and PD. In this study, we found significant differences in 13 amino acids and metabolites in brain exosomes. Tyrosine and phenylalanine, which are closely involved in dopamine metabolism, were significantly downregulated in the PD group compared to the control group. Tyrosine is taken up by dopaminergic neurons and catalyzed by tyrosine hydroxylase in the

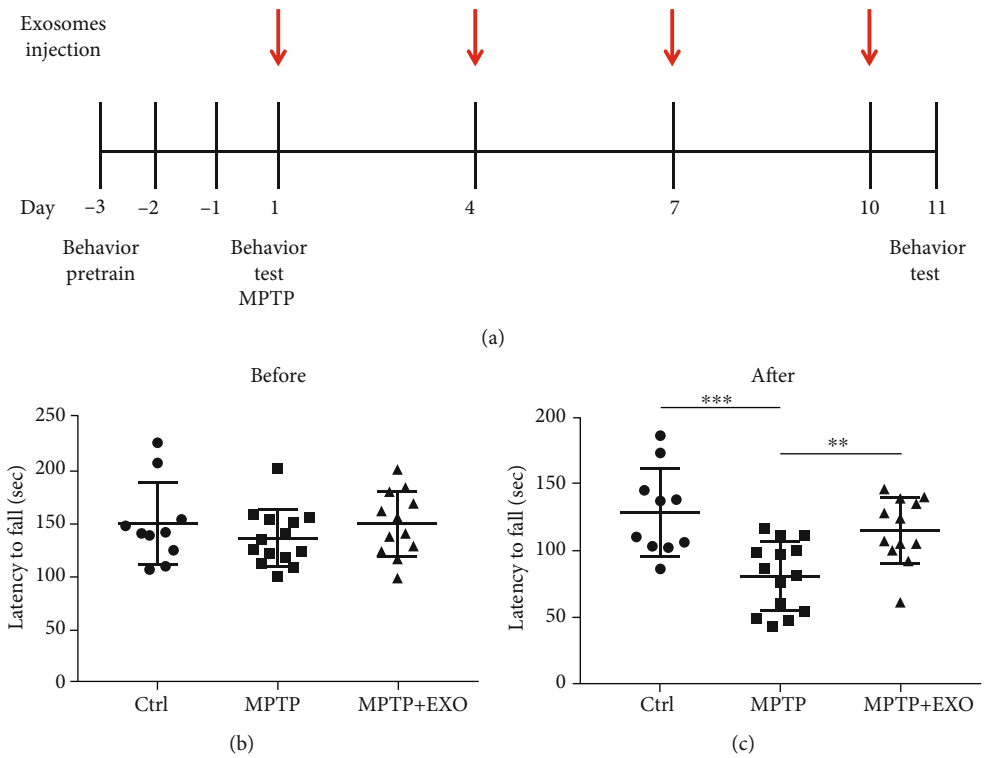

Figure 3: Exosomes improve behavioral performances in MPTP-induced mice. Protocol for MPTP administration, exosome administration, and behavioral test in Parkinson's disease model mice (a). Rotarod test for mice before MPTP injection (b), and after MPTP injection (c). All values are means ± SD, $n = 10 - 14$, $^{**}p < 0.01$, and $^{***}p < 0.001$.

cytoplasm to L-dopa, which is subsequently decarboxylated to dopamine. Phenylalanine also forms tyrosine via phenylalanine hydroxylase. The reduction of tyrosine and phenylalanine reflects the reduction of dopamine, which is one of the most important mechanisms in PD. The decrease in dopamine results in relative hyperfunction of the acetylcholine system. This transmitter disorder is the key to dyskinesia and other abnormal neurological activities. Our findings indicated that in PD mice, glutamic acid, glutamine, and glutamate were significantly reduced in serum exosomes; branched-chain amino acids (leucine, isoleucine, and valine) were reduced in brain exosomes; and alanine was increased in both serum and brain exosomes. Notably, there were significant differences in many lipids and fatty acids in both serum and brain exosomes between PD and control mice. The findings are similar to those of previous studies reporting that these metabolism pathway alterations are all indicative of mitochondrial dysfunction [44, 47]. In addition, decreased adenine in both serum and brain exosomes may be related to their participation in biological oxidation reactions. Uric acid, the final product of purine metabolism, can remove reactive oxygen and reactive nitrogen and reduce oxidative/-nitrative stress. These results confirmed that the metabolism of alanine, purine, and branched amino acids and lipids, which are closely involved in mitochondrial function and biological redox homeostasis, play an important role in the progression of PD. Moreover, the metabolites of exosomes were also indicative of alterations to carbohydrate metabolomics pathways. The serum and brain exosomes of PD mice accordantly exhibited a significant decrease in dulcitol and an increase in D-glucono-1, 5-lactone. In brain exosomes, phosphate and glucose were significantly reduced in PD mice. In serum exosomes, galactose and galactopyranoside were significantly increased in PD mice. It is not yet clear why these trends differ, but it may reflect the differential release of exosomes from different parts of the body. These results were consistent with previous results in body fluids [44]. The KEGG database revealed the differential metabolic pathways of phenylalanine and tyrosine metabolism, tryptophan metabolism, purine metabolism, branched-chain amino acid metabolism (leucine, isoleucine, and valine), etc. Other previous studies [48–51] also reported changes in purine metabolism, oxidative stress/redox homeostasis, energy metabolism, fatty acid metabolism, branched chain amino acids, phenylalanine and tyrosine metabolism, tryptophan metabolism, glycine derivation, and steroidogenesis in body fluids.

Growing evidence indicates that exosomes contribute to the progression of neurodegenerative disease [52]. Ghidoni et al. proposed the "Trojan horse" hypothesis of exosomes in neurodegeneration, a mechanism leading to the death of cells by shipping toxic agents in exosomes from cell to cell [53]. Indeed, many researchers believe that exosomes act as potential intercellular carriers of pathogenic proteins such as α-synuclein and cause impaired neuronal function [54]. In fact, a recent study by Han et al. showed that mice treated with serum exosomes from PD patients exhibited PD-relevant molecular, cellular, and behavioral phenotypes [55]. However, the opposing view is also considered feasible, that is, exosomes also offer neuroprotection, altering the

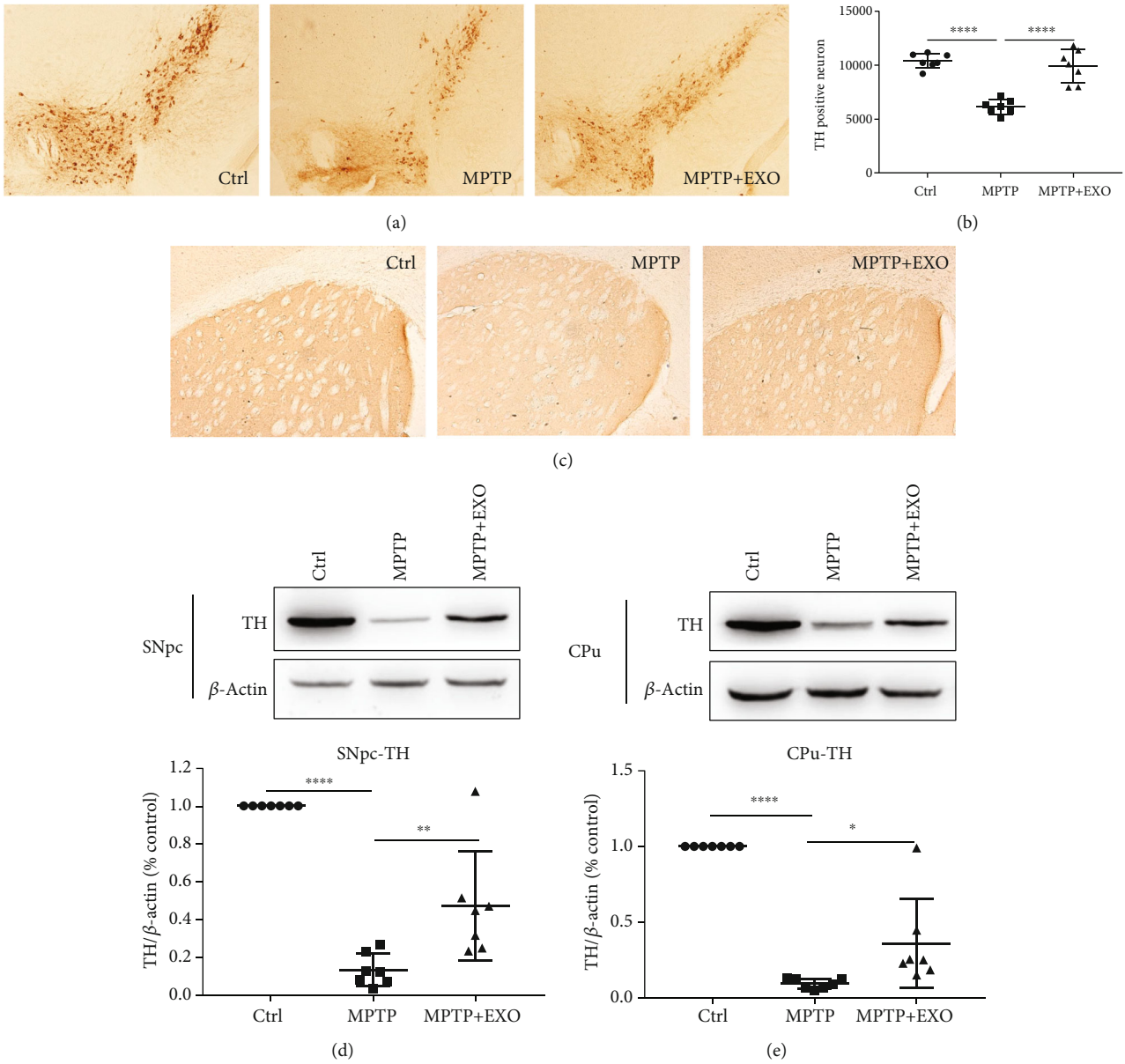

Figure 4: Exosomes prevent tyrosine hydroxylase (TH) loss in SNpc and CPu. Representative photomicrographs of TH-positive neurons in the SNpc region (a), quantitation of TH-positive neurons in SNpc (b), and representative photomicrographs of TH-positive neurons in the CPu region (c). Representative immunoblots and quantification of TH in the SNpc (d) and in the CPu (e). Error bars represent the means ± SD, $n = 7$, $^{*}p < 0.05$, $^{**}p < 0.01$, $^{***}p < 0.001$, and $^{****}p < 0.0001$.

abnormal cell's faulty programming by transmitting the "correct" information to the abnormal cell. There is no doubt that exosomes participate in the development process of PD, and the mechanism may derive from two aspects: first, exosomes are directly involved in information transmission and transport; second, exosomes indirectly affect biochemical reactions by altering the level of metabolites.

Based on the above mechanism, researchers have been studying and evaluating the feasibility of exosomes as therapeutic agents. Some studies have indicated that exosomes from different sources play a considerable role in protecting cells and alleviating the disease process. Research has revealed that exosomes from dental pulp stem cells inhibit 6-hydroxydopamine-induced apoptosis of dopaminergic neurons [56]. Similar findings indicated that exosomes from neurons, embryonic stem cells, neural progenitor cells, and astrocytes protect neurons [57]. Many studies have yielded similar results to the above, but they were based on exosomes of one cell type. It is undeniable that communication and transmission in the body generally involve the interaction of various types of cells. In this study, we focused on the blood-derived exosomes, which included exosomes derived from multiple cells rather than just one type of cell [58]. This setting allows our "therapeutics" to contain more comprehensive information. Exosomes released by different nerve cells carry different information and play different roles. Our study revealed that blood exosomes extracted from healthy volunteers have a neuroprotective effect on MPTP-

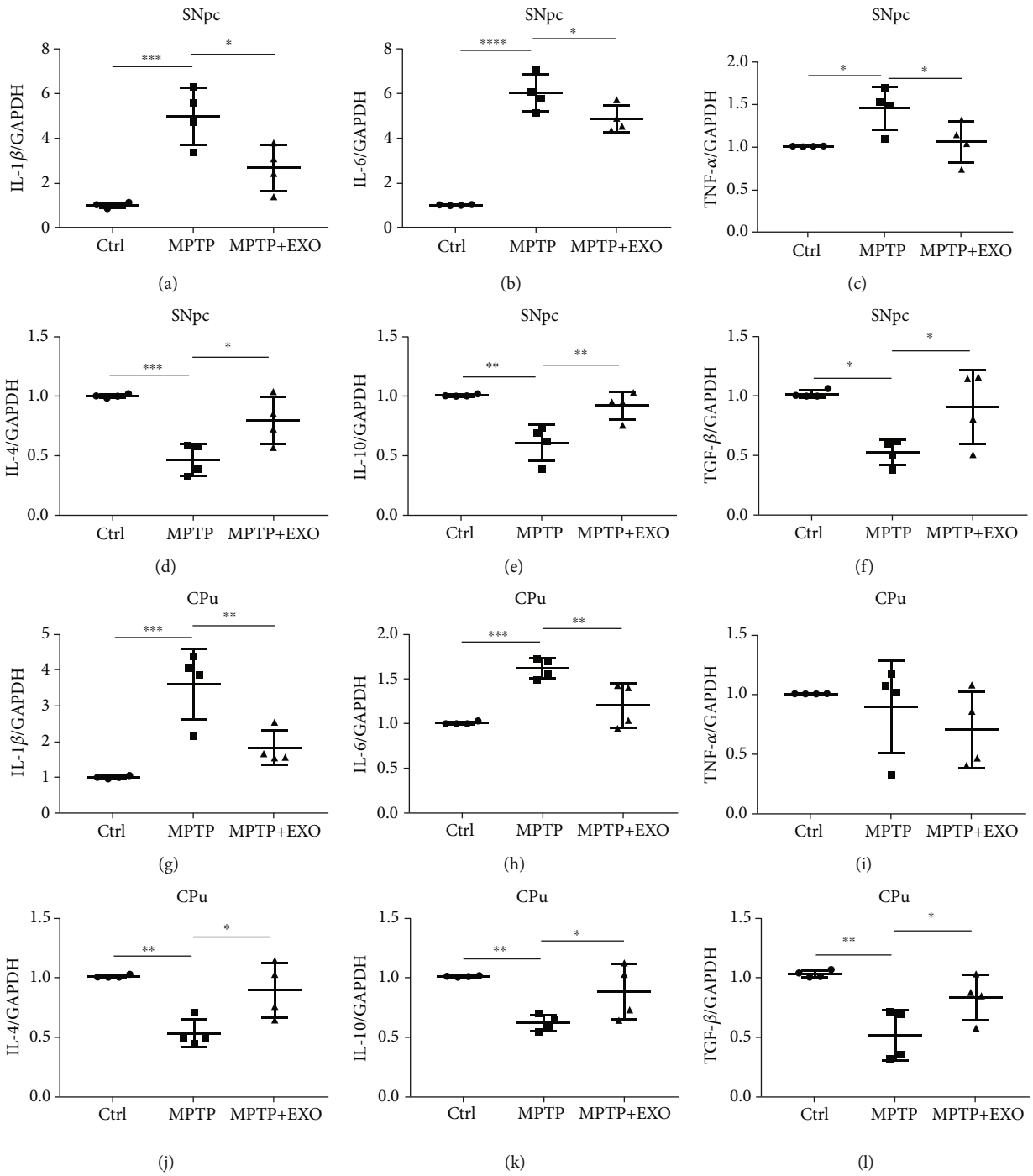

Figure 5: Exosomes attenuate neuroinflammation in SNpc and CPu. Data from qRT-PCR analyses of L-1β (a), IL-6 (b), TNF-α (c), IL-4 (d), IL-10 (e), TGF-β (f) in SNpc, and L-1β (g), IL-6 (h), TNF-α (i), IL-4 (j), IL-10 (k), TGF-β (l) in CPu. Error bars represent the means ± SD, $n = 4$, $^{*}p < 0.05$, $^{**}p < 0.01$, $^{***}p < 0.001$, and $^{****}p < 0.0001$.

treated mice. These protective effects were reflected by the restoration of the impaired motor coordination of mice, reduced loss of dopaminergic neurons, alleviated oxidative stress injury and neuroinflammation, and reduced cell apoptosis. We considered that the multiple neuroprotective effects in this study may be related to the source of exosomes, that is, blood exosomes are a complex composition comprising exosomes from a variety of nerve cells. There are two possible reasons for the therapeutic effects of blood exosomes. First, we can consider that some of the information carried by blood exosomes originates in the brain, for example, exosomes released by neurons cross the blood-brain barrier to the blood. Some of the information is consistent between the blood and the brain. Second, we speculate that intravenously injected exosomes entered the brain through the blood-brain barrier, altered the original proportion of exosomes in the brain, and successfully affected the physiological and pathological processes of the treated mice. The studies by

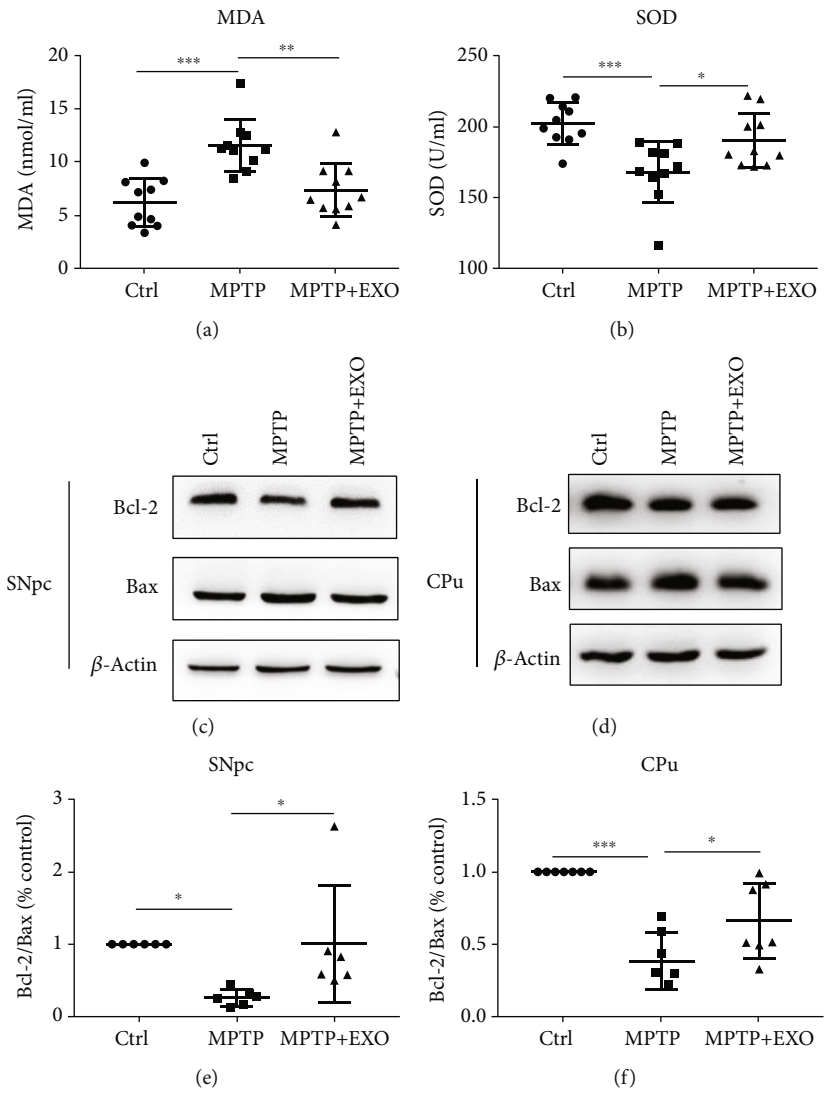

Figure 6: Exosomes alleviate oxidative stress injury in serum and the apoptosis in both SNpc and CPu. Effects of exosome treatment on the changes of MDA (a) and total SOD (b), $n = 10$. Representative bands of Bcl-2, Bax, and quantitative analysis results of Bcl-2/Bax in SNpc (c, e) and Cpu (d, f), $n = 7$. All values are means ± SD, $^{*}p < 0.05$, $^{**}p < 0.01$, and $^{***}p < 0.001$.

Qu et al. [59] and Peter et al. [60] provide strong support for this inference. They found that intravenous or intranasal injection of exosomes was targeted in relevant brain regions. Our results have suggested that exosomes are a promising target for the treatment of PD.

At present, the diagnosis of PD mainly depends on the assessment of motor symptoms according to the UK Parkinson's Disease Society Brain Bank clinical diagnostic criteria [61] and the patient's response to dopaminergic drugs. The degeneration of dopaminergic neurons before the onset of PD symptoms lasts several decades [62]. Therefore, identifying biomarkers of preclinical PD is the key to treat and predict this disease and distinguish it from other diseases with the same manifestation. After years of failing to find available biomarkers in metabolites of body fluids such as blood or urine, the focus has turned to exosomes in the hope of gaining more useful information. Recent studies have suggested α-synuclein in plasma neuronal exosomes as a promising biomarker for the early diagnosis and prognosis of PD [63, 64]. In this study, widely-targeted metabolomics analysis was used to analyze the metabolite differences in exosomes in the serum and brain between healthy mice and MPTP-treated mice and explore the potential biomarkers in exosomes and the potential mechanism underlying exosome involvement in PD. Given the significant differences between MPTP mice and controls regarding the level of the 25 metabolites in the serum and brain, it was necessary to explore the potential of serum metabolites as biomarkers to differentiate between control and MPTP mice. We performed ROC curve analysis using the nine metabolites that contributed most to the differentiation of MPTP mice and controls. The data from our study suggested that nine exosomal metabolites, which significantly differed in both the brain and the serum between groups, exhibited excellent performance in differentiating PD and control mice. These metabolites included phenylacetate, (S)-(-)-2-hydroxyisocaproic acid, D-glucono-1,5-lactone, cholesterol, triethyl phosphate, 1,2-dichloroethane, 2,4,6-trimethylphenol, and terpinolene (AUC > 90%).

Furthermore, 1,2-dichloroethane and (S)-(-)-2-hydroxyisocaproic acid have the ability to completely distinguish PD mice from control mice (AUC = 100%). Our study differs from previous reports in that we synchronously detected exosomal metabolites in the brain and serum. The advantage of this study was that the metabolites of serum exosomes could reflect the metabolites of brain exosomes, which can be difficult to acquire from clinical patients. Thus, these eight metabolites are potential clinical PD biomarkers.

However, the limitation of this study lies in the absence of a detailed mechanism for the treatment of PD by exosomes. Further research should focus on different metabolites or RNAs in exosomes, which can act as specific targets, to reveal the underlying mechanism of PD, provide feasible treatment options, and identify more accurate biomarkers.

5. Conclusion

In conclusion, through a series of experiments in behavior, pathology, and molecular biology, we confirmed that blood exosomes have protective effects on MPTP-treated PD model mice. This reflects the involvement of exosomes in the pathogenesis of neuron growth, oxidative stress, and neuroinflammation in PD. In addition, the widely-targeted metabolomics analysis revealed alteration of exosome metabolites and suggested the possibility of exosomes as potential biomarkers of PD. Our research provides novel suggestions for the treatment and prediction of PD.

Data Availability

All data generated or analyzed during this study are included in the manuscript.

Ethical Approval

Animal procedures were approved by the Animal Care and Use Committee of the Minzu University of China.

Conflicts of Interest

The authors declare no conflicts of interest.

Authors' Contributions

YC conceived and designed the experiments. TS, ZXD, and XL performed the experiments and analyzed the data. TS drafted the manuscript. YC and QSL reviewed and edited the manuscript. All authors read and approved the final manuscript.

Acknowledgments

This study was supported by the National Natural Science Foundation of China (81703492), Beijing Natural Science Foundation (7182092), and the MUC 111 project.

Supplementary Materials

Supplementary Figure 1: 2D and 3D PCA Plots indicated different metabolic characteristics in serum and brain tissue. Supplementary methods: the blood exosome isolation and validation methods. Supplementary Table 1: information of healthy volunteers. Supplementary Table 2: 69 differentially expressed metabolites in serum. Supplementary Table 3: 148 differentially expressed metabolites in the brain. *(Supplementary materials)*

References

[1] M. Delenclos, D. R. Jones, P. J. McLean, and R. J. Uitti, "Biomarkers in Parkinson's disease: Advances and strategies," *Parkinsonism & Related Disorders*, vol. 22, pp. S106–S110, 2016.

[2] A. Lee and R. M. Gilbert, "Epidemiology of Parkinson disease," *Neurologic Clinics*, vol. 34, no. 4, pp. 955–965, 2016.

[3] T. Pringsheim, N. Jette, A. Frolkis, and T. D. L. Steeves, "The prevalence of Parkinson's disease: a systematic review and meta-analysis," *Movement Disorders*, vol. 29, no. 13, pp. 1583–1590, 2014.

[4] G. E. Gillies, I. S. Pienaar, S. Vohra, and Z. Qamhawi, "Sex differences in Parkinson's disease," *Frontiers in Neuroendocrinology*, vol. 35, no. 3, pp. 370–384, 2014.

[5] L. V. Kalia and A. E. Lang, "Parkinson's disease," *Lancet*, vol. 386, no. 9996, pp. 896–912, 2015.

[6] R. Balestrino and A. H. V. Schapira, "Parkinson disease," *European Journal of Neurology*, vol. 27, no. 1, pp. 27–42, 2019.

[7] C. W. Olanow and J. A. Obeso, "The significance of defining preclinical or prodromal Parkinson's disease," *Movement Disorders*, vol. 27, no. 5, pp. 666–669, 2012.

[8] R. Cacabelos, "Parkinson's Disease: From Pathogenesis to Pharmacogenomics," *International Journal of Molecular Sciences*, vol. 18, no. 3, p. 551, 2017.

[9] A. Ascherio and M. A. Schwarzschild, "The epidemiology of Parkinson's disease: risk factors and prevention," *Lancet Neurology*, vol. 15, no. 12, pp. 1257–1272, 2016.

[10] M. A. Nalls, International Parkinson's Disease Genomics Consortium (IPDGC), N. Pankratz et al., "Large-scale meta-analysis of genome-wide association data identifies six new risk loci for Parkinson's disease," *Nature Genetics*, vol. 46, no. 9, pp. 989–993, 2014.

[11] V. Calabrese, A. Santoro, D. Monti et al., "Aging and Parkinson's disease: inflammaging, neuroinflammation and biological remodeling as key factors in pathogenesis," *Free Radical Biology & Medicine*, vol. 115, pp. 80–91, 2018.

[12] M. Schwartz and J. Kipnis, "A common vaccine for fighting neurodegenerative disorders: recharging immunity for homeostasis," *Trends in Pharmacological Sciences*, vol. 25, no. 8, pp. 407–412, 2004.

[13] M. G. Tansey and M. S. Goldberg, "Neuroinflammation in Parkinson's disease: its role in neuronal death and implications for therapeutic intervention," *Neurobiology of Disease*, vol. 37, no. 3, pp. 510–518, 2010.

[14] S. Phani, J. D. Loike, and S. Przedborski, "Neurodegeneration and Inflammation in Parkinson's disease," *Parkinsonism & Related Disorders*, vol. 18, pp. S207–S209, 2012.

[15] H. M. Gao and J. S. Hong, "Why neurodegenerative diseases are progressive: uncontrolled inflammation drives disease

progression," *Trends in Immunology*, vol. 29, no. 8, pp. 357–365, 2008.

[16] W. Le, J. Wu, and Y. Tang, "Protective Microglia and Their Regulation in Parkinson's Disease," *Frontiers in Molecular Neuroscience*, vol. 9, 2016.

[17] B. G. Trist, D. J. Hare, and K. L. Double, "Oxidative stress in the aging substantia nigra and the etiology of Parkinson's disease," *Aging Cell*, vol. 18, no. 6, article e13031, 2019.

[18] I. Ferrer, A. Martinez, R. Blanco, E. Dalfó, and M. Carmona, "Neuropathology of sporadic Parkinson disease before the appearance of parkinsonism: preclinical Parkinson disease," *Journal of Neural Transmission (Vienna)*, vol. 118, no. 5, pp. 821–839, 2011.

[19] S. Le Saux, H. Aarrass, J. Lai-Kee-Him et al., "Post-production modifications of murine mesenchymal stem cell (mMSC) derived extracellular vesicles (EVs) and impact on their cellular interaction," *Biomaterials*, vol. 231, p. 119675, 2020.

[20] G. Van Niel, G. D'angelo, and G. Raposo, "Shedding light on the cell biology of extracellular vesicles," *Nature Reviews. Molecular Cell Biology*, vol. 19, no. 4, pp. 213–228, 2018.

[21] J. Fauré, G. Lachenal, M. Court et al., "Exosomes are released by cultured cortical neurones," *Molecular and Cellular Neurosciences*, vol. 31, no. 4, pp. 642–648, 2006.

[22] I. Potolicchio, G. J. Carven, X. Xu et al., "Proteomic analysis of microglia-derived exosomes: metabolic role of the aminopeptidase CD13 in neuropeptide catabolism," *Journal of Immunology*, vol. 175, no. 4, pp. 2237–2243, 2005.

[23] A. R. Taylor, M. B. Robinson, D. J. Gifondorwa, M. Tytell, and C. E. Milligan, "Regulation of heat shock protein 70 release in astrocytes: role of signaling kinases," *Developmental Neurobiology*, vol. 67, no. 13, pp. 1815–1829, 2007.

[24] R. M. Johnstone, "Revisiting the road to the discovery of exosomes," *Blood Cells, Molecules, and Diseases*, vol. 34, no. 3, pp. 214–219, 2005.

[25] G. Raposo and W. Stoorvogel, "Extracellular vesicles: exosomes, microvesicles, and friends," *The Journal of Cell Biology*, vol. 200, no. 4, pp. 373–383, 2013.

[26] E. Emmanouilidou, K. Melachroinou, T. Roumeliotis et al., "Cell-produced alpha-synuclein is secreted in a calcium-dependent manner by exosomes and impacts neuronal survival," *The Journal of Neuroscience*, vol. 30, no. 20, pp. 6838–6851, 2010.

[27] C. Porro, M. A. Panaro, D. D. Lofrumento, E. Hasalla, and T. Trotta, "The multiple roles of exosomes in Parkinson's disease: an overview," *Immunopharmacology and Immunotoxicology*, vol. 41, no. 4, pp. 469–476, 2019.

[28] J. Howitt and A. F. Hill, "Exosomes in the Pathology of Neurodegenerative Diseases," *Journal of Biological Chemistry*, vol. 291, no. 52, pp. 26589–26597, 2016.

[29] M. D'Anca, C. Fenoglio, M. Serpente et al., "Exosome determinants of physiological aging and age-related neurodegenerative diseases," *Frontiers in Aging Neuroscience*, vol. 11, 2019.

[30] X. Wu, T. Zheng, and B. Zhang, "Exosomes in Parkinson's disease," *Neuroscience Bulletin*, vol. 33, no. 3, pp. 331–338, 2017.

[31] M. Shi, C. Liu, T. J. Cook et al., "Plasma exosomal α-synuclein is likely CNS-derived and increased in Parkinson's disease," *Acta Neuropathologica*, vol. 128, no. 5, pp. 639–650, 2014.

[32] A. Stuendl, M. Kunadt, N. Kruse et al., "Induction of α-synuclein aggregate formation by CSF exosomes from patients with Parkinson's disease and dementia with Lewy bodies," *Brain : a journal of neurology*, vol. 139, no. 2, pp. 481–494, 2016.

[33] H. Yu, T. Sun, J. An et al., "Potential roles of exosomes in Parkinson's disease: from pathogenesis, diagnosis, and treatment to prognosis," *Frontiers in cell and developmental biology*, vol. 8, p. 86, 2020.

[34] Z. G. Zhang and M. Chopp, "Exosomes in stroke pathogenesis and therapy," *The Journal of Clinical Investigation*, vol. 126, no. 4, pp. 1190–1197, 2016.

[35] Z. G. Zhang, B. Buller, and M. Chopp, "Exosomes - beyond stem cells for restorative therapy in stroke and neurological injury," *Nature Reviews. Neurology*, vol. 15, no. 4, pp. 193–203, 2019.

[36] Y. Song, Z. Li, T. He et al., "M2 microglia-derived exosomes protect the mouse brain from ischemia-reperfusion injury via exosomal miR-124," *Theranostics*, vol. 9, no. 10, pp. 2910–2923, 2019.

[37] Y. Zhang, M. Chopp, Y. Meng et al., "Effect of exosomes derived from multipluripotent mesenchymal stromal cells on functional recovery and neurovascular plasticity in rats after traumatic brain injury," *Journal of Neurosurgery*, vol. 122, no. 4, pp. 856–867, 2015.

[38] S. Huang, X. Ge, J. Yu et al., "Increased miR-124-3p in microglial exosomes following traumatic brain injury inhibits neuronal inflammation and contributes to neurite outgrowthviatheir transfer into neurons," *The FASEB Journal*, vol. 32, no. 1, pp. 512–528, 2017.

[39] M. Ding, Y. Shen, P. Wang et al., "Exosomes isolated from human umbilical cord mesenchymal stem cells alleviate neuroinflammation and reduce amyloid-beta deposition by modulating microglial activation in Alzheimer's disease," *Neurochemical Research*, vol. 43, no. 11, pp. 2165–2177, 2018.

[40] Z. X. Wei, G. J. Xie, X. Mao et al., "Exosomes from patients with major depression cause depressive-like behaviors in mice with involvement of miR-139-5p-regulated neurogenesis," *Neuropsychopharmacology*, vol. 45, no. 6, pp. 1050–1058, 2020.

[41] Y. Du, Y. Yu, Y. Hu et al., "Genome-wide, integrative analysis implicates exosome-derived microRNA dysregulation in schizophrenia," *Schizophrenia Bulletin*, vol. 45, no. 6, pp. 1257–1266, 2019.

[42] L. J. Vella, B. J. Scicluna, L. Cheng et al., "A rigorous method to enrich for exosomes from brain tissue," *J Extracell Vesicles*, vol. 6, no. 1, p. 1348885, 2017.

[43] S. Kim, S.-H. Kwon, T.-I. Kam et al., "Transneuronal Propagation of Pathologic α-Synuclein from the Gut to the Brain Models Parkinson's Disease," *Neuron*, vol. 103, no. 4, pp. 627–641.e7, 2019.

[44] J. Havelund, N. Heegaard, N. Færgeman, and J. Gramsbergen, "Biomarker Research in Parkinson's Disease Using Metabolite Profiling," *Metabolites*, vol. 7, no. 3, p. 42, 2017.

[45] M. Kori, B. Aydın, S. Unal, K. Y. Arga, and D. Kazan, "Metabolic biomarkers and neurodegeneration: a pathway enrichment analysis of Alzheimer's disease, Parkinson's disease, and amyotrophic lateral sclerosis," *OMICS*, vol. 20, no. 11, pp. 645–661, 2016.

[46] Y. Shao and W. Le, "Recent advances and perspectives of metabolomics-based investigations in Parkinson's disease," *Molecular Neurodegeneration*, vol. 14, no. 1, p. 3, 2019.

[47] M. H. A. Bakar, C. K. Kai, W. N. W. Hassan, M. R. Sarmidi, H. Yaakob, and H. Z. Huri, "Mitochondrial dysfunction as a central event for mechanisms underlying insulin resistance: the roles of long chain fatty acids," *Diabetes/Metabolism Research and Reviews*, vol. 31, no. 5, pp. 453–475, 2015.

[48] M. Trupp, P. Jonsson, A. Öhrfelt et al., "Metabolite and peptide levels in plasma and CSF differentiating healthy controls from patients with newly diagnosed Parkinson's disease," *Journal of Parkinson's Disease*, vol. 4, no. 3, pp. 549–560, 2014.

[49] P. A. LeWitt, J. Li, M. Lu, L. Guo, and P. Auinger, "Metabolomic biomarkers as strong correlates of Parkinson disease progression," *Neurology*, vol. 88, no. 9, pp. 862–869, 2017.

[50] T. Hatano, S. Saiki, A. Okuzumi, R. P. Mohney, and N. Hattori, "Identification of novel biomarkers for Parkinson's disease by metabolomic technologies," *Journal of Neurology, Neurosurgery, and Psychiatry*, vol. 87, no. 3, pp. 295–301, 2016.

[51] H. Luan, L.-F. Liu, N. Meng et al., "LC–MS-Based Urinary Metabolite Signatures in Idiopathic Parkinson's Disease," *Journal of Proteome Research*, vol. 14, no. 1, pp. 467–478, 2014.

[52] L. Vella, A. Hill, and L. Cheng, "Focus on extracellular vesicles: exosomes and their role in protein trafficking and biomarker potential in Alzheimer's and Parkinson's disease," *International Journal of Molecular Sciences*, vol. 17, no. 2, p. 173, 2016.

[53] R. Ghidoni, L. Benussi, and G. Binetti, "Exosomes: the Trojan horses of neurodegeneration," *Medical Hypotheses*, vol. 70, no. 6, pp. 1226-1227, 2008.

[54] B. M. Coleman and A. F. Hill, "Extracellular vesicles – their role in the packaging and spread of misfolded proteins associated with neurodegenerative diseases," *Seminars in Cell & Developmental Biology*, vol. 40, pp. 89–96, 2015.

[55] C. Han, N. Xiong, X. Guo et al., "Exosomes from patients with Parkinson's disease are pathological in mice," *Journal of Molecular Medicine*, vol. 97, no. 9, pp. 1329–1344, 2019.

[56] A. Jarmalavičiūtė, V. Tunaitis, U. Pivoraitė, A. Venalis, and A. Pivoriūnas, "Exosomes from dental pulp stem cells rescue human dopaminergic neurons from 6-hydroxy-dopamine-induced apoptosis," *Cytotherapy*, vol. 17, no. 7, pp. 932–939, 2015.

[57] M. Deng, H. Xiao, H. Peng et al., "Preservation of neuronal functions by exosomes derived from different human neural cell types under ischemic conditions," *The European Journal of Neuroscience*, vol. 47, no. 2, pp. 150–157, 2018.

[58] T. Ohmichi, M. Mitsuhashi, H. Tatebe, T. Kasai, O. M. Ali el-Agnaf, and T. Tokuda, "Quantification of brain-derived extracellular vesicles in plasma as a biomarker to diagnose Parkinson's and related diseases," *Parkinsonism & Related Disorders*, vol. 61, pp. 82–87, 2019.

[59] M. Qu, Q. Lin, L. Huang et al., "Dopamine-loaded blood exosomes targeted to brain for better treatment of Parkinson's disease," *Journal of controlled release : official journal of the Controlled Release Society*, vol. 287, pp. 156–166, 2018.

[60] N. Perets, O. Betzer, R. Shapira et al., "Golden exosomes selectively target brain pathologies in neurodegenerative and neurodevelopmental disorders," *Nano Letters*, vol. 19, no. 6, pp. 3422–3431, 2019.

[61] W. R. Gibb and A. J. Lees, "The relevance of the Lewy body to the pathogenesis of idiopathic Parkinson's disease," *Journal of Neurology, Neurosurgery, and Psychiatry*, vol. 51, no. 6, pp. 745–752, 1988.

[62] R. B. Postuma, D. Aarsland, P. Barone et al., "Identifying prodromal Parkinson's disease: pre-motor disorders in Parkinson's disease," *Movement Disorders*, vol. 27, no. 5, pp. 617–626, 2012.

[63] S. Lemprière, "Exosomal α-synuclein as a biomarker for Parkinson disease," *Nature Reviews Neurology*, vol. 16, no. 5, pp. 242-243, 2020.

[64] M. Niu, Y. Li, G. Li et al., "A longitudinal study on α-synuclein in plasma neuronal exosomes as a biomarker for Parkinson's disease development and progression," *European Journal of Neurology*, vol. 27, no. 6, pp. 967–974, 2020.

Hindawi
Oxidative Medicine and Cellular Longevity
Volume 2020, Article ID 2963540, 13 pages
https://doi.org/10.1155/2020/2963540

Research Article

Ellagic Acid Protects Dopamine Neurons via Inhibition of NLRP3 Inflammasome Activation in Microglia

Xue-mei He,[1,2] Yan-zhen Zhou,[3] Shuo Sheng,[1,2] Jing-jie Li,[1,2] Guo-qing Wang,[1,2] and Feng Zhang[1,2,4]

[1]*Key Laboratory of Basic Pharmacology of Ministry of Education and Joint International Research Laboratory of Ethnomedicine of Ministry of Education, Zunyi Medical University, Zunyi, Guizhou, China*
[2]*Department of Pharmacology, Key Laboratory of Basic Pharmacology of Guizhou Province and School of Pharmacy, Zunyi Medical University, Zunyi, Guizhou, China*
[3]*Department of Ear-Nose-Throat Surgery, The Affiliated Hospital of Zunyi Medical University, Zunyi, Guizhou, China*
[4]*Laboratory Animal Center, Zunyi Medical University, Zunyi, Guizhou, China*

Correspondence should be addressed to Feng Zhang; zhangfengzmc@163.com

Received 10 July 2020; Revised 20 September 2020; Accepted 5 November 2020; Published 19 November 2020

Academic Editor: Esmael Izadpanah

Neuroinflammation plays a crucial role in the pathological process of Parkinson's disease (PD). Nod-like receptor protein 3 (NLRP3) inflammasome was highly located in microglia and involved in the process of neuroinflammation. Activation of the NLRP3 inflammasome has been confirmed to contribute to the progression of PD. Thus, inhibition of NLRP3 inflammasome activation could be an important breakthrough point on PD therapy. Ellagic acid (EA) is a natural polyphenol that has been widely found in soft fruits, nuts, and other plant tissues with anti-inflammatory, antioxidant, and neuroprotective properties. However, the mechanisms underlying EA-mediated anti-inflammation and neuroprotection have not been fully elucidated. In this study, a lipopolysaccharide- (LPS-) induced rat dopamine (DA) neuronal damage model was performed to determine the effects of EA on the protection of DA neurons. In addition, the DA neuronal MN9D cell line and microglial BV-2 cell line were employed to explore whether EA-mediated neuroprotection was through an NLRP3-dependent mechanism. Results indicated that EA ameliorated LPS-induced DA neuronal loss in the rat substantia nigra. Further, inhibition of microglial NLRP3 inflammasome signaling activation was involved in EA-generated neuroprotection, as evidenced by the following observations. First, EA reduced NLRP3 inflammasome signaling activation in microglia and subsequent proinflammatory cytokines' excretion. Second, EA-mediated antineuroinflammation and further DA neuroprotection from LPS-induced neurotoxicity were not shown upon microglial NLRP3 siRNA treatment. In conclusion, this study demonstrated that EA has a profound effect on protecting DA neurons against LPS-induced neurotoxicity via the suppression of microglial NLRP3 inflammasome activation.

1. Introduction

Parkinson's disease (PD) is a chronic progressive neurodegenerative disease characterized by a deep selective loss of dopamine (DA) neurons in the substantia nigra (SN) [1]. Clinical manifestations include static tremor, slow movement, postural instability, stiffness, and other motor disorders [2]. So far, only a few drugs have been available for PD treatment, and most of them just relieve symptoms and could not prevent the death of DA neurons [3].

It was recognized that age-related excessive oxidative stress led to DA autooxidation, α-synuclein accumulation, and glial cell activation [4], which are the main causes of neuroinflammation [5]. Further, neuroinflammation, mediated by microglial activation and infiltrating T cells at sites of neuronal injury, was considered to be a prominent contributor to the pathogenesis of progressive PD [6]. Microglia are natural immune barriers in the immune system. While stimulated by external conditions, such as brain damage, inflammation, and pathogens, microglia readily become activated and undergo changes in morphology with hypertrophy and

function with phagocytosis. Most importantly, activated microglia could secrete a large number of proinflammatory factors, such as tumor necrosis factor-α (TNF-α), interleukin-1β (IL-1β), and IL-18 [7]. The accumulation of these proinflammatory factors contributes to the progressive loss of DA neurons. However, the neurotoxic factors, such as α-synuclein, released by the continuing damaged DA neurons, in turn, induce the secondary activation of microglia, and these activated microglia also secrete proinflammatory factors and further cause DA neuronal loss. Thus, a vicious cycle leading to prolonged neuroinflammation and progressive DA neurodegeneration emerges [8]. Collectively, inhibition of microglia-mediated neuroinflammation holds a promising potential for PD treatment.

Recently, inflammasomes are verified as intracellular proinflammatory pattern recognition receptors (PRRs) to initiate and propagate neuroinflammation. As a large multiprotein complex, inflammasome recruits pro-caspase-1 via ASC (the adaptor molecule apoptosis-associated speck-like protein containing a CARD) and then proceeds to cleave the cytokine precursors, such as pro-IL-1β and pro-IL-18, into mature IL-1β and IL-18 and finally mediates the immune responses against pathogen infection and tissue damage [9]. So far, five different types of inflammasomes have been identified, including NLRP1, NLRP3, NLRC4, Pyrin, and Absent in Melanoma 2 (AIM2) [10]. In particular, the NLRP3 inflammasome has been implicated in the process of neuroinflammation and is highly located in microglia [11]. Increasing evidence revealed that activation of the NLRP3 inflammasome played an important role in the progression of neurodegenerative diseases [12]. Therefore, inhibition of NLRP3 inflammasome activation could be an important breakthrough point in PD therapy.

Ellagic acid (2,3,7,8-tetrahydroxybenzopyrano [5,4,3-cde] benzopyran-5-10-dione, EA) is a polyphenol present in many plants, such as pomegranate plants, grapes, raspberries, blackberries, strawberries, and walnuts. EA exhibits a number of pharmacological activities, such as antioxidant and anti-inflammatory effects [13]. Recent studies confirmed that EA exerted neuroprotection against various neurological disorders. For example, EA generated neuroprotection and improved cognitive dysfunctions in a sporadic Alzheimer's disease (AD) animal model [14]. In addition, EA was indicated to confer neuroprotection against ischemic stroke [15]. However, the underlying mechanisms remain unclear. In this study, rat substantia nigral stereotaxic single injection of lipopolysaccharide- (LPS-) elicited DA neuronal loss was performed to investigate EA-exerted neuroprotection and the underlying mechanisms as well. These findings would provide evidence for the future application of EA on PD treatment.

2. Materials and Methods

2.1. Reagents. EA (purity > 95%), LPS (Escherichia coli O111:B4), 6-hydroxydopamine (6-OHDA), and apomorphine hydrochloride were obtained from Sigma-Aldrich (St. Louis, CA, USA). Enzyme-linked immunosorbent assay (ELISA) kits for TNF-α, IL-1β, and IL-18 were bought from Elabscience Biotechnology Co., Ltd. (Wuhan, China). The MTT assay kit was from Beijing Solarbio Science and Technology Co., Ltd. (Beijing, China). Small interfering RNA (siRNA) against NLRP3 was purchased from GenePharma (Shanghai, China). Anti-CR3 complement receptor (OX-42 Catalog No. Ab1211) and tyrosine hydroxylase (TH, Catalog No. Ab113) antibodies were bought from Abcam (Cambridge, MA, USA). Anti-caspase-1 (Catalog No. 22915-1-AP), ionized calcium-binding adapter molecule-1 (Iba-1, Catalog No. 10904-1-AP), β-actin (Catalog No. 20536-1-AP), TNF-α (Catalog No. 17590-1-AP), IL-1β (Catalog No. 66737-1-Ig), IL-18 (Catalog No. 10663-1-AP), rabbit IgG (Catalog No. SA00001-2), and mouse IgG (Catalog No. SA00001-1) antibodies were purchased from the Proteintech Group (Chicago, IL, USA). Anti-NLRP3 (Catalog No. orb101128) antibody was purchased from Biorbyt (Cambridge, United Kingdom).

2.2. Animal and Treatment. Male Wistar rats (200–250 g, 8–10 weeks) were bought from the Experimental Animal Center in the Third Military Medical University. All experimental procedures were carried out in accordance with the Chinese Guidelines of Animal Care and Welfare, and this study received approval from the Animal Care and Use Committee of Zunyi Medical University (Zunyi, China). Rats were acclimated to their environment for 1 week before the experiments. All the animals were randomly allocated to five experimental groups with six rats in each group: control, EA alone (50 mg/kg), LPS, LPS+EA (10 mg/kg), and LPS +EA (50 mg/kg). Anesthetized by 7% chloral hydrate (0.5 ml/100 g, v/w), rats received a single LPS (10 μg in 5 μl PBS) unilateral injection into the SN pars compacta followed by the coordinates 5.2 mm posterior to the bregma, 1.9 mm lateral to the midline, and 8.0 mm ventral to the surface of the skull [16]. EA was intragastrically administrated once a day for 7 consecutive days beginning 30 min before LPS injection. Seven days later, rat behavior changes were analyzed by the rotarod test. Afterwards, animals were sacrificed and the biochemical analysis was performed.

2.3. Rotarod Test. Apomorphine-induced rotation was widely employed for assessing the effects of lesions on the dopaminergic system and the success of treatment in PD animal models. Rats were tested for rotational behavior after receiving an intraperitoneal injection of apomorphine hydrochloride (0.5 mg/kg). Subsequently, a rotational behavior test was performed by the cylindrical arrangement containing thin steel rods with two parts by compartmentalization to permit the detection of two rats at the same time. Rats were trained to adapt at a speed of 10 rpm/min before the experiment started, with speed accelerating from 10 to 30 rpm over a period of 5 min until the rat slid off the steps. The duration time each rat stayed on the rod was recorded and calculated for analyzing the behavior changes of rats [17].

2.4. Immunohistochemical Analysis and Cell Counting in SN. Rat brains were cut with a horizontal sliding microtome into 35 μm transverse free-floating sections and immunostained with the corresponding antibodies. Then, brain slices were

incubated with 0.3% Triton X-100 and blocked with goat serum. Subsequently, brain slices were incubated with anti-TH (1 : 500), OX-42 (1 : 800), and NLRP3 (1 : 800) antibodies at 4°C overnight, respectively [18]. Digital images of TH-positive neurons, OX-42-positive microglia, and NLRP3-positive inflammasomes in midbrain SN were acquired by an Olympus microscope (Olympus, Tokyo, Japan). Representative fluorescence images were obtained, and the fluorescence intensity was calculated using ipwin32 software.

2.5. Cell Culture and Treatment. The mouse microglial BV-2 cell line was obtained from the China Center for Type Culture Collection (Wuhan, China). Cultures were maintained in minimum essential medium (MEM) supplemented with 10% heat-inactivated fetal bovine serum (FBS), 100 U/ml penicillin, and 100 μg/ml streptomycin at 37°C in the humidified atmosphere of 5% CO_2 and 95% air [19]. The DA neuronal MN9D cell line was purchased from the Cell Culture Center in the Institute of Basic Medical Sciences of the Chinese Academy of Medical Sciences (Beijing, China). MN9D cells were cultured in DMEM with 10% FBS and 1% penicillin-streptomycin on an atmosphere with 5% CO_2 at 37°C in the humidified atmosphere of 5% CO_2 and 95% air [20].

2.6. MTT Assay. Cell viability was evaluated by MTT assay. BV-2 and MN9D cells were cultured in 1×10^5/well in 96-well plates for 24 h. Afterwards, cells were treated with different concentrations of EA for 30 min followed by LPS (100 ng/ml) or 6-OHDA (100 μM) treatment for 24 h and then incubated with MTT solution (5 g/l) for 4 h. Formazan crystals in the cells were solubilized using 200 μl dimethyl sulfoxide (DMSO), and the absorbance was detected by an automated microplate reader within a 490 nm wavelength [21].

2.7. Western Blot Analysis. Total protein content was extracted from rat midbrain tissue and BV-2 cells using a lysis buffer containing protease inhibitors. Protein levels were quantified by BCA [22]. Protein (10 μg) from each sample was subjected to SDS-PAGE gel under the reduced conditions. Proteins were then transferred onto polyvinylidene fluoride (PVDF) membranes. The membranes were blocked with 5% nonfat milk for 2 h at room temperature and then incubated overnight at 4°C with the following primary antibodies: Iba-1 (1 : 800), NLRP3 (1 : 800), caspase-1 (1 : 800), TNF-α (1 : 1000), IL-1β (1 : 500), IL-18 (1 : 800), and β-actin (1 : 2000). Next, the membranes were incubated for 1 h with a horseradish peroxidase-conjugated anti-mouse IgG antibody or anti-rabbit IgG at 1 : 2000 dilution. The blot films were developed with an enhanced ECL Reagent.

2.8. ELISA. The levels of TNF-α, IL-1β, and IL-18 were measured by ELISA according to the manufacturer's instructions. The microplate reader was used to measure the absorbance at 450 nm.

2.9. Immunofluorescence Staining. Activated microglia were identified with an anti-OX-42 antibody. Cells were fixed with paraformaldehyde (4%) for 30 min. Later, cells were permeabilized using Triton X-100 (0.3%) for 15 min. Then, cells were blocked using a goat serum blocking solution for 60 min at 37°C. Thereafter, cells were incubated with 1 : 800 dilution of anti-OX-42 antibody overnight at 4°C. Following overnight incubation, cells were incubated in the dark for 30 min with goat anti-rabbit secondary antibody (1 : 1000) or goat anti-mouse secondary antibody (1 : 1000). Cells were also counterstained with DAPI for 5 min [23]. After rinsing cells with PBS, representative fluorescence images were obtained using an EVOS® Floid® Cell Imaging Station. The fluorescence intensity was calculated by using ipwin32 software.

2.10. RNA Transfection. BV-2 cells were cultured and seeded in a 6-well plate at a density of 1×10^5 cells/ml. The transfection of siRNA was performed complying with the manufacturer's protocol. A total of 2 μl of NLRP3 siRNA was diluted into 18 μl of transfection medium. GP-siRNA-Mate plus (180 μl) was used to transfect with siRNA dilution (20 μl). After transfection for 6 h, the transfection solution was removed and cells were rinsed with PBS and replaced with MEM containing 2% FBS and then treated with EA for 30 min followed by LPS (100 ng/ml) treatment for 24 h [19]. The gene sequences were as follows: sense, 5′-UUC UCC GAA CGU GUC ACG UTT-3′; antisense, 5′-ACG UGA CAC GUU CGG AGA ATT-3′.

2.11. Statistical Analysis. Results were indicated as the mean ± standard error of the mean (SEM). Statistical significance was analyzed by one-way analysis of variance (ANOVA) using GraphPad Prism software (GraphPad Software Inc., San Diego, CA, USA). Upon ANOVA demonstrating the significant differences, pairwise comparison between means was evaluated by Bonferroni's *post hoc* test with correction. A value of $p < 0.05$ was considered statistically significant.

3. Results

3.1. EA Attenuated LPS-Induced DA Neuronal Damage in SN In Vivo. Neuroprotective effects of EA on LPS-induced DA neuronal damage were investigated in rats. As shown in Figure 1(a), LPS reduced the time rats stayed on the rod, compared with the control group. However, EA (50 mg/kg) attenuated the LPS-caused decrease in the time rats remained on the rod, while no significant protection of EA (10 mg/kg) was discerned. To further confirm EA-mediated DA neuroprotection, the TH-positive neuronal number and TH protein expression were determined. As shown in Figure 1(b), EA (50 mg/kg) ameliorated the LPS-induced decrease in TH protein expression. Consistent with TH protein detection results, TH-positive neuronal counting indicated that EA exerted neuroprotection against LPS-induced DA neuronal loss (Figure 1(c)).

3.2. EA Ameliorated LPS-Elicited Activation of Microglia and NLRP3 Inflammasome Signaling In Vivo. Next, the effects of EA on microglia and NLRP3 inflammasome activation were investigated. To verify the connection between the NLRP3 inflammasome and microglia, the double-immunofluorescence

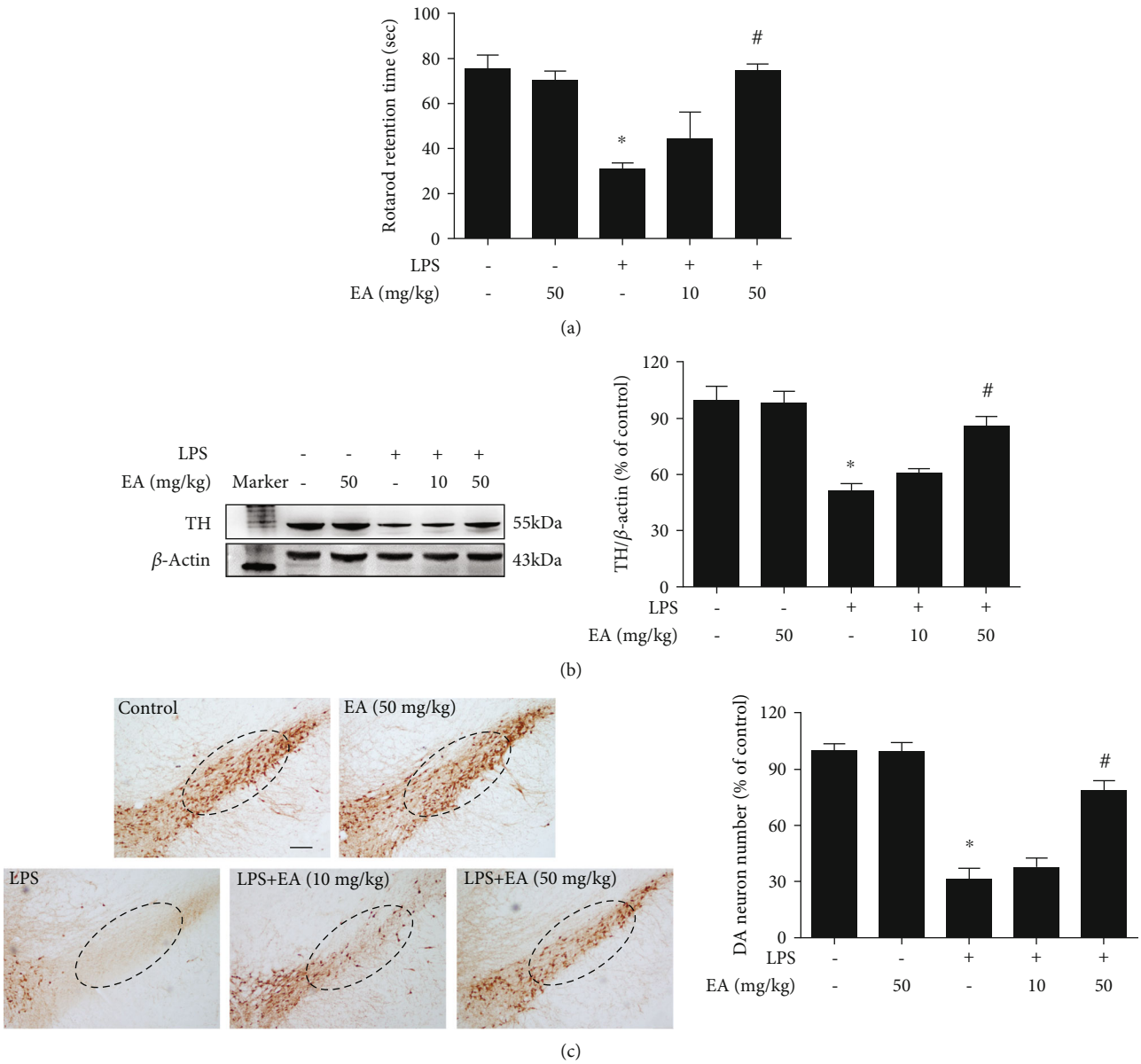

Figure 1: EA attenuated LPS-induced DA neuronal damage in SN *in vivo*. Rats were intragastrically given EA (50 mg/kg) for 7 consecutive days. Rat behavior changes were analyzed by the rotarod test (a). TH protein expression in the rat midbrain was tested by western blot assay (b). Brain sections were immunostained with an anti-TH antibody, and the number of TH-positive neurons in SN was counted (c). The "ellipse" presented the area of SN. Scale bar = 200 μm. Data were the mean ± SEM from 6 rats. $^{*}p < 0.05$ compared with the control group; $^{\#}p < 0.05$ compared with the LPS group.

calibration site was conducted. As shown in Figure 2(a), the NLRP3 inflammasome was activated and located in activated microglia. EA attenuated LPS-induced activation of the NLRP3 inflammasome in microglia. Also, EA inhibited Iba-1 protein expression induced by LPS (Figure 2(b)). In addition, EA suppressed LPS-induced activation of NLRP3 inflammasome signaling (Figure 2(c)) and proinflammatory cytokine (IL-1β, TNF-α, and IL-18) protein expressions (Figure 2(d)).

3.3. EA Had No Direct Neuroprotective Effects on DA Neurons. To further confirm whether EA produced direct neuroprotective actions on DA neurons, the effects of EA on 6-OHDA-induced DA neuronal damage *in vitro* were determined. First, as shown in Figure 3(a), 6-OHDA-induced neurotoxicity was not attenuated by EA treatment in MN9D cell-enriched cultures. Next, in TH-positive neuronal counting analysis (Figures 3(b) and 3(c)), 6-OHDA caused TH-positive neuronal loss and EA did not confer protection from 6-OHDA-induced neuronal damage. Similar results were indicated in the TH protein detection shown in Figure 3(d). These results demonstrated that EA did not generate direct neuroprotection on DA neurons.

3.4. EA Inhibited Microglial NLRP3 Inflammasome Activation In Vitro. The effects of EA on microglia and

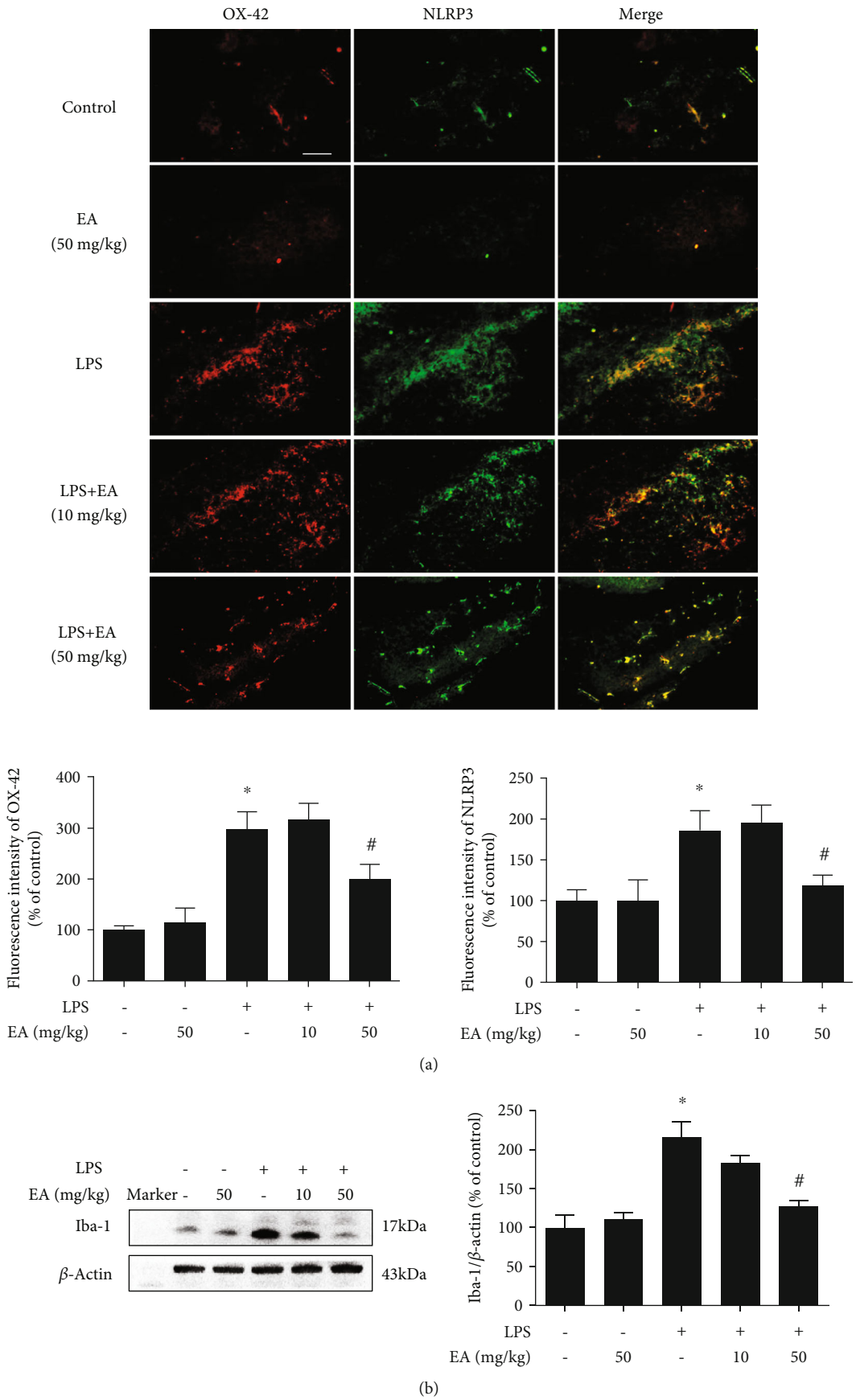

Figure 2: Continued.

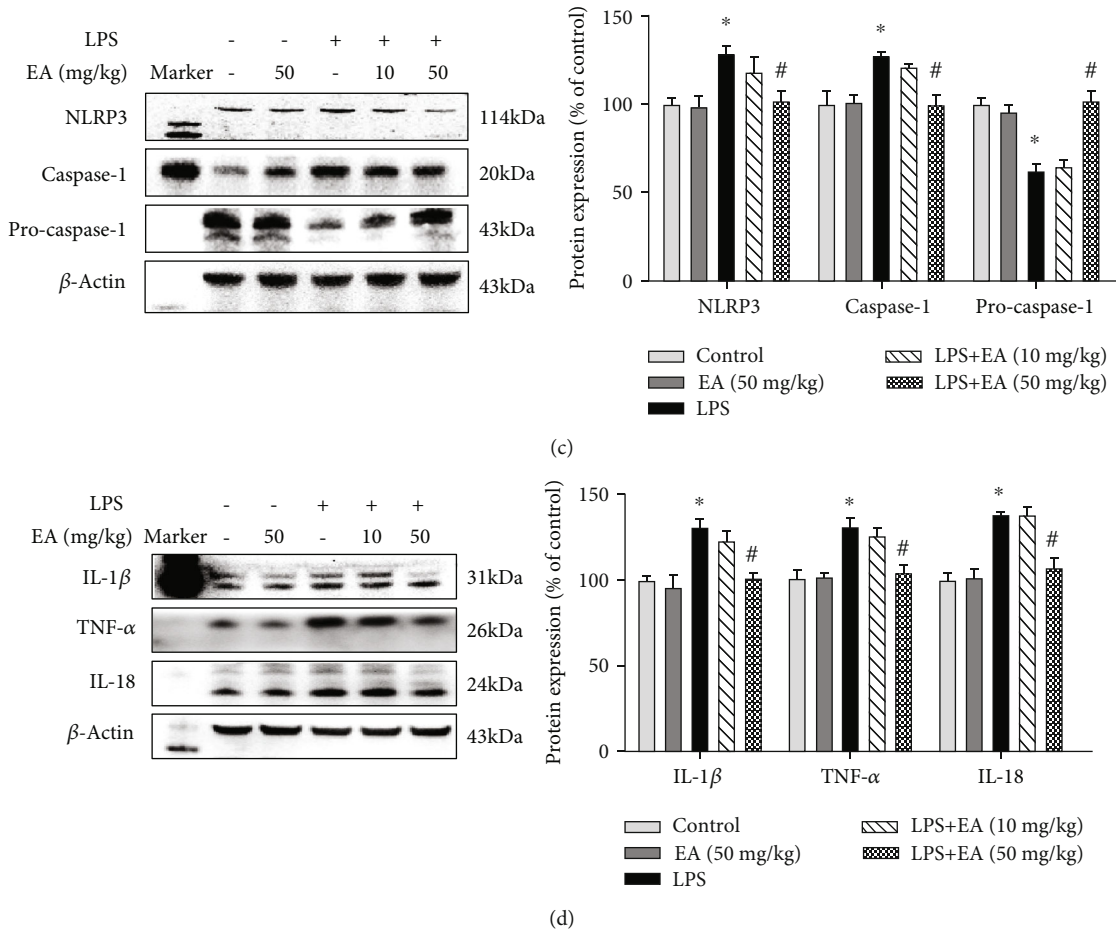

Figure 2: EA ameliorated LPS-elicited activation of microglia and NLRP3 inflammasome signaling *in vivo*. Rat brains were collected and stained by double immunofluorescence with anti-NLRP3 and anti-OX-42 antibodies (green fluorescence represented NLRP3 inflammasome, and red fluorescence represented microglia) (a). The protein expressions of Iba-1 (b); NLRP3, caspase-1, and pro-caspase-1 (c); and TNF-α, IL-1β, and IL-18 (d) in the rat midbrain were determined via western blot assay. Data were the mean ± SEM from 6 rats and expressed as a percentage of the control group. $^{*}p < 0.05$ compared with the control group; $^{\#}p < 0.05$ compared with the LPS group.

NLRP3 inflammasome signaling activation were further confirmed *in vitro*. First, BV-2 cells were employed to examine the effects of EA on LPS-induced microglial activation. As shown in Figure 4(a), immunofluorescence staining assay indicated that EA reduced LPS-induced microglial activation. Also, EA decreased LPS-induced higher protein expression of Iba-1 (Figure 4(b)). Then, EA inhibited the activation of microglial NLRP3 inflammasome signaling induced by LPS (Figure 4(b)). In addition, EA eliminated LPS-induced production of proinflammatory factors, such as TNF-α, IL-1β, and IL-18, in the culture medium (Figure 4(c)).

3.5. NLRP3 Inflammasome Signaling Inactivation Was Involved in EA-Mediated Anti-Inflammatory Properties. To investigate the role of NLRP3 inflammasome signaling in EA-mediated antineuroinflammation, NLRP3 siRNA was performed in BV-2 cell cultures. First, as shown in Figure 5(a), NLRP3 siRNA was transfected into BV-2 cells and the successful transfection with NLRP3 siRNA was evaluated by the NLRP3 protein level. After NLRP3 siRNA administration, both NLRP3 siRNA and EA inhibited LPS-induced NLRP3 inflammasome signaling activation. However, no significant difference of NLRP3 and caspase-1 protein expressions between the LPS+EA and LPS+EA+NLRP3 siRNA groups was discerned (Figure 5(b)). In addition, the effects of EA on proinflammatory factors' excretion with NLRP3 siRNA application were measured. In parallel with NLRP3 inflammasome signaling analysis, EA did not reduce LPS-induced release of proinflammatory factors again after NLRP3 siRNA treatment (Figure 5(c)). These observations indicated EA attenuated microglia-induced neuroinflammation via inhibition of NLRP3 inflammasome signaling activation.

3.6. EA Targeted Microglial NLRP3 Inflammasome to Produce DA Neuroprotection. Since microglia were the target of EA-generated DA neuroprotection, whether this neuroprotection resulted from inhibiting microglial NLRP3 inflammasome activation was then explored. As shown in Figure 6, compared with the MCM (LPS) group, both MCM (LPS+NLRP3 siRNA) and MCM (LPS+EA) protected against MCM (LPS)-induced neurotoxicity evidenced by cell viability and TH protein expression detection, whereas no significant difference of neuroprotection between these two

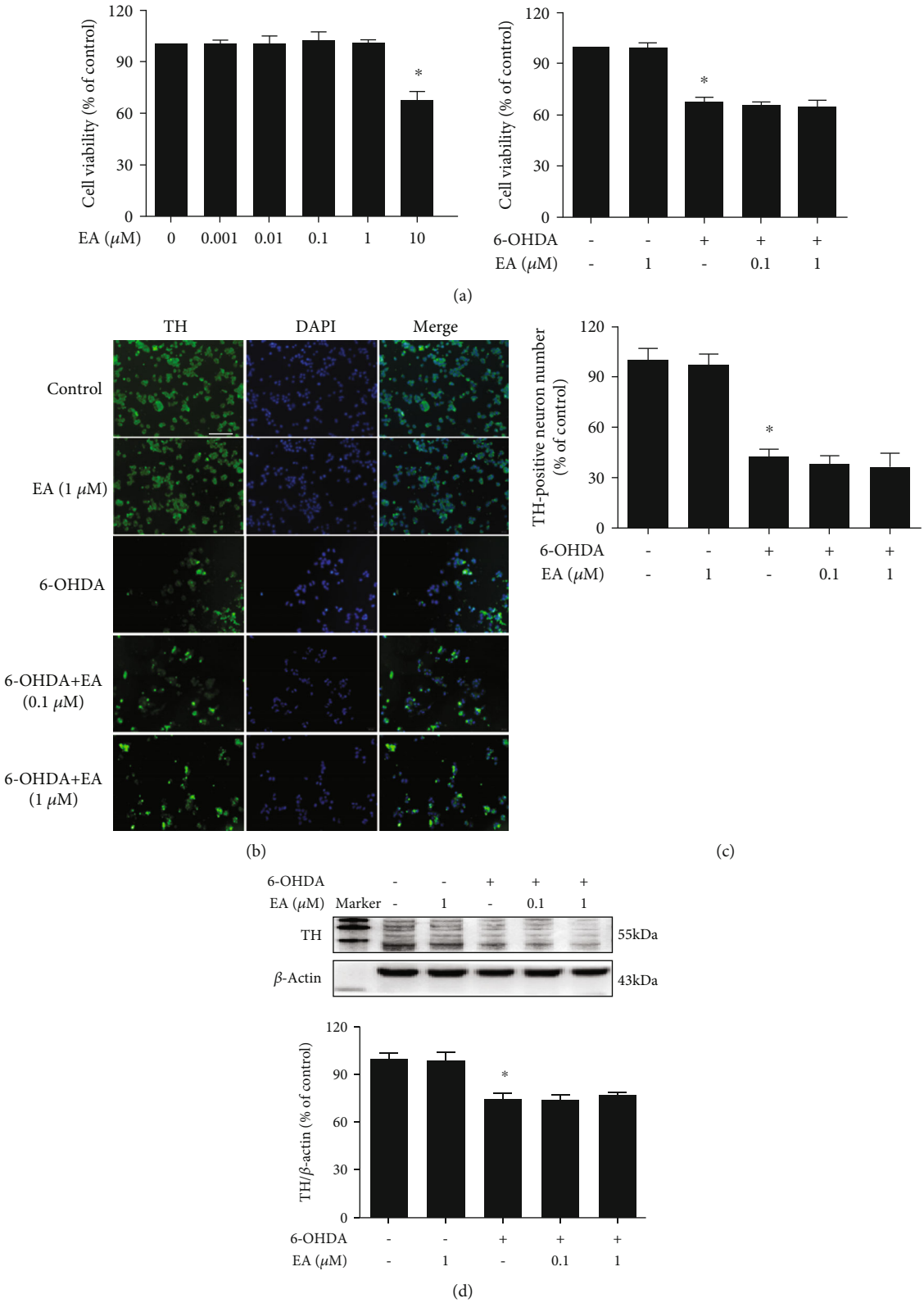

Figure 3: EA had no direct neuroprotective effects on DA neurons. MN9D cells were treated with EA (0.1 and 1 μM) for 30 min and then incubated with 6-OHDA (100 μM) for 24 h. Cell viability was determined by MTT assay (a). 6-OHDA-induced MN9D cell damage was evaluated by immunostaining (b) and cell counting (c). Scale bar = 100 μm. The protein expression of TH was detected by western blot assay (c). Data were the mean ± SEM from three independent experiments performed in triplicate. $^{*}p < 0.05$ compared with control cultures; $^{\#}p < 0.05$ compared with 6-OHDA-treated cultures.

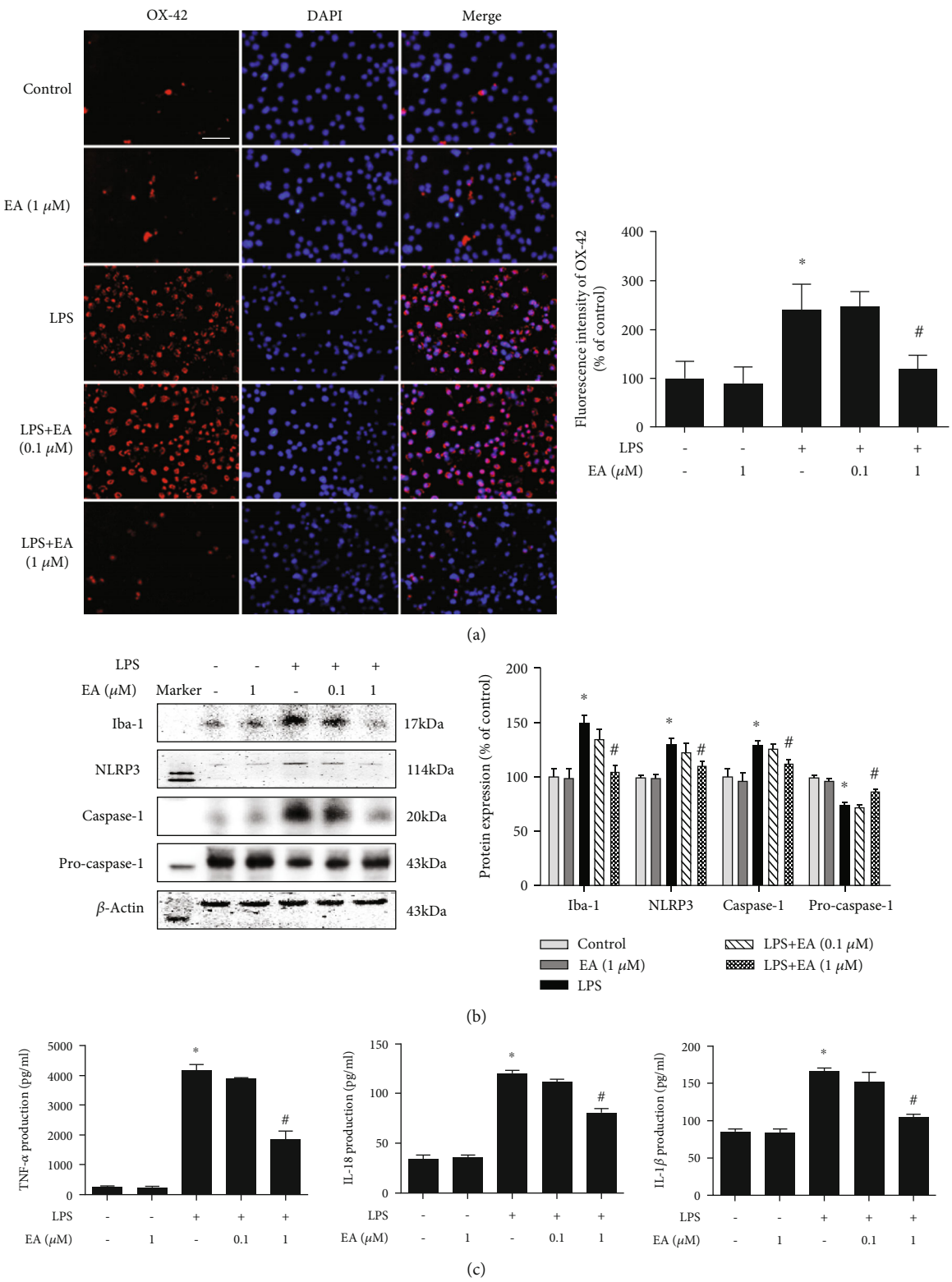

Figure 4: EA inhibited microglial NLRP3 inflammasome activation *in vitro*. BV-2 cells were treated with EA (0.1 and 1 μM) for 30 min and then incubated with LPS (100 ng/ml) for 24 h. Microglial activation was evaluated by immunostaining with an anti-OX-42 antibody (a) and quantitated by western blot analysis with an anti-Iba-1 antibody (b). Scale bar = 100 μm. The effects of EA on NLRP3 inflammasome signaling activation in BV-2 cells were detected via western blotting (b). The ratios of densitometry values of Iba-1, NLRP3, caspase-1, and pro-caspase-1 with β-actin were analyzed and normalized to each respective control cultures. The release of proinflammatory factors, such as TNF-α, IL-1β, and IL-18, in BV-2 cell culture medium was measured by ELISA (c). Data were the mean ± SEM from three independent experiments performed in triplicate. $^{*}p < 0.05$ compared with control cultures; $^{\#}p < 0.05$ compared with LPS-treated cultures.

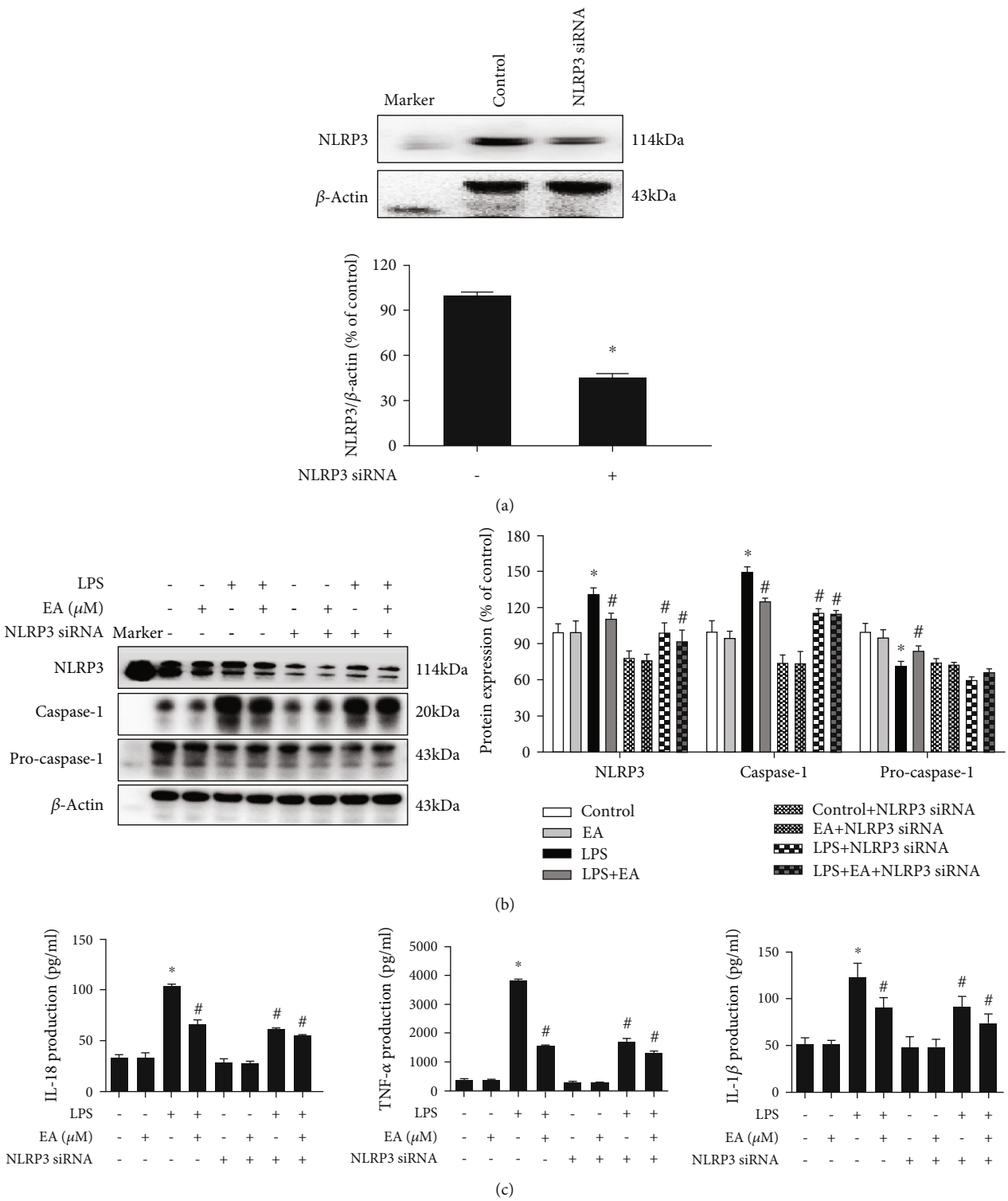

Figure 5: NLRP3 inflammasome signaling inactivation was involved in EA-mediated anti-inflammatory properties. BV-2 cells were treated with NLRP3 siRNA (40 nM). After 6 h of transfection, the transfection solution was removed and cells were rinsed with PBS. The silencing efficiency was assessed via NLRP3 protein expression detection (a). Moreover, BV-2 cells were treated with EA (1 μM) in the presence of NLRP3 siRNA and then exposed to LPS for 24 h. The protein expressions of Iba-1, NLRP3, caspase-1, and pro-caspase-1 in BV-2 cells were detected via western blot assay (b). The levels of TNF-α, IL-1β, and IL-18 in the culture medium were measured by ELISA (c). Data were the mean ± SEM from three independent experiments performed in triplicate. $^{*}p < 0.05$ compared with control cultures; $^{\#}p < 0.05$ compared with LPS-treated cultures.

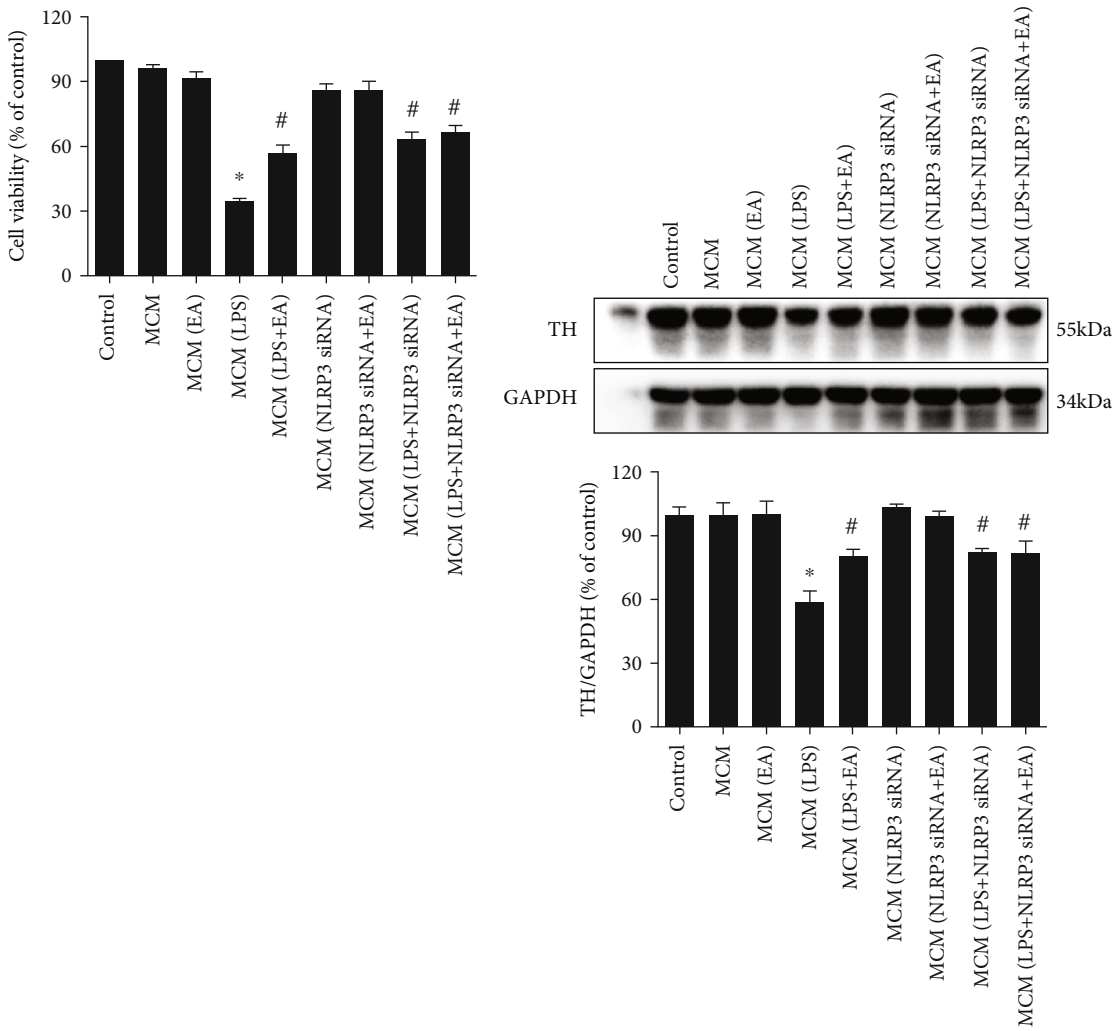

(a) (b)

Figure 6: EA targeted microglial NLRP3 inflammasome to produce DA neuroprotection. Microglia-conditioned medium (MCM) prepared from BV-2 cell cultures with administration of EA (MCM (EA)), LPS (MCM (LPS)), LPS+EA (MCM (LPS+EA)), NLRP3 siRNA (MCM (NLRP3 siRNA)), NLRP3 siRNA+EA (MCM (NLRP3 siRNA+EA)), NLRP3 siRNA+LPS (MCM (NLRP3 siRNA+LPS)), and LPS+NLRP3 siRNA+EA (MCM (LPS+NLRP3 siRNA+EA)) was harvested and added to MN9D cells incubated for 24 h. MN9D cell viability was determined by MTT assay (a). TH protein expression was tested by western blot assay (b). Data were the mean ± SEM from three independent experiments performed in triplicate. $^{*}p < 0.05$ compared with control cultures; $^{\#}p < 0.05$ compared with MCM (LPS)-treated cultures.

groups was exhibited. Further, MCM (LPS+NLRP3 siRNA +EA) did not exert more DA neuroprotection against MCM (LPS)-caused neuronal injury than MCM (LPS +NLRP3 siRNA) or MCM (LPS+EA) treatment.

4. Discussion

The present study is aimed at investigating the neuroprotective actions of EA on LPS-induced DA neuronal loss and evaluating the role of microglia-mediated neuroinflammation in this neuroprotection. Results indicated that EA protected DA neurons against LPS-induced neurotoxicity in SN. Further, inhibition of microglial NLRP3 inflammasome signaling activation was involved in EA-generated neuroprotection, as evidenced by the following observations. First, EA reduced NLRP3 inflammasome signaling activation in microglia and subsequent proinflammatory cytokines' excretion. Second, EA-mediated antineuroinflammation and further DA neuroprotection from LPS-induced neurotoxicity were not shown upon microglial NLRP3 siRNA treatment. Taken together, EA conferred neuroprotection against LPS-induced DA neuronal damage via inhibition of microglial NLRP3 inflammasome signaling activation (Figure 7).

Neuroinflammation is considered to be the most common feature of the aging brain and neurodegenerative disorders, including AD, PD, and amyotrophic lateral sclerosis (ALS) [5]. It is primarily mediated by activated glial cells, especially for microglia, and accompanied by the secretion of proinflammatory mediators [24]. As the first defense of immune surveillance, microglia readily become activated and predominately participate in the inflammatory response. In addition, astroglia could amplify microglia-mediated

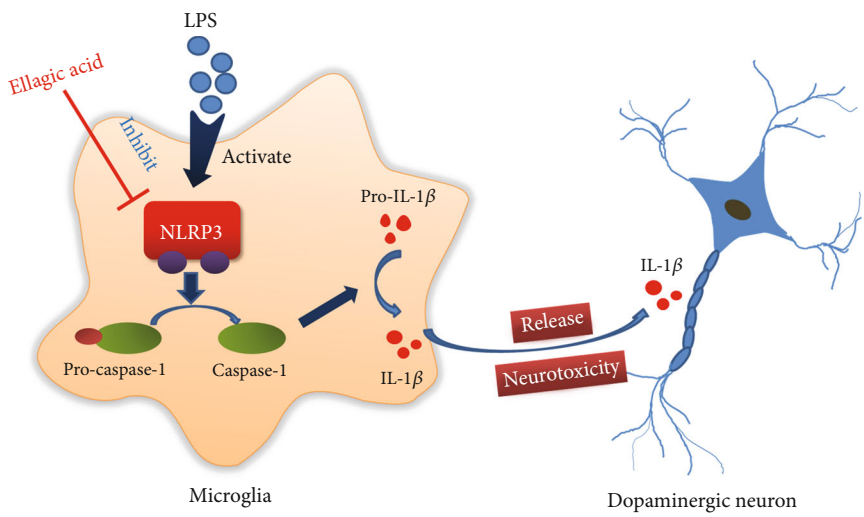

Figure 7: The mechanisms underlying EA-mediated dopamine neuroprotection.

neuroinflammation and result in the feedback loop of neuroinflammatory reactions [25]. In this regard, understanding the molecular mechanisms of PD can be found by investigating microglia-mediated neuroinflammation [26]. Therefore, to target microglia-derived proinflammatory cytokines might offer promising therapeutic approaches for PD management. In this study, EA protected DA neurons against LPS-induced neurotoxicity and reduced microglial proinflammatory factors' release, suggesting that EA-generated DA neuroprotection was closely associated with the inhibition of microglia-mediated neuroinflammation. Consistent with this finding, EA was previously confirmed to reduce the production of the proinflammatory cytokines, such as TNF-α and IL-6, in LPS-stimulated RAW 264.7 macrophage cells [27]. Furthermore, the dose of EA (50 mg/kg) presented beneficial effects on protection against LPS-induced DA neurotoxicity and inhibition of microglial NLRP3 inflammasome activation, whereas significant effects mediated by EA (10 mg/kg) were shown. This dose profile suggested that EA (10-50 mg/kg) was under the effective dose range in rats and guided that the selection of doses of EA complied with the dose-effect relationship. However, additional clinical studies are indeed needed to validate the dose range and dose-effect relationship of EA on humans corresponding to that in rats.

In addition, inflammasomes are multiprotein complexes responsible for intracellular sensors of environmental and cellular stress [28, 29]. As the inflammasome family member, the NLRP3 inflammasome is mainly involved in the response of neuroinflammation [11]. Upon cellular stress, assembly of NLRP3 inflammasome triggers caspase-1 activation and further caspase-1-mediated production of IL-1β and IL-18, thereby initiating neuroinflammation [30]. In PD patient brains, the NLRP3 inflammasome was potentially activated by insoluble α-synuclein aggregates and oxidative stress [31]. However, deficiency of NLRP3 inflammasome attenuated motor dysfunction and DA neurodegeneration in a PD mouse model [32]. Thus, inhibition of NLRP3 inflammasome activation might be beneficial for PD intervention. The present study demonstrated that EA could inhibit NLRP3 inflammasome signaling activation. Similar results exhibited that EA prevented monocrotaline-induced rat pulmonary artery hypertension via inhibiting the activation of the NLRP3 inflammasome and caspase-1 in the lungs and release of proinflammatory cytokines, such as IL-β, in serum [33]. On the other hand, this study indicated that EA-mediated DA neuroprotection was present in neuron-microglia cocultures but not in neuron-enriched cultures, implying that microglia were at least essential for EA-generated neuroprotection. Moreover, EA was found to reduce LPS-induced proinflammatory factors' production. Collectively, EA-inhibited microglial activation, and the subsequent proinflammatory factors' release might be attributed to the inhibition of microglial NLRP3 inflammasome activation. This conclusion was verified by the following observations: (1) EA inhibited microglial NLRP3 and pro-caspase-1 activation and IL-1β production; (2) EA could not further suppress LPS-induced proinflammatory factors' release and produce DA neuroprotection after neuron-microglia cocultures treated by NLRP3 siRNA.

Interestingly, EA not only decreased IL-β and IL-18 production via inhibition of NLRP3 inflammasome activation but also reduced TNF-α secretion. Why did EA suppress TNF-α production during EA-inhibited NLRP3 inflammasome activation? The amount of evidence indicated that the NLRP3 inflammasome participated in NF-κB-mediated inflammatory processes of diseases [34, 35], which suggested that there was crosstalk between the NLRP3 inflammasome and NF-κB signaling pathways. Thus, we speculated that EA-reduced TNF-α production might be associated with the regulation of the NLRP3 inflammasome/NF-κB signaling.

To date, current PD therapy is focused on symptom control and fails to delay the progressive neurodegenerative process. Actually, various side effects of the available drugs present huge challenges for long-term application. Therefore, more potential therapeutic candidates are urgently essential for halting the progression of PD. Recent studies demonstrated that inhibition of neuroinflammation would

attenuate DA neurodegeneration. Thus, anti-inflammatory agents might provide new avenues for PD treatment. However, the low success of translating promising anti-inflammatory candidates from animal studies to clinical trials was indicated. Therefore, an urgent approach for a novel anti-inflammatory alternative design was prompted [28]. Since activation of the microglial NLRP3 inflammasome was verified to play a pivotal role in the progression of neurodegenerative disorders, such as AD, PD, and ALS, inhibition of NLRP3 inflammasome activation might become a promising therapeutic target for these neurodegenerative disorders. Here, the present study demonstrated that EA conferred DA neuroprotection against LPS-induced neurotoxicity and modulation of microglial NLRP3 inflammasome signaling activation was revealed to participate in this neuroprotection. These findings suggested that EA could open a new window on neurodegenerative disorder treatment. However, the current study on EA only stays in animal experiments, and the follow-up hopes to be used as a clinical drug application for future studies.

5. Conclusion

This study demonstrated that EA has a profound effect on protecting DA neurons against LPS-induced neurotoxicity via suppression of microglial NLRP3 inflammasome signaling activation. These findings suggest that EA might be a potential benefit for PD treatment.

Abbreviations

6-OHDA: 6-Hydroxydopamine
AD: Alzheimer's disease
DA: Dopamine
DMSO: Dimethyl sulfoxide
EA: Ellagic acid
ELISA: Enzyme-linked immunosorbent assay
FBS: Fetal bovine serum
Iba-1: Ionized calcium-binding adapter molecule-1
IL-1β: Interleukin-1β
IL-18: Interleukin-18
LPS: Lipopolysaccharide
MCM: Microglia-conditioned medium
MEM: Minimum essential medium
NLRP3: Nod-like receptor protein 3
OX-42: Anti-CR3 complement receptor
PBS: Phosphate-buffered saline
PD: Parkinson's disease
PVDF: Polyvinylidene fluoride
siRNA: Small interfering RNA
SN: Substantia nigra
TH: Tyrosine hydroxylase
TNF-α: Tumor necrosis factor-α.

Data Availability

Data in this manuscript were available from the corresponding author on reasonable request.

Conflicts of Interest

The authors declared no conflicts of interests.

Authors' Contributions

FZ conceived and designed the experiments. All the authors participated in the experiment performance and data analysis. FZ, YZZ, and XMH wrote, revised, and checked the article. All authors revised and approved the final manuscript. Xue-mei He and Yan-zhen Zhou contributed equally to this work.

Acknowledgments

This study was supported by the National Natural Science Foundation of China (No. 81760658), the Foundation for High-Level Innovative Talents of Guizhou Province (No. 20164027), the Innovation Research Group project of the Department of Education of Guizhou Province (No. 2016038), the Foundation for Excellent Young Talents of Zunyi Medical University (No. 201603), and the Master Start Foundation of Zunyi Medical University (No. F-898).

References

[1] Y. Zhang, V. L. Dawson, and T. M. Dawson, "Oxidative stress and genetics in the pathogenesis of Parkinson's disease," *Neurobiology of Disease*, vol. 7, no. 4, pp. 240–250, 2000.

[2] T. J. Collier, N. M. Kanaan, and J. H. Kordower, "Aging and Parkinson's disease: different sides of the same coin?," *Movement Disorders*, vol. 32, no. 7, pp. 983–990, 2017.

[3] A. J. Lees, J. Hardy, and T. Revesz, "Parkinson's disease," *The Lancet*, vol. 373, no. 9680, pp. 2055–2066, 2009.

[4] A. Raichur, S. Vali, and F. Gorin, "Dynamic modeling of alpha-synuclein aggregation for the sporadic and genetic forms of Parkinson's disease," *Neuroscience*, vol. 142, no. 3, pp. 859–870, 2006.

[5] L. Qian, P. M. Flood, and J. S. Hong, "Neuroinflammation is a key player in Parkinson's disease and a prime target for therapy," *Journal of Neural Transmission (Vienna)*, vol. 117, no. 8, pp. 971–979, 2010.

[6] E. Hansson, "Long-term pain, neuroinflammation and glial activation," *Scandinavian Journal of Pain*, vol. 1, no. 2, pp. 67–72, 2010.

[7] F. Zhang, J. Liu, and J. S. Shi, "Anti-inflammatory activities of resveratrol in the brain: role of resveratrol in microglial activation," *European Journal of Pharmacology*, vol. 636, no. 1-3, pp. 1–7, 2010.

[8] W. Dauer and S. Przedborski, "Parkinson's disease: mechanisms and models," *Neuron*, vol. 39, no. 6, pp. 889–909, 2003.

[9] L. Franchi, R. Munoz-Planillo, and G. Nunez, "Sensing and reacting to microbes through the inflammasomes," *Nature Immunology*, vol. 13, no. 4, pp. 325–332, 2012.

[10] Y. He, H. Hara, and G. Nunez, "Mechanism and regulation of NLRP3 inflammasome activation," *Trends in Biochemical Sciences*, vol. 41, no. 12, pp. 1012–1021, 2016.

[11] M. T. Heneka, M. P. Kummer, A. Stutz et al., "NLRP3 is activated in Alzheimer's disease and contributes to pathology in APP/PS1 mice," *Nature*, vol. 493, no. 7434, pp. 674–678, 2013.

[12] L. C. Freeman and J. P.-Y. Ting, "The pathogenic role of the inflammasome in neurodegenerative diseases," *Journal of Neurochemistry*, vol. 136, Supplement 1, pp. 29–38, 2016.

[13] F. Firdaus, M. F. Zafeer, E. Anis, M. Ahmad, and M. Afzal, "Ellagic acid attenuates arsenic induced neuro-inflammation and mitochondrial dysfunction associated apoptosis," *Toxicology Reports*, vol. 5, pp. 411–417, 2018.

[14] F. Moura, K. de Andrade, J. F. dos Santos, and M. F. Goulart, "Lipoic acid: its antioxidant and anti-inflammatory role and clinical applications," *Current Topics in Medicinal Chemistry*, vol. 15, no. 5, pp. 458–483, 2015.

[15] Q.-s. Liu, R. Deng, S. Li et al., "Ellagic acid protects against neuron damage in ischemic stroke through regulating the ratio of Bcl-2/Bax expression," *Applied Physiology, Nutrition and Metabolism*, vol. 42, no. 8, pp. 855–860, 2017.

[16] C. Latchoumycandane, V. Anantharam, H. Jin, A. Kanthasamy, and A. Kanthasamy, "Dopaminergic neurotoxicant 6-OHDA induces oxidative damage through proteolytic activation of PKCδ in cell culture and animal models of Parkinson's disease," *Toxicology and Applied Pharmacology*, vol. 256, no. 3, pp. 314–323, 2011.

[17] T. Wang, L. Wang, C. Li et al., "Hydroxysafflor yellow A improves motor dysfunction in the rotenone-induced mice model of Parkinson's disease," *Neurochemical Research*, vol. 42, no. 5, pp. 1325–1332, 2017.

[18] F. Zhang, J. S. Shi, H. Zhou, B. Wilson, J. S. Hong, and H. M. Gao, "Resveratrol protects dopamine neurons against lipopolysaccharide-induced neurotoxicity through its anti-inflammatory actions," *Molecular Pharmacology*, vol. 78, no. 3, pp. 466–477, 2010.

[19] C. Chen, Y. Z. Wei, X. M. He et al., "Naringenin produces neuroprotection against LPS-induced dopamine neurotoxicity via the inhibition of microglial NLRP3 inflammasome activation," *Frontiers in Immunology*, vol. 10, p. 936, 2019.

[20] Y. Dong, M. L. Heien, M. M. Maxson, and A. G. Ewing, "Amperometric measurements of catecholamine release from single vesicles in MN9D cells," *Journal of Neurochemistry*, vol. 107, no. 6, pp. 1589–1595, 2008.

[21] J. van Meerloo, G. J. L. Kaspers, and J. Cloos, "Cell sensitivity assays: the MTT assay," *Methods in Molecular Biology*, vol. 731, pp. 237–245, 2011.

[22] S. Hirano, "Western blot analysis," *Methods in Molecular Biology*, vol. 926, pp. 87–97, 2012.

[23] J. G. Donaldson, "Immunofluorescence staining," *Current Protocols in Cell Biology*, vol. 69, no. 1, pp. 431–437, 2015.

[24] W. Shao, S. Z. Zhang, M. Tang et al., "Suppression of neuroinflammation by astrocytic dopamine D2 receptors via αB-crystallin," *Nature*, vol. 494, no. 7435, pp. 90–94, 2013.

[25] M. Jo, J. H. Kim, G. J. Song, M. Seo, E. M. Hwang, and K. Suk, "Astrocytic orosomucoid-2 modulates microglial activation and neuroinflammation," *The Journal of Neuroscience*, vol. 37, no. 11, pp. 2878–2894, 2017.

[26] G. Q. Wang, D. D. Li, C. Huang et al., "Icariin reduces dopaminergic neuronal loss and microglia-mediated inflammation in vivo and in vitro," *Frontiers in Molecular Neuroscience*, vol. 10, p. 441, 2018.

[27] C. S. Seo, S. J. Jeong, S. R. Yoo, N. R. Lee, and H. K. Shin, "Quantitative analysis and in vitro anti-inflammatory effects of gallic acid, ellagic acid, and quercetin from Radix Sanguisorbae," *Pharmacognosy Magazine*, vol. 12, no. 46, pp. 104–108, 2016.

[28] Y. Yan, W. Jiang, L. Liu et al., "Dopamine controls systemic inflammation through inhibition of NLRP3 inflammasome," *Cell*, vol. 160, no. 1-2, pp. 62–73, 2015.

[29] Z. L. Hu, T. Sun, M. Lu, J. H. Ding, R. H. du, and G. Hu, "Kir6.1/K-ATP channel on astrocytes protects against dopaminergic neurodegeneration in the MPTP mouse model of Parkinson's disease via promoting mitophagy," *Brain, Behavior and Immunity*, vol. 81, pp. 509–522, 2019.

[30] F. Di Virgilio, "The therapeutic potential of modifying inflammasomes and NOD-like receptors," *Pharmacological Reviews*, vol. 65, no. 3, pp. 872–905, 2013.

[31] R. Gordon, E. A. Albornoz, D. C. Christie et al., "Inflammasome inhibition prevents α-synuclein pathology and dopaminergic neurodegeneration in mice," *Science Translational Medicine*, vol. 10, no. 465, article eaah4066, 2018.

[32] E. Lee, I. Hwang, S. Park et al., "MPTP-driven NLRP3 inflammasome activation in microglia plays a central role in dopaminergic neurodegeneration," *Cell Death and Differentiation*, vol. 26, no. 2, pp. 213–228, 2019.

[33] B. Tang, G. X. Chen, M. Y. Liang, J. P. Yao, and Z. K. Wu, "Ellagic acid prevents monocrotaline-induced pulmonary artery hypertension via inhibiting NLRP3 inflammasome activation in rats," *International Journal of Cardiology*, vol. 180, pp. 134–141, 2015.

[34] W. Zhao, D. R. Beers, S. Bell et al., "TDP-43 activates microglia through NF-κB and NLRP3 inflammasome," *Experimental Neurology*, vol. 273, pp. 24–35, 2015.

[35] L. Bai, J. Li, H. Li et al., "Renoprotective effects of artemisinin and hydroxychloroquine combination therapy on IgA nephropathy via suppressing NF-κB signaling and NLRP3 inflammasome activation by exosomes in rats," *Biochemical Pharmacology*, vol. 169, article 113619, 2019.